ISSN 0727-0097

TWENTY SEVENTH NEWCASTLE SYMPOSIUM

on

"ADVANCES IN THE STUDY OF THE SYDNEY BASIN"

2nd to 4th April, 1993

NEWCASTLE NSW AUSTRALIA

DEPARTMENT OF GEOLOGY, THE UNIVERSITY OF NEWCASTLE, NSW 2308

THE UNIVERSITY OF NEWCASTLE

New South Wales 2308

DEPARTMENT OF GEOLOGY

Publication No. 545

COVER : Prospecting the Main Greta Coal Seam, discovered in a waterhole in Deep Creek by Geological Survey party in 1886. The Abermain Colliery is now situated near left bank of waterhole.

From David, 1907 "The Geology of the Hunter River Coal Measures NSW" Memoirs Geological Survey, New South Wales.

DEPARTMENT OF GEOLOGY

THE UNIVERSITY OF NEWCASTLE

TWENTY SEVENTH NEWCASTLE SYMPOSIUM

on

"ADVANCES IN THE STUDY OF THE SYDNEY BASIN"

2nd to 4th APRIL, 1993

NEWCASTLE NSW 2308 AUSTRALIA

C.F.K. DIESSEL
CONVENER

INDEX

AUTHOR INDEX

Note : Acceptance of abstracts and presentation of papers does not necessarily imply acceptance of the ideas and concepts by the participants of the Newcastle Symposium or The University of Newcastle.

PREFACE

Welcome to the 27th Newcastle Symposium. It does not seem so long ago that I was writing the Preface to last year's Symposium, yet time has been marching on, and the flood of interesting papers we received over the past weeks indicates that our contributors made good use of the past 12 months, which enabled us to put together an exciting program. Once again, the papers to be presented are the product of both fundamental and applied research and, while they cover a wide range of topics, there is the usual emphasis on the many aspects of coal.

Coal is also the subject of the Keynote Address to be given by Dr Alan Davis, Director of the Coal & Organic Petrology Laboratories at Penn State University and President of the International Committee of Coal Petrology (ICCP). He is still well-remembered in this country from his years with the Queensland Geological Survey, before he took up his present position in the United States. Dr Davis has a high reputation in petrography-based coal research, and is currently on study leave at the University of New South Wales.

Once again, the final list of papers differs slightly from the one publicised in the Second Circular due to some last-minute withdrawals. In spite of this, we have a full program which made it necessary to provide for 3 parallel sessions on Sunday morning. I hope the choice of session will not be too agonising for our visitors, particularly, since there are poster papers and trade exhibits to view as well.

Finally, I wish to thank you for your attendance and trust that you will have an enjoyable weekend in Newcastle.

Claus F.K. Diessel
Convener

FOREWORD

Welcome to the 27th Newcastle Symposium on "Advances in the Study of the Sydney Basin". Offers for papers have been overwhelming with 34 being accepted for presentation covering topics even more diverse than last year.

Prior to the presentation of papers at the weekend, the traditional pre-Symposium Excursion will be held and ably led by two of the oldest and most active participants of the Newcastle Symposium, Claus Diessel and David Branagan. They will take delegates to localities throughout the Lower Hunter Valley, which contain features critical to the geological understanding and industrial development of the region.

In the evening, after the excursion, there will be a Sheep Roast organised by the Newcastle Geology Graduates' Society. This is a function rarely missed by delegates as it provides them with an opportunity to catch up on the latest developments in their particular fields. More importantly, it allows them to renew friendships with colleagues that they have not seen since the last symposium or other symposia.

The Keynote Speaker is Dr Alan Davis from the Coal & Organic Petrology Laboratories, Pennsylvania State University, who will speak on "The influence of chemical and geological factors on coal maceral phenomena". It will be an interesting lecture.

Since writing the foreword for last year's Newcastle Symposium, much has happened in the Geology Department. Ron Boyd joined our staff in July, 1992, bringing with him much-needed expertise in sedimentology and sequence/seismic stratigraphy. He has settled in rapidly and has developed a rapport with both students and staff alike. In October he gained a large ARC grant to study the application of sequence stratigraphy of the northern Sydney basin.

As many of you were aware at the last Symposium, Claus Diessel was contemplating retirement. This is now official. Whilst he may have retired from teaching, however, he certainly has not retired from research, which he pursues avidly in his well-equipped laboratory, ably assisted by Larissa Gammidge, his ARC-funded Professional Officer. Claus is now Professor Emeritus and an Honorary Associate of the Department.

I had hoped to tell you that the Chair in Geology had been filled. Alas, this is not so and will not be filled until after the review of the department has been completed, prior to the end of Semester I. Present indications are that there are a number of potential candidates interested in applying for this position.

In December 1992, Colin Murray-Wallace resigned to take up a position at the University of Wollongong. His position has been advertised and a large number of applications were received. Amongst them are some excellent candidates, one of whom will be chosen in the near future.

The high profile of the Department has again been maintained in the twelve months since the last symposium, with staff travelling to the USA, UK, NZ, Germany and Czechoslovakia to present papers at International Conferences. On the Australian scene, in February this year, nine staff and postgraduate students attended the New England Orogen '93 Conference at the University of New England. After this conference, Phil Seccombe convened another successful Specialist Group in Economic Geology meeting.

Our students also have done well with Sue Keay achieving one of the best results seen in the department for many years – First Class Honours and a University Medal. She is leaving soon for Canberra to pursue a PhD at the Research School of Earth Sciences. We wish her all the best for the future.

I would like to thank Professor Raoul Mortley, our new Vice Chancellor, for agreeing to perform the opening ceremony of the Symposium. We wish him well in his new rôle which, in these times, will not be an easy one.

Finally, I would be remiss if I did not thank that dynamic duo Geraldene MacKenzie and Claus Diessel for their untiring efforts that they and the staff have put into the organisation of this Symposium.

Robin Offler
Head of Department

PROGRAM
27th NEWCASTLE SYMPOSIUM

"ADVANCES IN THE STUDY OF THE SYDNEY BASIN"

FRIDAY	2 APRIL 1993
10:00 - 17:30 EXCURSION	**HISTORY OF GEOLOGY IN THE LOWER HUNTER VALLEY** ***LEADERS :*** *David Branagan (University of Sydney) and Claus Diessel (University of Newcastle)* The excursion will visit localities in the Lower Hunter Valley which played a key role in the geological understanding and industrial development of the region, including the Muree and Ravensfield quarries, abandoned mines in the Maitland area, the Walka Waterworks, road and rail cuttings, the old copper prospect at Pokolbin and the use of local building materials. Lunch will be provided. *Because access is restricted, there will be only one bus with a maximum of 53 participants.*
18:30 - 23:00	**UNIVERSITY OF NEWCASTLE GEOLOGY GRADUATES' SOCIETY** **SHEEP ROAST - UNIVERSITY UNION**

SATURDAY	3 APRIL 1993	
08:30 - 09:00	**REGISTRATION** - Foyer of the Geology Department	
09:00 - 09:05 Lecture Theatre B01	**WELCOME** by the Head of the Geology Department, Associate Professor Robin Offler	
09:05 - 09:10	**OPENING** of the 27th NEWCASTLE SYMPOSIUM by the Vice Chancellor of the University of Newcastle, Professor R.J. Mortley	
TECHNICAL SESSION 1	**LECTURE THEATRE B01** **Chair David Branagan, The University of Sydney**	
09:10 - 09:40	*Konrad Moelle et al.* *Inst Coal Research*	The Newcastle Earthquake - Some of its 'After Effects'
09:40 - 10:10	*Jack Rynn* *Earthquake Research Cntr*	Earthquakes & Geology - are they related? The dilemma of causal relationships
10:10 - 10:50	**MORNING TEA** In the FOYER OF THE GREAT HALL	
10:50 - 11:20	*Chris Jenkins et al.* *Sydney Univ*	Geology of the offshore Sydney Basin : New results from direct sampling and geophysics
11:20 - 11:50	*Graham Bradley* *Consultant Geologist*	A new tectonic and depositional model for the offshore Sydney Basin (NSW/P10)
11:50 - 12:30	****** KEYNOTE ADDRESS ****** *Alan Davis* *Coal & Organic Petrology Laboratories* *Penn State University*	The Influence of Chemical and Geological Factors on Coal Maceral Phenomena
12:30 - 12:35	*CHAIR*	SUMMARY & VOTE OF THANKS
12:40 - 13:45	**LUNCH**	in the UNIVERSITY UNION

SATURDAY	3 APRIL 1993	
TECHNICAL SESSION 2A	**LECTURE THEATRE E01** Chair Brian Engel, The University of Newcastle	
13:45 - 14:15	*Richard Glen* *Geol Surv NSW*	The Lochinvar Anticline, the Hunter Thrust & Regional Tectonics
14:15 - 14:45	*N.Z. Tadros* *Dept Min Resources*	Review of the stratigraphy of the Gunnedah Basin
14:45 - 15:15	*David Briggs* *UNSW*	Chronostratigraphic correlation of Australian Permian depositional sequences
15:15 - 15:45	AFTERNOON TEA in the Foyer of the GREAT HALL	
15:45 - 16:15	*Peter Watson* *Univ Queensland*	Episodic fossil concentrations in a Hawkesbury sandstone shale lens at Somersby, NSW
16:15 - 16:45	*Chris Herbert* *Macquarie Univ*	Marine environments in the Early to Middle Triassic Narrabeen Group
16:45 - 17:15	*Rod Feldtmann et al.* *Univ Wollongong*	Shoalhaven Group in the western coalfield
17:15 - 17:45	*Thann Naing* *Macquarie University*	Trace fossils of the Sydney Basin
17:45 - 17:50	*CHAIR*	SUMMARY & VOTE OF THANKS
19:00 FOR 19:30	SYMPOSIUM DINNER	in the UNIVERSITY UNION

SATURDAY	3 APRIL 1993	
TECHNICAL SESSION 2B	**LECTURE THEATRE B01** Chair Konrad Moelle, The Institute of Coal Research	
13:45 - 14:15	*Bill Vlahovic* *Pacific Power*	Southern Newnes Plateau coal deposits – geology, coal resources and proposals for mining
14:15 - 14:45	*Robert Whiteley et al.* *Coffey Partners*	Detection of abandoned mine workings with radiowave methods
14:45 - 15:15	*Ross Seedsman et al.* *Coffey Partners*	Designing for subsidence, pillar stability and floor heave with low strength claystone floors
15:15 - 15:45	AFTERNOON TEA in the Foyer of the GREAT HALL	
15:45 - 16:15	*Andrew Newland et al.* *BHP*	A comparison of explosive and non-explosive seismic sources in an in-seam seismic borehole to borehole survey
16:15 - 16:45	*Hossein Memarian* *Wollongong Univ.*	Fracturing history of coal cliff sandstone at Coalcliff
16:45 - 17:15	*Paul Woolton* *IMS Pty Ltd*	A box full of squiggly lines
17:15 - 17:45	*Michael Vickers* *Sydney Univ.*	Strike-slip deformation at Kangaroo Tops, southern New England orogen : 10 km of sinistral displacement recorded on the Yarrowitch Fault
17:45 - 17:50	*CHAIR*	SUMMARY & VOTE OF THANKS
19:00 FOR 19:30	SYMPOSIUM DINNER	in the UNIVERSITY UNION

SUNDAY	4 APRIL 1993	
TECHNICAL SESSION 3A	**LECTURE THEATRE E01** Chair Phil Seccombe, The University of Newcastle	
09:00 - 09:30	*Jeff Bembrick* *Pacific Power*	Salinity Variations in the Upper Hunter
09:30 - 10:00	*F.L. Sutherland et al* *Australian Museum*	Barrington Volcano - Repeated gem eruptions (zircon, sapphire & ruby) at the edge of the Sydney Basin
10:00 - 10:30	*David Branagan* *Univ Sydney*	The Cox's Gap Incidents
10:30 - 11:00	MORNING TEA	in the Foyer of the GREAT HALL
11:00 - 11:30	*Judy Bailey* *Newcastle Univ*	The usefulness of petrographic, chemical & combustion indices and char character in predicting burn-off for Australian coals
11:30 - 12:00	*Dick Sanders et al.* *Quality Coal Consulting*	Mineral matter .... ash .... What's the difference?
12:00 - 12:30	*Susan Keay* *Univ Newcastle*	Magma-mixing in granitoids of the Lachlan Fold Belt : basement rocks of the Sydney Basin
13:00 - 13:05	*CHAIR*	SUMMARY & VOTE OF THANKS
13:05 - 14:15	LUNCH	in the UNIVERSITY UNION

SUNDAY	4 APRIL, 1993	
TECHNICAL SESSION 3B	**LECTURE THEATRE B01** Chair Claus Diessel, The University of Newcastle	
09:00 - 09:30	*John Wilmshurst et al.* *CSIRO*	A fluorescence laser microprobe for coal assessment
09:30 - 10.00	*Ron Wilkins et al.* *CSIRO*	The use of small lasers for the fusibility assessment of coals
10:00 - 10:30	*Michael Ellacott et al.* *CSIRO*	Integrated fluorescence alteration and reflectance study of Volador-1, Gippsland Basin, Victoria
10:30 - 11:00	MORNING TEA	in the Foyer of the GREAT HALL
11:00 - 11:30	*Darryl Stevenson* *Newcastle Univ*	Determination of marine influences on the Greta & Pelton seams by the use of selected palaeoenvironmental indicators
11:30 - 12:00	*John Gibson* *Newcastle Univ*	The use of dispersed organic matter in the investigation of hydrothermal fluids within the Copeland goldfields
12:00 - 12:30	*Ross Jenkins* *Newcastle Univ*	Organic maturation in the Early Permian Manning Group
12:30 - 12:35	*CHAIR*	SUMMARY & VOTE OF THANKS
13:05 - 14:15	LUNCH	in the UNIVERSITY UNION

SUNDAY	4 APRIL, 1993	
TECHNICAL SESSION 3C	LECTURE THEATRE CG04 Chair Ron Boyd, The University of Newcastle	
09:00 - 09:30	*M.M. Faiz et al.* *Univ Wollongong*	Two kilometres of post-Permian sediment – did it exist?
09:30 - 10.00	*Xianwen Yu* *Univ NSW*	Hydrogeological properties of the Botany sands aquifer, Sydney
10:00 - 10:30	*Michael Hill et al.* *Dept. Mineral Resources*	The geology and resources of the northern part of the southern coalfield
10:30 - 10:35	*CHAIR*	SUMMARY & VOTE OF THANKS
10:30 - 11:00	MORNING TEA	in the Foyer of the GREAT HALL
13:05 - 14:15	LUNCH	in the UNIVERSITY UNION

14:00 - 18:00	7th SAA PETROGRAPHY WORKSHOP -- PROVISIONAL PROGRAM .	
	(1)	Report on the 44th Meeting of the ICCP University Park, Pennsylvania State University, USA - July 1992 – Claus Diessel & Alan Davis, President, ICP
	(2)	Proposed ICCp vitrinite re-classification scheme and implications for AS 2856, Coal-Maceral Analysis. Alan Davis & Claus Diessel & Committee Members
	(3)	Discussion of the revision of AS 2418, Parts 1-7, released as draft DR 91222-T, "Solid Mineral Fuels - Glossary of Terms". Report and update by ?Ray Smith/TBF
	(4)	SAA RRE 1990 - final version. Report by ?Ken Hall/TBF
	(5)	SAA RRE 1992 - Report by ?Harold Read/TBF
	(6)	Next SAA RRE - ?analysis of a coal using gridded slides. ?Ken Hall to report/TBF

THE NEWCASTLE EARTHQUAKE – SOME OF ITS 'AFTER EFFECTS'

K.H.R. MOELLE, G. LI, O. SANO, H. CANTLE & G. DEAN-JONES
The Institute of Coal Research, Newcastle University

INTRODUCTION

An earthquake of moderate intensity (Richter scale magnitude ML 5.6 and Moment magnitude M 5.3) shook the City of Newcastle, NSW on the 28th December, 1989. Seismologists have identified a steep thrust fault (NW–SE trend, 75°NE dip) at 11.5 km depth, as the focal plane for this seismic event. The epicentre has been defined by the co-ordinates 32.95°S, 151.61°E, approximately 15 km south-west of Newcastle (Rynn *et al.*, 1992).

A comparison of pre- and post-earthquake performances of several surface or near-surface engineering structures in several districts of Newcastle has revealed considerable discrepancies and unexpected changes, the most notable being in the failure rates of an extensive water supply and sewerage disposal pipe network laid at shallow depth. A significant percentage (>15%) of buildings that had been damaged during the 1989 earthquake and subsequently repaired were found to be affected by serious recurrent damage which could not be attributed to faulty workmanship or to unsuitable materials being used in restoration and repair work. The considerable variations in observed failure occurrences in the post-earthquake period have major engineering implications. This paper discusses some results of an on-going research programme centred on pipe damage, and presents interpretative opinions on the observed post-earthquake changes, based on a comprehensive statistical study of failure data for pipes laid at shallow depths recorded since 1977, and on rainfall data from 1867 to the present.

THE STATISTICAL STUDY ON PIPE FAILURE AND RAINFALL DATA

A statistical study involving significance tests, regression and time series analyses has been conducted on pipe failure and rainfall records maintained by the Hunter Water Corporation Limited, Newcastle, NSW.

The Hunter Water Corporation Limited divides the Greater Newcastle District into three major regions: the Central Region (Newcastle City), the Southern Region (Lake Macquarie City), and the Northern Region (Maitland and Port Stephens areas). These regions have been further divided, respectively, into 8, 8, and 12 'performance areas' based on pipe failures. The pipe network of the Hunter Water Corporation covers an area of more than 5300 km^2. Most of the pipes are made of brittle cast iron, and are sensitive to differential ground movements. Such a large

pipe network thus acts as a very useful sensor to ground movements in the geological environment of the Newcastle Coal Measures.

The most frequently observed and typical pipe failure modes include holes in the pipes caused by corrosion, longitudinal fractures, and 'broken backs'—a term used to describe the circumferential fracturing of pipes which is generally attributed to bending stresses caused by differential ground movements. Because they represent an index of sensitivity to ground movement, broken back type failures are the focus of this investigation.

Sewer pipe chokes are a further important part of this study, as chokes are linked to cracks developed in the sewer mains, and subsequent vegetation ingress in search of water.

Most analysed data cover a period from July 1977 to October 1992, whereas broken backs have been recorded only since 1985. Rainfall data analyses cover a considerably longer period, from 1867 to October 1992.

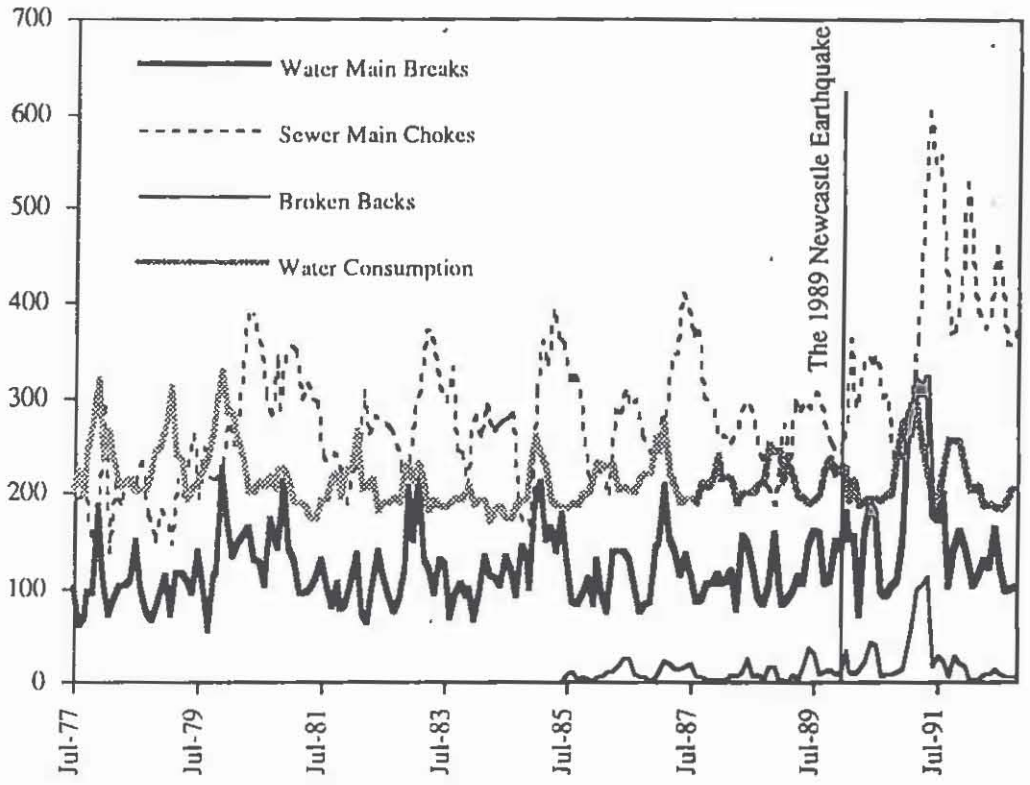

Fig. 1. Monthly variations of water main breaks, 'broken backs,' sewer main chokes and water consumption.

Water Main Breaks:	monthly number of water pipe breaks for the Greater Newcastle District.
Sewer Main Chokes:	monthly number of sewer pipe blockage for Greater Newcastle District.
Broken Backs:	monthly number of transverse fractures of water pipes for the Central and Southern regions. 'Broken Backs' are a sub-data set of the Water Main Breaks.
Water Consumption:	monthly water usage for the entire area analysed (unit: mL).

THE NEWCASTLE EARTHQUAKE—SOME OF ITS 'AFTER EFFECTS'

THE BEHAVIOUR PATTERN OF THE PIPE NETWORK AND THE EFFECTS OF PIPE AGING

Figure 1 displays the monthly variations of four data sets, recorded from July 1977 to October 1992, including water main breaks, occurrences of broken backs as a sub-set of the water main breaks, sewer chokes and water consumption; an explanation of the four data sets is given in Fig. 1. The significant increase in water main breaks and sewer chokes, commencing approximately 12 to 14 months after the Newcastle Earthquake, is obvious (Fig. 1) when compared with all previous records. This increase in pipe failures coincided with the notable increase in claims for recurrent earthquake damage to houses.

Some results of the statistical study on the data shown in Fig. 1 are summarised as follows:

(1) The performance patterns of water mains and sewer mains prior to the 1989 Newcastle Earthquake.

A time series analysis has revealed that the monthly variations in water main breaks, sewer pipe chokes, broken backs and water consumption (Fig. 1) followed a cyclic pattern during the pre-earthquake period. As presently understood, the periodic nature of water main breaks is characterised by a dominant 5-year cycle, a 2 to 3-year cycle, a one-year cycle, as well as by a half-year cycle, as a less significant event. The investigations of this aspect have not been completed. The time series study has also established the sequential occurrences of water main breaks, sewer pipe chokes and water consumption on a yearly basis, which shows that peak water consumption is followed approximately 4-5 months later by the highest incidence of broken back failures.

(2) The differences in pipe break frequencies before and after the 1989 Newcastle Earthquake.

Approximately 12 to 14 months after the 1989 Newcastle Earthquake, significant increases in water main breaks and sewer chokes (Fig. 1) began to be experienced in the Greater Newcastle District. The increase in water main breaks was attributable predominantly to broken back type failures, indicative of enhanced differential ground movements after the earthquake.

To establish quantitatively the difference in water main breaks in the pre- and post-earthquake periods, significance tests, using the Paired Student-*t* Test, have been conducted with paired break rate data. The data pair for each performance area consist of the pre-earthquake break rate averaged from 1985 to 1989, and the post-earthquake break rate averaged from 1990 to 1992. The break rate tested is specified by Equation (1) which gives normalised values:

$$R_i = \frac{N_i}{L_i Y} \qquad (1)$$

where R_i = pipe break rate for a particular performance area, N_i = count of pipe breaks for the performance area, L_i = total pipe length in the performance area, and Y = number of years considered. The results of the tests are given in Table I, which demonstrates significant differences in break rates before and after the earthquake.

Table I.

SIGNIFICANCE TESTS ON PIPE BREAK RATES
BEFORE AND AFTER THE EARTHQUAKE

Cases	Probability One-tail (%)	Probability Two tails (%)	Comments on Difference
Water main Breaks (the Greater Newcastle District)	0.02	0.03	Highly significant
'Broken Backs' (Central & Southern Region)	0.07	0.13	Highly significant
'Broken Backs' (Central Region)	2.02	4.03	Significant
'Broken Backs' (Southern Region)	0.05	0.10	Highly significant

(3) The effects of pipe aging

The detected differences shown in Table I have to be interpreted with caution. Considering an aging pipe system, it is likely that any comparison of break rates between two consecutive time periods should reveal systematic differences. Both linear and non-linear regression studies have been performed to examine the possible effects of pipe aging. These studies do not support the assumption that break rates in the Newcastle District are increasing with time at a noticeable rate, hence the significant increase in pipe breakage after the Newcastle Earthquake cannot be attributed exclusively to the aging of the pipes.

THE EFFECTS OF METEOROLOGICAL PATTERNS ON PIPE FAILURES

The two most important factors contributing to underground pipe failures are pipe deterioration due to corrosion, and movements caused by reactive clay. Reactive clays are a prime factor in the majority of water main breaks recorded by other utilities in the world, especially as a cause for the broken back failures. As pipe aging is excluded as an important cause for the failure increase after the earthquake, the role played by reactive clays must thus be carefully assessed.

Reactive clays occur selectively in several areas of the Greater Newcastle District and, depending on the seasonal variations in ground moisture conditions, the clays may apply shrink-swell induced stresses to the pipelines. Seasonal variations in rainfall should represent an important factor in this context, however a cross-correlation study has established only a vague relationship between rainfall and pipe breaks. This low correlation is mainly due to the high level of random variations in both rainfall and pipe breaks. Water consumption (Fig. 1), however, exhibits a much more regular annual periodic change than rainfall, and has thus been used here as an indirect measure of the ground moisture conditions.

A FFT (Fast Fourier Transformation) analysis has been applied to reveal any periodicity of rainfall from January 1867 to October 1992. Two characteristic rainfall cycles have been identified: a one-year cycle, as expected, and a five-year cycle. A non-linear regression analysis has confirmed the existence of

these two characteristic cyclic components. Similar analytical methods applied to data on the pipe break and sewer choke occurrences from July 1977 to October 1992 have revealed that pipe breaks and sewer chokes also exhibit a strong five-year cycle component, as discussed above. Consequently, drought conditions are important causal factors in the pipe failures observed.

The identified influence of rainfall on pipe failures can be confirmed qualitatively by comparing the monthly number of pipe breaks with monthly rainfall, as shown in Fig. 2. Both data sets presented in Fig. 2 have been normalised. Two interesting aspects are apparent. Firstly, high incidents of pipe breaks in the past have always occurred during drought periods. A cross-correlation study has confirmed this observation by showing that a peak of drought is followed approximately 2-3 months later by a peak of water main failures. Secondly, recent rainfall records (1977-1992) confirm the existence a 5-year cycle component. Figure 2 demonstrates that the last two major drought periods were approximately 10 years apart, and that here have been two 5-year rainfall cycles. The first of these droughts occurred in 1980, and the second in 1991. During both dry periods high pipe failure rates were recorded, and it is suggested that they were drought induced. The significantly higher failure rate after the earthquake corresponds exactly to the occurrence of the 1991 drought.

The significant question then arises: is the observed post-earthquake pipe failure increase in 1991 attributable to the earthquake, or to some dramatic change in climate conditions? Engineers in Newcastle have been faced with the same question when dealing with the increase in claims for house damage which occurred during the same period. There has been a general consensus that damage to houses observed in 1991 was the result of the extremes in climate conditions, and had little or nothing to do with the 1989 Newcastle Earthquake. The present authors' opinions on this question are discussed in the following sections.

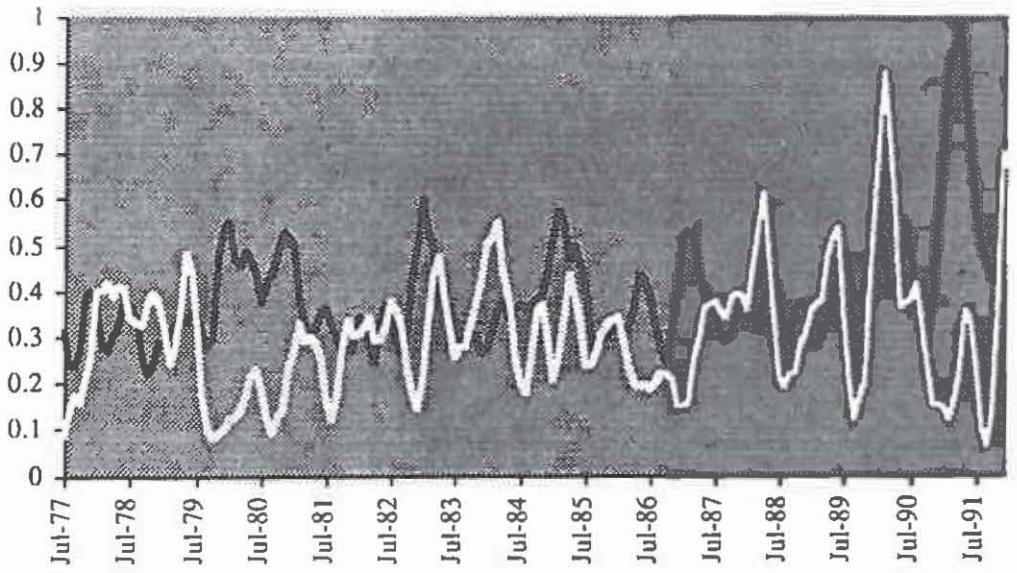

Fig. 2. Monthly number of pipe breaks and monthly rainfall (white line: rainfall, black line: break. Both data sets have been normalised).

K.H.R. MOELLE, G. LI, O. SANO, H. CANTLE and G.L. DEAN-JONES

EVIDENCE SUGGESTING THE EFFECTS OF THE 1989 NEWCASTLE EARTHQUAKE ON PIPE FAILURES

Cantle and Moelle (1993) have discussed the relationship between the pipeline orientation and the broken back failure rates. The most important finding of that study, in the context of this paper, is that the previously established directionally random distribution of broken backs over the area prior to the earthquake has changed to a directional preference after the earthquake, with NE–SW and NW–SE maxima. Such a change, after a seismic event with strong directional attributes, implicates the earthquake in the development of post-earthquake pipe failures.

It is known that the Hunter Mooki Thrust has been active over a long period of time; geometrically and kinematically related low angle thrust faults have been found in rocks of the Triassic Narrabeen Groups and the overlying Hawkesbury Sandstone. A strongly developed pervasive joint set in the rocks of the Newcastle Coal Measures also trends NW–SE, and it is not surprising that any ground movement would occur along planes with this spatial attitude, and may have affected the breaks in water pipes.

The pattern of sequential occurrences of pipe breaks has also changed after the earthquake. Time series analyses of the post-earthquake data have demonstrated the 4–5 month time-lag of broken back failures after the peak of water consumption has shortened to two months. This observed time shift is of significance. It is conceivable that in the Newcastle District the transportation/diffusion rates of ground water or moisture may have changed, as a result of stress-induced cracks in soils and underlying rocks, or because of the opening of previously closed joints in the rocks during the earthquake. Such changes in transportation/diffusion rates of ground water or moisture may have caused the shortening in time-lag after the peak of water consumption. A specific investigation on the effects of clay movements on pipe breaks is currently being conducted.

Figure 3 shows the observed yearly variations of water consumption for the entire Newcastle District, as well as those of broken back failures for the Central and Southern Regions.[1] The pre-earthquake broken back data cover the period July 1985 to December 1989, and the post-earthquake data from January 1990 to October 1992. Seasonal reactive clay movements occur as a result of changes in soil moisture conditions that are reflected by variations of water consumption, as discussed above. It follows that there should be a good correlation between the occurrence of broken back failures and water consumption. A study on water consumption and pre-earthquake broken back failure data has, indeed, confirmed such a close correlation, which is shown schematically in Fig. 3. However, the post-earthquake broken back data (Fig. 3) have significantly deviated from the pre-earthquake data trend. A speculation on this observed phenomenon is that either some factors affecting soil movement may have changed after the earthquake, or that other unknown physical processes may have caused differential ground movements in the post-earthquake period.

---

[1] Recording of broken backs for the Northern Region commenced only recently.

THE NEWCASTLE EARTHQUAKE—SOME OF ITS 'AFTER EFFECTS'

A regression model of pipe breaks has been developed, which adequately describes the monthly variation of the pipe breaks in the pre-earthquake period, taking into consideration the climatic data. However, even after allowing for the dry period of 1991, this model does not predict the high pipe break rates observed. This further suggests that rainfall leading to reactive clay movements is not the exclusive factor in the failure increase, and that the behaviour pattern of the pipe system has changed after the earthquake.

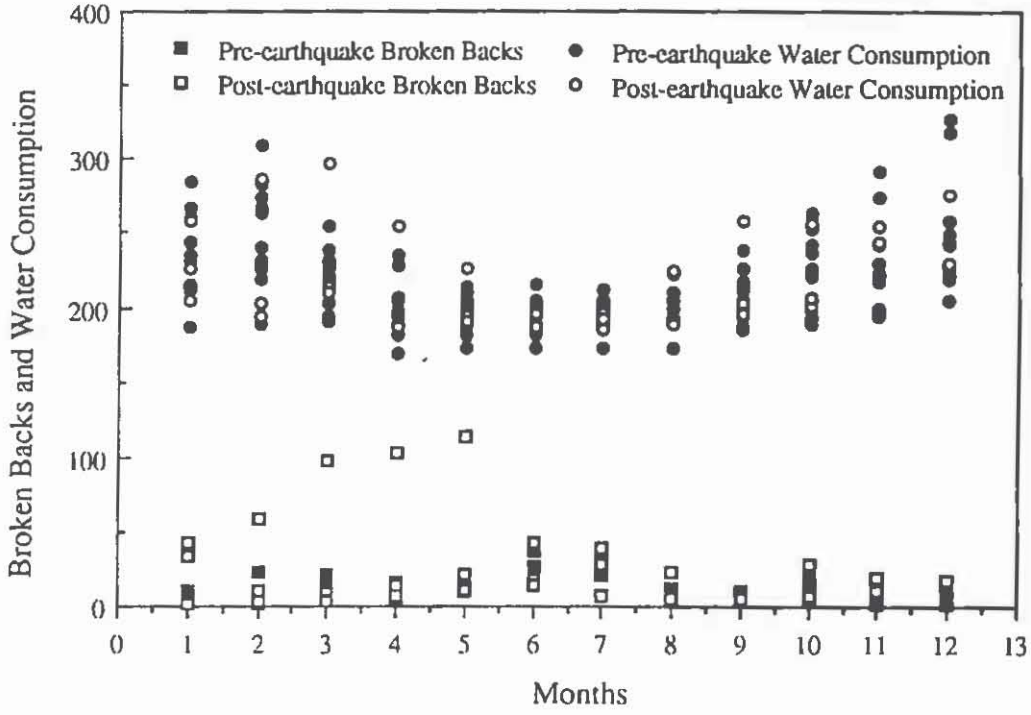

Fig. 3. Variations of water consumption (unit: mL) and 'broken backs.'

DISCUSSIONS

This study has provided strong evidence for enhanced ground movements in the post-earthquake period. The causes for the movements, whether reactive clay movements as claimed by some authors, or other, warrant detailed investigation. Although lack of rainfall has been a contributing factor to the unusually high incidence of failures after the earthquake, this study has shown that it is not the sole cause. Consequently, it is not justified to consider reactive clay movements as being the most influential factor in causing the observed damage after simply noting that there has been a climate extreme in the post-earthquake period. In view of the established evidence, the role played by the mechanical events directly associated with the 1989 Newcastle Earthquake must be considered in any analytical assessment.

An on-going research programme is being conducted to assess the effects of reactive clays and the earthquake. Apart from the possible reasons suggested in the preceding section for the earthquake effects, the release of stored strain energy due to the earthquake may also be an important aspect. It is shown (Fig. 1) that the increase in pipe breakage in the post-earthquake period has been

gradual, extending over a period of approximately 12 to 14 months. The cause for this development is not yet clear, although it is suggested here that the 1989 Newcastle Earthquake has caused a distortion of the coal measures rocks, mainly involving movements along the joint systems, bedding planes and coal plies, followed by a slow relaxation and release of stored strain energy from the rockmass. Such a concept is plausible for a sequence of sedimentary rocks that consists of very brittle and stiff conglomerates, sandstones and cherts interbedded with coal seams, claystones, mudstones and tuffs. The envisaged kinematic model relies heavily on bedding plane and joint plane movements and a high energy absorption in the coal seams. Bedding plane faults with movements of up to 40 m net displacement do occur in the Newcastle Coal Measures, and it is conceivable that seismic energy has been stored in those fault planes and in other planar structural elements.

The long energy release period may be attributable to the high regional horizontally arranged compressive stress, generally exceeding 10 MPa, which existed prior to the seismic event and whose magnitude and vectorial direction have not changed significantly after the earthquake. It is the aim of a further on-going research programme to identify the mechanism for the initial deformation of the rockmass and for the subsequent energy release processes.

CONCLUSIONS

The rockmass of the Newcastle and Tomago Coal Measures, distorted by the 1989 Newcastle Earthquake, appears to have been significantly affected by this seismic event. It is suggested that a complex and short distortion episode is now being followed by a slow release of stored strain energy. That energy has not been accumulated by the seismic event alone. The lithological complexity and structural setting of the Newcastle Coal Measures are possible causes for the observed phenomena. Other interpretations have been offered for discussion, possibly not always based on facts and data, and thus speculative. Definitive explanations of the observed facts are not possible at this stage of the investigations, however appropriate paths for research are being identified.

ACKNOWLEDGMENTS

The authors are indebted to engineers of the Hunter Water Corporation Limited, especially Mr Gregory Clinton for many useful discussions and exchange of data. Financial support provided by the Hunter Water Corporation Limited for this research project is gratefully acknowledged.

REFERENCES

CANTLE H. and K.H.R. MOELLE, 1993: Performance of the Newcastle water supply system since the 1989 Earthquake. *Proceedings 1993 National Earthquake Conference*, Memphis, Tennessee.

RYNN, J.M.W., E. BRENNAN, P.R. HUGHES, I.S. PEDERSEN and H.J. STUART, 1992: The 1989 Newcastle, Australia, Earthquake: The Facts and the Misconceptions. *Bulletin of the NZ National Soc. for Earthquake Engineering*, Vol. 25, No. 2, 77–146.

EARTHQUAKES & GEOLOGY – ARE THEY RELATED? THE DILEMMA OF CAUSAL RELATIONSHIPS

J. RYNN
The Centre for Earthquake Research in Australia, Indooroopilly

INTRODUCTION

Earthquakes are the most violent and intriguing geological process in shaping our Earth. They are the most devastating natural disaster known to human civilization in terms of life and economic loss. As the population increases, with consequent expansion in building stock and infrastructure, the scope of earthquake disasters, and hence vulnerability of urbanised areas anywhere on Earth, also increases (Berz, 1991). Relationships between earthquakes and geology in continental regimes, considering the Sydney-Newcastle region, are an enigma - some proclaim they exist, others shun them, while most have not considered them relevant from the practitioner's standpoint. Such understanding, however, is vital for earthquake mitigation to identify potential earthquake sources and prepare response to potential damage in urbanised areas.

Earthquake mitigation programs of many nations worldwide, including Australia, received an impetus through the United Nations International Decade of Natural Disaster Reduction (IDNDR) 1990-2000 (Littleton, 1990). The accepted approach is through earthquake zonation mapping - maps of potential ground shaking and damage derived by multidisciplinary analyses with outcomes of practical (not academic) use to the community (Shah, 1991).

The 1989 Newcastle earthquake is the most significant geological event since European settlement of Australia - indeed, the most devastating in terms of socio-economic losses of any known natural disaster. It has shown, not only to Australia but also to the international community, the importance of geology in earthquake mitigation in terms of causative structures and control on damage by alluvial sediments (Moelle, 1991; Rynn et al, 1992).

This paper briefly outlines the challenges facing seismology and geology for integration into the multidisciplinary approach to earthquake zonation mapping, and hence disaster preparedness for the community. Some factual observations and probable speculations that proport to be potential causal relationships between earthquakes and geology are highlighted.

J.M.W. RYNN

ROLE OF GEOLOGY WITH SEISMOLOGY AND ENGINEERING

Seismological information with a sound geological base must be provided in a practical manner to engineering for implementation into earthquake load codes and design procedures, bearing on geotechnical practice (site specific surveys for building foundations) and structural design. Unfortunately, questions are always asked after a disastrous event. The case of the 1989 Newcastle earthquake was no different. Practitioners in engineering, local government and emergency services asked the questions: Where was it located? What was the cause? How can the damage pattern be explained? Will it happen again? Where will it happen again? The earth sciences, together, must take these challenges and research the problems to provide suitable and satisfactory explanations.

The Question of Scale

The scale for geology can be considered in three points:

GLOBAL : The plate tectonics model - Australia relates to continental tectonics

REGIONAL : Considering eastern Australia with the terrestrial accreted marine (Tasmanides) with major faults, lineaments, fold belts, basins, etc. (e.g. Grimstone et al, 1990) and the marine environment (for sea-floor spreading) of fracture zones and ancient ridges (e.g. Veevers, 1991)

LOCAL : Considering the Sydney Basin as the "local" geological zone (Herbert and Helby, 1980) wherein specific areas such as the Newcastle-Lower Hunter region can then be considered (e.g. Collins, 1991): Near-shore marine geology must also be included (e.g. Jenkins, 1992)

POTENTIAL EARTHQUAKE SOURCES - THE SPECULATIONS?

Two types of sources are usually identified:

known faults - these are active, with contemporary activity and usually some surface expression; such as the San Andreas Fault or other plate margin situations;

areal sources - identified by areas of uniform activity, usually scattered, to which no mapped faults can be definitely attributed, such as continental situations.

The latter are termed "buried" or "blind" sources by Coppersmith (1991) and can denote possible thrust faults which do not reach the surface or be associated with folding.

For NE Australia, Rynn (1988) considered such "areal" sources in terms of current activity being confined between known geological structures as source zones for probabilistic hazard mapping. The source of the 1989 Newcastle earthquake is clearly of a "blind" type, as no definitive feature can be assigned as a causative structure for this event.

Sutherland (1992) claims a "predictive model" relating seismicity to volcanic "hot spots" for the Sydney basin. This appears to have both a problem of scale - broad, ill-defined regional geology compared

to small, local earthquake occurrences - and of time - volcanic ages up to 10 million years to explain recent, <200 years, activity. Neither earthquake distributions nor epicentral errors were depicted. In addition, no account was taken of the off-shore activity. Figure 1 shows the comparison between the "scattered" activity and the "linear" volcanic migration trends.

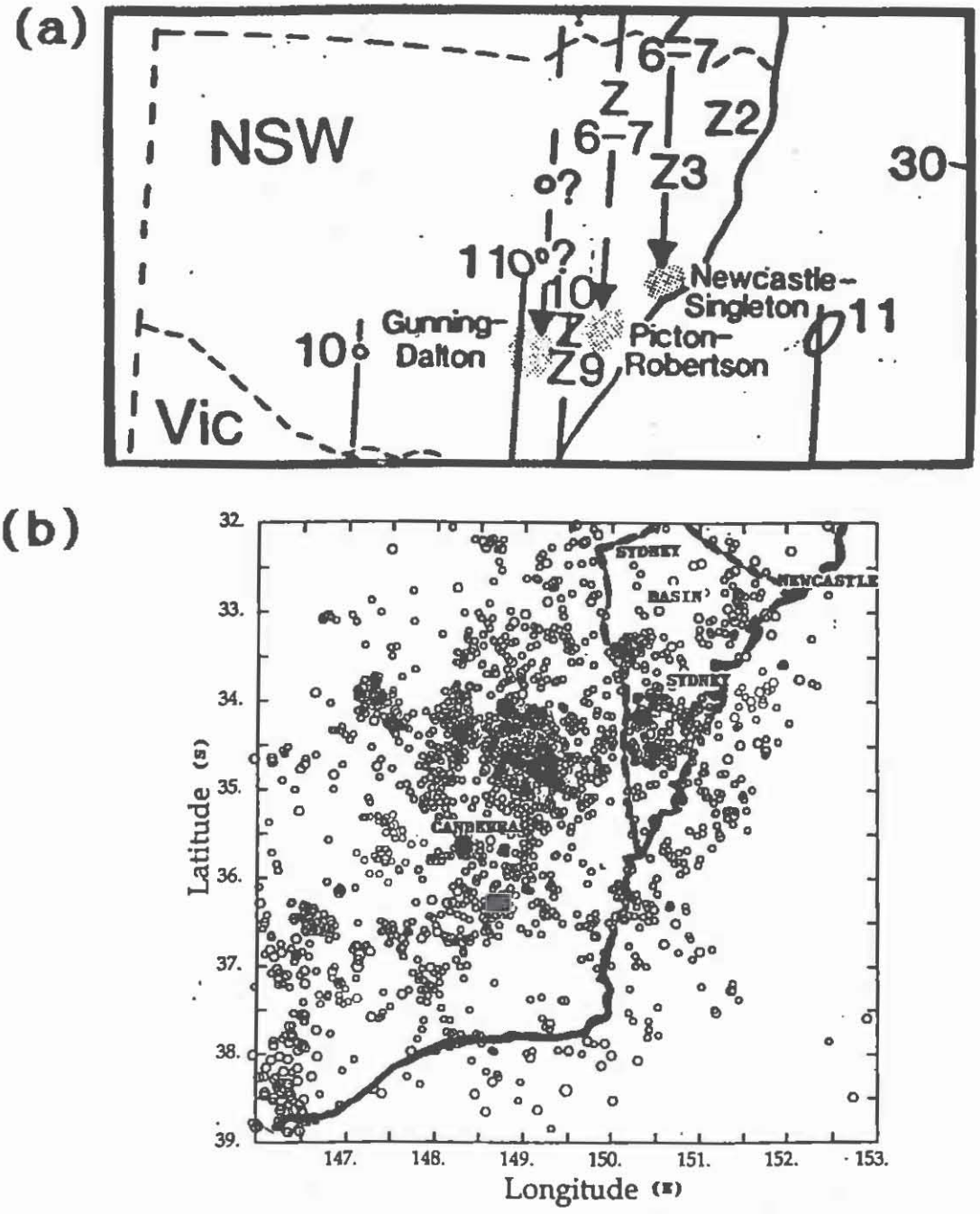

Fig. 1: Predictive model (?) of Sutherland's (1992) linear volcanic trends (a) compared with earthquake occurrences (1958-1991) in SE NSW (b) (RSES, ANU data: J. Weekes, pers.comm., 1991)

A more realistic attempt to identify potential sources for the Sydney Basin is shown in Figure 2, as used in current earthquake zonation mapping of the Sydney region (Rynn, 1992). Potential sources are based on significant earthquakes in relation to major structures in the near-vicinity of the epicentres - for example : Kurrajong Fault in the Lapstone Structure - 1919 Kurrajong earthquake (?); Lachlan Lineament - 1872 Bathurst earthquake (?); Nepean Fault - 1973 Picton earthquake.

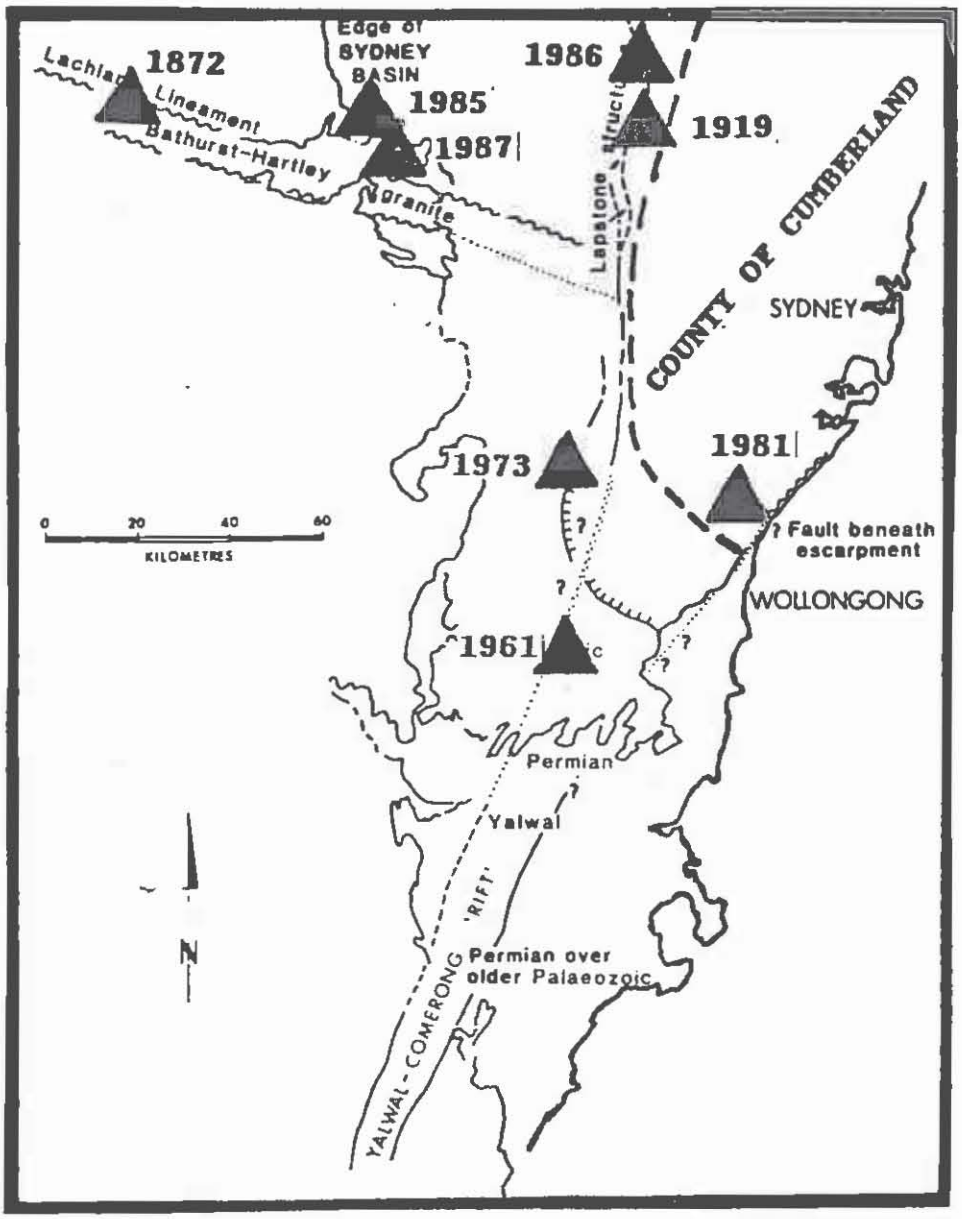

Fig. 2: Major geological structures and significant earthquakes considered as potential earthquake sources in the Sydney region (Based on Branagan and Pedrami, 1990; From Rynn, 1992)

EARTHQUAKES AND GEOLOGY - ARE THEY RELATED?

GEOLOGICAL CONTROLS TO DAMAGE

With international acceptance that potential damage to the built environment from earthquakes is increasing, preparedness in earthquake mitigation requires knowledge of the causative (geological) process therein. Earthquake damage patterns are traditionally considered in terms of the macroseismic data (observations of damage and/or felt reports) presented as isoseismal maps. These represent contours of subjectively assigned intensity values (MM) based on the Modified Mercalli Scale of Intensity (for Australia, per Elby, 1966) and pertain to "average" rock conditions.

The significance in geological controls is in understanding the surface ground motions and/or failures which caused the damage. Considering the 1989 Newcastle earthquake as an example (Rynn et al, 1992), the damage pattern in the Newcastle-Lower Hunter region clearly shows an extreme dependence upon the geology - specifically the major damage coincides with the areas of Holocene sediments (alluvials). Detailed causative geological conditions (of the alluvials) are, however, much more complex than usually considered, as shown in Figure 3 for the Hamilton (Newcastle) area.

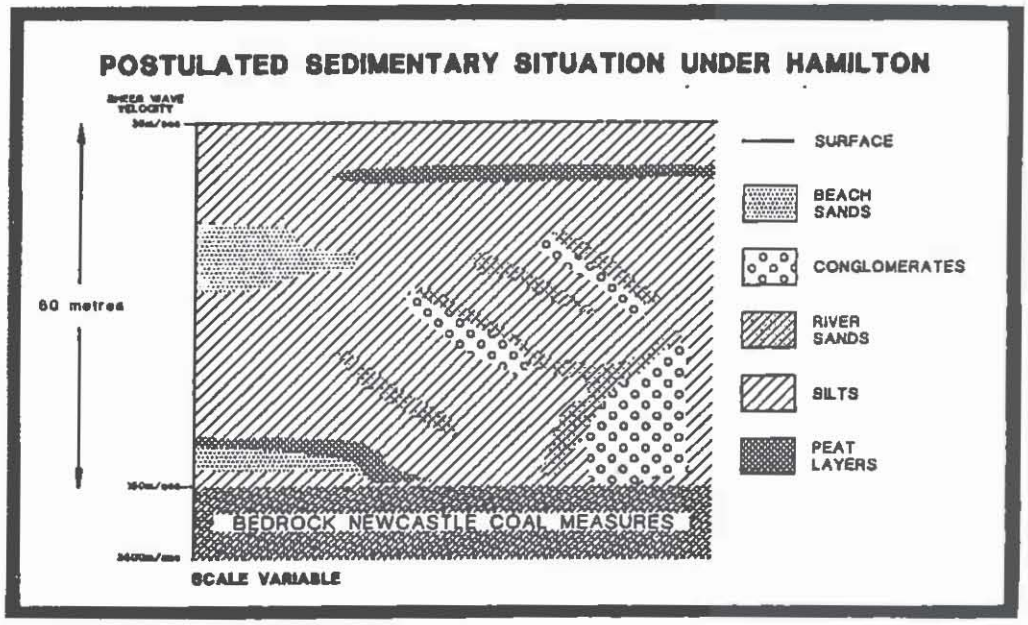

Fig. 3: Illustration of complexity of recent alluvial cover (Holocene sediments) in the City of Newcastle

Other important aspects include:
(a) Attenuation of seismic energy with distance
In Australia, this is based on MM intensities (macroseismic observations) and usually taken for "average" rock conditions.
Studies are in progress to quantify attenuation for alluvial areas as distinct from the hard-rock areas.
(b) Amplification
It is now recognized that amplification of seismic energy at the surface, particularly in sedimentary areas, may reach values of 10 or

greater. This is related to difference in shear wave velocities of the surface/sub-surface/basement rock units (Jacob, 1990). The enigmatic problems highlighted by this parameter relate to differences between geological and geotechnical (engineering) definitions of surface sediments (including "soils") and methods of evaluation: for example for 1989 Newcastle, estimates of 2 - 8 and 4 - 14, respectively (Rynn et al, 1992; Coffey and Partners, 1990). The necessity for geophysical studies complimentary to geology is evident.

(c) Liquefaction

This is the other parameter of equal importance with amplification. Although only one observation of liquefaction is known for 1989 Newcastle, the occurrence of possible "hidden" liquefaction in the sub-surface alluvials is real. This is evident in the far-field (>50km).

(d) Lateral Spreading

With various sedimentary situations in the Newcastle City area, some observed damage may be a result of lateral spreading. A suggested example (Rynn et al, 1992) is for Carrington Chambers (Figure 4).

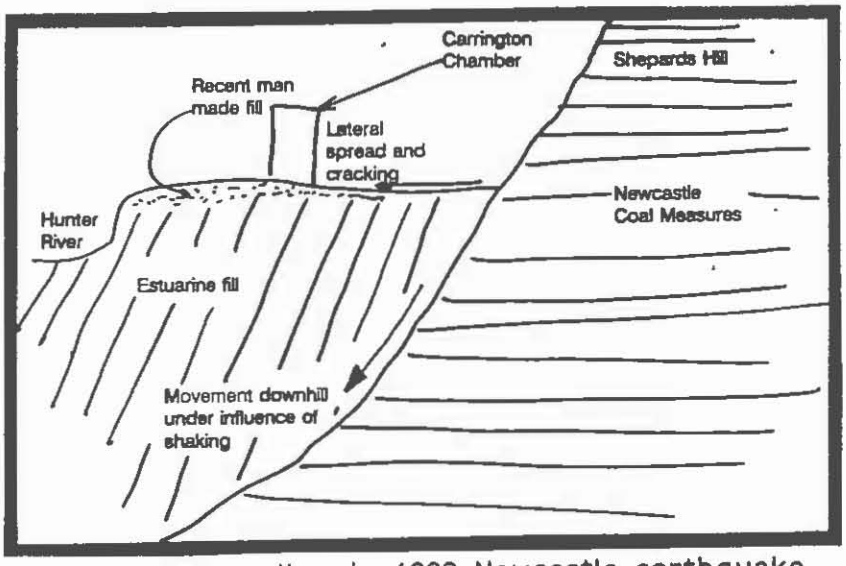

Fig. 4: Lateral spreading in 1989 Newcastle earthquake.

International observations

Brennan (1993) presents clear evidence of all such above factors in geological controls to damage in similar sedimentary situations from other worldwide continental earthquakes (1727 Newburyport, USA ML 5.0; Maitland, Australia ML 5.5; 1884 Colchester, UK ML 6.5; 1976 Tangshan, China ML 7.9; 1983 Leige, Belgium ML 4.9), and indeed for pate margin regions (San Francisco Marina District in 1989 Loma Prieta earthquake ML 7.1).

POST-EARTHQUAKE DAMAGE

Latent and recurrent defects in the aftermath of an earthquake are of most concern to the affected community. In the case of Newcastle, these have been continually identified from early 1990 through to the present, 3 years later. Geological factors, as well as built environment, historical and human factors, influence these effects.

EARTHQUAKES AND GEOLOGY - ARE THEY RELATED?

(a) Shrink/Swell conditions and reactive clays
Continuing damage to Newcastle's built environment well after the 1989 earthquake has caused great concern to the insurance industry. Brunsdon et al (1991) invoked the influence of reactive clays and then shrink/swell conditions as the reason. This has been questioned through the need to consider in more detail possible geological factors including changes to ground surface, liquefaction, climatic changes, groundwater changes and geological conditions of reactive clays in the Newcastle area (Rynn et al, 1992; K.H.R. Moelle, pers com. 1992).

(b) Long-term effects on buried lifelines
Recent research by Cantle and Moelle (1993) has identified serious effects on Newcastle's buried water and sewage pipe systems. This has been related in part to the responses of clay soils and other alluvial sediments to climatic conditions and to the directivity of earthquake waves across the City. (Details discussed by Moelle et al, This Symposium). Consequences for local authorities in all urbanised areas to potential infrastructure damage, both at the time of any earthquake and in the long-term are of great importance.

SUMMARY

The 1989 Newcastle earthquake has stimulated a great international interest in the role of geology for the fundamental disciplines of seismology, geology and engineering in regard to potential earthquake damage in urbanised areas. A close co-operation with geology must be afforded through these researchers to provide the practitioners in local government, land-use planning, engineering design and emergency services to reduce potential losses in future devastating earthquakes.

ACKNOWLEDGMENTS

This paper is part of the continuing multidisciplinary research by the CERA team. Many colleagues have contributed with special mention of K.H.R. Moelle (ICR, University of Newcastle) for his geological guidance, E. Brennan for his slides of geological controls on damage and engineers I.S. Pedersen and P.R. Hughes for their continuing questioning and encouragement on behalf of all practitioners. Funding in part was kindly provided by Emergency Management Australia (formerly NDO) and the Newcastle City Council for the IDNDR earthquake zonation mapping program for Australia.

REFERENCES

Berz, G., 1991. Natural disasters and insurance and reinsurance. Earthquakes and Volcanoes, 22, 3, 99-102.

Branagan, D.F. and Pedrami, H., 1990: The Lapstone Structural Complex, NSW. Aust. J. Ear. Sci., 37, 23-36.

Brennan, E., 1993: Geological controls in continental earthquake effects. 1993 US Nat. Earthquake Conf., Proc. (in press).

Brunsdon, D.R., Forbes, J.G. and Douglas, D.J., 1991. Factors influencing the structural behaviour of residential buildings in

Newcastle following the 1989 earthquake. Report to Insurance Council of Australia, Irwin Johnston and Part. and D.J. Douglas and Parts, 56pp.

Cantle, H.E. and Moelle, K.H.R., 1993. Performance of the Newcastle water supply system since the 1989 earthquake. 1993 US Nat. Earthquake Conf., Proc. (in press).

Coffey and Part. Int., 1990. Newcastle earthquake study - Geotechnical aspects. In R.E. Melchers (Ed) "Newcastle Earthquake Study", The Institution of Engineers, Australia., 109-147.

Collins, W.J., 1991. A reassessment of the "Hunter-Bowen Orogeny": Tectonic implications for the southern New England Fold Belt. Aust. J. Em. Sci., 38, 409-423.

Coppersmith, K.J., 1991. Seismic source characterisation for engineering seismic hazard analyses. 4th Int. Conf. Seismic Zonation, Stanford, Proc.,1, 3-60.

Eiby, G.A., 1966. The Modified Mercalli Scale of Earthquake Intensity and its use in New Zealand. NZ. Jour. Geol. Geophys.,9, 1/2, 122-124.

Gaull, B.A., Michael- Leiba, M.O. and Rynn, J.M.W., 1990. Probabilistic earthquake risk maps of Australia. Aust. J. Ear. Sci., 37, 119-187.

Grimstone, L.R., Mallett, C.W. and Hammond, R.L., 1987. Ancestral Pacific Margins in eastern Australia. Proc. Pacific Rim Congress 87, The Aust. Inst. Min. Metall., 709-722

Herbert, C. and Helby, R., 1980. A guide to the Sydney Basin. Dept. Miner. Scs. Geol. Surv. NSW Bull., 26, 603pp

Jacob, K., 1990. Seismic hazards and the effects of soils on ground motions for the Greater New York City Metropolitan Region. New York Metro. Section ASCE Seminar Proc.

Jenkins, C.J., 1992. GLORIA imagery and geological structure of the NSW continental margin (offshore Sydney Basin). Adv. Stud. Syd. Bas., 26th Newcastle Symp., Proc., 9-14.

Littleton, C.J., 1991. The International Decade for Natural Disaster Reduction - An Australian point of view. Multidisp. Sci.,18, 1, 10-12.

Moelle, K.H.R., 1991. A geological picture of the Newcastle earthquake area - This is not a Newcastle fault, or is it? In J.M.W. Rynn (Ed) "What We Have Learnt From The Newcastle Earthquake" Conf. 24-25 October, 1991, Proc.

Rynn, J.M.W., 1988: The assessment of seismic risk in NE Australia. Inst. Eng., Aust., CE Times., CE30, 2, 45-46.

Rynn, J.M.W., 1992. Earthquake zonation for City of Sydney and Environs. Final Report on Project 3/91 "Earthquake Zonation of Urbanised Areas of Australia" to Australian IDNDR Co-Ordination Committee, Natural Disasters Organisation, Canberra, 59pp.

Rynn, J.M.W., Brennan, E., Hughes, P.R., Pedersen, I.S. and Stuart, H.J., 1992. The 1989 Newcastle, Australia, earthquake - The facts and the misconceptions. Bull. NZ Nat. Soc. Eq. Eng., 25, 2, 77-144.

Shah, H. (Ed), 1991. Proceedings of 4th International Conference on Seismic Zonation, Stanford University, August 1991, Volumes 1-3.

Sutherland, F.L., 1 992. Late Thermal events - NE New South Wales - SE Queensland - Links to Sydney Basin seismicity? Adv. Stud. Syd. Bas., 26th Newcastle Symp., Proc., 1-8.

Veevers, J.J., Powell, C.McA. and Roots, S.R., 1991. Review of seafloor spreading around Australia - 1. Synthesis of patterns of spreading. Aust. J. Ear. Sci., 38, 373-389.

GEOLOGY OF THE OFFSHORE SYDNEY BASIN : NEW RESULTS FROM DIRECT SAMPLING AND GEOPHYSICS

C.J. JENKINS, J.B. KEENE, R. HELBY & RIG SEISMIC CRUISE 112B SHIPBOARD PARTY
Ocean Sciences Institute, University of Sydney

The joint Sydney University/Australian Geological Survey cruise 112B of the 'Rig Seismic' in September 1992 conducted an extensive program of coring and dredging on the NSW continental shelf and slope east of Newcastle-Sydney-Wollongong. In this report we present new data about rock units on the continental slope.

Previous geophysical work (Jenkins & others, subm.) has shown that the slope is remarkably bare of post-rift sediment: for example, 30% of the lower slope is bare of sediment and earlier dredging by Sydney University obtained serpentinites, granites, greywackes, monzonites from the slope as well as sediments. The lower-middle slope consists of 2-3 basement ridges, some of which may define half-grabens. The upper slope is composed of thicker post-rift sediment accumulations - the shelf-edge sediment wedge - which overlies a buried, gently inclined palaeoshelf.

Cruise 112B obtained samples from the lower and middle slope. Lower slope samples south of Sydney canyon were of Palaeozoic (?Carboniferous) deep-water volcaniclastics/greywackes with pervasive cleavage. North of the canyon however, all samples from the Lower slope were of Upper Cretaceous volcaniclastic sandstones. Dating is by means of palynology. Some of those samples had strong tectonic fabric which could be due to normal (rift) faulting or to strike-slipe motions at breakup (for which there is also some geophysical evidence). Further sampling of Cretaceous rocktypes from higher on the slope showed quartzose sandstone types as well, and we now picture a complex sediment supply into the rifting basin.

Sydney Basin basement was obtained from outcrops at ~1200m water depth east of Manly. A Scythian (Hawkesbury-Wianamatta) palynological assemblage is present. Offshore of Newcastle, volcanic lithologies were encountered, rhyolitic

volcanics and a basalt in separate dredgings. Seismic and bathymetric data show that an igneous complex of probable Cretaceous age underlies an area of submerged pinnacles (dykes ?) at 1200m E of Wyong.

Post-rift sedimentation is represented by Palaeocene-Eocene greensands of remarkably wide distribution. Miocene-Recent sediments are of mixed terrigenous-pelagic carbonate composition. Pliocene sediments with almost no terrigenous content are also collected.

Analysis of the samples in terms of dating, lithostratigraphic correlations, tectonic structures, petrophysics, thermal history and tectonic location (geophysical framework) is continuing.

A NEW TECTONIC & DEPOSITIONAL MODEL FOR THE OFFSHORE SYDNEY BASIN (NSW/P10)

G. BRADLEY
Naremburn

This paper presents an alternative tectonic and sedimentary model to the most recently published model for the offshore Sydney Basin (Grybowski, 1992). The new model is consistent with the well documented foreland origin of the basin, and with the known distribution of the three distinctive clastic suites. Although the clastic fill was dominated by the interplay between arc-derived acid-intermediate volcanic sands and craton-derived quartz-rich sands (Conaghan et al., 1982), basic volcaniclastic sands of distinctive appearance, and the erosion products of deeply weathered basic volcanics make intermittent, locally significant contributions to the clastic fill. These distinctive clastics, were derived from the Offshore Uplift (Figure 3).

The offshore Sydney Basin is dominated by three structural elements (Figures 1 and 2):

1) The "Offshore Syncline", in the immediate offshore;
2) The "Offshore Uplift" - an easterly dipping tilted fault block; and
3) The Newcastle Syncline - a later structure which cross-folds the first two in the north of the permit. The Offshore Syncline and Offshore Uplift are separated by a complex fault zone interpreted to be a strike-slip fault overprinted by thrusting, then by extensional faulting prior to the onset of Tasman Sea spreading.

The top of the Offshore Uplift is defined by high amplitude reflectors inferred by Grybowski (1992) to be basement to the Sydney Basin. However, compelling evidence suggests this is not so, and that the uplift is a long-lived, emergent, volcanically active feature, which became quiescent near the Permo-Triassic boundary and was finally buried by middle Triassic sediments.

The key evidence supporting this interpretation comes from easterly sourced ash-flows in the Late Permian; distinctive easterly sourced Permo-Triassic clastics (dark green volcanic sandstones, and red-brown claystones); the onlapping

geometry of strata overlying the high amplitude reflectors of the Offshore Uplift, and the fault-propagation fold geometry visible along its western boundary:

1) Sporadic ash-flows and pervasive ash-falls are characteristic of the Late Permian Coal Measures. One well documented ash-flow eruption was directed towards the SW/WSW, and clear-felled trees in the Lower Pilot Coal swamp (Diessel, 1985). Welding did not occur in the ash-flow, indicating that it propagated from a point beyond the maximum range of welding (30-50 km: Macdonald, 1972; and Walker, 1984), but within the blast radius. Documented blast radii are generally less than 25-30 km (eg. the 20 x 30 km zone of total devastation at Mount St. Helens - Lipman and Mullineaux, 1981; and Macdonald, 1972). The evidence points to a very large eruption responsible for the Lower Pilot Coal event, at a minimum range of around 30 km. If the blast propagated from beyond the maximum documented range of welding, it must have been exceptionally large to account for its blast effects, and a range of 30-40 km is seen as most likely. The crest of the Offshore Uplift is about 25 km of the coast, and it is considered that the eruption originated from the uplift just east of its crest. The minimum distance to the magmatic arc volcanoes further east exceeds 200 km (Figure 6), and hence cannot be the source of the ash flows.

2) Distinctive dark green to dark greenish-grey sands derived from an easterly source were deposited during the Late Permian (Ward et al., 1986, pp 45-48) and during the Early Triassic (Ward, 1972). The distinctive Early Triassic "red-beds" were also derived from an easterly source, and include interbeds of red-brown, olive-brown to olive-grey sandstones with highly labile volcanic-lithic clasts which would not have survived transport over long distances. Work by Ward (1972) indicated that these volcanic sediments were derived from a basic volcanic source petrographically very similar to the mid-Permian Gerringong Volcanics. It is inferred that the Offshore Uplift was the source of these sediments, and that the red beds and associated sands were eroded from the Uplift after episodes of lateritic weathering. The last detritus derived from the Offshore Uplift was deposited as the Garie Formation - an eroded and re-deposited bauxitic paleosol.

3) Seismic data clearly images the Offshore Uplift as a large easterly dipping tilted fault block. The overlying strata are more shallowly dipping and exhibit a very marked onlapping relationship to the tilted fault block. It is inferred from this and the above evidence that the Offshore Uplift was an emergent actively eroding high until the end of the Early Triassic, and was an active volcanic arch until near the Permo-Triassic boundary. The Uplift

was progressively onlapped from east to west during the Late Permian and Early Triassic (by coal measures and Narrabeen Group), and finally buried beneath strata of Middle Triassic age (Newport Formation, Hawkesbury Sandstone, Wianamatta Group, and possibly younger strata : Figures 7 and 8).

The key implications of the new model are:

1) The Offshore Uplift evolved contemporaneously with Sydney Basin sedimentation (and is not a later breakup structure, as proposed by Grybowski, 1992);
2) The crest of the Offshore Uplift is composed of Wianamatta Group - Figure 8 (not Early Permian Conjola Subgroup, as proposed by Grybowski, 1992);
3) The high amplitude reflectors marking the top of the uplift are mid-Permian and younger volcanics (Figure 8) (not Late Carboniferous - Grybowski, 1992);
4) The fault bounding the west of the Offshore Uplift is a major structure separating Permo-Triassic ages (to the west) from Middle Triassic and Jurassic/Cretaceous ages.

The proposed model is supported by Early/Middle Triassic-aged rocks (latest Scythian to Anisian) recently dredged from about 4500 m subsea on the continental slope some 90 km offshore from Sydney (Jenkins et al., in prep). Grybowski's (1992) model would have predicted Early Permian or older ages.

Evolution of the Offshore Sydney Basin

The Sydney Basin was initiated by rifting in the Late Carboniferous. Rift volcanism was greatest along the present-day Meandarra Gravity High (Murray et al., 1989), but extended eastwards as far as the Offshore Uplift (Figure 4). During the earliest Permian, compressional tectonism (related to the Peel-Manning Thrust/Subduction Complex) began to propagate southwards, and westwards beneath the Sydney Basin (as floor thrusts and blind thrust splays: Figure 4). By Early Permian, the Sydney Basin had become a well developed foreland basin with active thrusting on the Peel-Manning Thrust (Figure 5). During the early Permian, major sinistral strike-slip motion occurred along a major crustal weakness which now corresponds to the western edge of the Offshore Uplift. By this stage the Offshore Uplift had evolved into a fault-propagation fold with quiescent to sporadic volcanism. A major compressional event occured in the mid Permian, and was probably caused by docking of a micro-continent north of Port Stephens. This event caused the Hunter-Mooki to emerge as the dominant thrust front, then caused the major westwards (sinistral) swing in the thrust along the Hunter Lineament. The Newcastle Syncline emerged as the new foredeep, cutting across and refolding the older north-south

foreland folds. The mid Permian event caused major arching of the Offshore Uplift, reactivated stalled magmatic diapirs and caused renewed volcanism, which continued through into the Late Permian (Figure 6).

Foreland tectonism continued throughout the Late Permian and Early Triassic. The Offshore Uplift continued to grow as a major fault propagation fold, while being progressively onlapped by coal measures and Narrabeen Group strata (Figure 7). Foreswell monoclines propagated towards the west and south during this time, and by mid Triassic resulted in major uplift in the south of the basin, which caused the reversal of paleocurrents from dominantly southeast-directed to northeast-directed (Hawkesbury Sandstone), and the Offshore Uplift was inundated by sediment. Final thrust movements, and growth on the foreswell monoclinal flexures occurred in the earliest Late Triassic.

Early Jurassic ages (C. classoides - J1) are recorded from diatremes in the Sydney Basin, and indicate that sedimentation had recommenced in the Sydney Basin by the Early Jurassic. Apatite fission track, and vitrinite studies are consistent with burial of the Sydney Basin 3-3.5 km deeper than present-day on the coast near Sydney, and about 2-2.5 km deeper on the coast near Newcastle (Grybowski, 1992). This burial would have occurred through the Jurassic to the early Cretaceous, before uplift and arching commenced prior to mid Cretaceous breakup on the east coast. Down-to-basin growth faulting would be expected in the Sydney Basin during the rift event, and would be superimposed on the thrust faulting (Figure 7 and 8). Major uplift of the basin occurred prior to breakup, and massive erosion of up to 3.5 km occurred at the edge of the continental shelf, decreasing to about 1-1.5 km about 100 km inland. The Sydney Basin was subjected to late-stage episodes of compression, which caused brittle deformation, fracturing and high angle reverse faults.

Acknowledgements

This paper summarises the key geological findings of a study completed by me for Ampolex Limited. I would like to thank Ampolex Limited and Santos Limited, for approval to publish. The work relied heavily on inferences drawn from the 1991 vintage seismic data shot by the current Joint Venture, and builds on the earlier technical work by Grybowski (1992) for Santos Limited.

References

Conaghan, P.J., and J.G. Jones, K.L. McDonnel and K. Royce, 1982 : A dynamic fluvial model for the the Sydney Basin. Geol. Soc.of Aust. - Jour.29, pp 55-70.

Diessel, C.F.K., 1985: Tuffs and tonsteins in Coal Measures of New South Wales, Australia. In proceedings of the 10th International Congress of

OFFSHORE SYDNEY BASIN - NEW TECTONIC MODEL

Carboniferous Stratigraphy and Geology, Madrid, 1983, Volume 4, pp 197-210.

Jenkins, C.J., J.B. Keene, R. Helby and shipboard scientific staff (in prep) : Rig Seismic Cruise 112-B September-October, 1992. Offshore Sydney Basin Continental Slope Dredge Samples.

Lipman, P.W. and D.R. Mullineaux, (Editors), 1981 : The 1980 Eruptions of Mount St. Helens, Washington. U.S. Geology Survey, Professional Paper 1250.

MacDonald, G.A., 1972 : Volcanoes. Prentice-Hall Inc N.J.

Murray, C.G, E. Scheibner and R.N. Walker, 1989 : Regional Geological Interpretation of a Digital Coloured Residual Bouguer Gravity Image of Eastern Australia, with a Wavelength Cut-off of 250 km. Aust. Jour. of Earth Sci. - Jour.36, pp 423-449.

Walker, R.G. 1984 : Facies Models, Second Edition. Geoscience Canada Reprint Series 1, McMaster University Ontario.

Ward, C.R. 1972 : Sedimentation in the Narrabeen Group, Southern Sydney Basin, New South Wales. Geol. Soc.of Aust. - Jour.19 (3), pp 393-409.

Ward, C.R., G.M. Bradley, C.G. Skilbeck and Robyn Stutchbury, 1986 : A Guide to Cored Rocks in the Sydney Basin. Earth Resources Foundation, The University of Sydney.

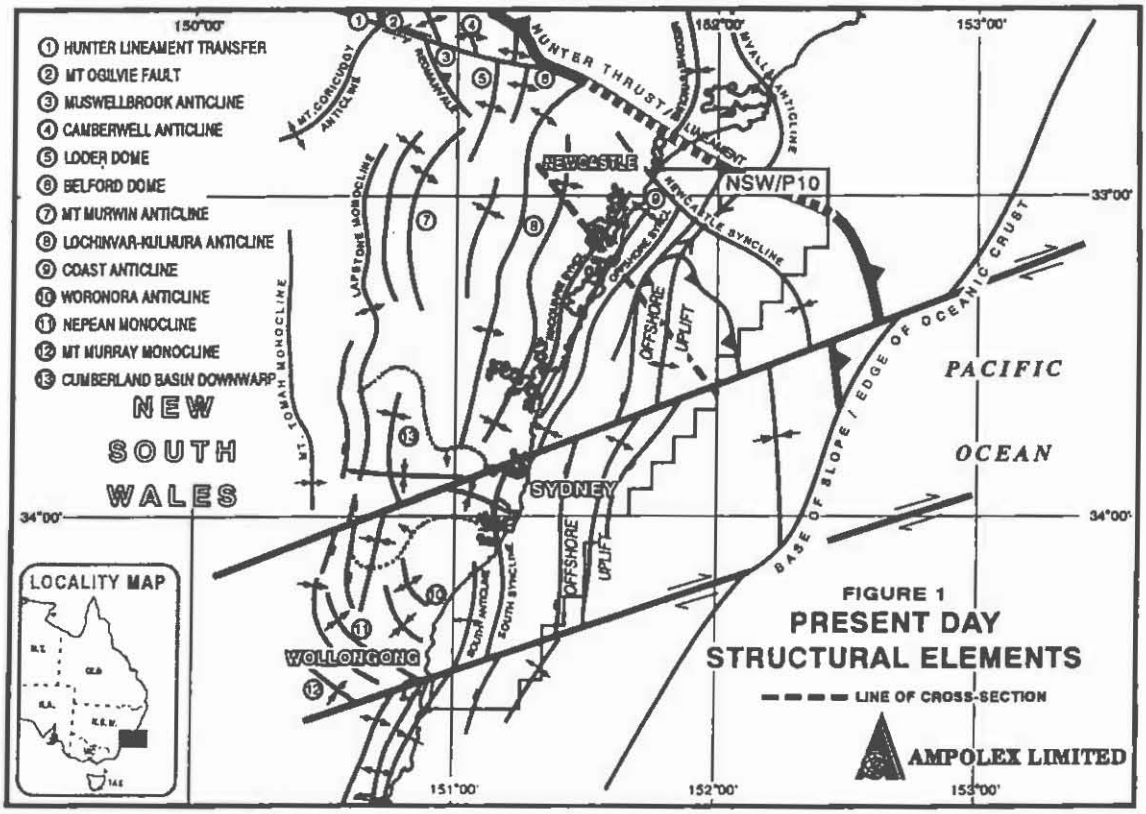

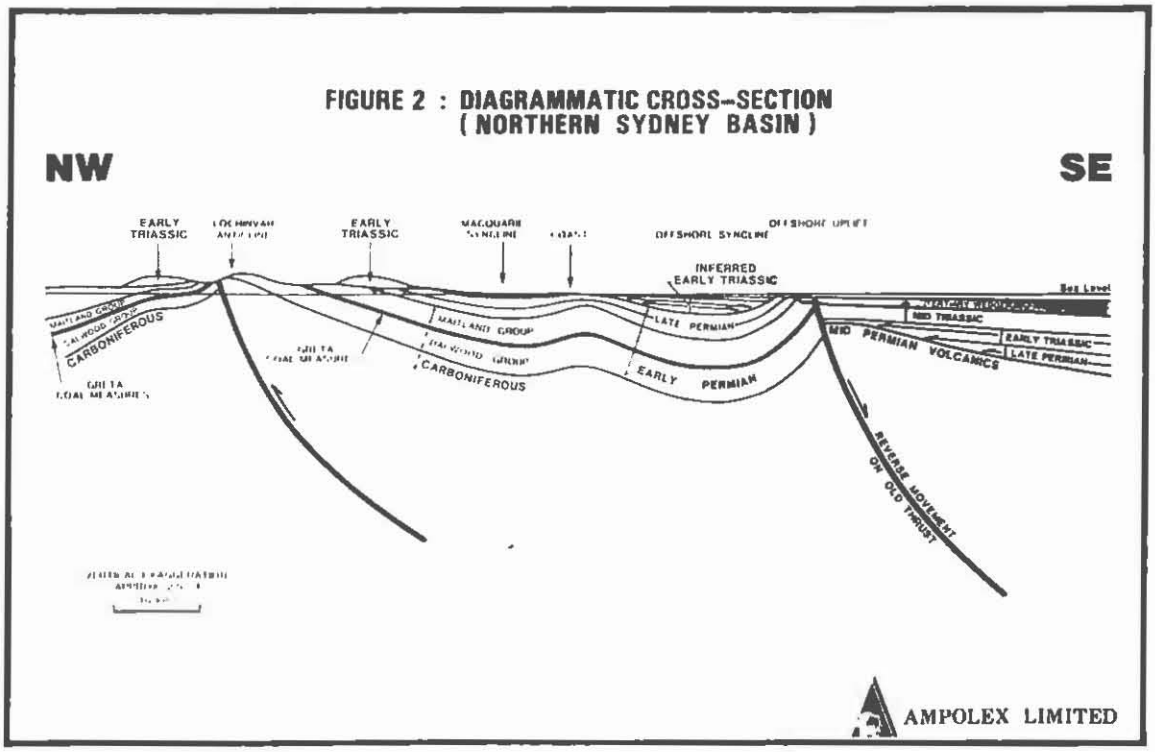
FIGURE 2 : DIAGRAMMATIC CROSS-SECTION
(NORTHERN SYDNEY BASIN)
NW
SE
EARLY TRIASSIC
EARLY TRIASSIC
OFFSHORE SYNCLINE
OFFSHORE UPLIFT
INFERRED EARLY TRIASSIC
CARBONIFEROUS
MAITLAND GROUP
CARBONIFEROUS
LATE PERMIAN
EARLY PERMIAN
MID PERMIAN VOLCANICS
MID TRIASSIC
EARLY TRIASSIC
LATE PERMIAN
REVERSE MOVEMENT ON OLD THRUST
AMPOLEX LIMITED

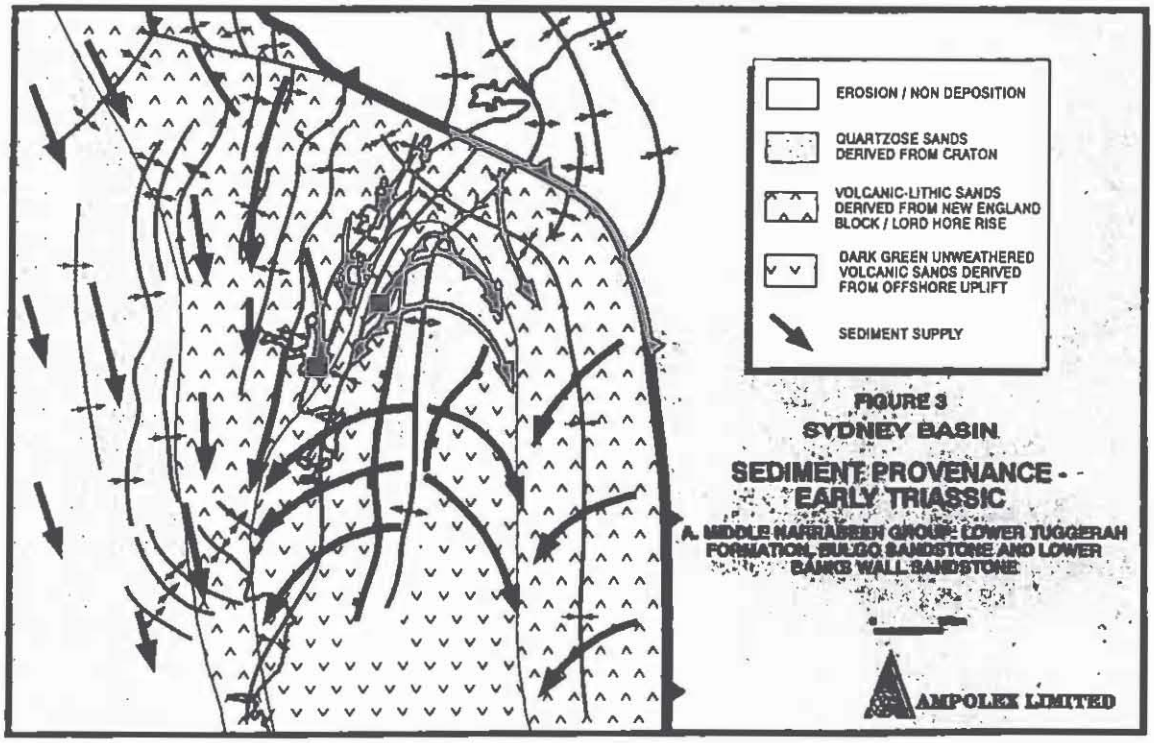
EROSION / NON DEPOSITION
QUARTZOSE SANDS DERIVED FROM CRATON
VOLCANIC-LITHIC SANDS DERIVED FROM NEW ENGLAND BLOCK / LORD HORE RISE
DARK GREEN UNWEATHERED VOLCANIC SANDS DERIVED FROM OFFSHORE UPLIFT
SEDIMENT SUPPLY
FIGURE 3
SYDNEY BASIN
SEDIMENT PROVENANCE - - EARLY TRIASSIC
A. MIDDLE NARRABEEN GROUP: LOWER TUGGERAH FORMATION, BULGO SANDSTONE AND LOWER BANKS WALL SANDSTONE
AMPOLEX LIMITED

OFFSHORE SYDNEY BASIN - NEW TECTONIC MODEL

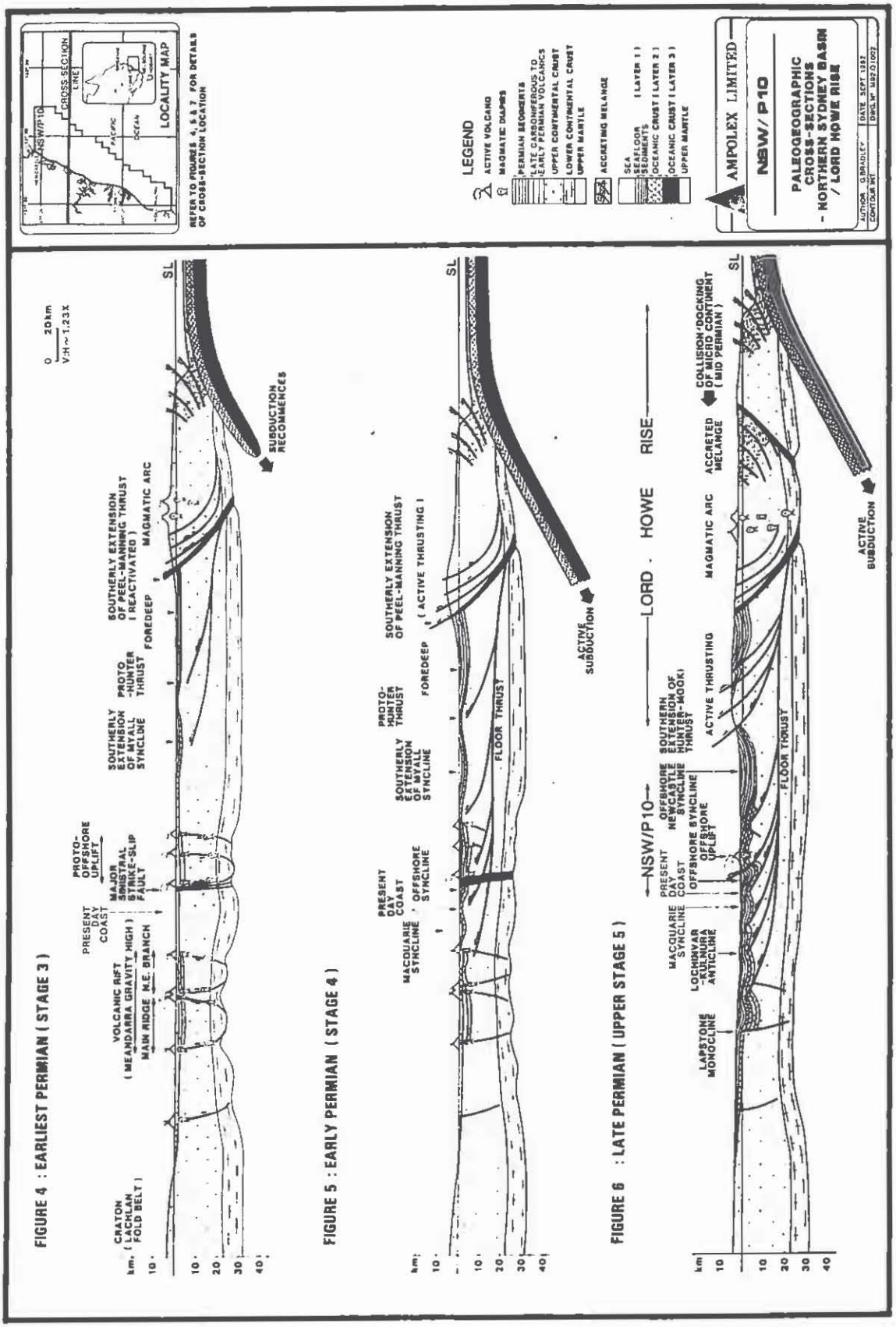

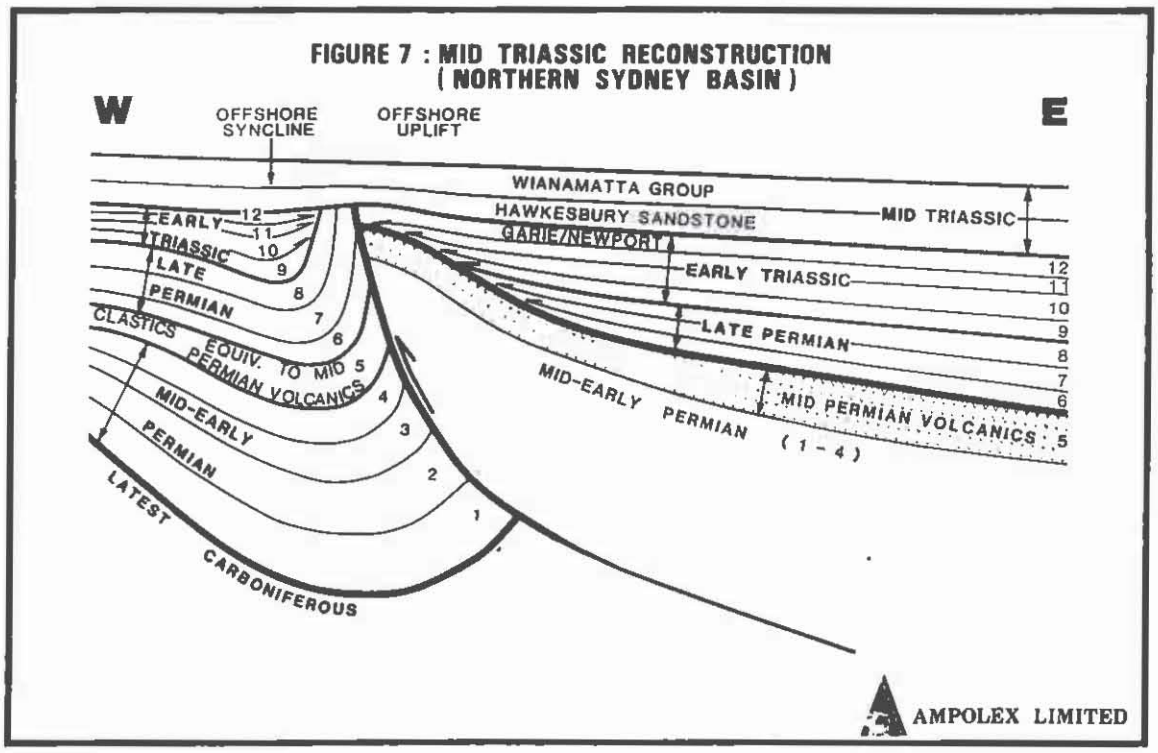
FIGURE 7 : MID TRIASSIC RECONSTRUCTION
(NORTHERN SYDNEY BASIN)
W
E
OFFSHORE SYNCLINE
OFFSHORE UPLIFT
WIANAMATTA GROUP
HAWKESBURY SANDSTONE
GARIE/NEWPORT
MID TRIASSIC
EARLY TRIASSIC
LATE PERMIAN
MID PERMIAN VOLCANICS
MID-EARLY PERMIAN (1 - 4)
EARLY TRIASSIC
LATE PERMIAN
CLASTICS EQUIV. TO MID PERMIAN VOLCANICS
MID-EARLY PERMIAN
LATEST CARBONIFEROUS
12
11
10
9
8
7
6
5
4
3
2
1
AMPOLEX LIMITED

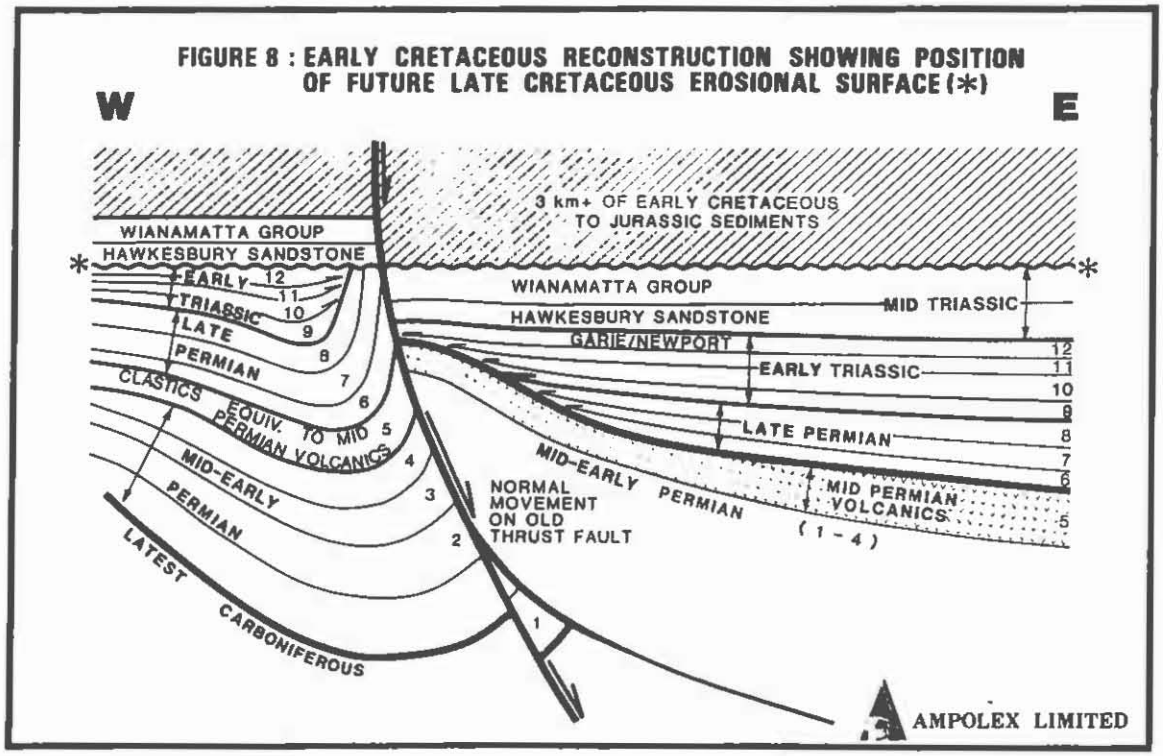
FIGURE 8 : EARLY CRETACEOUS RECONSTRUCTION SHOWING POSITION OF FUTURE LATE CRETACEOUS EROSIONAL SURFACE (*)
W
E
3 km+ OF EARLY CRETACEOUS TO JURASSIC SEDIMENTS
WIANAMATTA GROUP
HAWKESBURY SANDSTONE
*
*
EARLY TRIASSIC
LATE PERMIAN
MID PERMIAN VOLCANICS
MID-EARLY PERMIAN (1 - 4)
NORMAL MOVEMENT ON OLD THRUST FAULT
CLASTICS EQUIV. TO MID PERMIAN VOLCANICS
MID-EARLY PERMIAN
LATEST CARBONIFEROUS
12
11
10
9
8
7
6
5
4
3
2
1
AMPOLEX LIMITED

THE INFLUENCE OF CHEMICAL & GEOLOGICAL FACTORS ON COAL MACERAL PHENOMENA

A. DAVIS
Penn State University, USA

ABSTRACT

The molecules or structures which are responsible for the absorption and emission phenomena involved in the fluorescence behaviours of materials are referred to as fluorophores. The π-electrons present in organic compounds with conjugated double bonds have the mobility necessary for the display of fluorescence behaviour. It follows that aromatics and conjugated aliphatic polyenes can be fluorescent. Other organic structures which fluoresce are the aliphatic aldehydes, substituted aromatics and heteroaromatics. The walls of spores and pollen are composed of a material referred to as sporopollenin; this complex biopolymer is thought to have a carotenoid structure and so contains a central conjugated double-bond system made up of isoprene units. Isoprene units also constitute the terpenoid structures of resins. The fluorescence behaviour of cutin and suberin has been attributed to the presence of aromatic phenols, and that of algae to carotenoid and aromatic structures diluted by saturated aliphatics. The fluorescence of wood-derived materials of low maturity is derived from biopolymers, notably lignin which contains cross-linked phenolic units.

The trend of vitrinite fluorescence intensity with coal rank has two peaks (Fig. 1), reflecting changes in the nature of the fluorophores which take place with organic maturation. The highest vitrinite/huminite fluorescence intensities are found in the least mature materials, corresponding to peats and lignites. This mode of fluorescence has been referred to as primary fluorescence; within the range of primary fluorescence, intensity decreases to a minimum at about the subbituminous C/B boundary (Rrand = 0.45-0.50%). A plausible explanation in the case of organic matter derived from ligno-cellulosic tissues is that the primary fluorescence is due to the presence of lignin-derived structures, and that the decrease in fluorescence intensity through this rank range is due to the progressive quenching which accompanied polymerization. Also, the increasing conjugation of double bonds results in greater

delocalization of π-electrons, so that the emitted light has higher wavelengths. By subbituminous-B rank, the quenching and electron delocalization which have taken place permit very little visible fluorescence.After the near extinction of vitrinite primary fluorescence, fluorescence intensity increases with further increase in maturity to a second mode, one of less intense fluorescence, centred at high volatile A bituminous rank (ca. Rmax = 0.9%; Fig. 1). This so-called secondary fluorescence has been attributed to the presence of either "bitumen" or a "mobile phase" incorporated into the structure of the vitrinite. Although the mobile phase may possibly contain petroleum-like substances derived from liptinite and lipoid substances, it is suggested that it also contains molecular fragments which have been derived by oligomerization as the aromatic network of the vitrinite structure becomes increasingly polymerized.

From the vitrinite secondary fluorescence peak there is a decline in intensity with further increase in rank (Fig. 1), a trend which is mirrored by decrease in the yields of chloroform-soluble materials. Visible fluorescence is essentially lost at low volatile bituminous rank (Rrand = 1.8%). Presumably, this is because of the progressive elimination of the mobile phase by aromatic condensation. The residual aromatic network is too highly polymerized to fluoresce in the bituminous range. Not only will quenching be intense because of the size and concentration of the macromolecules, but also the π-electrons will be highly delocalized; together, these factors have produced the loss of fluorescence, even though the organic matter contains abundant structures which, in isolation, could be potential fluorophores.The quenching mechanism described above is also a major factor in determining the relative fluorescence behaviours of the maceral groups. The strong fluorescence displayed by some liptinite macerals, notably alginite, is contributed to by the dilution of aromatic or other fluorophores in an environment of non-fluorophoric saturated aliphatics. Inertinite, at the other extreme, generally is non-fluorescent because of the high degree of concentration quenching; the low levels of fluorescence displayed by some semi-inertinite could be due to the presence of residual mobile phase.

The alteration of vitrinite fluorescence intensity with time, obtained when an air objective is used, has been shown to result mainly from photochemical oxidation. The alteration responses obtained in various media have been compared; a latex sleeve was used to connect the microscope objective and specimen so that the gaseous environment could be controlled during dry fluorescence measurements. Figure 2 shows how both the negative (intensity decrease) and positive (intensity increase) components of dual alteration which occur in an air medium are prevented by the use of a nitrogen atmosphere. Support for the conclusion that the overall reaction is a photooxidation has come from FTIR studies and the staining of the irradiated coal surfaces with safranin 0, a cationic dye. Both techniques demonstrate an increase in the proportion of carboxylic functional groups on the surface. In addition to the dominant influence of rank over fluorescence behaviour, there appears also to be some influence exerted by the environment of deposition. Vitrinite fluorescence intensities have been measured on coals from marine- and freshwater-influenced

locations. Figure 3 shows a clear positive relationship between telocollinite fluorescence intensity and the total sulphur contents of various whole-seam channel samples of high volatile A bituminous coals from the northern Appalachian Basin. Moreover, a more detailed study of vertical subsections collected from marine- or brackish-influenced seams shows consistent increases in these same two properties from bottom to the top of the seams. High sulphur values occurring at the tops of coal seams are common and are taken to result from the greater availability at these horizons of sulphate- bearing waters associated with the marine sediments which terminated peat deposition. The same relationship just was not found for subsections of coals from freshwater sites. Speculation on the cause of this relationship, as well as on the coincidence of a maximum content of aliphatic CH_2 groups with the region of marine influence, has centred on the theory, advanced by some, that concentration of bacterial lipids would be favoured by the relatively high pH values associated with marine waters. Comparison of the hopane abundances (a triterpenoid lipid used as an index of bacterial reworking of organic sediments) in some "marine" and "freshwater" coals suggests that this may be the case, although confirmation is needed.

Figure 4 shows the differences in fluorescence alteration (change in intensity) with time between severely weathered and freshly collected high and medium volatile coals. In both cases, intensity values (at time zero) are lower for the weathered than for the fresh vitrinite.

Alteration patterns were collected on a series of coals protected from oxidation by briquetting and on equivalent particulate coal stored for up to 194 months. Measurements were made on similar particles of telocollinite from the fresh (original) and stored samples. A marked change in alteration pattern for coals of mean maximum reflectance of > 0.60% and < 1.00% was noted. In each case, storage results in less time to reach a minimum value in the negative component of the pattern and the rate of increase for the positive component was enhanced. This response was not unexpected because, as shown in Figure 4, severely weathered bituminous coals lose the negative component of alteration and become largely positive. However, the rank dependence of these changes for the more subtle oxidation that occurs during storage was not anticipated. Furthermore, changes in alteration patterns were observed following as little as 50 months of storage and before thermoplastic properties were completely lost.

For coals stored > 3 years a greater proportion of the initial fluorescence intensity was lost for those in the in the 0.90 - 1.00% reflectance range than for higher or lower ranks. Coals in this high volatile bituminous range typically have the highest vitrinite fluorescence intensity, fluidity, and chloroform extraction yields. All of these factors are believed to be manifestations of the presence of a "mobile" phase in these coals. These observations imply that changes in the concentration, chemistry, and/or physical mobility of the mobile phase of coal may be involved in the deterioration of thermoplastic properties during storage and weathering. The relation between fluorescence properties and thermoplastic behaviour of coals has been well

documented by the Newcastle group. The correspondence among fluorescence intensity, the yield of chloroform-soluble materials and Gieseler fluidity observed by the Penn State group extends to coals (including low-rank and oxidised samples) hydrogenated in the absence of a solvent. It is the creation of smaller molecular fragments, analogous to the "mobile" phase of untreated coals, which provides the linkage among these phenomena. The extractable materials produced within the hydrogenated coals contain a proportion of aromatic and hydroaromatic structures capable of promoting a thermoplastic response; these groups are considered responsible for solvation and hydrogen-stabilisation of the molecular units which are cleaved off during thermal treatment.

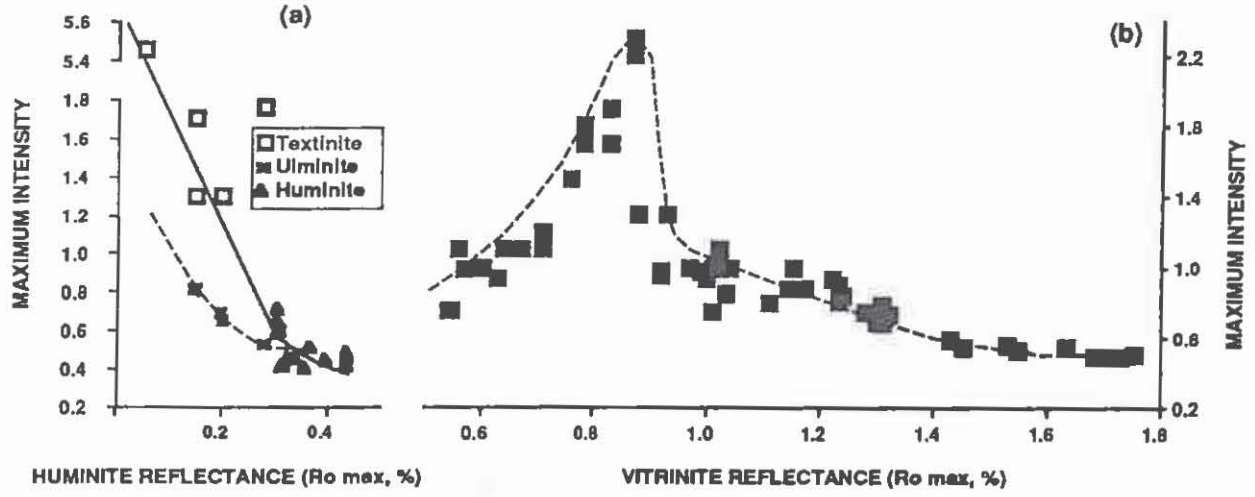

Fig. 1 Variation in intensity of vitrinite fluorescence with rank: a) primary fluorescence in UV irradiation; b) secondary fluorescence in blue–light irradiation (DAVIS et al., in press).

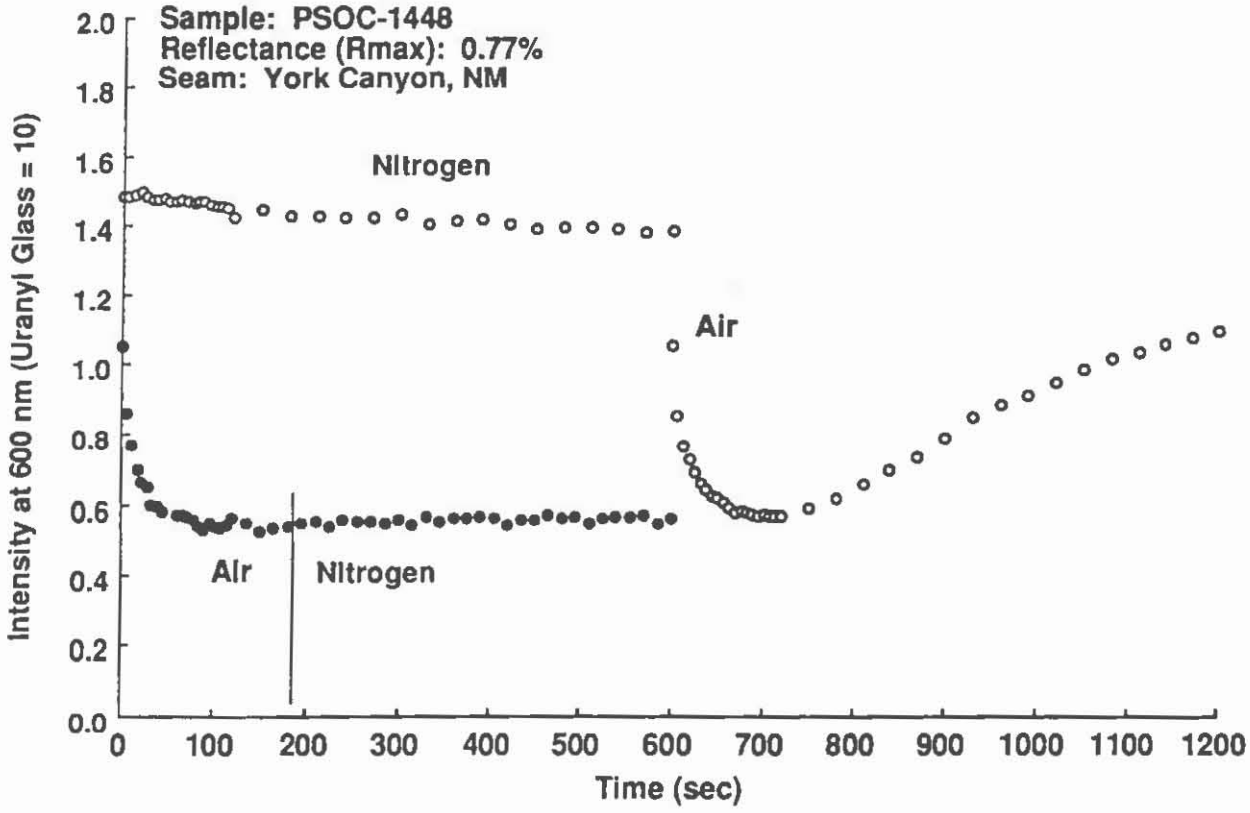

Fig. 2 Fluorescence alteration of a particle of hvAb vitrinite in successive media: (o) nitrogen then air, (o) air then nitrogen. Response at 600 nm to blue–light irradiation (DAVIS et al., 1990).

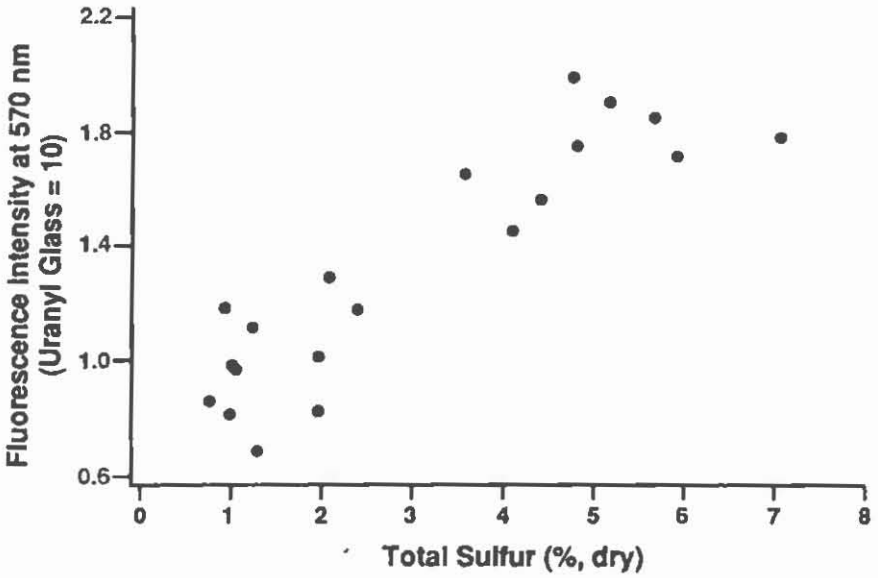

Fig. 3 Relation between vitrinite fluorescence intensity and total sulphur for northern Appalachian hvAb coals (RATHBONE and DAVIS, in press).

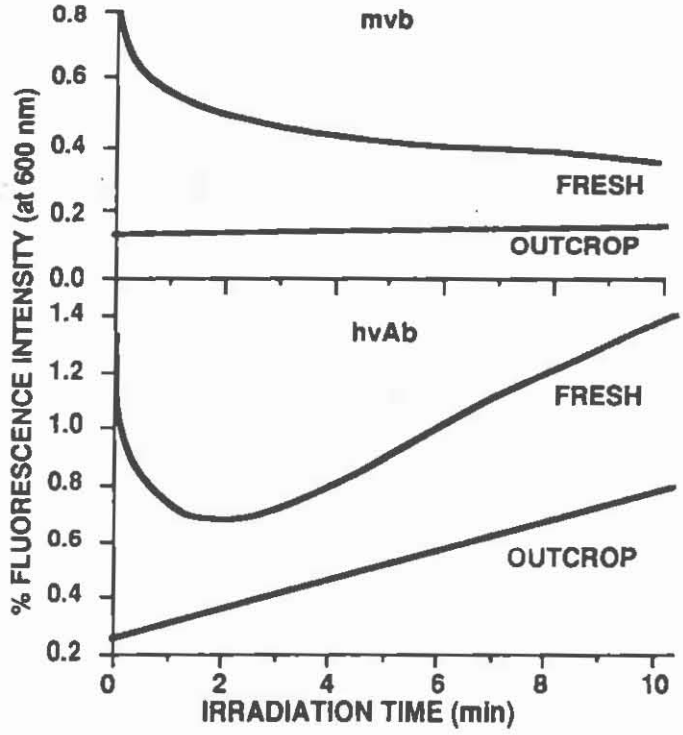

Fig. 4 Patterns of fluorescence alteration of vitrinite in fresh and weathered hvAb and mvb coals (MITCHELL et al., 1991).

THE LOCHINVAR ANTICLINE, THE HUNTER THRUST & REGIONAL TECTONICS

R.A. GLEN
NSW Department of Mineral Resources

INTRODUCTION

The enigmatic Lochinvar Anticline is the largest structure in the northern part of the Sydney Basin and lies at right angles to the WNW-trending Hunter Thrust which marks the mountain front of the New England Orogen and the boundary between its external and frontal zones (Glen and Beckett 1989).

This paper reports a new interpretation of the anticline, based on mapping carried out for the Newcastle Coalfields Map (Hawley et al., to be published by the NSW Department of Mineral Resources). This work suggests that the Lochinvar Anticline is a composite structure and formed from a combination of (W)NW-trending structures (caused by NE-SW compression) with (sub)meridional ones caused by approximately E-W compression.

STRUCTURES CAUSED BY NE-SW COMPRESSION

1. The Lochinvar Anticline is cut off to the north by the WNW trending Hunter Thrust. Mapping of Upper and Lower Carboniferous ignimbrite sheets in the hangingwall of the thrust compiled by Roberts and Engel (1989, unpubl.) clearly shows firstly, that bedding above the thrust lies parallel to the thrust, and secondly, that the Hunter Thrust cuts off the northern end of the Lochinvar Anticline.

2. The northern part of the Lochinvar Anticline is cut by the WNW-trending Radfordslee Fault and extensions eastward along fault segments mapped by Roberts and Engel (1989) to the north of Maitland where, as a south dipping ramp, it it responsible for the major plunge culmination in the Buchanan Monocline (called the Oakhampton Syncline). This fault is interpreted to be the eastern extension of the Hunter River Cross Fault mapped by Glen and Beckett (1989) to the west in the Hunter coalfield. Its extension east of the Oakhampton Syncline is uncertain, but it could extend to the coast.

3. The central part of the Lochinvar Anticline is cut by the poorly outcropping Greta Fault, first mapped by David (1907) as a SW-dipping structure with south over north vertical movment. The western end of the fault dies out in a NW-plunging anticline just west of Branxton. The eastern end of the Greta Fault dies out within the Early Permian Dalwood Group (Rutherford Formation), with shortening along the fault transferred into anticlinal folding to the southwest.

4. Other WNW-trending structures occur in the Molly Morgan Range area (Fig. 1) where outcrops of the Ravensfield Sandstone in the Farley Formation (Dalwood Group) indicate the presence of WNW-trending contractional faults and folds overprinted by meridional folds.

STRUCTURES CAUSED BY E-W TO ESE-WNW COMPRESSION.

1. The eastern limb of the Lochinvar Anticline is a region of over-steep east dips ranging from 60° to 80° (and locally overturned) that was called the Buchanan Fault by LLoyd (1956) and Buchanan Monocline by Blayden (1971). This structure is similar to the Mt Thorley Monocline on the westen side of the Loder Anticline in the Hunter Coalfield to the west (Glen and Beckett 1989). Several authors have suggested that this monocline reflects the presence of a blind, west-dipping thrust at depth (Kendall 1964, Greer and Campbell 1966 cited by Blayden 1971, and Blayden 1971). I agree.

2. An east-dipping thrust, corresponding to the Elderslee Fault of David (1907) lies along the western limb of the Lochinvar Anticline, and is inferred to pass southward into the Black Creek Syncline (Glen and Beckett 1989).

3. Based on east-west structures in the Molly Morgan Range area, a major NNE-trending, fault lies along the lower (eastern) boundary of the Greta Coal Measures in the western limb of the Lochinvar Anticline. This fault is parallel to bedding in the overlying Gretas, but cuts off folded units in the underlying Dalwood Group. South of Tyrells Vineyard, outcrop is poor and the position of the fault is based on thinning of the Greta Coal Measures, Branxton Formation and Muree Sandstone above the fault as it ramps laterally up and then down section to the south.

4. The axial trace of the Lochinvar Anticline itself consists of two separate, non joining splaying anticlines, north and south of the Greta Fault. The anticline north of the Greta Fault is best defined by outcrop of the Allendale Sandstone which defines a south-plunging box fold. The anticline south of the Greta Fault is defined by closures of the Lochinvar and Allendale formations immediately south of the fault, and by closures in the Greta Coal Measures, Fenestella beds and Muree Sandstone farther south. Strike changes in the Gretas and Muree Sandstone in the southern part of the eastern limb indicate additional poorly defined open folds in this area.

R.A.GLEN

FORMATION OF THE LOCHINVAR ANTICLINE

Relations in the Molly Morgan Range area serve as a template for interpreting the relations between (W)NW and N-S (NNE) sets of structures in the Lochinvar Anticline. They indicate that WNW and E-W-trending structures predate meridional ones which overprint them. Applying this as a whole to the Lochinvar Anticline, I argue for two phases of deformation. Early NNE-SSW compression led to formation of the north dipping Hunter Thrust, the Radfordslee Fault, the south dipping Greta Fault and the Hunter River Cross Fault which dips south in this area. (Near)parallel folds also formed in this event, with footwall synclines developed below major thrusts and anticlines developed in the hanging walls of such structures and along strike of these faults as fault shortening gave way laterally to fold shortening.

Later deformation in response to E-W shortening led to reactivation of early (W)NW faults as strike-slip (tear) faults and folding of rocks in separate (W)NW-trending panels south of the Hunter Thrust. East-west shortening led to formation of a hangingwall anticline above a west-dipping blind imbricate thrust developed along the eastern side of the folds. Backthrusting along the western edge of the anticline led to formation of a NNE east-dipping thrust(s). Stage 2 deformation of the Lochinvar Anticline thus involved formation of a thrust pop-up structure bounded by oppositely dipping thrusts at depth. Subsequent (or late stage 2) deformation involved NE-SW extension, leading to the formation of NW-trending normal faults.

REGIONAL IMPLICATIONS

The pattern of NE directed compression followed by E-W compression in the Lochinvar Anticline is similar to that documented from the Hunter Coalfield farther west where the Hunter Thrust is folded about meridional folds (Glen and Beckett 1989) and where NE compression has been partitioned into N-S and E-W thrusting (Glen and Beckett in press). In Permian rocks of the foreland basin, structures caused by NE-SW compression followed by E-W compression extend from Muswellbrook southeast to Maitland. The area north of Maitland marks the most easterly extent of (W)NW-trending structures. Here the Hunter Thrust dies out in the hinge of the Bolwarra Anticline, outcrops of Ravensfield Sandstone define an east-west syncline at Aberglasslyn, and the Mindaribba Syncline curves from a WNW trend in the west into a meridional series of splay folds in the east. Roberts et al (1991) showed that in Carboniferous rocks in the hangingwall of the Hunter Thrust, WNW-trending folds extend as far as the NE-trending Glenoak Fault, a splay of the Williams River Fault: structures to the east are meridional to NNE in trend with little or only minor evidence of contractional structures in other orientations.

Several major points follow from this:

LOCHINVAR ANTICLINE AND HUNTER THRUST

1. The area from Muswellbrook to Maitland occupies a recess caused by a major indentation in the combined New England and offshore Currarong orogens. This recess is of fundamental crustal significance and is probably the cause of persistent stress build-ups like the one which caused the 1989 Newcastle Earthquake.

2. Multiple deformation in this area reflects stress heterogeneities in an area of complex geometry. First phase structures represent compression from the northeast, as the thrust front from the New England Orogen migrated from northeast to southwest. Second phase structures represent westward migration of the thrust front from the offshore Currarong Orogen. In this regard, the dominant NNE-trending structures in the central and southern parts of the Sydney Basin reflect shortenings induced by westward thrusting in the Currarong Orogen.

3. As the Hunter Thrust dies out to the southeast, Permian rocks lie with original relationship on Carboniferous rocks. Strain discontinuities between these areas of allochthonous and autochthonous relationships are taken up by (sub)meridional faults in Carboniferous and Early Permian strata. These are thus tear faults as suggested by Roberts and Engel (1987) and Roberts et al. (1991).

4. Major faults in the inverted northern part of the Sydney Basin probably sole into a floor thrust (see also Glen and Beckett, 1989). Eastward dying out of the Hunter Thrust does not mean that the floor thrust similarly stops, and this detachment may underlie much or even all of the Sydney Basin. Similarly, the Hunter River Cross Fault may persist at depth as a WNW-trending splay off, or ramp in, the floor thrust, and probably continues to the coast.

ACKNOWLEDGEMENTS

I thank John Roberts for kindly sharing the unpublished mapping compiled by Brian Engel and himself in the Branxton and Paterson 1:100 000 sheet areas, and Jeff Beckett, Shawn Hawley and John Brunton for discussions about Newcastle geology. Published with permission, Director-general, NSW Department of Mineral Resources

REFERENCES

BLAYDEN, I. D., 1971: On the structural evolution of the Macquarie Syncline, New South Wales. Ph. D., thesis, Univ. Newcastle, Newcastle, (unpubl.).

DAVID, T.W.E., 1907: Geology of the Hunter River Coal Measures. NSW Geol. Survey, Memoir 4.

GLEN, R.A., 1989, and BECKETT,J., 1989. Thin-skinned tectonics in the Hunter Coalfield of New South Wales. Aust. J. Earth Sci., 36, 589-593.

GLEN, R.A., 1989, and BECKETT, J., in press: Hunter Valley Coalfield 1:100 000 Map (Second Edition). Department of Mineral Resources, Sydney.

HAWLEY, S., GLEN, R.A., and BAKER, C.J., in press: Newcastle Coalfield 1:100 000 Geological Map. Department of Mineral Resources, Sydney.

LLOYD, J.C., 1956: East Maitland Coal District. Bloomfield, Buchanan-Maitland and Dagworth-Greta areas. NSW Dept. Mines Tech. Rept., 1, 35-37.

ROBERTS, J., AND ENGEL, B.A., 1987: Depositional and tectonic history of the southern New England Orogen. Aust. J. Earth Sci., 34,1-20.

ROBERTS, J., ENGEL, B., and CHAPMAN,J., (Editor) 1991: Geology of the Camberwell, Dungog and Buladelah 1:100 000 sheets 9133,9233,9333. NSW Geol. Survey, Sydney.

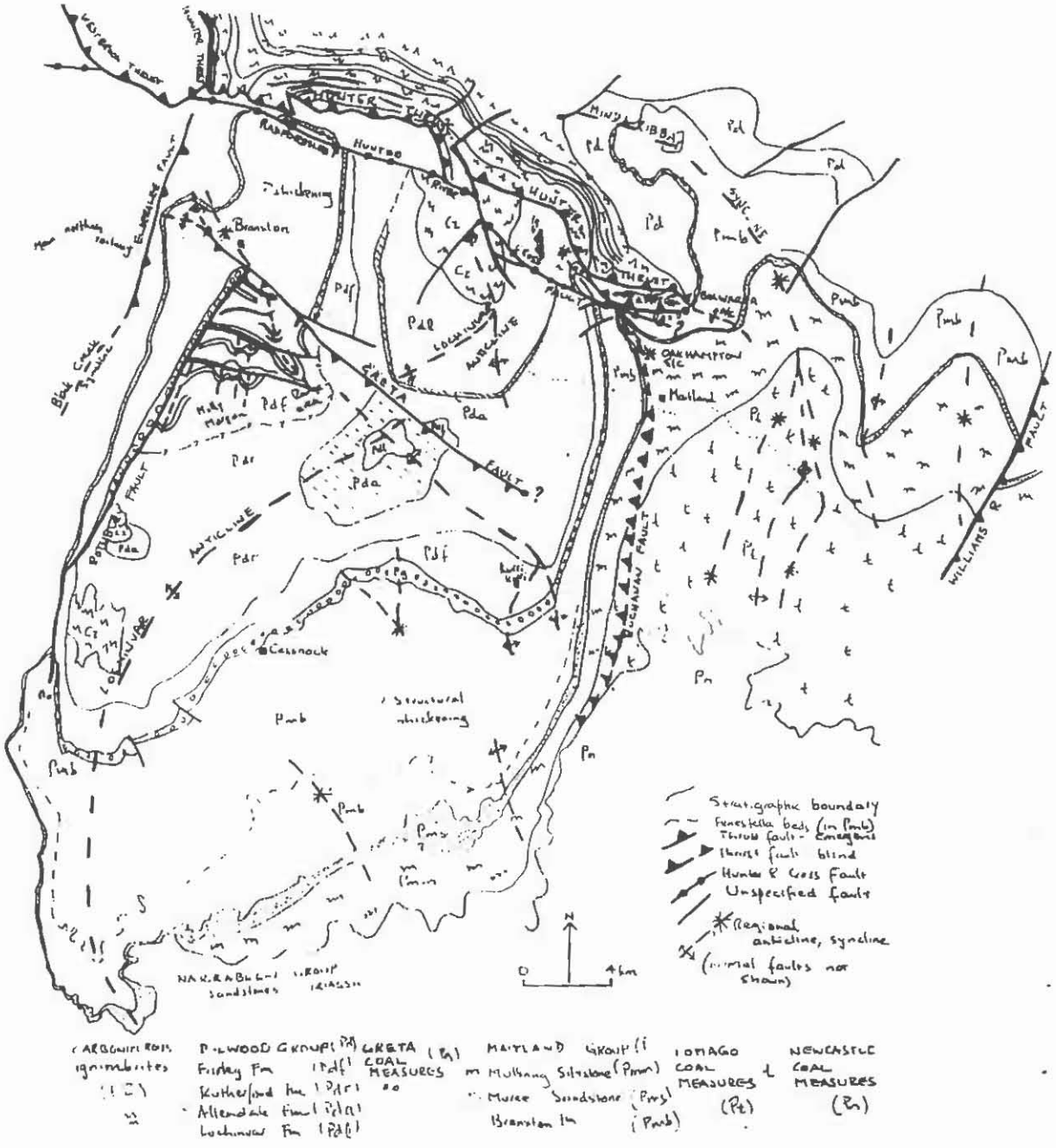

FIG. 1. SOLID GEOLOGY (INTERPRETATIVE) MAP OF LOCHINVAR ANTICLINE & RELATIONSHIP TO THE HUNTER THRUST. BASED ON NEW MAPPING TOGETHER WITH COMPILATION OF OLDER DATA FROM HANLEY et al. (IN PRESS).

P.Jen 2/93

REVIEW OF THE STRATIGRAPHY OF THE GUNNEDAH BASIN

N.Z. TADROS
NSW Department of Mineral Resources

INTRODUCTION

Before 1981, stratigraphic schemes were constructed for localised areas of the Gunnedah Basin and many of these schemes concentrated on selected parts of the sequence. Based on limited information, Russell (1981) amalgamated previous schemes into a unified stratigraphy for the Gunnedah Basin north of the Liverpool Range, but rigorous definition of many of the stratigraphic units was not possible. Extensive drilling in the north of the Liverpool Range between 1981 and 1985 provided detailed knowledge of its rocks and allowed a comprehensive review of the stratigraphy. The region to the south has been subject to extensive stratigraphic studies and the lithostratigraphic schemes are continuously being reviewed and updated.

Table 1 shows the existing and new stratigraphy. Three Groups are proposed for the Permian section, Bellata Gp (new, includes 3 formations) & Millie Gp.(new, includes two formations) and Black Jack Group (elevated from Formation status, comprises 7 formations). Two members are abandoned and three are created and three are elevated to Formation status. The Triassic Digby (consists of two new members) and Napperby Formations are redefined and a third formation is created. Fig.1 should be consulted wherever reference is made to the distribution of stratigraphic units. Formal definition of coal units in this review has been limited to the Hoskissons Coal and the Melvilles Coal Member. **Other seams have been described in detail in Tadros (in press). Lack of space forced the exclusion of many figures, but the reader is advised to refer to the Gunnedah Basin Memoir (Tadros in press) for more comprehensive treatment of the stratigraphy and sedimentology of the Gunnedah Basin.**

FLOOR OF THE GUNNEDAH BASIN

E.Permian silicic (Boggabri Volcanics, Hanlon 1949) to mafic volcanics. (Werrie Basalt) form the basement for the Gunnedah Basin E of the Rocky Glen Ridge. The top of the volcanics is deeply weathered, indicating an unconformity. Metavolcanics of the Lachlan Fold Belt form the basement underneath the Gilgandra Sub-basin.

PERMIAN STRATIGRAPHY

BELLATA GROUP (BGp) (new, N.Z.Tadros)

Named after Bellata some 50km north of Narrabri and comprises all of the E. Permian lithostratigraphic units in the Gunnedah Basin namely Leard, Goonbri and Maules Creek Formations. The BGp unconformably overlies the basal volcanics and the contact with the overlying L.Permian Millie Group varies from conformable to unconformable. Age is E.Permian Stage 3 to Upper Stage 4a (McMinn 1993). The BGp is broadly correlated with the Greta Coal Measures in the Sydney Basin, except that the Goonbri Fm is time equivalent of the upper Dalwood Group. The BGp comprises mainly fluvial lacustrine coal measure deposits.

LEARD FORMATION (LF) Brownlow (1981) **(Redefinition, N.Z.Tadros)**

Named after the Leard State Forest, the LF is the basal unit in the Gunnedah Basin sequence, of E. Permian age & consists of flint (pelletoidal) claystone (cs). Loughnan (1975) described E.Permian flint clays from the Wingen, Muswellbrook, Willow Tree & Gunnedah areas. Tadros (1982) described a 17.4 m section in DM Boggabri DDH 2 & extended the correlation to the western side of the Boggabri Ridge. The term has since been used to encompass all pelletoidal css which rest on the weathered volcanics in the northern Gunnedah Basin. **Type section & Lithology** as in Brownlow (1981) **Thickness** *range:*up to 17.5m. **Relationships & boundary criteria** The LF is a diachronous unit (Thomson 1986) best described as a discontinuous veneer overlying weathered surfaces on the Boggabri Volcanics (& Werrie Basalt?) with gradational boundary. The upper boundary is the lowermost occurrence of lithic sediments which constitute the overlying **Maules Creek**

Formation (MCF) (Brownlow 1981). In the Maules Creek Sub-basin (MCSB) area, the LF exists below the lower seams of the MCF distal to the Boggabri Ridge (Thomson 1986). Close to the ridge the LF underlies the upper seams. Further, clastic units & coal seams extend from the MCF into the LF indicating that deposition of the LF & MCF occurred at the same time in different parts of the basin (Thomson 1986). In the Mullaley Sub-basin (MSB) intercalations of pelletoidal cs & lithic sediments locally occur in the basal few metres of the MCF.

Age & evidence E.Permian Lower Stage 4 palynological zone age (Morgan 1976a,e). Weathering of the basal Volcanics spanned the L.Carboniferous-E.Permian, until the Boggabri Ridge was covered during deposition of the Porcupine Formation (Thomson 1986).

GOONBRI FORMATION (GF) (Thomson 1986 unpubl.; **Redefinition, N.Z.Tadros**)

Named after Goonbri Mountain (GR 334092, Boggabri 1:100 000 sheet) the GF exists in the MCSB in the subsurface N. of the mountain, in the central parts of the Bellata Trough Etheridge (1987) & the Bohena Trough (Tadros in press). **Type section** (New) DM Bellata DDH 1 between 1007.1m & 1112.7m. Thomson's (1986b) type section lacked definition of the lower boundary (drilling terminated within the unit). **Thickness** *MCSB* >125m; *MSB*, Bellata Trough 105.6m; Bohena Trough 79m. **Lithology** (in new type section) Mainly dark organic-rich sl, thin layers of coal, & graded sl-cs laminite, coarsening-up through burrowed, graded sl-cs & laminated fn-grained ss & sl to fn & medium-grained, moderately well sorted ss. The ss is up to 3m thick, overlain in places by coal & root-penetrated & disturbed sl & v fine ss. The ss is composed of approximately equal proportions of angular quartz & rock fragments, with 3%-5% feldspar (microcline). The GF has interbeds of pelletoidal reworked weathered volcanics near its base (Etheridge 1987).

Relationships & boundary criteria Unconformably overlies & onlaps Boggabri Volcanics & LF if present, is conformably overlain by the MCF, & the first appearance of coal marks its top (Thomson 1986). A disconformity between MCF&GF in DM Bellata DDH1 is indicated by absence of sediments containing lower Stage 4; McMinn 1986, Etheridge 1987).

Age & evidence E.Permian Stage 3 of Price (1976), McMinn (1981 & in press).

Correlations A time equivalent to the Dalwood Group.

MAULES CREEK FORMATION (MCF)(Brownlow 1981; **Redefinition, N.Z.Tadros**)

Named after the village of Maules Creek, the MCF onlaps the E & W sides of the Boggabri Ridge & crops out between the ridge & the Mooki Fault System. *MSB*, mainly in the subsurface except a few outcrops near Gunnedah.

Type section as in Brownlow (1981). **Thickness** *MCSB* >800m; *MSB* <100m.

Lithology *MCSB*: (as in Type section, Brownlow 1981). *MSB:* a northern quartz-rich ss zone, a central volcanogenic-rich zone & a SE zone characterised by fine-grained sediments rich in coal (Thomson (1986b).

Relationships & boundary criteria The MCF overlies & onlaps the Leard & Goonbri Formations & underlies the Porcupine Formation. The lower boundary is taken at the base of the lithic sediments above the pelletoidal cs. *MCSB*: top of the MCF has generally been eroded. *MSB*: disconformable, sharp up. boundary in the west (Runnegar 1970, Bourke & Hawke 1977) & intergradational in the centre & S (Beckett et al. 1983). MCF is overlapped by the Porcupine Formation along the E side of the MSB.

Age & evidence *MCSB*: Morgan (1976a,b) assigned E.Permian L.Stage 4 to MCF (Brownlow 1981). *MSB*: McMinn (in press) assigned the majority of the MCF to Up. Stage 4, with only the base occasionally extending into L.Stage 4. **Correlations** Rowan Formation of the Greta Coal Measures.

MILLIE GROUP (MGp) (New, N.Z.Tadros)

Named after Parish of Millie, SW of Gunnedah, the Group is comprises marine sediments of the Porcupine & Watermark Formations. The MGp has limited surface exposure, but extends in the subsurface over almost the entire area of the MSB. The boundary with the underlying BGp is conformable in the central part of the sub-basin, intercalating in the S & unconformable over basal volcanics along the sub-basin margins. The base is diachronous, ranging from Permian Upper Stage 4 paly. zone in the SE to Lower Stage 5b in the N & W (McMinn in press). The formations of The MGp have been correlated with the Maitland Gp.

PORCUPINE FORMATION (PF) (**Redefinition; S.McDonald, G.Skilbeck & N.Z.Tadros**)

Named after Porcupine Hill, SE of Gunnedah, by Hanlon (1949), the PF is present in subsurface of MSB. *Outcrops*:Gunnedah-Curlewis area & Deriah Forest area. *MCSB:* one hole intersection in the NE & two isolated outcrops N. of Mt. Kaputar (Russell 1981).

Type section DM Ferrier DDH2 (249066mE, 1535912mN), 172.4m from 330.0m to 502.4m. **Thickness** W: 0m-10m, N: 20m-60m, S&SE: 30m - >160m. **Lithology** *Base:*fining-up from a massive paraconglomerate with a poorly sorted ss & sl matrix, through orthoconglomerate with moderately sorted lithic ss/sl matrix, to

an homogeneous bioturbated mixture of ss & ms with a few clasts & traces of *Zoophycus* burrows. Clasts are composed dominantly of silicic volcanics. *Top:* fining-up bioturbated sl-dominated homogeneous mixture of sl & ms with rare clasts & indistinct lamination. Sporadic traces of *Zoophycus* **Relationships & boundary criteria** *central MSB*: the PF conformably overlies, & in some places intercalates with the Maules Creek Fm. Along the MSB margins the PF is unconformable over basement rocks. Upper boundary is gradational & is typified by a transitional facies consisting of bioturbated homogeneous mixture of sl&ms with rare erratics & can be widely correlated across the MSB. This transitional facies grades upwards to the base of the Watermark Formation which is an intensely bioturbated & burrowed (*Zoophycus*) sandy sl&ms, with bryozoans & shell fossils (McDonald & Skilbeck (1991).
Age & evidence Diachronous, ranging from Permian Upper Stage 4 in the southern MSB, to Lower Stage 5b in the N. (McMinn 1993). **Correlations** Snapper Point Formation (Herbert 1980), Branxton Formation & Murce Sandstone in the Sydney Basin (Beckett et al. 1983).

WATERMARK FORMATION **(WMF) (Redefinition; N.Z.Tadros, S.McDonald & G.Skilbeck).**
Named after Mount Watermark 10km W of Breeza by Hanlon (1949) to describe a shaly marine unit, and extended by Russell (1981) & Beckett et al. (1983) to the Gunnedah - Narrabri - Coonabarabran region; herein the name is applied to the MSB. *Outcrops*: W of Gunnedah & Mount Watermark.
Type section & Thickness DM Brown DDH1 (228989mE, 1547008mN), 178m from 199m to 377m., maximum 230m in the SE. **Lithology** *Lower part:* fining-up sequence of sandy sl at the base, silty ss, dark-grey sl, through to sl/cs laminite at the top. Common brachiopod shells & bryozoans zones. Intense bioturbation has destroyed most of the primary sed. structures, but where preserved, parallel lamination predominates (Hamilton 1987). *Upper part:* two lithologically distinctive units forming a major upward-coarsening succession. *Lower unit:* present only in the S (absent N. of Boggabri), a finely laminated sl & cs, with little or no bioturbation, have fissile mechanical state (Hamilton 1987), sporadic erratics, secondary calcite "cone-in-cone" replacement zones, & glendonite crystals. *Upper unit:* well-developed coarsening-up sequences of grey laminated sl, silty ss & sl/ss laminite at the top, with strongly bioturbated horizons. The percentage of ss increases towards the top. The WMF is sporadically topped by well-sorted clean fine to coarse-grained ss. **Relationships & boundary criteria** lower boundary is fining-up transitional with PF (see upper boundary of PF). The upper boundary is commonly gradational but can be recognised by a change from well-sorted, clean, fine to coarse-grained ss to a coal-bearing, organic matter rich sequence of lithic ss, sl, cs & cg (Hamilton 1987). **Age & evidence** WMF spans much of the Permian Lower Stage 5b to Lower Stage 5c palynological zone (McMinn in press). **Correlations** Mulbring Siltstone & Berry Siltstone (Beckett et al. 1983).

BLACK JACK GROUP (Variation of Published Name & Redefinition, N.Z.Tadros)
Named as a formation after Black Jack MT. SW of Gunnedah, by Hanlon (1949), Russell (1981), Beckett at al. (1983); as coal measures by Britten & Hanlon (1975), but no clear definition was given to its lower boundary & there is some confusion concerning its upper boundary. *Outcrops:* along a N-NW trending zone of discontinuous hills between Breeza & N of Boggabri, otherwise in subsurface of MSB.
Type section & Thickness DM Springfield DDH1 (228904mE, 1524844mN), 265.6m from 348.7 to 614.3; range W 50m - SE 470m, average 200m. **Lithology** a *lower part* (Brothers Subgroup) consisting of 3 units: 1) basal lithic coal-bearing (Pamboola Fm), 2) a dominantly lithic ss, cs & cg (Arkarula Fm) & 3) a quartz-rich ss (Brigalow Fm); a *middle part* (Coogal Subgroup) consisting of two units: 1) Hoskissons Coal at the base overlain in the east by organic-rich ms-dominated unit (Benelabri Mudstone Member), which occupies the basal part of 2) a quartz-rich ss sequence (Clare Sandstone), and an *upper part* (Nea Subgroup) comprising two units 1) a dominantly lithic conglomeratic unit (Wallala Fm) & at the top 2) a tuffaceous coaly unit (Trinkey Fm).
Relationships & boundary criteria Conformable with the underlying sediments of the Millie Group but unconformably & erosively overlain by the Triassic Digby Fm.
Age & Evidence: L.Permian age extending from L.Stage 5c to Up.Stage 5. *M. bitriangularis* first appears in the upper zone above the Hoskissons Coal (McMinn in press).
Correlations Illawarra, Wittingham & Wollombi Coal Measures.

BROTHERS SUB-GROUP (New, N.Z.Tadros)
Named after Parish of Brothers west of Breeza, this subgroup comprises 3 formations with outcrops mainly near Gunnedah.
Type section & Thickness a composite of the contained formations.
Lithology dominantly lithic sandstones and siltstones with coal seams in the lower part (Pamboola Fm), and burrowed silty ss in the upper part in the E (Arkarula Fm) & quartz-rich ss (Brigalow Fm) in the W and NW.

Relationships & boundary criteria *Lower boundary* as that of the the Pamboola Fm. *Upper boundary* as that of the Arkarula and Brigalow Formations.
Age & evidence L..Permian spanning L.Stage 5c to Up.Stage 5. (McMinn in press).
Sediments of this subgroup are either marine or influenced by marine conditions except along the W & NW sub-basin margins.

PAMBOOLA FORMATION (PMBF) (New, N.Z.Tadros)
Named after Pamboola Creek near type section, the formation mainly occurs in the subsurface of the MSB, absent only in the W.
Type section & Thickness: DM Denison DDH1 (385054m E, 1585274m N) 46.5m from 176.5 to 223m, *range: SE* 0m->206m, *N* up to 89m.
Lithology: Lithic ss, sl, cs, cg & intercalated coals in generally coarsening-up & sporadic fining-up sequences. The PMBF consists of: a) interbeds, 3-15m thick, of fine to c-grained ss with finely macerated organic matter & coaly fragments & erosive pebbly bases; b) lenticular bedded, fn-grained ss & sl intercalated with parallel laminated ss & cs containing abundant burrows c) intercalated minor units of ripple, parallel & wavy-laminated ss, sl & cs fining-up to carbonaceous cs & capped by coal seams.
Relationships & boundary criteria: Conformably overlies the WMF. The boundary is marked by a change from well-sorted clean ss to either erosively & pebbly-based thick interbeds of fine to c-grained lithic ss, or to carbonaceous sl & cs with abundant plant debris. Boundary with overlying Arkarula Fm.: *S*; marked by a change from a coal bearing sequence of ss, sl & cs to a distinctive unit of fn. to medium-grained ss with sporadic zones of vc detritus & abundance of subvertical mud-lined worm burrows, *N*; boundary is characterised by a change to a unit containing well-sorted medium-grained ss, poorly-sorted strongly bioturbated silty ss & a distinctive bioturbated silty ss with silicic volcanic pebbles. PMBF contains Melvilles C. Mb. **Age & evidence** L.Permian, spanning L.Stage 5a-c (McMinn in press). **Correlations** Lower Tomago Coal Measures, Nile Subgroup & Pheasants Nest Formation.

MELVILLES COAL MEMBER (MCMb) (Redefinition, N.Z.Tadros)
A seam named after Melville's Well near Gunnedah by Hanlon (1949) & a coal Mb by Britten & Hanlon (1975); widely distributed over the E half of the MSB & crops out near Gunnedah. **Type section & thickness** seam 8 in DM Clift DDH4 (235518mE, 1536744mN), 3.11m between 111.47m & 114.58m, *range* to 5.03m. **Lithology** consists of moderate to high vitrinite coal with subordinate layers of fn-grained ss, carbonaceous sl/cs & tuff. Generally, the MCMb has a consistent lithotype profile. Pyrite lenses, nodules & framboids are present throughout the MCMb; sometimes concentrated towards the top.
Relationships & boundary criteria The MCMb is present roughly in the middle of the PMBF sequence. **Age & evidence** L.Permian within the L.Stage 5c. **Palaeoenvironment** Blanket peat in a lower delta plain environment.

ARKARULA FORMATION (ARKF)(Variation to published name & redefinition, N.Z.Tadros)
Named as a member after Arkarula Homestead, W of Gunnedah, by Britten & Hanlon (1975), but herein elevated to a formation status to encompass the overlying Allara Shale Mb (Britten & Hanlon 1975) and to extend its coverage over much of the MSB south of Narrabri except in the W &NW.
Type section & Thickness: DM Millie DDH1 (206200m E, 1563016m N), 23m from 340.m to 363m, *range*: 51m. **Reference section in the N.** DM Turrawan DDH2A (189881mE, 1632521mN), 39m from 316m to 355m *range* up to 51m. **Lithology** overall up-finning sequence of fn. to medium-grained ss at the base with distinctive subvertical mud-lined worm burrows & sporadic zones of vc detritus, overlain by alternating sequences of a poorly sorted silty ss & sl. At the top, the ARKF contains finely interbedded ss & sl fining-up to laminated organic-rich sl & fn-grained ss with lenticular bedding, oscillation ripples, load casts, mud cracks & mud drapes. From about 25km SW of Boggabri northward to Narrabri changes to well sorted medium-grained ss with thin pebbly base. The ss may coarsen up & locally become conglomeratic, or may change into a poorly sorted strongly bioturbated silty ss & mud dominated sequences. A distinctive unit of a poorly sorted pebbly ss, crudely fining-up & erosively based may develop in the mud dominated sequence. This unit contains silicic volcanic clasts up to pebble size in a bioturbated medium-grained silty ss matrix. In the northernmost part of the Sub-basin, the unit may contain mud-dominated sequences with abundant disarticulated brachiopod shells (Hamilton 1987). **Relationships & boundary criteria:** The lower boundary is marked by appearance of the distinctive burrowed ss above the coal-bearing PMBF. The upper boundary is gradational, but easily recognisable, through carbonaceous cs to the Hoskissons Coal. The unit grades laterally to the W into, & locally in the N. overlain by, the Brigalow Fm. **Age & evidence:** L.Permian, spanning the paly. boundary between Lower & Upper Stage 5 & contains Spinose acritarchs (McMinn in press). **Correlations** Kulnura Marine Tongue in the Sydney Basin.

NEW STRATIGRAPHY FOR THE GUNNEDAH BASIN

BRIGALOW FORMATION **(BRGF) (New, N.Z.Tadros)**
After Parish of Brigalow, which contains the type section; present in the N & W of MSB.
Type section & thickness DM Brigalow DDH2 (361568m E, 574703m N), 7.5m between 508.5m & 516m, *range:* up to 28m.
Lithology Dominantly quartzose ss, medium & c-grained to pebbly, medium-bedded with sharp base, commonly erosively overlying the ARKF. Medium scale tabular & trough cross-stratification are dominant. Subordinate fn-grained ss finely-interbedded with sl & carbonaceous sl also occur (Hamilton 1987). **Relationships & boundary criteria** In the NW MSB, the BRGF overlies & is intergradational laterally, in a southeasterly direction with the ARKF. Locally in the W., where the ARKF is absent, the unit overlies the PMBF. The unit has an overall finning-up character & is overlain by the Hoskissons Coal (Tadros in press). **Age & evidence** contains the first appearance of *D. parvithola* which marks the boundary between L.Permian L & Up. Stage 5 paly. zones (McMinn in press). **Correlations** Marrangaroo Conglomerate in the W Sydney Basin.

COOGAL SUBGROUP (New, N.Z. Tadros)
Named after Parish of Coogal, W of Gunnedah, this subgroup has limited outcrop in the Gunnedah-Curlewis area, but extends in the subsurface over much of the MSB from a few km N of Narrabri, S to Quirindi & westward to the western margin of the MSB. **Lithology** Thick coal at the base (Hoskissons Coal) overlain by organic-rich mudstone-dominated unit (Benelabri Mudstone Member) in the east and middle of the sub-basin & quartz-rich sandstone (Clare Sandstone) in the west. **Relationships & boundary criteria** *Lower boundary* Arkarula and Brigalow Formations, up. boundary Wallala Fm. **Age & evidence** L.Permian Upper Stage 5 associated with the *M. bitriangularis* paly. zone.(McMinn in press).

HOSKISSONS COAL **(HC) (Variation of Published Name & Redefinition)**
Named as informal seam by Hanlon (1949), a Mb by Britten & Hanlon (1975). Extends over much of the MSB except N of Narrabri. **Type section & thickness** as in Tadros (1988). **Lithology** as described in Tadros (1988). **Relationships & boundary criteria:** Overlies the ARKF in center & S. & BRGF in the W&N; overlain by the Benelabri Mudstone Mb. in the E, & with Clare Sandstone (CLSS) in the W. Along the MSB W margin, the HC is split by the CLSS. **Age & evidence** spans the change from *D. paravithola* to *M. bitriangularis* (McMinn in press). **Correlations** Bayswater & Woonona C Mbs., Lithgow & Ulan Coals (Beckett et al. 1983; Hunt et al. 1986).

CLARE SANDSTONE **(CLSS) (Variation of name & Redefinition, N.Z.Tadros)**
Named "Clare Sandstone Member" after Clare Homestead near Gunnedah by Waters (1971) to describe a 28.8m section of ss containing quartz pebbles in Gunnedah Colliery old Bore 2 (W128.596) and in outcrops, but the name was never formalised. Britten & Hanlon 1975, confirmed its informal status and since 1980, the name has been strongly associated, through field usage and in literature (Beckett et al. 1983, Hamilton & Beckett 1984, Hamilton 1985,1987,1991; Hamilton et al. 1988; Tadros 1985,1988,1991) with quartz-rich ss encountered above the Hoskissons Coal in the regional drilling in the Mullaley Sub-basin. These sandstones have been mapped in detail (Tadros in press) and have distinct lithological characteristics and mappable boundaries. The strong association of the "Clare Sandstone" with this mappable unit favours retaining the name, but it is proposed herein to elevate the Member to a Formation status & assign a new type section & extend its usage to encompass the area from Narrabri to Quirindi and westward to E of Coonabarabran.
Type section & thickness Dm Wallala DDH1 (247698mE, 1527836mN), 65.5m between 195.5m & 261.0 m, *range:* up to >95m. **Lithology** Medium & c-grained quartz-rich ss with quartz cg locally developed. The ss generally forms medium-bedded units with low angle medium-scale tabular & trough cross stratification. The CLSS sporadically changes to fining-up thinner interbeds of ss/sl rich in plant debris & organic matter and topped with coal. Sed. structures include small-scale trough crossbeds, fn climbing ripples, ripple-cross lamination, wavy & parallel laminations, clay drapes & laminated mud layers. At the top of the CLSS is fining-up sequence of interlaminated thin sl&cs sequence topped with the Breeza seam (Tadros in press). Sporadic coarsening-up sequences may also develop with internal erosional surfaces & palaeosols towards the top (Tadros 1986,1993).
Relationships & boundary criteria: The lower boundary is defined by the top of the HC or the top of the lowermost split of the HC, & the upper boundary by the top of the Breeza seam. In the E half of MSB the CLSS inter-fingers with, & overlies, the BLMBF. Along the extreme W margin the CLSS splits the HC.
Age & evidence L.Permian Up.Stage 5 (McMinn in press).
Correlations Blackmans Flat Conglomerate in the W Sydney Basin.

BENELABRI MUDSTONE MEMBER **(BLMb) (New, N.Z.Tadros)**

Named after Parish of Benelabri; is present over much of the eastern half of the MSB from Turrawan (25km S of Narrabri to Caroona; absent in the W&SW parts of the MSB & between Breeza & Quirindi.
Type section & thickness DM Denison DDH1 (385054mE, 1585274mN), 25.8m between 114.9m & 140.7m; *range:* up to 35m. **Lithology** An overall coarsening-up sequence of interbedded organic-rich ms, sl & quartzose ss. The sequence is distinctly cyclical. Each cycle is represented by coarsening-up sequence, 3-5m thick, consisting of organic-rich ms at the base, grading to ms/sl & graded sl/ss laminite with common burrows, which in turn passes into mainly ss at the top. Coal may develop in the lower cycles (contains Caroona seam in the SE). Upper cycles are more sand-dominant. Lenticular & flaser bedding, ripple lamination & dessication cracks are common (Tadros 1986, 1993). The BLMb is often terminated by the Howes Hill seam (Tadros in press). **Relationships & boundary criteria** Underlain by the HC, often with gradational boundary & overlain by the quartz-rich :Clare Sandstone Locally, where the overlying Clare Sandstone is absent or removed by erosion, the BLMb may also be partly eroded & directly overlain by the Wallala Formation. **Age & evidence** On paly. evidence, L.Permian Up.Stage 5 associated with the appearance of *M. bitriangularis* (McMinn in press). **Correlations** Denman, Dempsey & Baal Bone Formations in the Sydney Basin based on paly. assemblage (McMinn 1982).

NEA SUBGROUP (New, N.Z.Tadros)
Named after Parish of Nea NW of Breeza; generally has poor outcrops, but extends in the subsurface over much of the MSB from a few km N of Narrabri S to Quirindi & W to the western margin of the MSB. **Type section** composite of those of the contained formations. **Lithology** Lithic conglomerate ss, sl,cs & coal in the lower part (Wallala Fm) and fn-grained, tuffaceous coaly sequence in the upper part (Trinkey Fm).
Relationships & boundary criteria underlain by the Clare SS & overlain by the Digby Formation.
Age & evidence L.Permian Upper Stage 5, lies within the *M. bitriangularis* paly. zone.(McMinn in press).

***WALLALA FORMATION* (WLAF) (New N.Z.Tadros)**
Named after Parish of Wallala containing the type section, the WLAF is present in the E MSB between Boggabri & Caroona-Quirindi area. **Type section & thickness** DM Wallala DDH3 (252539mE, 1524344mN), 55.5m from 170m to 225.5m. *range:* up to 55.5m. **Lithology** Fining-up sequence of lithic cg, ss, sl, cs & coal, with minor amounts of tuff & tuffaceous sediments. Variably stratified granule to pebble cg consisting of varying proportions of silicic & mafic volcanics, cherts & jaspers in a lithic sand or clay matrix dominates the sequence particularly in the E & SE. The cg forms planar, medium to thickly-bedded units up to 5m thick, interbedded towards the top with low angle cross-bedded, coarse to fn-grained ss,sl&cs. Laterally, the cg shows a gradual & progressive decrease in clast size towards the W. Locally in some areas in the SE, the basal part of the unit is quartz-lithic, but the quartz content decreases rapidly upwards. At the top, the WLAF sequence commonly fines-up to thinly bedded, fn-grained ss,sl & cs & in the south culminates with a coal seam.
Relationships & boundary criteria Overlies the CLSS & underlies the Trinkey Formation. The lower boundary is marked by the top of the Breeza seam & its equivalents (see Tadros in press). The upper boundary is marked by the base of the Clift seam, which is present mainly in the S, but where the seam is absent, the boundary is marked by rapid increase in tuff & tuffaceous sediments (Tadros in press).
Age & evidence Fine grained sediments within the unit indicate Late Permian Up. Stage 5.(McMinn in press). **Correlations** Gap Sandstone of the W Sydney Basin (Beckett et al. 1983).

***TRINKEY FORMATION* (TKYF) (New, N.Z.Tadros)**
Named after Parish of Trinkey which contains the type section, the TKYF is present mainly in the subsurface from Narrabri to Quirindi to E of Coonabarabran.
Type section & Thickness DM Trinkey DDH1 (205418mE, 1525491mN), 141.7m from 531.3m to 673m *range:* up to 258m in SE. **Lithology** Dominated by finely-bedded cs,sl & fn-grained ss sequence intercalated with tuff, tuffaceous sediments & abundance of carbonaceous coaly matter & tuffaceous stony coal seams. Tuffs range from thinly bedded to massive. *Sed. structures:* thin laminations, small scale crossbedding, distorted bedding, root traces & abundant plant debris. The TKYF contains minor fining-up sequences of crossbedded, lithic ss with scour bases & sl & cs showing fu cross-lamination, climbing ripples & root traces. The TKYF also contains up to 40m of medium to thickly-bedded, lithic, granule to pebble cg sequences consisting of chert & silicic volcanic clasts in a dominantly tuffaceous ss matrix. Cg beds are confined mainly to the SE MSB between Gunnedah, Mullaley & Quirindi. Bed thickness & clast size increase towards the SE where the cg forms a significant part of the sequence (Tadros in press).
Relationships & boundary criteria: Overlies the WLAF & underlies Digby Formation. The lower boundary is marked by the base of the Clift seam in the S., or where the seam is absent, by rapid increase of tuff & tuffaceous sediments, either as discrete beds or as matrix in the cg. The upper boundary is recognised by

lithological contrasts between the generally fn-grained tuffaceous coaly sequence of the TKYF & the basal cg beds of the Digby Formation (**DGYF**) which are free of coal, carbonaceous & coaly matter & tuff & tuffaceous sediments; even in the few occurrences where these cgs are in contact with cg of the TKYF, they differ in composition allowing easy recognition of the boundary. DGYF cgs are mainly clast-supported with the matrix & cement forming less than 30% of the total volume of the rock. Clasts are often larger in size than those of the TKYF ranging up to cobble grade & are richer in colours because of abundance of red & green jaspers & to a lesser extent volcanics of different colours. Matrix is generally ss, similar to the clasts in composition. Cement is clayey but can be ferrugenous close to the surface & in outcrops. TKYF cgs are generally matrix-supported, rich in green volcanic clasts, tuff & tuffaceous matter & the clasts are generally small ranging from granule to pebble grade. Matrix is also rich in tuffaceous material & forms up to 70% of the rock. The boundary is erosive & represents Permo-Triassic unconformity surface (Tadros in press).
Age & evidence L.Permian Up.Stage 5c (McMinn in press).
Correlations broadly equivalent to Farmers Creek Formation of the W Sydney Basin.

TRIASSIC STRATIGRAPHY

DIGBY FORMATION (**DGYF**) (**Redefinition** Feng Xu Jian, C.R. Ward & N.Z. Tadros)
Named Digby Series or Digby Beds by Kenny (1929) after Parish of Digby, Digby Conglomerate (Russell 1981); the Digby Formation (Beckett et al. 1983) is present over much of the Gunnedah Basin except in the MCSB S of Deriah Forest. Discontinuous outcrops form a belt extending south from Narrabri to Willow Tree at the foot of the Liverpool Range. South of the Range, they reappear in the Murrurundi & the Binnaway-Wollar areas. **Type section & Thickness** DM Wilson DDH1 (181157mE, 1524330mN), 147m from 297m to 444m, *range:* 2m-204m. **Lithology** Lithic cg in the lower part & quartz ss with minor quatzose cg & ms beds at the top in the upper part. In the S basin area N of the Liverpool Range, the lower part of the quartz ss section is gradational from lithic to quartz lithic ss. **Relationships & boundary criteria** Unconformably & erosively overlies the Permian Black Jack Group in the MSB, metamorphic rocks of the Lachlan Fold Belt in the west & basement volcanics in the east. A basin-wide greyish-brown mudsone bed (a palaeosol), a few centimetres to 1m thick, marks a disconformity on the upper boundary beneath sediments of the Napperby Formation.
Age & evidence E.Triassic, *Lunatisporites pellucidus*, (equivalent to the *Punctatisporis walkomii* Zone of McMinn in press) *Protohaploxpinus samoilovichii* & *Artrisporites tenuispinosus* (equivalent to the *Artrisporites wollarensis* Zone of McMinn in press) palynological zones.

BOMERA CONGLOMERATE MEMBER (**BOMb**) (New name Feng Xu Jian, C.R. Ward & N.Z. Tadros)
Named after Parish of Bomera, the BOMb is present over much of the Gunnedah Basin except in the MCSB S of Deriah Forest. Discontinuous outcrops form a belt extending south from Narrabri to Willow Tree at the foot of the Liverpool Range. South of the Range, they reappear in the Murrurundi area.
Type section & Thickness DM Wilson DDH1 (181157mE, 1524330mN), 74m from 370m to 444m, *range:* to 113.5m **Lithology** Lithic, clast-supported pebble cg with subordinate lithic ss. Conglomerate consists of pebbles of varying composition, mainly red & green jasper, grey & dark grey laminated chert, silicic & mafic volcanics & white vein quartz in a lithic ss matrix. Volcanic pebbles of different colours are observed more in the basal part of the unit, jasper is relatively abundant in the middle, whereas light to dark grey chert & white vein quartz pebbles are common in the upper part (Jian 1991)
Relationships & boundary criteria Unconformably & erosively overlies the Permian Black Jack Group over a large part of the MSB. It also overlies metamorphic rocks of the Lachlan Fold Belt in the west & basement volcanics in the east. The unit is unconformably overlain by the Napperby Formation in the northern part of the basin in the Narrabri area, by sediments of the Ulinda Ss Member with a well-defined contact in the middle part, but gradationally in the southern part & in the Bellata area. The upper boundary is therefore marked by a sharp change in composition from lithic cg to sl & cs of the basal Napperby Group in the north, or to quartz ss of the Ulinda Sandstone Member in the middle, or to lithic & quartz-lithic ss of the basal part of the Ulinda Sandstone Member in the south & in the Bellata area (Jian 1991).
Age & evidence: The unit is barren of microfloral assemblages, but its age can be deduced from its position below the Ulinda Sandstone Member within the *Lunatisporites pellucidus* palynological zone (*Punctatisporis walkomii* Zone of McMinn in press).

ULINDA SANDSTONE MEMBER (**UDAMb**)(New, Feng Xu Jian, C.R. Ward & N.Z. Tadros)
Named after Parish of Ulinda, the Mb is present over much of the Gunnedah Basin except in the MCSB S of Deriah Forest. Discontinuous outcrops form a belt extending S from Boggabri to Willow Tree. South of the Liverpool poRange, they reappear in the Murrurundi area & in the SW in the Binnaway-Wollar area.
Type section & Thickness DM Wilson DDH1 (181157mE, 1524330mN), 73m from 297m to 370m.

N.Z. TADROS

Lithology Mainly quartzose ss, with subordinate quartzose cg&cs. Small to moderate amount of ms occurs at the top of the unit, especially in the south. In the SE part of the basin & locally in the Bellata area in the far north, the lower part of the UDA Mb is quartz-lithic & locally, lithic cg is present in places towards the base. A 2m flint clay bed is present in the middle of the UDAMb & is made up of kaolinitic interclasts set in well-crystallised matrix of vermicular kaolinite. A cs bed, 0.2m thick, occurs in the upper part of the unit, & consists of fine-grained well-crystallised kaolinite with minor amounts of anatase.
Relationships & boundary criteria Underlain, with well-defined contact, by the BOMb in the middle, & by transitional boundary in the S. In the west, where the BOMb. is absent, the unit rests on sediments of the Black Jack Group. In the westernmost areas, where the Permian sediments are also absent, the unit rests on metamorphosed basement rocks. It is unconformably overlain by the sls & css of the basal unit of the Napperby Fm. The upper boundary is marked by the top of a basin-wide ms bed (a palaeosol), up to 1m thick, & characterised by distinct geophysical response (marked increase in gamma & decrease in neutron log responses) (Jian 1991). **Age & evidence** E.Triassic *Protohaploxpinus samoilovichii* & *Artrisporites tenuispinosus* palynological zones (*Artrisporites wollarensis* zone of McMinn in press) The fine sediments within the quartz-lithic lower part of the Mb in the south contain E.Triassic *Lunatisporites pellucidus* palynological Zone (equivalent to *Punctatisporis walkomii* Zone of McMinn in press).

NAPPERBY FORMATION **(Redefinition, Feng Xu Jian, C.R. Ward & N.Z. Tadros)**
Named after a prominent outcrop of Napperby Beds or Series of Kenny (1929) on Parish of Tunmallalee, the Napperby Formation (Russell 1981, Beckett et al. 1983) is present over much of the Gunnedah Basin except in the Maules Creek Sub-basin S of Deriah Forest. Discontinuous outcrops form a belt extending south from Narrabri to Willow Tree at the foot of the Liverpool Range. South of the Range, they reappear in the Murrurundi area & in the southwest in the Binnaway-Wollar area south into the Sydney Basin.
Type section & Thickness DM Parkes DDH 3 (373941mE, 1607497mN), 148m from 275m to 423m, *range:* 30m-250m. **Lithology** An overall coarsening-up sequence; a) a lower part consisting of four coarsening-up & thickening sequences, each is up to around 10m thick, ascending up. from dark grey cs to interlaminated & thinly interbedded lithic ss & cs & finally to parallel-bedded & low-angle crossbedded off-white lithic ss. Bioturbation & burrows are common; b) a middle part dominated by dark grey cs, sl & interlaminated lithic ss & sl units in the SE part of the basin. In the middle & NE sectors, it consists mainly of lithic ss & cs organised into small coarsening-up sequences, together with crossbedded or parallel-bedded ss & rootlet-penetrated ms that forms fining-up sequences. In the W part of the basin, the lower part of the unit consists of dark grey silty-cs, the middle part of massive or parallel-bedded & crossbedded ss, & the upper part of further dark grey shaley sediment. Bioturbation & burrows are common (Jian 1991), & c) an upper part consisting mainly of off-white, medium-grained, crossbedded lithic ss, with rare ms clasts. Parallel-bedded & cross-bedded lithic ss, with irregularly interbedded ss/ms containing plant rootlets is dominant in the middle & S parts, . Along the W side of the basin, the unit consists mainly of dark grey cs & massive or parallel-bedded ss with ms clasts & crossbedded ss. Minor matrix-supported cg is present in the SW area.
Relationships & boundary criteria The lower boundary with the Digby Fm is disconformable & is marked by the upper surface of a basin-wide ms horizon (a palaeosol), a few centimetres to 1m thick. The upper boundary is either the base of the Deriah Fm or the regional unconformity surface overlain by the Middle Triassic to Jurassic Garrawilla Volcanics or the Jurassic Purlawaugh & Ukebung Formations & the Pilliga Sandstone (see Tadros in press for litho. descriptions of these units).
Aage & evidence: L.Early to Mid.Triassic; upper *Protohaploxpinus samoilovichii*, upper *Artrisporites tenuispinosus* (both are approximate equivalents of *Artrisporites wollarensis* Zone of McMinn in press) & lower *Artrisporites parvispinosus* palynological zones (McMinn in press).
Notes Talbragar Formation (Dulhunty 1973), Wallingarah Creek Formation (Higgins & Loughnan 1973, Bourke & Hawke 1977) & Wallingarah Formation (Loughnan & Evans 1978). Napperby Formation (Russell 1981, Beckett et al. 1983, Etheridge 1987). Bourke & Hawke (1977) & Etheridge (1987) also recognized two unnamed units at the top of the Triassic section referred to as "Unit 1" & "Unit 2". Martignoni (1986) introduced the terms "Eulah Sandstone" & "Deriah Formation" for the upper section of the Triassic sequence. Jian (1991) redefined the upper sequence as the Deriah Formation. Sediments of the two formations have a very close resemblance to those of the Wianamatta Group in the Sydney Basin (Hamilton 1987). However, palynological evidence suggests that the lower part of the unit can be correlated with the Gosford Formation & its equivalents (including the Newport Formation); the middle part with the Hawksbury Sandstone & the Ashfield Shale, & the upper part with the Bringelly Shale at the top of the Sydney Basin Triassic succession.

DERIAH FORMATION **(Redefinition, Feng Xu Jian, C.R. Ward & N.Z. Tadros)**
Named after Deriah State Forest to the east of Narrabri by Marignoni (1986) to describe the equivalent interval to the informally named "Unit 2" of Bourke & Hawke (1977). The term has been retained, but

redefined to include both "Unit 1" & "Unit 2" as originally identified by Bourke & Hawke (1977). The unit is present mainly in the N of the Gunnedah Basin, & to a lesser extent in the S & central areas.

Type section & Thickness DM Moema DDH1 (384420mE, 1672128mN), 160.6m from 174.5m to 335.1m, *range*,4.9m-160.6m.

Lithology The **lower part** of the formation consists dominantly of fine to medium-grained green lithic ss rich in volcanic fragments, with rare dark grey slitstone & cs beds at the top of the sequence. Mud clasts are very common in the ss, & are especially abundant at the base of the unit. The basal part of this sequence consists of coarse to very coarse-grained granule-bearing & often calcite-cemented feldspatholithic ss, up to 5m in thickness, characterised by common occurrence (up to 10%) of perthitic feldspar particles. The **upper part** consists of off-white lithic ss & dark grey to grey brown ms with plant rootlets & minor coaly laminations. A 25m lava succession of a Middle Triassic age (Morgan 1976, Dulhunty 1986) also occurs (DM Moema DDH1a) within this upper part (Jian 1991).

Relationships & boundary criteria The lower boundary with the Napperby Formation is very distinct in the northeastern part of the basin, where the medium-grained green lithic sss, with ms clasts that mark the base of the Deriah Formation are in contact with the mainly off-white, medium-grained, crossbedded lithic ss, rare in ms clasts. In the southern areas, the unit contrasts with the light green parallel-bedded & cross-bedded lithic ss, with irregularly interbedded ss & ms containing plant rootlets of the underlying Napperby Formation. The unit is disconformably overlain by medium-grained pebbly ss beds or coal seams of the Jurassic Purlawaugh Formation in the northern part of the basin, & by the Jurassic Garrawilla Volcanics in the southern & central areas. (Jian 1991)

Age & evidence Late Mid. Triassic, indicated by an upper *Artrisporites parvispinosus* (McMinn in press), characterised by the first occurrence of *Cadargasporites senectus*.

Correlations Palynological evidence suggests that the unit can be correlated with the Bringelly Shale at the top of the Sydney Basin Triassic succession.

Notes The Deriah Formation is proposed as a separate Triassic stratigraphic unit for several reasons. (1) the coarse to very coarse-grained ss at the base contrasts markedly to the fine to medium-grained ss of the Napperby Formation. (2) the different ss composition (indicating sudden change in provenance), with an abundance of green volcanic rock fragments, typically with clay rims, & light-coloured perthitic feldspars. (3) A lava horizon with a Middle Triassic age occurs within the upper part of the sequence, suggesting contemporaneous volcanic activity. (4) The unit has a distinctly different palynological assemblage, with the presence of an upper *A. parvispinosus* (McMinn in press) characterised by the first occurrence of *C. senectus*, distinguishing it from the underlying formations.

REFERENCES:

Beckett, J., Hamilton, D.,S., and Weber, C.,R., 1983. NSW Geol. S., QN, 51, 1-16. **Bourke, D.J., and Hawke, J.M., 1977.** NSW Geol.S. - QN 29, 7-18. **Britten, R.A. and Hanlon, F. N., 1975.** 2 Coal AusIMM M 6. **Brownlow, J.W., 1981.** Coal Geol. Gp. GSA J.2, 125-160. **Dulhunty, J.A., 1973.** J. Geol. Soc. Aus., 20(3), 319-328. **Dulhunty, J.A., 1986.** R. Soc.NSW, J. Proc. 119, 29-32. **Etheridge, L.T., 1987.** NSW Geol. S. QN 66, 1-21. **Hamilton, D.S., 1985.**Sed. Geol., 45; pp 35-75. **Hamilton, D.S., 1987.** Uni. Syd. thesis, Ph.D. **Hamilton, D.S., 1991.** Aus. J. E. Sc., 38, pp. 95-113. **Hamilton et al., 1988.** APEA J.28,218-241. **Higgins, M.L., and Loughnan, F.C., 1973.** Aus.IMM Proc. 246, 3-40. **Hanlon, F.N., 1949.** R. Soc. N.S.W. - J.& Proc. 82, 241-250 & 251-245. **Hunt, J.W., Brakel, A.T. & Smyth, M., 1986.** Geol.Soc. Aus. - J. Coal Geol. Gp.V. 6, 59-76. **Jian, Xu Feng, 1991.** Uni. NSW (Sydney) Thesis Ph.D. **Kenny, E.J., 1929.**NSW Dep. M. Ann. Rep. for 1928, p. 117-118. **Loughnan, F.C.,1975.** J.Sed. Pet.,45,591-598. **Loughnan, F.C., & Evans, P.R., 1978.** J. & Proc. R. Soc. NSW 111, 107-120. **Martignoni, J. 1986.** Uni.NSW, Dep. App. Geol.Thesis, B.Sc. **McDonald,S.J. & Skilbeck,C.G., 1991. 25yh Newcastle Symp. 138-145. McMinn, A., 1981.** NSW Geol.S., Paly. Rep. 1981/4 (GS 1981/025). **McMinn, A., 1982.** NSW Geol.S. - Rep. Paly. 1982/1 (unpublished) (GS 1982/002). **McMinn, A., in press.** In: **Tadros, N.Z. (ED),** NSW Geol. S., Memoir Geol,12. **Morgan, R., 1976.** NSW Geol.S.- Rep.Paly. 1976/10 (unpublished) (GS 1976/077) **and several other unpubl. GS reports for full listing see tadros (in press). Runnegar, B.N.,1970.** J.Geol.Soc.Aus. 16, 697-710. **Russell, T.G., 1981.** NSW Geol.S.-Rep. GS 1981/045 (unpublished). **Tadros,N.Z.,1982.** NSW Geol.S. On 48,1-18.**Tadros, N.Z., 1986.**NSW Geol. S. QN, 65, 20-34. **Tadros,N.Z.,1985.** NSW Geol.S. QN 59,1-18. **Tadros, N.Z., 1988.** NSW Geol.S. QN, 71, 1-18. **Tadros, N.Z. (ED), in press,** Gunnedah Basin, NSW. NSW Geol. S. Memoir Geology, 12. **Thomson,S.,1986.** Uni.N.Engl.,MSc Th. **Waters, D.D, 1971.** Uni. N'castle - B.Sc. H. Thesis.

N.Z. TADROS

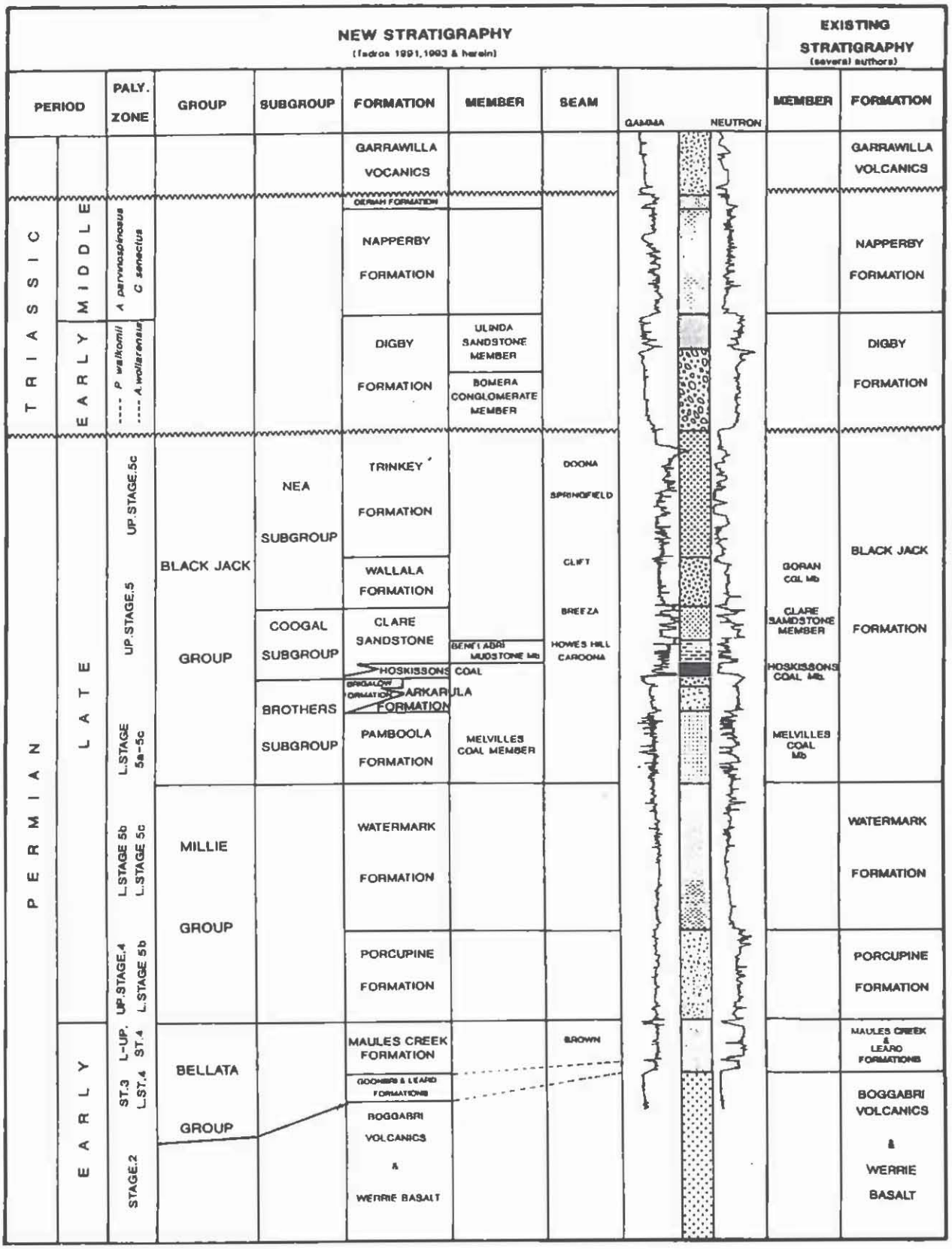

Table 1. New stratigraphy for the Gunnedah Basin.

NEW STRATIGRAPHY FOR THE GUNNEDAH BASIN

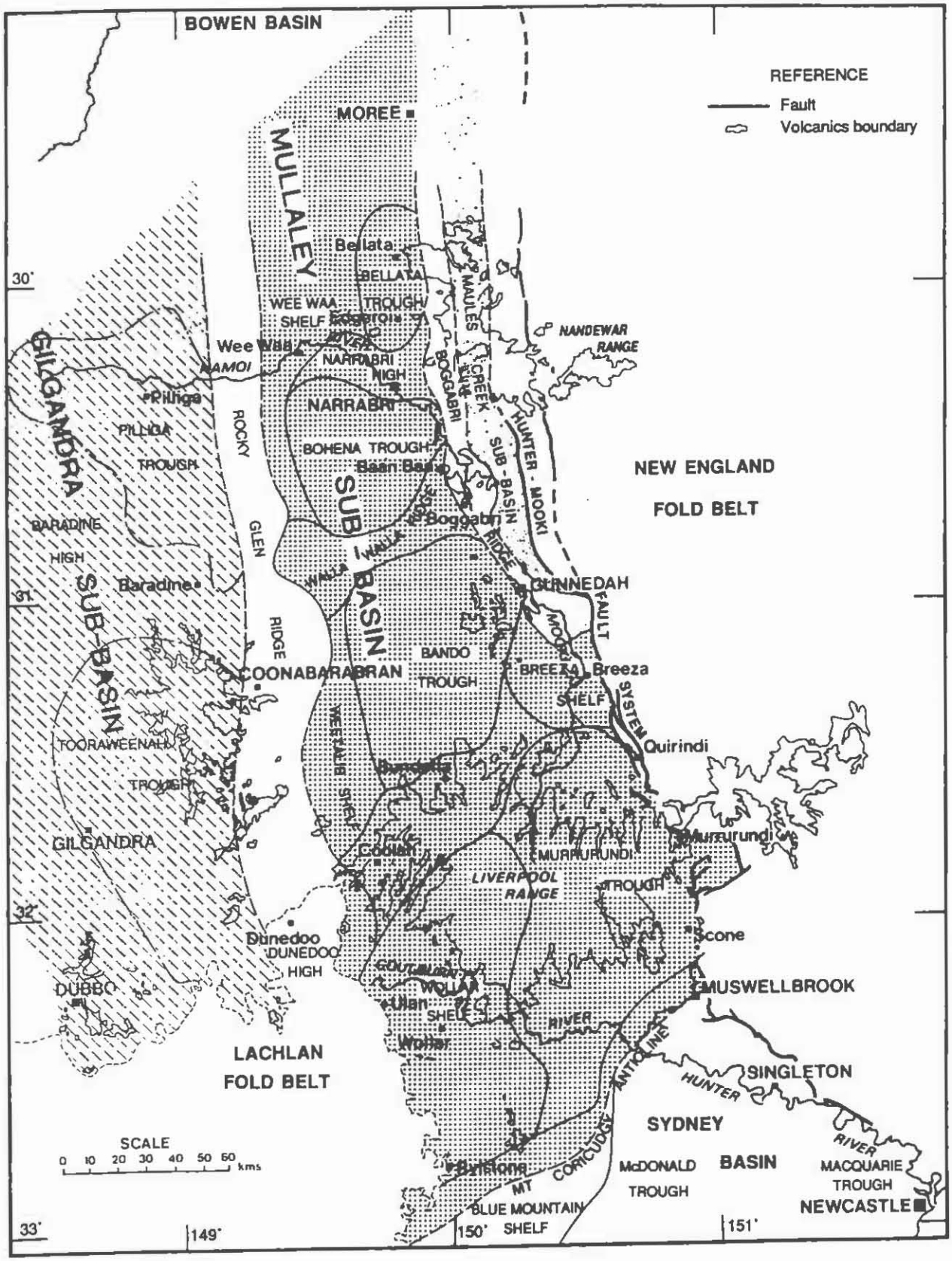

Figure 1. Gunnedah Basin. (Modified after Tadros in press).

CHRONOSTRATIGRAPHIC CORRELATION OF AUSTRALIAN PERMIAN DEPOSITIONAL SEQUENCES

D.J.C. BRIGGS
University of New South Wales

Eastern Australian Permian successions have long presented difficulties for international correlation, both because of problems inherent in their isolated and high-latitude palaeogeographic location, and because of secondary difficulties resulting from incomplete knowledge of Permian biotas and successions both locally and internationally. Slowness and persistent controversy in the development of an international chronostratigraphic framework for the Permian have exacerbated these problems. Recent studies of palynomorphs, foraminifera and macrofauna have however provided a clearer picture of local biostratigraphic successions, and recent systematic studies, mainly of brachiopods and foraminifera, have turned up some additional international links. Furthermore, recognition of the importance of the depositional sequence as the most natural unit for interregional correlation has led to the development of a chronostratigraphic scheme for the Permian that appears to be a considerable improvement on previously published schemes (Ross and Ross, 1987). These advances make reassessment of the international correlation of the eastern Australian Permian timely.

LOWER PERMIAN DEPOSITIONAL SEQUENCES OF WESTERN AUSTRALIA

The primary difficulty caused by the provincialism of eastern Australian Permian biotas can be attacked best by comparisons with basins that are palaeogeographically and palaeoclimatically intermediate with the traditional standard successions of Russia and the Tethys. For the Lower Permian the marine successions of Western Australia are of prime importance in this regard, as they on the one hand can be tied to the eastern Australian succession using microfloral, microfaunal and macrofaunal links, and on the other hand can be related to international chronostratigraphic units by virtue of their ammonoid faunas. Unfortunately the Late Permian of Western Australia contains marine macrofaunas at only two levels, neither of which can be closely tied to the eastern Australian succession.

The Permian of Western Australia is characterized by great lateral persistence of lithostratigraphic units, reflecting much greater tectonic stability than prevailed in eastern Australia. Investigations currently under way in the Canning Basin are delineating a succession of depositional sequences that, except in the lower, glacially influenced part of the sequence, have sheet-like geometries that can be traced laterally for great distances (O'Brien *et al.*, 1992). The Carnarvon Basin Permian has not yet been investigated from a sequence stratigraphic point of view, but the remarkable lateral persistence of its formations undoubtedly implies a similar situation. Detailed sedimentological studies (Hocking et al., 1985) permit recognition of a succession of basin-wide transgressive-regressive cycles, corresponding approximately to (in descending order) (a)

the Baker Formation-Coolkilya Sandstone-Mungadan Sandstone (b) the Quinnanie Shale-Wandagee Formation-Nalbia Sandstone (c) the Bulgadoo Shale-Cundlego Formation (d) the Madeline/Coyrie Formation-Mallens Sandstone, (e) the Billidee Formation - Keogh Formation, (f) the Cordalia Sandstone - Moogooloo Sandstone, (g) the Callytharra Formation, (h) the Carrandibby Formation and (i) the Lyons Formation. An unconformity marked by karstification separates the Callytharra Formation (cycle g) from the overlying Wooramel Group (cycles e and f). As in eastern Australia, these cycles typically consist of a narrow transgressive phase at the base below a much thicker regressive phase. The Perth Basin is continuous offshore with the Carnarvon Basin, and contains lithological equivalents of the Lyons Formation (Nangetty Formation), Carrandibby Formation (lower Holmwood Shale), Callytharra Formation (upper Holmwood Shale, including Woolaga and Fossil Cliff Members), Wooramel Group (Irwin River Coal Measures including High Cliff Sandstone) and lower Byro Group (Carynginia Formation).

Figure 1 summarizes microfloral, microfaunal and macrofaunal evidence that permits correlation of this succession with that of eastern Australia (Briggs, this volume). While caution should be exercised in attaching chronological significance to biostratigraphic links over such large distances, the consistency of these links makes any substantially different alternative correlation seem unlikely. The biostratigraphic links are:

1. Incoming of *Microbaculispora tentula*. This spore, whose incoming marks the base of APP1.2, occurs in the Nangetty Formation (Segroves, 1970), Lyons Formation (Kemp et al., 1977) and throughout the Grant Formation (Foster and Waterhouse, 1988).

2. Range of *Lyonia* Archbold. This productid genus has a restricted range both in eastern Australia, where it is confined to the *Lyonia* n. sp. Zone (sequence II1), and in Western Australia, where it is confined to the Lyons Formation (Carnarvon Basin).

3. The macrofaunal assemblage described by Foster and Waterhouse (1988) from the base of the middle member of the Grant Formation (Carrandibby sequence) in WMC Calytrix 1 contains a strophalosiid most closely comparable to *Strophalosia concentrica* Clarke, and the gastropod *Paraplatyschisma* aff. *twelvetreesi* (Dun), which together suggest correlation with the "*Trigonotreta* n. sp. Zone" and sequence II2 in eastern Australia. *Eurydesma playfordi* Dickins, which has its type occurrence in the Carrandibby Formation, is closely allied to the eastern Australian species *Eurydesma burnettensis* Waterhouse which typifies the "*Trigonotreta* n. sp. Zone".

4. *Ammodiscus oonahensis* foram Zone. The presence of this zone in the upper Grant Formation, upper Lyons Group, and Holmwood Shale (below the Fossil Cliff Member) in western Australia, and the Quamby Formation ("*T.* n. sp. Zone" correlative) in Tasmania (Palmieri, 1990) support the correlation implied by the macrofaunal elements listed above under point (3). [Palmieri's record of the *A. oonahensis* Zone from the Allandale Formation is incorrect; this formation and the underlying upper Lochinvar Formation are now known to belong to the succeeeding *H. woodwardi* Zone (Palmieri, pers. comm., 1992].

5.The incoming of *Diatomozonotriletes townrowi* in western Australia occurs in the uppermost Grant Formation in parts of the Canning Basin (Powis, 1984), and within the Holmwood Shale at or below the base of the Fossil Cliff Member (Foster et al., 1985); in eastern Australia this event occurs low in palynological stage APP2.1. The true distribution in western Australia of *Verrucosisporites pseudoreticulatus*, the index species of APP2.1, is presently unclear due to reported confusion of this species with *Granulatisporites confluens*(Foster and Waterhouse, 1988).

6. The *Howchinella woodwardi* foram zone enters the eastern Australian succession in sequence II3; in western Australia this zone enters the succession in the Fossil Cliff Member and Callytharra Formation (Callytharra sequence) (Palmieri, 1990).

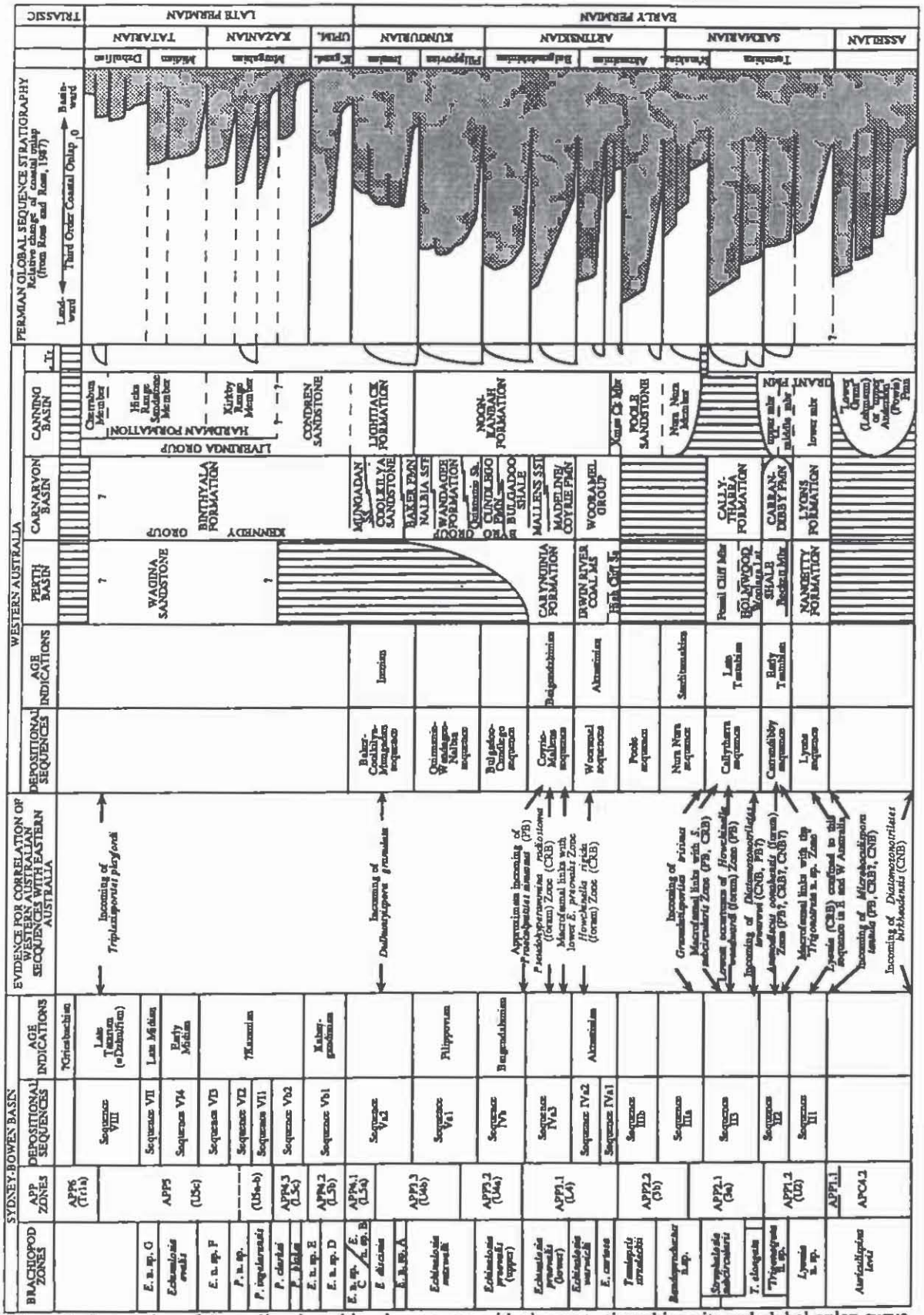

Figure 1. Correlation of Australian depositional sequences with chronostratigraphic units and global onlap curve.

7. The bivalve *Deltopecten waterfordi* Dickins has been figured from the Glencoe Formation in Tasmania (Runnegar, 1969, p. 88); in Western Australia this species occurs in the Fossil Cliff Member and the Callytharra Formation.

8. The incoming of the spore *Granulatisporites trisinus* marks the base of APP2.2, which in eastern Australia lies within sequence IIIa; in western Australia this incoming is recorded within the Nura Nura Member (Lehmann, 1986, fig. 4). *G. trisinus* is apparently absent in the Fossil Cliff Member and Callytharra Formation (Foster et al., 1985), which previously have been correlated with the Nura Nura Member, but which contains a different ammonoid fauna, of Tastubian rather than Sterlitamakian affinities (see below).

9. The *Howchinella rigida* foram Zone, which in eastern Australia corresponds roughly to the *Echinalosia warwicki* Zone, in western Australia is found within the Jimba Jimba Calcarenite member of the Billidee Formation (Palmieri, 1990).

10. Macrofaunal links exist between the lower *E. preovalis* Zone of eastern Australia and the Coyrie-Mallens sequence of western Australia. A bivalve resembling *Pseudomyalina mingenewensis* (Etheridge) from the Mingenew Formation (Coyrie Formation correlative, Perth Basin) occurs in the Tiverton Formation at Homevale (Runnegar, 1969) in collections from "Zone 10" of Campbell (1961), within the lower *E. preovalis* Zone. *Aulosteges lyndonensis* Coleman from the Madeline Formation closely resembles the eastern Australian *Taeniothaerus homevalensis* Briggs, and *Aulosteges ingens* Hosking from probable Coyrie Formation is closest to *Taeniothaerus acanthophorus* (Fletcher). *T. homevalensis* is restricted to the lower *E. preovalis* Zone, while *T. acanthophorus* occurs in both the lower and the upper *E. preovalis* Zones.

11. The incoming of *Praecolpatites sinuosus*, defining the base of APP3.2, was thought by Backhouse (1991) to lie a short distance above the Irwin River Coal Measures in the Perth Basin, but, from the general succession of microfloras, to be at slightly lower level than in eastern Australia, where this incoming lies near the base of sequence IVb.

12. The *P. radiostoma* foram Zone typifies lower *Echinalosia preovalis* Zone units in eastern Australia and the lower Byro Group in WA (Palmieri, 1990).

13. The incoming of *Dulhuntyispora*, marking the base of APP4, lies within sequence Va2 in eastern Australia, and approximately at the base of the Kennedy Group (ie base of Coolkilya Sandstone) in western Australia (Kemp et al., 1977).

INTERNATIONAL CHRONOSTRATIGRAPHIC CORRELATIONS

Sequence II1/Lyons sequence. This sequence is not directly dated in either eastern or western Australia, and is constrained only by the early Tastubian age of sequence II2. The Asselian age adopted earlier (e.g. Briggs, 1989) remains possible, but an earliest Tastubian age now seems more likely in the light of Early Permian zircon dates obtained from older stratigraphic units in New South Wales by Roberts et al. (1991).

Sequence II2/Carrandibby sequence. In the Perth Basin this sequence contains the ammonoid *Juresanites jacksoni* (Etheridge), considered Tastubian by Glenister *et al.* (1973, p. 1033) based on sutures closest to the lower Tastubian *J. kazakhorum* Ruzentsev.

Sequence II3/Callytharra sequence. Assessment of ammonoid evidence for the age of units of this sequence in western Australia (Woolaga and Fossil Cliff Members, Perth Basin; Callytharra Formation, Carnarvon Basin) has been distorted by the correlation by earlier workers of the latter two units with the younger (Sterlitamakian) Nura Nura Member (Canning Basin). The only firm ammonoid evidence is that provided by *Metalegoceras kayi* Glenister, Windle and Furnish from the Fossil Cliff Member, which resembles the Upper Tastubian *M. distale* Ruzhentsev (Glenister *et al.*, 1973, p. 1046). All other ammonoids from the Callytharra sequence give less precise ages,

compatible with the Late Tastubian age implied by *M. kayi*. On the basis that *Uraloceras* Ruzhencev first appears in the Upper Tastubian, Glenister and Furnish (1961, p. 686) took the incoming of *Uraloceras irwinense* Teichert and Glenister in the Woolaga Limestone Member of the Perth Basin to indicate a Late Tastubian age, and suggested a Sterlitamakian age for the stratigraphically higher Fossil Cliff Formation. The chronostratigraphic significance thus attached to *U. irwinense* no longer exists now that this species has been transferred by Glenister *et al.* (1990) to the Asselian - Sterlitamakian genus *Svetlanoceras* Ruzhentsev. Glenister and Furnish (1961, p. 686) concluded that *Metalegoceras* n. sp. from the Callytharra Formation was "compatible with either a late Sakmarian or an Artinskian age". It would be incorrect to interpret the expression "late Sakmarian" in this context to mean specifically and exclusively Sterlitamakian: Glenister *et al.* (1973, p. 1031) used the same expression for the age of the Fossil Cliff Formation while explicitly stating that the precise age could be either late Tastubian or Sterlitamakian (ibid., p. 1047).

Sequence IIIa/ Nura Nura sequence. *Propopanoceras ruzhencevi* Glenister and Furnish indicates a Sterlitamakian age for the Nura Nura Member based on its resemblance to a species from the Urals (Glenister and Furnish, 1961, p. 686).

Sequence **IIIb/Poole sequence.** Either Sterlitamakian or Aktastinian, based on the age of younger and older sequences; no direct evidence is available.

SequencesIVa1-2/ Wooramel sequences. These sequences are considered Aktastinian, following the assessment of the age of the Wooramel Group by Archbold (1991). The Wooramel Group was regarded as Baigendzhinian by Cockbain (1980) because of the presence of the ammonoid *Pseudoschistoceras simile* Teichert, but Archbold (1991) pointed out that the Baigendzhinian age assigned to *Pseudoschistoceras* was based on a very small number of described occurrences, and argued that the affinities of the brachiopods of the Wooramel Group on balance indicated an Aktastinian age.

Uraloceras lobulatum and *U. whitehousei* of Armstrong *et al.* (1967) from the lower Tiverton Formation (*E. warwicki* and basal *E. preovalis* Zones) were assigned an "Artinskian, probably Aktastinian" age by their authors based on their closest resemblances, despite some consistent differences, to species mostly from the Aktastinian of the Urals. Bogoslovskaya and Pavlova (1988) placed *U. lobulatum* in the new genus *Gobioceras* Bogoslovskaya, but accepted a "mid-Artinskian" age for the species.

Sequence IVa3 / Coyrie-Mallens sequence Glenister and Furnish (1961, p. 687) dated the ammonoids *Neocrimites* sp. and *Propinacoceras* n. sp. from the Coyrie Formation as Baigendzhinian, noting striking similarity of the former to *N. fredericksi* (Emiliancev) from the type Baigendzhinian. The presence of *Neocrimites* in itself is significant as this genus first appears in the Baigendzhinian (Glenister and Furnish, 1961, p. 728). The productoids *Magniplicatina undulata* Waterhouse and *Anidanthus paucicostatus* Waterhouse from the *E. preovalis* Zone resemble forms from the Artinskian of Russia.

Sequence IVb/ Bulgadoo-Cundlego sequence. Occurrences of *Neocrimites* in units of sequence IVb in eastern Australia (basal Gebbie Formation (*sensu* Malone et al.), the lower South Curra Limestone and the basal Elderslie Formation) confirm the Baigendzhinian or younger age implied by the correlation sequence IVa3.

Sequence Va1/ Quinnanie-Wandagee-Nalbia sequence. An Early Kungurian (Filippovian) age is suggested by the ages of the preceding and succeeding sequences. The ammonoid *Bamyaniceras australe* (Teichert), found in the Quinnanie-Wandagee-Nalbia sequence in the Carnarvon Basin, was taken by Glenister and Furnish (1961, p. 687) to indicate a Baigendzhinian age, but this species must range well into the Kungurian as it occurs up to the same level as the Irenian (late Kungurian) species *Paragastrioceras wandageense* Teichert (see below). The lower *E. maxwelli* Zone contains the brachiopod *Megousia* Waterhouse, which seems to first appear in Kungurian or "Leonardian" strata worldwide.

Sequence Va2/ Baker-Coolkilya-Mungadan sequence. Ammonoids apparently from this sequence in the Carnarvon Basin include two species of chronostratigraphic significance, indicating an Irenian age. *Paragastrioceras wandageense* closely resembles *P. kungurense* Mirskaya from the Irenian of central Cisuralia (Bogoslovskaya, 1976). Some confusion exists as to whether the sole known specimen came from the Baker Formation (Glenister and Fuurnish, 1961) or the underlying Nalbia Sandstone (Cockbain, 1980, p.103), but Archbold and Dickins (1991, p. 3) support the former position. *Daubichites goochi* (Teichert) from the Coolkilya Sandstone and *Daubichites* sp. from the same locality as *P. wandageense* indicate correlation with "Chihsian Stage" of Kozur (1977), implyng an immediately pre-Kubergandinian age.

Sequence Vb1. An earliest Late Permian (i.e. Kubergandinian) age was suggested by Dickins *et al.* (1989) for the Mangarewa Formation (*sensu* Waterhouse) of New Zealand and the basal Blenheim Formation (*sensu* Dickins) of the northern Bowen Basin, both of which belong to sequence Vb1. A Kubergandinian age for this sequence is consistent with its position immediately above the Irenian sequence Va2.

Sequence Vb2 and sequences VI1-3. This interval may be correlated broadly with the Kazanian based on the links of preceding and succeeding sequences, but direct evidence is limited. This interval corresponds to the range of "Fauna IV" as first defined in the northern Bowen Basin, and in the western Bowen Basin includes towards the top the occurrence of *Atomodesma bisulcatum* Dickins in the Crocker Formation which Dickins (1961) compared with Kazanian species from Timor and Siberia.

Sequence VI4. In the Denison Trough this sequence contains the youngest foram zones of Palmieri (1990), said to share direct links with units as young as early Midian in peripheral Tethyan areas (Palmieri, 1990 and pers. comm.).

Sequence VII . This sequence is a probable correlative of the *Plekonella multicostata* Zone of New Zealand, which shares several links with "early Chhidruan" or "Kalabaghian" faunas in Pakistan and Timor (Waterhouse, 1982, p. 101). The Kalabagh - lowermost Chhidru Formation was assigned by Kozur (1977) to the Abadehian, or late Capitanian (=late Midian) of Ross and Ross (1987).

Sequence VIII . The incoming of *Triplexisporites playfordi* within this sequence provides a link with uppermost Permian (Dzhulfian *sensu* Ross and Ross) units in the Canning Basin (upper Hardman Formation: Kemp *et al.*, 1977) and Salt Range (Chhidru Formation: Balme, 1970). In Australia the top of the Permian is conventionally taken at either the first appearance of, or the appearance of "appreciable numbers" of, the spore *Lunatisporites pellucidus*, events which in the Sydney-Bowen Basin occur somewhat above the base of the Narrabeen and Rewan Groups. This correlation may need to be revised in the light of Balme's (1979) discovery of an earliest Triassic microflora in East Greenland, apparently stratigraphically lower than the*Taeniaesporites* (or *Lunatisporites*) dominated microfloras, and locally associated with early Griesbachian marine macrofossils. From Balme's description this microflora, his "*Protohaploxypinus* Association", appears to be comparable to the "Tr1a microfloras" of the basal Narrabeen Group. This comparison suggests that sequence boundary VIII, at the base of the Rewan and Narrabeen Groups, may closely coincide with the Permian-Triassic boundary.

In the time scale of Ross and Ross (1987), the "Djulfian", comprising the Wuchiapingian and Changhsingian, is equated with the Upper Tatarian or Vjatska Substage (Zone of *Suchonellina fragiloides*). Correlation of sequence VIII with the Upper Tatarian is supported by the presence of conchostracans typical of the Vjatska Substage in the "Belmont series" or upper Newcastle Coal Measures (Kozur, 1977, p. 96).

CORRELATION WITH THE SEQUENCE STRATIGRAPHIC CURVE OF ROSS AND ROSS (1987)

Ross and Ross (1987) published detailed curves showing eustacy and relative change of coastal onlap for the Carboniferous and Permian Periods. These curves appear to have been derived mainly from studies of North American successions, but were correlated with successions in Europe and Tethys, and were claimed to be globally applicable. Ross and Ross (1987) made no attempt to correlate these curves with successions in the Gondwanan region, presumably because of the then insurmountable difficulties associated with correlation with the region.

Figure 1 shows a correlation of Australian Permian depositional sequences with the global sequence stratigraphic curve of Ross and Ross (1987), using the chronostratigraphic correlations outlined above. The correlation is reasonably firm in the Sakmarian to Kungurian interval, where control is relatively precise, due largely to the ammonoid data from western Australia. Late Permian chronostratigraphic correlations are much less firmly based, but nevertheless an apparent correlation (shown by dashed lines) appears to be recognizeable. Comparison with the correlation chart of depositional sequences in the Sydney - Bowen Basin (Briggs, this volume) reveals many agreements in terms of relative importance of sequence boundaries, and degree of coastal onlap of depositional sequences, between the Ross and Ross curve and their proposed correlatives in eastern Australia. Among these points of similarity may be noted the particular importance in both of sequence boundaries I, II, IIIb, IVa, IVb, Va, Vb1, and VII, and the overall (second order) pattern of coastal onlap, which reaches a broad peak throughout the Sakmarian to Ufimian interval, and thereafter declines markedly into the Late Permian. These similarities appear to corroborate the proposed correlations, which permit far more precise international correlation of eastern Australian successions than has been possible up to the present.

REFERENCES

ARCHBOLD, N.W., 1991: Studies on Western Australian Permian brachiopods 10. Faunas from the Wooramel Group, Carnarvon Basin. Proc. R. Soc. Vict. 103, 55-66.

ARCHBOLD, N.W., & DICKINS, J.M., 1991: Australian Phanerozoic Timescales: 6. A standard for the Permian System in Australia. Bur. Min. Res., Aust. Rec. 1989/36.

ARMSTRONG, J.D., DEAR, J.F., & RUNNEGAR, B.N., 1967: Permian ammonoids from eastern Australia. J. geol. Soc. Aust, 14, 87-97.

BACKHOUSE, J., 1991: Permian palynostratigraphy of the Collie Basin. Rev. Palaeobotany Palynology, 67, 237-314.

BALME, B.E., 1970: Palynology of Permian and Triassic strata in the Salt Range and Surghar Range, West Pakistan. *In* B. Kummel and C. Teichert (eds), Stratigraphic boundary problems: Permian and Triassic of West Pakistan. Univ. Kansas , Spec. Publ. 4, 305-453.

BALME, B.E., 1979: Palynology of Permian-Triassic boundary beds at Kap Stosch, East Greenland. Meddelelser om Gronland, Bd. 200 *(6)*, 1-37, 3 pls.

BOGOSLOVSAKAYA, M.F., 1976: Kungurian ammonoids from central Cisuralia. Paleont. J., 1976(4), 417-424.

BOGOSLOVSKAYA, M.F., & PAVLOVA, Ye. Ye., 1988: On the development of the ammonoids of the Family Spirologeoceratidae. Paleont. J. *1988(2)*, 104-108.

BRIGGS, D.J.C., 1989: Can macropalaeontologists, palynologists and sequence stratigraphers ever agree on eastern Australian Permian correlations? Adv. Stud. Syd. Bas., 23rd Newcastle Symp.: 11-17.

CAMPBELL, K.S.W., 1961: New species of the Permian spiriferoids *Ingelarella* and *Notospirifer* from Queensland and their stratigraphic implications. Palaeontographica A, 117, 159-192.

COCKBAIN, A.E., 1980: Permian ammonoids of the Carnarvon Basin - a review. Geol. Surv. W. A., Ann. Rep. 1979, 100-105.

DICKINS, J.M., 1961: Permian pelecypods newly recorded from eastern Australia. Palaeontology, 4, 119-130, pl. 16.

DICKINS, J.M., ARCHBOLD, N.W., THOMAS, G.A., & CAMPBELL, H.J., 1989: Mid-Permian correlations. Compte Rendu XIe Congres Internationale Stratigraphie et Geologie du Carbonifere (Beijing, 1987), 2, 185-198.

FOSTER, C.B., PALMIERI, V. & FLEMING, P.J.G., 1985: Plant fossils, Foraminiferida, and Ostracoda from the Fossil Cliff Formation (Early Permian, Sakmarian), Perth Basin, Western Australia. Spec.Publ. S. A. Dept Mines Energy, 5, 61-105.

FOSTER, C.B. & WATERHOUSE, J.B., 1988: The *Granulatisporites confluens* Oppelzone and Early Permian marine faunas from the Grant Formation on the Barbwire Terrace, Canning Basin, Western Australia. Aust. J. Earth Sci 35, 135-157.

GLENISTER, B.F., BAKER, C., FURNISH, W.M., & THOMAS, G.A., 1990: Additional Early Permian ammonoid cephalopods from Western Australia. J. Paleont. 64, 392-399.

GLENISTER, B.F., & FURNISH, W.M., 1961: The Permian ammonoids of Australia. J. Paleont. 35, 673-736.

GLENISTER, B.F., WINDLE, D.L. Jnr, & FURNISH, W.M., 1973: Australian Metalegoceratidae (Lower Permian ammonoids). J. Paleont. 47, 1031-1047.

HOCKING, R.M., MOORS, H.T., & VAN DE GRAAFF, W.J.E., 1987: Geology of the Carnarvon Basin Western Australia. Bull. Geol. Surv. W.A., 133.

KEMP, E.M., BALME, B.E., HELBY, R.J., KYLE, R.A., PLAYFORD, G., & PRICE, P.L., 1977: Carboniferous and Permian palynostratigraphy in Australia and Antarctica - a review. BMR J. Aust. Geol. Geophys., 2, 177-208.

KOZUR, H., 1977: Beitrage zur Stratigraphie des Perms. Teil 1. Probleme der Abgrenzung und Gleiderung des Perms. Freiberger Forschungshefte C319, 79-121.

LEHMANN, P.R., 1986: The geology and hydrocarbon potential of the EP 104 permit, northwest Canning Basin, Western Australia. APEA J., *26*, 261-284.

O'BRIEN, P.E., LINDSAY, J.F., JACKSON, M.J., KENNARD, J.M., SOUTHGATE, P.N., & SEXTON, M.J., 1992: Sequence stratigraphy of Permian siliciclastics in the Fitzroy Trough, Canning Basin, Western Australia. Geol. Soc. Aust. Abst. 32, 111.

PALMIERI, V., 1990: Permian foraminifera of Australia. Geol. Soc. Aust. Abst. 25, 53-4.

POWIS, G.D., 1984: Palynostratigraphy of the Late Carboniferous sequence, Canning Basin, W.A. In Purcell, P.G. (ed.), The Canning Basin, W.A. 429-438.

ROBERTS, J., CLAOUE-LONG, J.C. & JONES, P.J., 1991: Calibration of the Carboniferous and Early Permian of the southern New England Orogen by shrimp ion microprobe zircon analyses. Adv. Stud. Syd. Bas., 25th Newcastle Symp., 38-43.

ROSS, C.A., & ROSS, J.R.P., 1987. Late Palaeozoic sea levels and depositional sequences. Cushman Found. Foram. Research. Spec. Publ. 24, 151-168.

RUNNEGAR, B., 1969: The Permian faunal succession in eastern Australia. Geol. Soc. Aust., Spec. Publ. 2, 73-98.

SEGROVES, 1970: The sequence of palynological assemblages in the Permian of the Perth Basin, Western Australia. 2nd Int. Gondwana Symp. Sth Africa, 511-529.

WATERHOUSE, J.B., 1982: New Zealand Permian brachiopod systematics, zonation, and palaeoecology. Geol. Surv. N. Z., Paleont. Bull. 48.

EPISODIC FOSSIL CONCENTRATIONS IN A HAWKESBURY SANDSTONE SHALE LENS AT SOMERSBY, NSW

P.S. WATSON
University of Queensland

Hawkesbury Sandstone shale lenses are usually finely laminated. Light silty laminae representing higher energy, oxygenating phases are coupled with dark, finer grained, clay laminae reflecting lower energy, reducing conditions. The fish bearing lens at Somersby was similarly finely laminated but the fish, if viewed as sedimentary particles, did not occur as regularly and cyclically as other sedimentary particles. Nor were they restricted to the finer grained layers but sometimes occurred in silty/sandy bands where they, uncharacteristically, retained finely preserved features.

The deposition of fossil fish in the Glendale fish lens, and likely to some extent in the other lenses, appears to have been episodic rather than cyclic/regular. Mortality horizons of varying fossil concentrations were separated by varying thicknesses of barren mudstone.

Fossil fish horizons appeared to represent closed basin conditions when water levels fluctuated widely, fish were concentrated and susceptible to asphyxiation. Barren horizons and barren lenses appear to reflect open basin conditions, wide spacing or escape of biota, oxygenation and hence rapid disintegration and disappearance of remains.

In such small basins, gradients are exaggerated with increased likelihood of sedimentation via fluidised sediment/turbidity flow. This is possibly the critical factor in whether a plant or animal is buried and preserved or not. The case of one mortality horizon where fossil fish, plants and pebbles occur variously throughout an interval up to 15 cm thick points to this possibility.

In this particular case the source of the sediment was likely collapse of unstable margins brought about by lowering water level or by crevasse splays or by channel avulsion triggering off collapse of small scale alluvial fans. The presence of abraded plant fossils point to this latter.

Other quite different mortality horizons reflecting more open basin conditions also existed in the lens. They may be the model for fossil fish occurrences in other lenses. The texture of the mudstone needs to be explained. Fish lenses in the southern parts of the Hawkesbury Sandstone have very fine grained shales and correspondingly exquisite fossil preservation, features likely to overbank and overload deposition of suspension fines which then settle out particle by particle in quiet protected basins.

But in this lens the texture is somewhat coarse and grainy and fossil preservation correspondingly mediocre and indistinct. Some process of pelletal flocculation seems to have been at work with silt and fine sand particles trapped within the floccules. This is more typical of estuarine or marine environments but in a fresh water regime it suggests agitated water with a high rate of interparticulate collisions and this points back to principally channel deposition of fines. If the lake was quiet and protected, flocculation must have occurred upstream. Suspension of floccules rather than particles requires higher energy current and so the hydrodynamic regime in this north easterly part of the floodplain may have been more turbulent than to the south, or the muds were more mature by this stage.

Like the sediment, the flora and fauna also appeared to have been allochthonous. The assemblage was restricted to fish and plants and this bias suggests their provenance was elsewhere, unlike the Lagerstatten at Beacon Hill and Hornsby.Heights lenses. The fish were not washed in from outside but swam in and were trapped. The "Hawkesbury Lakes" were interconnected or the Glendale lake was connected to a much larger lake or lagoon where the fish were nurtured and grew. Fish appeared to be migrating from a Narrabeen Group lagoon, perhaps near a coast, up the river system to final domicile in the Wianamatta aquatic regime. The Glendale lake was just above the Narrabeen/Hawkesbury boundary and had a mingling of both types of fish.

There was also bias in the size of the fossil fish and fish less than 1-2 years of age appeared to be missing, with rare exceptions. This suggests that significant precipitation, and hence spawning, had not occurred in the catchment area for 1-2 years and this further points to the fluctuating nature of the hydrologic regime and probably the climate.

MARINE ENVIRONMENTS IN THE EARLY TO MIDDLE TRIASSIC NARRABEEN GROUP

C. HERBERT
Macquarie University

INTRODUCTION

Early to Middle Triassic Narrabeen Group sediments in the Sydney Basin have traditionally been regarded as dominantly of alluvial to lacustrine origin. Recently authors have recognised marine influences in some formations. For example, Conolly (1969) regarded Bald Hill Claystone red-beds as marine bay deposits and Bunny and Herbert (1971) suggested a marine influence in the Newport Formation. Uren (1980) suggested an estuarine influence for the Dooralong Shale. Most recently, Naing (1990) identified brackish marine horizons in the Bald Hill Claystone and Newport Formation from a study of trace fossils, and here I describe further evidence that sea-level changes controlled sedimentation throughout the entire Narrabeen Group.

Sedimentary facies change markedly from dominantly alluvial in western and southern areas to increasingly more marine to the northeast (figs 1 and 2). Thus vertically stacked sandstone sequences in the Blue Mountains appear to be dominantly alluvial (although with minor estuarine influence) whereas to the northeast, as seen in coastal outcrops, marine shoreline sands and offshore siltstones were deposited.

Marine conditions were dominant where the Narrabeen Group attained its greatest thickness indicating that fluvial sedimentation rates were insufficient to overcome the more rapid subsidence rates in the northeastern part of the basin.

Only those formations showing marine influences in coastal outcrops along the Central Coast will be discussed here, with brief reference to southwestern parts of the basin. Formations are described from the base of the Narrabeen Group to the top.

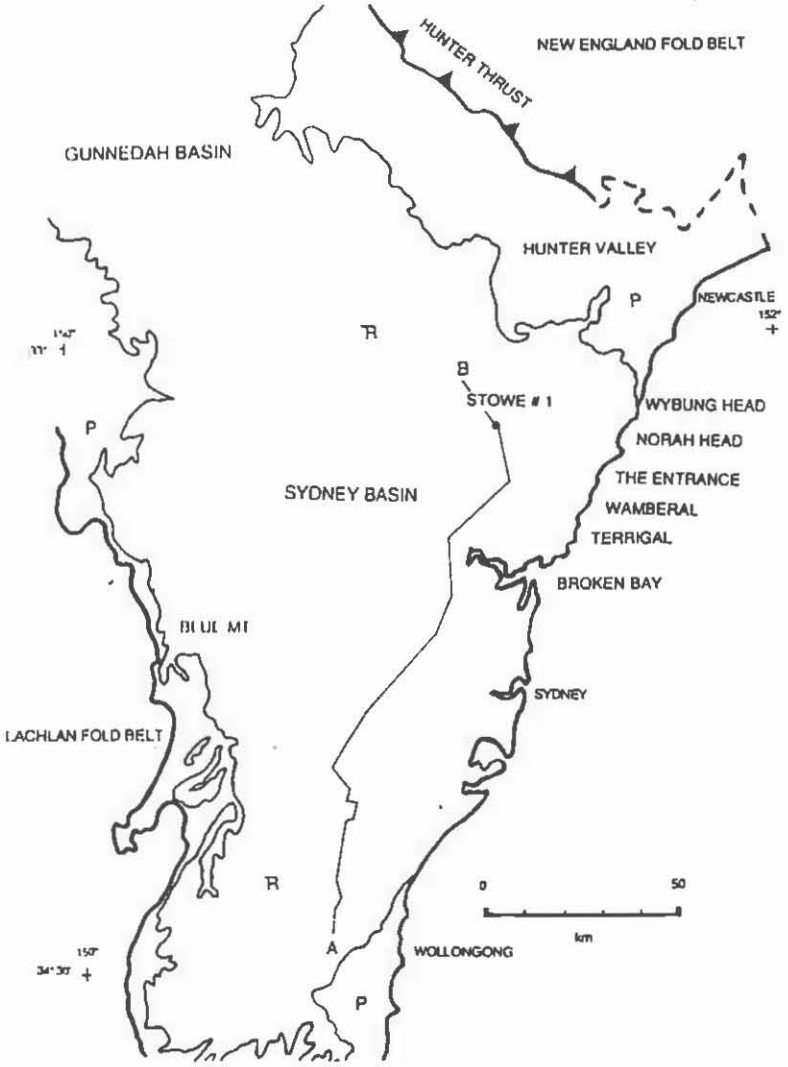

Figure 1. Locality map. Narrabeen Group occurs in outcrop and subsurface across the entire basin within the inner thin line shown on the map.

Figure 2. South to north cross-section of the Narrabeen Group. See figure 1 for location.

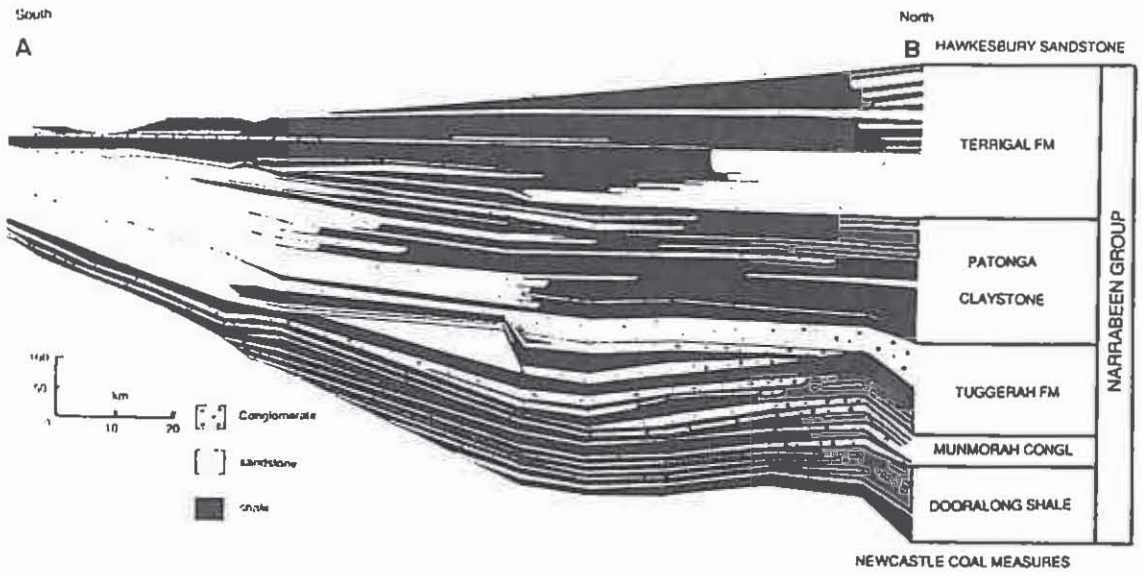

MARINE ENVIRONMENTS - NARRABEEN GROUP

DOORALONG SHALE

At Wybung Head, the Dooralong Shale consists of interbedded green-grey sandstone and green and grey shale in units about 10m thick. Sandstones have erosive bases, consist of coarse sand with conglomerate, and were deposited by low-sinuosity rivers and estuaries. Each coarse-grained sandstone is transgressively overlain by variably bioturbated shale and fine- to medium-grained sandstone. The latter sandstone grades up into both coarsening-up and fining-up sandstone/shale sequences indicating, deposition in a complex of coastal-plain environments including alluvial and estuarine channels, floodplains, lakes, lagoons, with associated crevasse splays, subdeltas and lacustrine to lagoonal shorelines. Abundant acritarchs in the Dooralong Shale are consistent with a paralic interpretation (Grebe 1970).

TUGGERAH FORMATION

Only the top of the Tuggerah Formation can be observed on the coast at Norah Head where it is composed of stacked, erosively based, fluvial/estuarine sandstones and conglomerate. Trough crossbedding shows that paleocurrents trended in both southeast and northwest directions indicating the possibility of tidal influence. Bioturbation and tetrapod tracks support a fluvial/estuarine interpretation.

The two topmost sandstones, each about 8m thick, are interbedded with thin, strongly bioturbated, red-brown siltstones which were deposited during a transgression before deposition of the overlying red-brown, marine siltstone of the Patonga Claystone.

PATONGA CLAYSTONE

The Patonga Claystone crops out along the coast between Wamberal and The Entrance and consists dominantly of red-brown siltstone with interbedded green-grey, fine to medium-grained sandstone. The siltstone is mostly massive and homogeneous, bioturbation having completely obliterated bedding except where grey mottling or interbedded fine-grained sandstone provide a colour contrast. Foraminifera identified by Crespin(1938), bioturbation and stratigraphic setting indicate that the red-bed siltstone was deposited in a marine bay environment.

In coastal outcrop sandstones are seen to be sharp-based and, in places,

channel into underlying siltstone. However, well logs from bores located further inland (e.g. DM Stowe DDH1) indicate stacked, gradational, coarsening-up, shale to sandstone sequences as much as 30m thick comprising progradational sequences. Sedimentary structures, tetrapod tracks and a diverse assemblage of trace fossils such as *Thalassinoides, Ophiomorpha, Turimettichnus, Rhizocorallium* , and bilobed trails indicate that the sandstones were deposited as barrier-islands with tidal inlets and tidal deltas.

In addition laminated, grey and red-brown shale with *Skolithus* and *Turimettichnus* (decapod crustacean) burrows, and desiccation cracks indicate deposition in tidal flats within lagoonal areas behind the barriers.

TERRIGAL FORMATION

McDonnell (1974) interpreted the entire Terrigal Formation to have been deposited on an alluvial plain with in-channel and floodplain environments. However, the marine-shoreline interpretation presented here is consistent with observed sedimentary features. McDonnell's point-bar sandstones are interpreted here as barrier-island, tidal inlet and tidal delta sandstones while his fine-grained floodbasin deposits are interpreted as tidal-flat and lower shoreface to offshore sediments.

Between Broken Bay and Terrigal, the Terrigal Formation consists of thick sandstones (as much as 25m) interbedded with grey, and rare red-brown and purple, shale. Sandstones are both interbedded with, and in places, erosively channel underlying shale. They contain a variety of trace fossils including many different forms of *Thalassinoides*, *Skolithus*, *Turimettichnus* and tetrapod tracks. I interpret these sandstones to have been deposited as a complex of barrier islands, tidal inlets and tidal deltas similar to those occuring in the Patonga Claystone.

Finer-grained sediments immediately below the sandstones are variably bioturbated and, in particular, contain distinctive vertical branching, tubular structures *(Barrenjoeichnus)* concentrated in certain horizons. The finer-grained sediments were probably deposited in a shallow, lower shoreface to offshore marine environment. In addition laminated siltstone and fine-grained sandstone, in places with *Skolithus*, *Turimettichnus* and desiccation cracks, grade upwards into siltstone with roots, and are interpreted as tidal flats behind barrier-islands. Other fossils include amphibians and many fishes, such as sharks and two species of the almost exclusively marine genus *Saurichthys.*

Mytilid bivalves were described from the partly equivalent Newport Formation at Warriewood, near Sydney (Grant-Mackie et al. 1987).

WESTERN SYDNEY BASIN

From the north-coastal Sydney Basin the Narrabeen Group passes westwards into a sandy sequence typified by spectacular cliff exposures in the Blue Mountains. This sandstone is generally thought to have been deposited by a low-sinuosity fluvial system that entered the basin from the northwest (Ward 1972, Goldbery and Holland 1973). However, bioturbation in many horizons throughout the Grose Subgroup and Caley Formation indicates that estuarine conditions penetrated the fluvial system at times.

Thin interbedded shales vary from green, grey and brown to red-brown. Some contain palaeosols which, in some places are superimposed on previously-bioturbated shale, particularly in central areas of the basin. Red-brown siltstones in the Mount York Claystone appear to be homogeneous in hand-specimen, but thin-sections show that pervasive bioturbation destroyed bedding. It is suggested that many of the more extensive shales represent marine transgressions, some of which almost covered the entire basin.

PALAEOGEOGRAPHY

Overview

The following discussion is restricted to the Patonga Claystone and Terrigal Formation only. During Patonga-Terrigal time alluvial sediments were derived from the New England Fold Belt via the Gunnedah Basin. Rivers flowed along the axis of the Gunnedah Basin into the Sydney Basin in a southeasterly direction across the western, more slowly subsiding, part (fig. 3). At times the alluvial plain passed southeastwards through a paralic environment into a marine shoreline complex of barrier islands, tidal inlets and tidal deltas located in the rapidly subsiding part of the basin between Broken Bay and The Entrance. Fine-grained, marine sediments were deposited offshore, in the lower Hunter Valley to Newcastle region, but have now been mostly lost by modern erosion.

Relative Sea-level Change

Cycles of relative sea-level rise and fall by the combined effect of the

changing rate of eustatic sea-level and the rate of subsidence/uplift can explain the pattern of vertically stacked fluvial/estuarine to barrier-island sandstones and intercalated coastal-plain to marine shales. The lateral distribution of these facies can also be related to regression and transgression as a consequence of sedimentation rate versus varying accommodation space.

During relative sea-level fall (fig. 3A) the depositional surface was subaerially exposed and eroded. Rivers flowed directly to the shoreline with no intervening paralic environment and with little, or no, alluvial deposition. Soil profiles developed on interfluvial areas. Most sediment was deposited as shoreface sands and offshore silts.

As relative sea-level started to rise (fig. 3B) coarse-grained sandy alluvium aggraded and estuarine conditions progressed upstream. Meanwhile, shoreline sediments were reshaped by the initial transgression into proto barriers or shoals. Thus the bayline moved landwards, transgressing at a faster rate than the relatively static shoreline (the bayline is the boundary between fluvial and paralic/delta-plain environments whereas the shoreline is the boundary between paralic/delta-plain and marine environments).

When the rate of relative sea-level rise reached its maximum (fig. 3C) and sedimentation could not keep pace, rapid transgression resulted in the deposition of thin, commonly bioturbated sandstone and shale over previous alluvial/estuarine sandstones. If the rate of sea-level rise was sufficient the alluvial plain was pushed back to the basin margin and an almost basinwide paralic shale resulted. Further to the east at the shoreline, transgressive barrier islands matured from the original shoreline shoals into a full suite of tidal inlet, tidal delta and back-barrier tidal flats.

During relative sea-level stillstand and initial fall (fig. 3D) the bayline moved basinwards and regressive sedimentation resumed in a variety of coastal-plain environments including alluvial channels and floodplains, shallow lakes and estuaries, with associated crevasse splays and microdeltas. Barrier-island complexes at the shoreline also regressed, but at a slower rate in the deeper water, marine and more rapidly subsiding part of the basin.

Subsequent relative sea-level fall (fig. 3A) exposed the basin to erosion to conclude the cycle. The Narrabeen Group contains many such sedimentary cycles. About 5 cycles occur in the Patonga Claystone and 7 in the Terrigal Formation. Along the Central Coast cycles average about 30m thick, but generally thin towards the western basin margin.

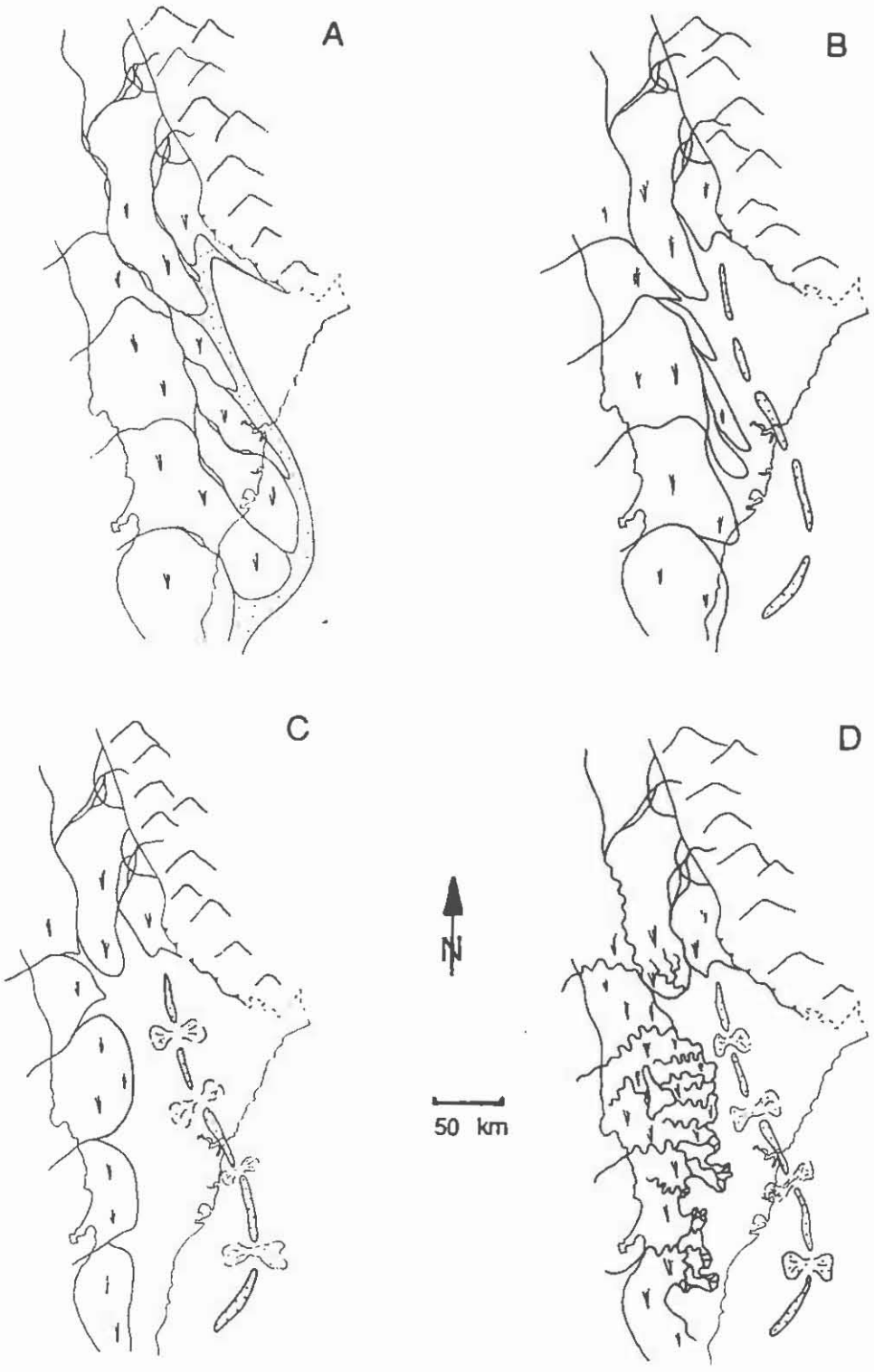

Figure 3. Palaeogeographic reconstruction for the Patonga Claystone and Terrigal Formation during relative sea-level fall (A), initial sea-level rise(B),maximum rate of sea-level rise (C), and sea-level highstand (D).

REFERENCES

Bunny, M.R. and Herbert, C., 1971: The Lower Triassic Newport Formation, Narrabeen Group, southern Sydney Basin. Records of the Geological Survey, N.S.W., 13(2), 61-81.

Conolly J.R., 1969: Models for Triassic Deposition in the Sydney Basin. Spec. Publ. Geol. Soc. Aust., 2, 209-223.

Crespin, I., 1938: Report on No. 1 Bore, Kulnura, N.S.W. Dep. Min N.S.W. File Nos Ms38/7661, Ms39/2884 and WCR29.

Goldbery, R. and Holland, W.N., 1973: Stratigraphy and sedimentation of redbed facies in Narrabeen Group of Sydney Basin, Australia. Bull. Am.Ass. Petrol. Geol., 57(7), 1314-1334.

Grant-Mackie, J.A., Branagan, D.F. and Grenfell, H.R., 1987: A new mussel (Mytilidae, Bivalvia) from the Sydney Basin Triassic. Rec. Geol. Surv., N.Z. 9, 53-55.

Grebe, H., 1970: Permian plant microfossils from the Newsastle Coal Measures/Narrabeen Group boundary, Lake Munmorah, New South Wales. Rec. Geol Surv. N.S.W., 12(2), 125-136.

Naing, T., 1990: Palaeoenvironmental studies of the Middle Triassic Uppermost Narrabeen Group, Sydney Basin. Ph.D thesis (unpubl.), Macquarie University, Sydney.

Uren, R., 1980: Notes on the Clifton Sub-Group, Northeastern Sydney Basin., in A Guide to the Sydney Basin., Bull. Geol. Surv. N.S.W. 26, 162-168.

Ward, C.R., 1972: Sedimentation in the Narrabeen Group, southern Sydney Basin, New South Wales. J. Soc.Geol. Aust., 19(3), 393-409.

SHOALHAVEN GROUP IN THE WESTERN COALFIELD

R. FELDTMANN[1] & A. HUTTON[2]
[1] Esso Australia, Melbourne
[2] University of Wollongong

INTRODUCTION

The Shoalhaven Group is the extensive basal unit of the Permian sequence in the southern Sydney Basin and although some units were defined as early as the last century, it has not received the attention that perhaps it might given its important position in the stratigraphy of the basin and the influence it had on deposition of the Illawarra Coal Measures. Recent studies have focused on stratigraphic intervals within the sequence (for example, recent studies by Bann (1990) and Mifsud (1990) re-examined units cropping out along the southernmost extremity of the basin) but few papers have attempted basin-wide correlations. As a consequence, outcrops along the western and southwestern margins of the basins are referred to by unit names that have been defined on the coastal sections. As a result, the terminology used is often vague and stratigraphically equivalent units are given different names. For example, Mladek (1959), McElroy and Relph (1961) and Packham (1968) use different names for the same units in the Bullio area.

Feldtmann (1991) reviewed the sequence in the Lithgow area and recognised five facies types in the Shoalhaven Group (Table 1) - horizontally stratified diamictite (DMS), shoreface conglomerate (SFC), massive sandstone (MSD), hummocky cross-stratified sandstone (HCS) and massive bioturbated siltstone (MBS); these lithofacies, together with vertical and lateral facies variations, were the basis for interpreting environments of deposition.

In this paper we use data given in Feldtmann (1991) and earlier work by Hutton (1978) to describe the geology of the Shoalhaven Group in the Marangaroo and Bullio areas and give interpretations of the environments of deposition. Data from the two areas indicate that the deposition of the Shoalhaven Group, and later, deposition of the lower Illawarra Coal Measures was strongly influenced by the palaeotopography. Stratigraphic relationships suggest that the term Megalong Conglomerate should be re-introduced, instead of Snapper Point Formation, for the basal conglomerate and sandstone; the definition of the boundary of the Megalong Conglomerate should also be modified to allow for an interbedded relationship between that unit and the overlying Berry Formation.

MARRANGAROO-LITHGOW AREA

In the Lithgow-Marrangaroo area of the Western Coalfield, the Shoalhaven Group was

first called the Upper Marine Series (Carne, 1908) and renamed the Capertee Group by McElroy (1962). The currently-accepted term, Shoalhaven Group, was introduced by McElroy *et al.* (1969) after stratigraphic continuity was established with the coastal exposures.

The Shoalhaven Group has a maximum thickness of 125 m in Elecom drill hole ELN 31 and thins rapidly westward from this hole such that 2 km south of Ben Bullen it is 26 m thick and at Marangaroo it is inferred to be 15 to 20 m thick as the unconformity with the granitic basement is not exposed but its position can be estimated to within 5 m.

MEGALONG CONGLOMERATE

The Megalong Conglomerate was named by *McElroy et al.* (1969) for the unconformable basal unit of the Shoalhaven Group in the Western Coalfield. However in 1983, Bembrick proposed that the unit be termed the Snapper Point Formation, presumably to bring it line with the nomenclature used in the Southern Coalfield.

The type section for the Megalong Conglomerate is located in the Megalong Valley where it comprises 60 m of cobble conglomerate which extends from Tallong in the south to well northwest of Lithgow. In the Marrangaroo-Lithgow area, the unit comprises poorly-sorted, polymict conglomerate at the base which grades upwards to a medium-grained, lithic sandstone. The upper sandstone of the Megalong Conglomerate in the study area is not laterally extensive or continuous and is only well developed where the basal conglomerate is thin or absent, suggesting that the sandstone and conglomerate are lateral variants of one depositional unit with conglomerate more abundant proximal to source and sandstone abundant distal to source.

In her recent study, Bann described the Snapper Point Formation as a series of marine fossiliferous sandstones, with a few ice-rafted clasts up to boulder size, that were deposited in a near-shore environment. The description given above for the lowermost unit of the Sholahaven Group in the Lithgoow-Marrangaroo area does not fit the description of the Snapper Point Formation given by Bann,; a common name for the lowest unit is the two areas appears to be inconsistent with stratigraphic principles.

The boundary between the Megalong Conglomerate and the overlying Berry Formation is gradational with the upper sandstone of the former grading upwards into siltstone. Where this transition is apparent, the top of the Megalong Conglomerate should be placed at the base of the lowermost bluish-grey siltstone bed. However, where the contact is interbedded siltstone and conglomerate,the boundary should be placed at the top of the uppermost, well-defined bed of conglomerate as suggested by McElroy *et al.* (1968).

Further work is being undertaken to determine if the Megalong Conglomerate should be further divided and formal stratigraphic names defined.

Facies

Three facies were recognised in the Megalong Conglomerate - horizontally stratified diamictite, shore face conglomerate and massive sandstone.

Horizontally Stratified Diamictite (DMS)

The horizontally stratified diamictite is a highly irregular, poorly- to very poorly-sorted polymict conglomerate with clasts up to 2.2 m diameter and a silty sandstone matrix

comprising between 30 and 80% of the rock. This facies ranges in thickness from 50 m in ELN 31 to 13 m south of Ben Bullen and less than 3 m at the new Thompsons Creek Dam where facies DMS comprises massive conglomerate overlain by interbedded sandstone and conglomerate beds 0.3 to 0.6 m thick.

At each locality where this facies is found, the clast composition is extremely variable but generally the dominant clast type strongly correlates with the nearby basement rocks; two main types of conglomerates are recognised.

1. Metasediment Pebble-Cobble Conglomerate. At most localities, quartzite is the dominant clast, such as near Mt Airly on the Glen Davis road; at Thompsons Creek Dam, the composition is less dominated by quartzite and slate and volcanic fragments (with a distinctive green colour) are co-dominant. Quartzite clasts are up to 1.6 m diameter. Some of the beds of the quartzite-dominated DMS facies are poorly-sorted and crudely-stratified breccias. The matrix is a fine-grained to very fine-grained sandstone composed of microcrystalline quartz, metamorphic rock fragments and minor ankerite, siderite, sericite and kaolinite.

   In rail cuttings between Wallerawang and Rydal, conglomerate beds up to 1 m thick have considerable lateral continuity with little variation in either grain size or bed thickness for 4 to 5 km.

2. Granite Boulder Conglomerate. Near Lithgow and Marrangaroo, DMS facies is characterised by clast-supported conglomerate composed of well-rounded spherical to ellipsoidal granite boulders (up to 75% of the rock and up to 2 m diameter) and a poorly- to very poorly-sorted carbonate-cemented, immature feldspathic litharenite matrix (with a grit to fine-grained conglomerate texture) comprising monocrystalline quartz (straight and undulose extinction), partially-replaced K-feldspar and granite fragments with a still finer grained matrix of quartz, K-feldspar, granite fragments, clays minerals and calcite.

   Texturally, the porphyritic granite clasts are similar to the pink granites of the Bathurst Batholith basement. Angularity of the granite clasts increases with decreasing grain size.

   The granite boulder DMS facies is inferred to be of limited lateral extent although it is found in three cuttings over a distance of 4 km. A finer-grained lateral equivalent is exposed in road cuttings 4 km south of Lithgow; these outcrops consist of a matrix-supported conglomerate (clasts up to 0.9 m diameter but generally smaller) fining upwards to a pebbly coarse-grained sandstone. Clast generally comprise <30% of the rock.

Environment of Deposition. Emplacement of clasts up to 2 m diameter would require enormous energy and potential mechanisms include debris flows, ice rafting, rock falls and possibly glaciofluvial deposition. The preferred environment of deposition is a subaqueous mass flow for the following reasons:

i. the beds are commonly sheet-like with little basal erosion;
ii. beds show no obvious stratification except crude layering;
iii. beds contain a variety of clast types;
iv. clasts are angular, poorly-sorted and have a random fabric; and,
v. there is inverse tail grading of large clasts in the granite boulder conglomerate.

However, apparent uniformity over a wide area and absence of a lenticular geometry are not features generally found in subaqueous mass flows.

Shore Face Conglomerate (SFC)

The shore face conglomerate is best exposed at Ben Bullen where it overlies basement rocks with a sharp angular unconformity and is characterised by a well- sorted, well-rounded, clast-supported ologomictic pebble to cobble conglomerate. Crude stratification is well developed approximately 2 m above the unconformity where clast size decreases to predominantly pebble size; clasts are almost entirely quartzite derived from the Devonian basement metasediments.

Environment of Deposition. The environment for the SFC facies is interpreted as a beach or, more likely, a shoreface environment. The facies has some similarity with fluvial facies but has lateral continuity and good segregation of clasts into distinct bodies which have well-defined stratification; graded bedding is not common. The rounded grains indicate significant reworking, perhaps by longshore drift or wave action.

Massive Sandstone Facies (MSD)

Facies MSD consists of a massive structureless, medium to coarse-grained sandstone containing pebble- to boulder-sized clasts (maximum size of 40 cm) which commonly exhibit crude layering. Clast content is variable ranging from sporadic clasts to pebbly sandstone-conglomerate layers up to 0.3 m thick. Maximum measured thickness of this facies is 14 m. On the Great Western Highway, north of Lithgow, the facies is 5 m thick; the top sandstone is interbedded with the bioturbated siltstone facies with beds of both facies 0.5 to 1.5 m thick.

The sandstone is a well- to very well-sorted, angular to subangular, loosely-packed, grain-supported immature subphyllarenite with no preferred orientation or alignment of the framework grains. Matrix content varies from 10 to 55% with XRD analysis showing predominantly quartz, muscovite and kaolinite with siderite and ankerite.

Environment of Deposition. A nearshore environment is inferred because:

i. pebble beds are well sorted and well segregated into distinct uniform layers that are laterally continuous for 50 m (a characteristic of marine gravels);
ii. the sandstones are interbedded with the overlying bioturbated siltstones of the MBS facies of the Berry Formation,; and,
iii. medium- to coarse-grained sands of the type in this facies are typical of foreshore and backshore zones.

The isolated clasts were deposited as dropstones after ice-rafting. Grain size appears to have been too coarse to allow wave-generated structures to be formed or preserved.

BERRY FORMATION

The Berry Formation was given by David and Stonier in 1891 for a sequence of marine rocks in the upper Shoalhaven Group that crop out on the South Coast. The term was later applied to the Western Coalfield by McElroy *et al.* (1968) who argued that the unit was a contiguous mappable unit along the western margin of the Sydney Basin. In ELN 31, the Berry Formation attains a thickness of 80 m but elsewhere around the Lithgow-Marrangaroo it is thinner; it is absent at Marrangaroo. The maximum thickness recorded is 210 m in the Grose Valley (Goldberry, 1972).

SHOALHAVEN GROUP

Facies

Two facies were recognised in the Berry Formation - massive bioturbated siltstone and hummocky cross-stratified sandstone.

Massive Bioturbated Siltstone (MBS)

This facies comprises bluish-grey or mid to dark grey sandy, massive micaceous siltstone to fine-grained sandstone which is moderately to strongly bioturbated and contains rare pebbles, cobbles and boulders which are generally quartzite, granite or phyllite. Sandstone lenses and sandy siltstone beds are common and these are generally iron-stained and more resistant to weathering. The siltstone is a well- to very well-sorted, angular to subangular, loosely-packed sublitharenite in which quartz is dominant (50 to 75%) with recrystallised schistose, phyllitic and cherty rock fragments. The finer-grained components are mostly quartz, muscovite/sericite and minor kaolinite.

The MBS facies is easily eroded and undercut cliffs commonly form where it occurs. Laminated bedding is preserved at some localities but generally bioturbation destroys any structure. Burrows are vertical, horizontal or U-shaped.

Environment of Deposition. The absence of sedimentary structures indicates deposition in a quiescent environment, thus allowing settling of fine-grained sediment which was reworked by burrowing organisms that were abundant. The abundance of bioturbation indicates a marine shelf environment with uniform conditions for long periods. Periodically, large ice-rafted clasts were deposited as ice melted.

Hummocky Cross-Stratified Sandstone (HCS)

This facies occurs at the top of the Berry Formation and was only observed at Pipers Flat where it attains a thickness of 6 m. Cosets of hummocky cross-stratified laminae are commonly 10 to 50 cm thick and are interbedded with bioturbated beds of similar thickness and composition and in which bioturbation generally has destroyed structure. These two lithologies are commonly gradational one to another.

The mineralogy of the sandstone in the HCS facies is similar to the siltstone of the MBS facies with quartz dominant and generally have a 14:1 ratio with other components. Muscovite is generally aligned as are other larger grains.

Environment of Deposition. The environment for facies HCS is interpreted as marine, above storm wave-base but below fair weather wave-base with the hummocky cross-beds forming as sand is moved from the upper shoreface and were redeposited below fair weather wave-base. During fair weather sediment accumulated very slowly and burrowing organisms reworked the sediment, gradually destroying bedding. Bioturbated units were sharply truncated during the next storm event.

BULLIO AREA

The thickness of the Shoalhaven Group varies considerably ranging from less than 20 m at Pulpit Rock near the Wombeyan Caves Road at Bullio to 114 m, two kilometres to the east. As at Marrangaroo-Lithgow, the sequence is interpreted as a shallow marine sequence. However, at Bullio fossils are evidence of this environment.

FELDTMANN and HUTTON

MEGALONG CONGLOMERATE

Basal Conglomerate

The basal unit in the Bullio area is a conglomerate which unconformable overlies the Palaeozoic granitic and metasediment basement and is interpreted to be a lateral equivalent of the Megalong Conglomerate of the Marrangaroo-Lithgow area. This conglomerate unit is a discontinuous polymictic pebble and cobble conglomerate with a sand to fine-grained sand matrix, which grades laterally to a conglomeratic sandstone near the Wingecarribee River. The conglomerate is generally found in low lying areas of the palaeotopography.

Clasts are generally 10 to 20 cm in diameter (rarely up tp 50 cm) and are well rounded. Composition of the clasts is approximately 65% metamorphic (dominantly white to dark grey quartzite with phyllite, slate, granite, porphyritic volcanic fragments; metamorphic clasts are generally flattened whereas igneous clasts are spherical. As in the Marrangaroo-Lithgow area, many of the clasts are thought to have been derived from the basement rocks in the local area. Imbricate textures were found at Pulpit Rock.

The conglomerate is both clast- and matrix-supported with the matrix composed of quartz, muscovite, sericite, clay minerals and rock fragments with the same compositions and proportions as the clasts.

Environment of Deposition. The inferred environment of deposition is a subaqueous mass flow.

Cross-bedded Sandstone

Immediately above the conglomerate and gradational with it, is a fine- to medium-grained, cross-bedded silty sandstone with tabular cross-bed sets 0.1 to 0.4 cm thick. At some localities, the conglomerate and cross-bedded sandstone are interbedded with beds 10 to 50 cm thick; cross-bed sets range in thickness from 0.1 to 0.4 m. The sandstone commonly forms a low cliff topography where it crops out.

Environment of Deposition. This sandstone is thought to have been deposited in a nearshore environment and is equivalent to Facies MSD of the Marrangaroo-Lithgow sequence.

Terminology

Herbert (1971) described similar conglomerates, which he termed the Tallong and Yadboro Conglomerates, at the base of the southern Sydney Basin sequence and suggested that these units had been deposited under terrestrial and fluvial, or fluvioglacial, conditions in valleys and channels which had been eroded into the older Palaeozoic basement. The conglomerates of Herbert are thought to be stratigraphic equivalents of the basal conglomerate unit at Bullio and are also probably correlatives of the units described by Packham as "basal breccia-like conglomerate" of the Megalong Conglomerate.

Given the similarity in lithology, stratigraphic position and environment of deposition, the conglomerate and sandstone unit at Bullio should be given the name Megalong Conglomerate.

SHOALHAVEN GROUP

BERRY FORMATION

The uppermost unit of the Shoalhaven Group is a massive micaceous siltstone unit, up to 100 m thick, with numerous pebble clasts and occasional angular boulders up to 0.5 m diameter. Most of the clasts are well-rounded and discoidal, grey to greenish-grey quartzite derived from the basement metasediments. At the locality where this unit is best exposed, the lower half of the unit contains a higher proportion of pebble clasts, including several pebble layers, than the upper half of the unit.

The siltstone is poorly-sorted, textually-immature, loosely-packed and composed dominantly of quartz (40%), rock fragments (15%, dominantly metamorphic, sedimentary and chert), muscovite/sericite (5%) and clay minerals.

Fossils include common to abundant animal burrows, filled with dark grey silt, rare *Notospirifera* brachiopods (near the base of the unit), rare plant remains and *Notoconularia inornata* (Dana). The latter fossil has also been found in the Dalwood Formation in the Hunter Valley and in the Nowra Sandstone and Wandrawandrian Siltstone (Thomas, 1969).

Environment of Deposition. The absence of sedimentary structures indicates deposition in a quiescent environment, thus allowing settling of fine-grained sediment which was reworked by burrowing organisms. The abundance of bioturbation, together with the sparse macrofossils, indicates a marine shelf environment with uniform conditions for long periods; ice-rafted pebbles were deposited after melting of ice.

Terminology

The bioturbated siltstone unit is almost identical to Facies MBS in the Marrangaroo-Lithgow area and occupies the same stratigraphic interval. It should therefore be included in the Berry Formation.

DEPOSITIONAL SYNTHESIS

The marine sediments of the Shoalhaven Group were deposited in a transgressive environment that advanced over undulating topography, resulting in a sea level rise associated with a global ice thaw. Basal diamictites of the Megalong Conglomerate were deposited in areas adjacent to topographic highs by the process of debris flow. With a rise in sea level, proximal facies retreated with the transgressing shoreline and distal debris flows were interbedded with finer-grained sediment that accumulated between the flows. In these areas, gentle coastal gradients allowed wave action to rework freshly eroded sediment depositing it as beach gravels that fined upwards into sands.

The shelf deposits of the later Berry Formation were deposited in distal marine settings. The last phase of deposition of the Berry Formation occurred during a regression which permitted reworking of sediment by storm activity. The regression continued until the marine shelf was abandoned and deposition took place on the broad coastal plain which had formed. During the early stages of this deposition of the Illawarra Coal Measures, the topographic high continued to influence sedimentation patterns.

REFERENCES

Bann, K., 1990: Sedimentology and diagenesis of the Early Permian Snapper Point

Formation, Southern Sydney Basin, NSW. BSc(Hons) Thesis, University of Wollongong.

Bembrick, C.S., 1983: Stratigraphy and sedimentation of the Late Permian Illawarra Coal Measures in the Western Coalfield, Sydney Basin, New South Wales. *J. Roy. Soc. N.S.W.*, 116, 105-117.

Carne, J.E., 1908: Geology and Mineral Resources of the Western Coalfield. *Mem. Geol. Surv. N.S.W.*, 6, 43-47.

Feldtmann, R., 1991: The geology of the lower Sydney Basin, Western Coalfield, New South Wales. BSc(Hons) Thesis, University of Wollongong.

Goldberry, R., 1972: Geology of the western Blue Mountains. *Bull. Geol. Surv. N.S.W.*, 20, 56-78.

Herbert, C., 1971: Palaeodrainage patterns in the southern Sydney Basin. *Rec. Geol. Surv. N.S.W.*, 14(1), 5-18.

Hutton, A.C., 1978: Geology of an area south-east of Bullio, New South Wales. BSc(Hons) Thesis, University of Wollongong.

McElroy, C.T., 1962: Explanatory notes for the Sydney 1:25,000 geological sheet. 2nd Edition, *Bur. Min. Resour. Geol. Geophys.* Canberra.

McElroy, C.T. and Relph, R.E., 1961: Explanatory notes to accompany geological maps of the inner catchment areas, Warragamba storage. *Tech. Rep. Dept Mines N.S.W.*, 6, 65-88.

McElroy, C.T., Branagan, D.F., Raam, A and Campbell, K.S.W., 1969: in Packham, G.H., (ed.), The Geology of New South Wales. *J. Geol. Soc. Aust.*, 16, 357-369.

Mladek, H.V., 1959: The geology of the Berrima, Wingecarribee, Bullio District. MSc (Qual.) Thesis, University of Sydney.

Mifsud, J., 1990: The sedimentology and diagenesis of the upper Pebbly Beach Formation, southern Sydney Basin. BSc(Hons) Thesis, University of Wollongong.

Packham, G.H., 1968: The Geology of New South Wales. *J. Geol. Soc. Aust.*, 16, 654p.

Thomas, G.A., 1969: *Notoconularia*, a new conularid genus from the Permian of eastern Australia. *J. Paleont.*, 43, 1283-1290.

Table 1. Facies Terminology for the Shoalhaven Group in the Marrangaroo-Lithgow Area.

Facies Code	Lithology	Sedimentary Structures	Interpretation
DMS	poorly-sorted diamictite	horizontally stratified, random clast orientation, matrix supported	sub-aqueous debris or mass flows
SFC	pebble to cobble conglomerate	clast supported, horizontally stratified	shore face, wave-worked gravels
MSD	sandstone, fine to coarse	massive	near-shore but above wave-base
HCS	sandstone, fine to silty	hummocky and swaily cross-stratification	near-shore, between storm and fair weather
MBS	siltstone	massive, bioturbated	quiet marine shelf

TRACE FOSSILS AS PALAEOENVIRONMENTAL INDICATORS IN THE EARLY TO MIDDLE TRIASSIC, NARRABEEN GROUP

T. NAING
Macquarie University

GEOLOGY

Coastal Triassic rocks between Sydney and Broken Bay total about 180 m in thickness (Figure 5) and comprise the uppermost part of the Narrabeen Group (in ascending stratigraphic order: the Bald Hill Claystone, Garie Formation, Newport Formation (Figure 1). Environmentally-diagnostic body fossil are rare, and, where they occur are nowhere unequivocally indicative of marine affinities. Allochthonous plant macrofossils and palynomorphs occurs sporadically. For the above reasons, many previous workers have interpreted these formations to be of fluvial or fluvio-lacustrine origin.

TRACE FOSSILS DISCOVERY

Trace fossils occur abundantly at specific stratigraphic levels within the uppermost Narrabeen Group rocks, particularly within the Newport Formation. These trace fossils have received very little attention and have not been systematically studied. This study shows that the trace fossil assemblage is relatively diverse, comprising almost 100 different ichnotaxa including varietal categories (Figure 2). These include several new ichnogenera and ichnospecies. Among the more notable are two large bioglyph-bearing dwelling-burrows of probable crustacean origin (*Turimettichnus conaghani* and *T. webbyi*) and one (*Pytiniichnus trifurcatum*) made either by a small reptile or an amphibian; a multi-stage spiral star-shaped feeding-trace (*Helikospirichnus veeversi*),probably made by a worm or worm-like deposit-feeder; several new species and varieties of *Rhizocorallium* (the first record of this ichnogenus in the Triassic of Australia); a new species and new variety of the saltatorial running vertebrate trackway *Moodieichnus* (an ichnogenus previously known only from the Late Permian of North America); and a new ichnogenus of vertical/steeply-inclined, cylindrical, branching dwelling-burrows (*Barrenjoeichnus mitchelli*). These new trace fossils are associated with *Thalassinoides*, *Skolithos*, *Ophiomorpha*, *Chondrites*, *Rhizocorallium*, *Palaeophycus*, and *Planolites*,

all of which are known to have unequivocally brackish- to shallow-marine palaeoecological affinities and, which globally, are characteristic of the *Skolithos* ichnofacies.

ASSEMBLAGE ZONES

At least four diverse assemblage zones can be identified, characterised by one or more particular index ichnogenera which lend their names to zones defined in ascending stratigraphic order as follows: *Turimettichnus-Ophiomorpha* assemblage zone; *Skolithos-Diplocraterion* assemblage zone; *Helikospirichnus* assemblage zone; and *Rhizocorallium-Thalassinoides* assemblage zone. An intervening ichnotaxonomically less-diverse and relatively impoverished assemblage zone is interpreted to have predominantly non-marine palaeoecological affinities and can be referred to the *Scoyenia* assemblage zone. This stratigraphic pattern of alternating ichnologically diverse and impoverished assemblage zones confirms the suggestions of previous workers Conolly (1969), Bunny & Herbert (1971), and Retallack (1977) regarding the presence of brackish-/shallow-marine palaeoenvironmental influence in the Newport Formation. This allows, for the first time, the stratigraphic resolution of four marine tongues which are named here after their respective type localities (Figures 4b & 5). These are, in ascending order: the Turimetta Head Tongue (2 m to 3 m thick; extending from at least the middle part of the Bald Hill Claystone almost to the top); The St Michaels Cave Tongue (4 m to 5 m thick; encompassing the Garie Formation and the lower part of the Lower Member of the Newport Formation); the Bangalley Head Tongue (3 m to 5 m thick; extending from the uppermost part of the Lower Member into the lower part of the Middle Member of the Newport Formation); and the Palm Beach Tongue (3 m to 4 m thick; comprising the uppermost part of the Middle member of the Newport Formation) (Figure 5).

PALAEOENVIRONMENTAL ANALYSIS

Trace fossils assemblages in each of these marine tongues indicate a brackish- to very shallow-marine low-energy palaeoenvironment typical of modern coastal lagoons and estuaries, implying the presence of a protecting coeval topographic barrier of some kind to the east (Figure 3 & and Herbert this conference). This lagoon is herein called the `Newport Lagoon' and its development in the central-eastern part of the Sydney Basin coincides approximately with the geographic and depocentral axis of the basin which trends NW-SE and intersects the present coastline in the Sydney metropolitan area. The non-marine affinities of the impoverished and less diverse trace fossil assemblages in the intervening and overlying strata are consistent with fluvial/fluvio-lacustrine environmental interpretations for these thicker and predominantly sandstone-dominated intervals. Palaeocurrent and petrographic data from these

fluvial sediments show that streams debouched episodically into the Newport Lagoon from northwest, west and southwest, and were sourced from both the cratonic Lachlan Fold Belt to the southwest and New England Orogen to the northeast (Figure 6). These interpretations are supported by Herbert (this symposium) who suggests even more extensive paralic and marine influence throughout the entire Narrabeen Group. The development of the Newport Lagoon in the geographic and depocentral axis of the basin attests to the presence of short-lived marine trangressions in the latest Early and early Middle Triassic at the end of a period of declining piedmont clastic alluviation from the coeval New England Orogen.

REFERENCES

Bembrick, C. S., 1980: Geology of the Blue Mountains, Western Sydney Basin., in C. Herbert & R. Helby (eds.), A guide to the Sydney Basin, Dept. Min. Res., Bull. Geol. Surv. N.S.W., (26), 134-161.

Bunny, M. R. & Herbert, C., 1971: The Lower Triassic Newport Formation, Narrabeen Group, southern Sydney Basin. Records of the Geological Survey. N.S.W., 13(2), 61-81.

Conolly, J. R., 1969: Models for Triassic Deposition in the Sydney Basin. Spec. Publ. Geol. Soc. Aust., 2,, 209-223.

Cowan, E. J., 1985: A Basin Analysis of the Triassic System, central Coastal Sydney Basin. B.Sc. Hons Thesis (unpubl.), School of Earth Sciences, Macquarie University, Sydney.

Herbert, C., 1970: A synthesis of Narrabeen Group Nomenclature, Sydney Basin. New South Wales. Geol. Surv., Quart. Notes., (1), 3-10.

Herbert, C., 1983: Sydney Basin Stratigraphy., in C. Herbert (ed.), Geology of the Sydney 1:100,000 sheet 9130. Geol. Surv. N.S.W., Dept. Min. Res., 7-34.

Loughnan, F. C. & et al., 1964: The Red Beds of the Triassic Narrabeen Group. J. Geol. Soc. Aust. (11), 65-78.

Mcdonnell, K. L., 1983: The Sydney Basin: from Late Permian to Middle Triassic. Ph.d thesis (unpubl.), School of Earth Sciences, Macquarie University, Sydney.

Uren, R., 1980: Notes on the Clifton Sub-Group, Northeastern Sydney Basin., in A Guide to the Sydney Basin., Bull. Geol. Surv. N.S.W. (26), 162-168.

Ward, C., 1972a: Sedimentation in the Narrabeen Group, southern Sydney Basin, New South Wales. J. Geol. Soc. Aust., 19(3), 393-349.

Ward, C., 1972b: Mineralogical changes as marker horizons for stratigraphic correlation in the Narrabeen Group of the Sydney Basin N.S.W. J. Proc. R. Soc., N.S.W., 104(1), 77-88.

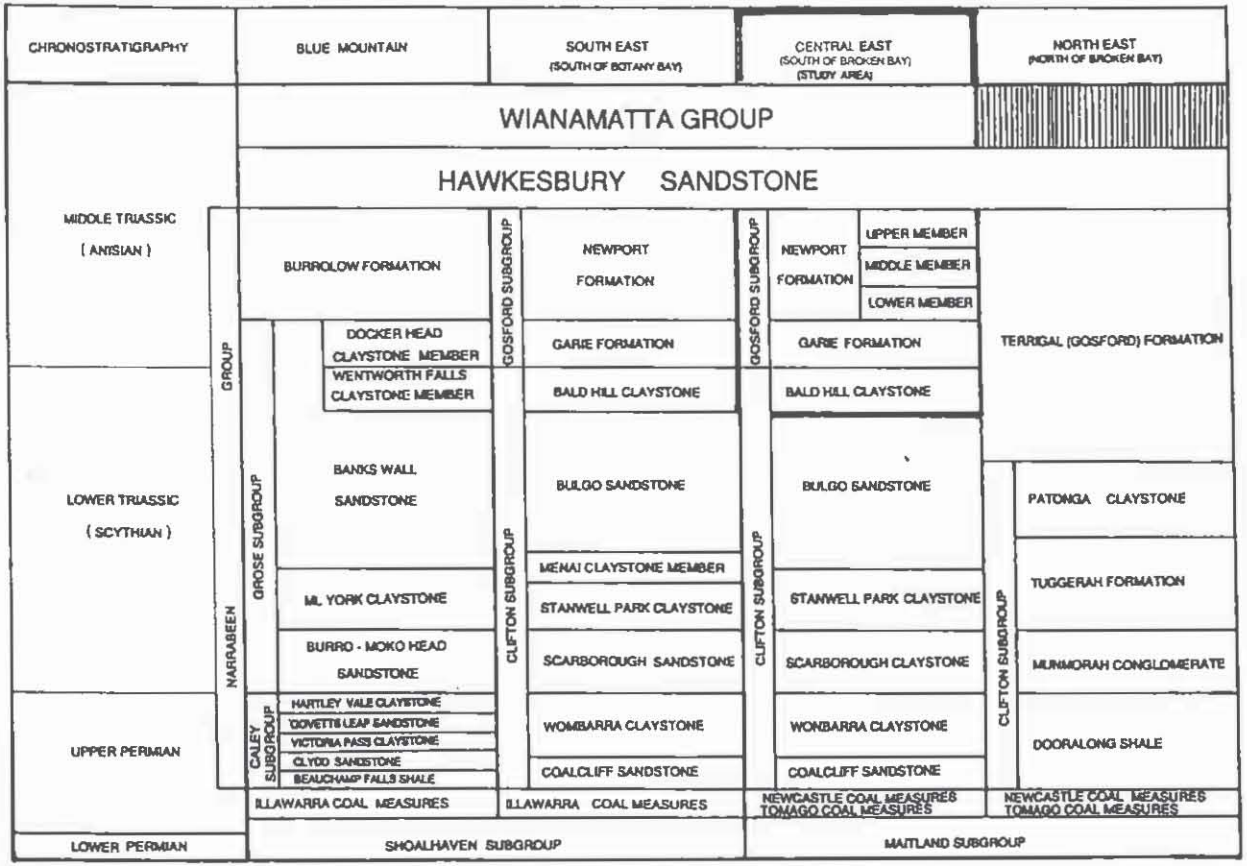

Figure 1. Comparative stratigraphic nomenclature of the Triassic System (including underlying Permian System) in different parts of the Sydney Basin. Source: Herbert, 1970 & 1983; Ward, 1972a & b; Loughnan et al., 1964; Bembrick, 1980; Uren, 1980; Mcdonnell, 1983; and Cowan, 1985.

TRACE FOSSILS IN THE NARRABEEN GROUP

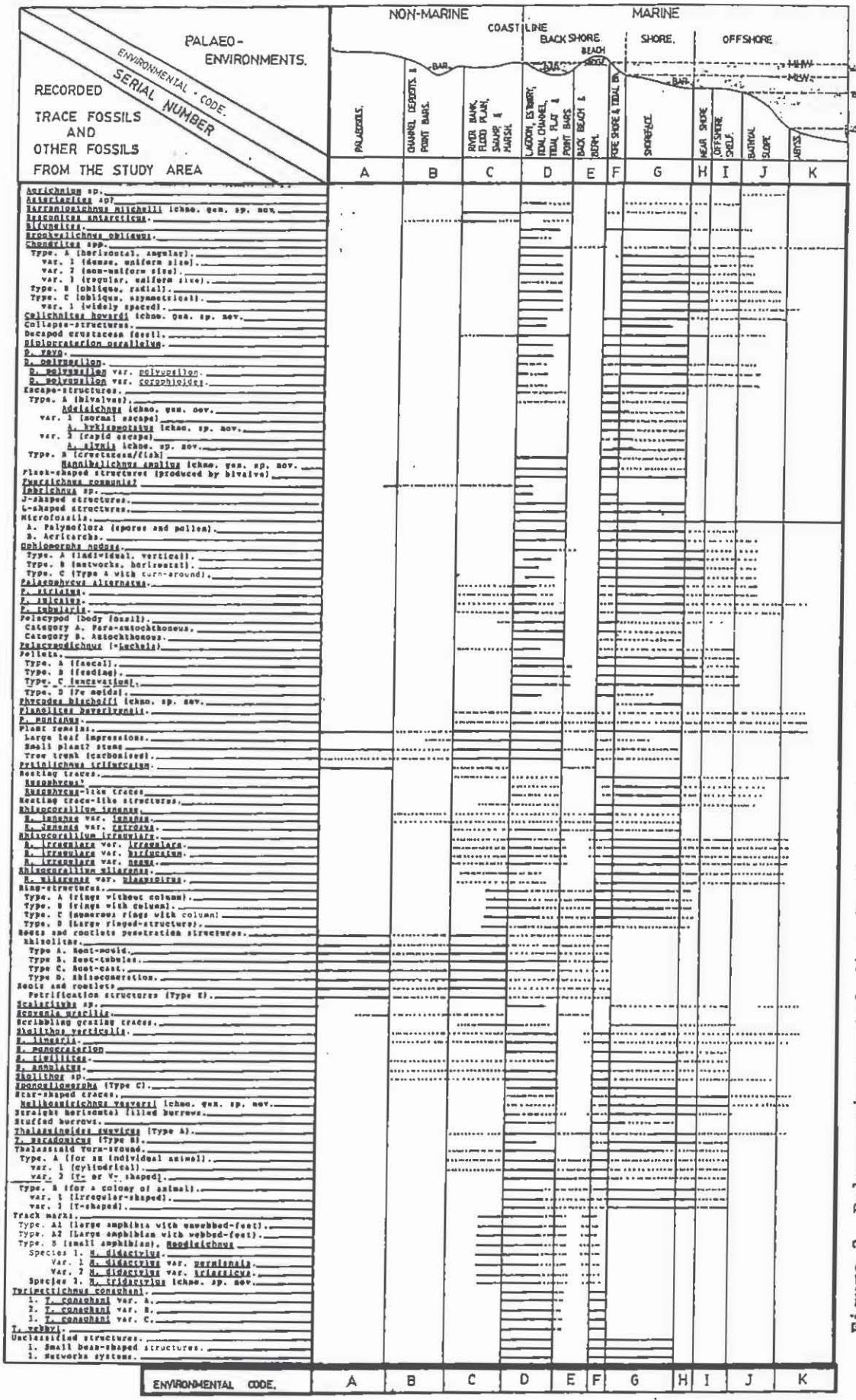

Figure 2. Palaeoenvironmental distribution of trace fossils, body fossils, and plant remains in the study area. The major environmental distribution of indices shows unequivocally a complex environment of shallow coastal estuary or lagoon, open shallow-marine and non-marine (fluvial and emergent) areas. Solid horizontal lines show inferred environmental range of individual trace fossils in the study area and dotted lines show the total range of individual trace fossils globally according to the literature.

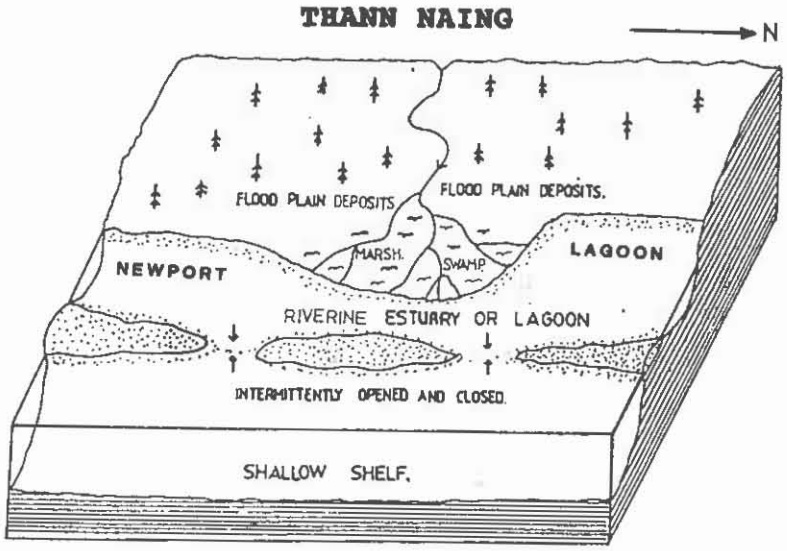

Figure 3. Block diagram palaeoenvironmental reconstruction of the study area during deposition of the Bald Hill Claystone and Newport Formations. The overall study area is interpreted to represent a fluvially-dominated coastal estuary or lagoon (termed here the "Newport Lagoon".

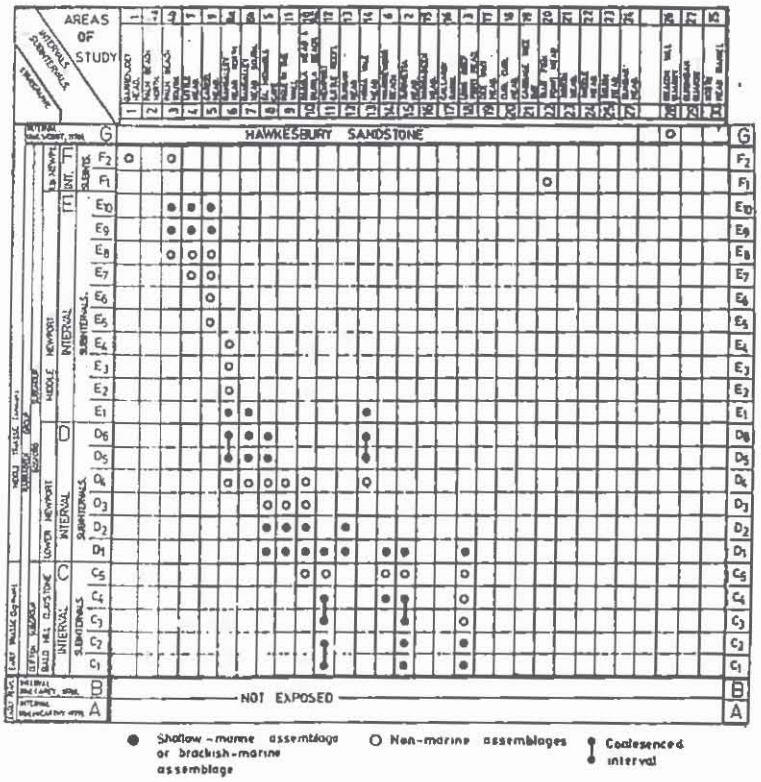

Figure 4a. Stratigraphic distribution (vertical axis) versus geographic distribution (horizontal axis) of the trace fossils subintervals in the study area. Open circles indicate non-marine affinity of the trace fossil assemblages (or suites) and solid circles indicate marine affinity of these assemblages. (Solid circles with connected bars indicate locally coalesced).

TRACE FOSSILS IN THE NARRABEEN GROUP

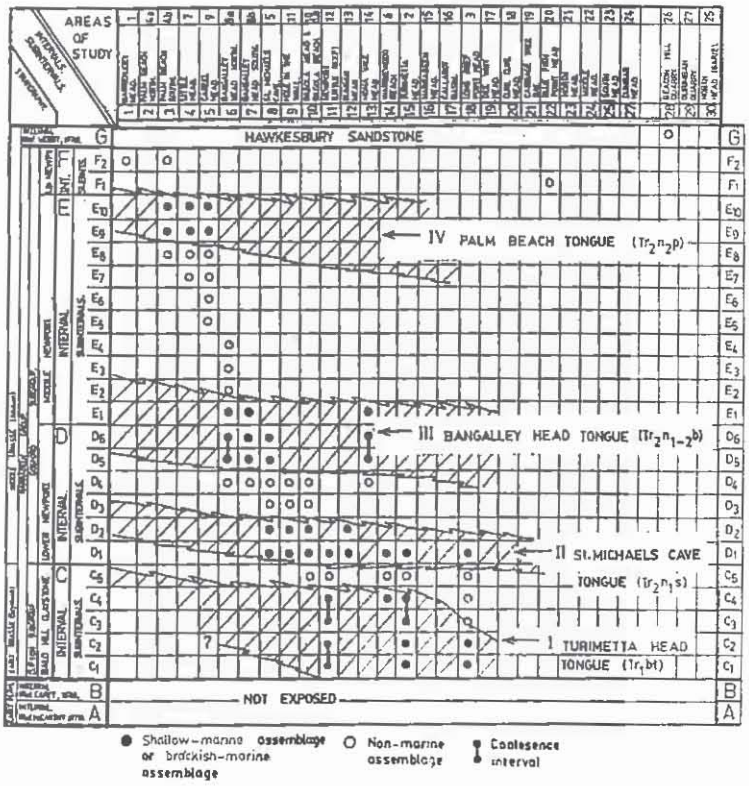

Figure 4b. Stratigraphic distribution versus geographic distribution (as in Fig. 4a) with interpreted four marine-influenced episodes. These episodes were named after the type localities.

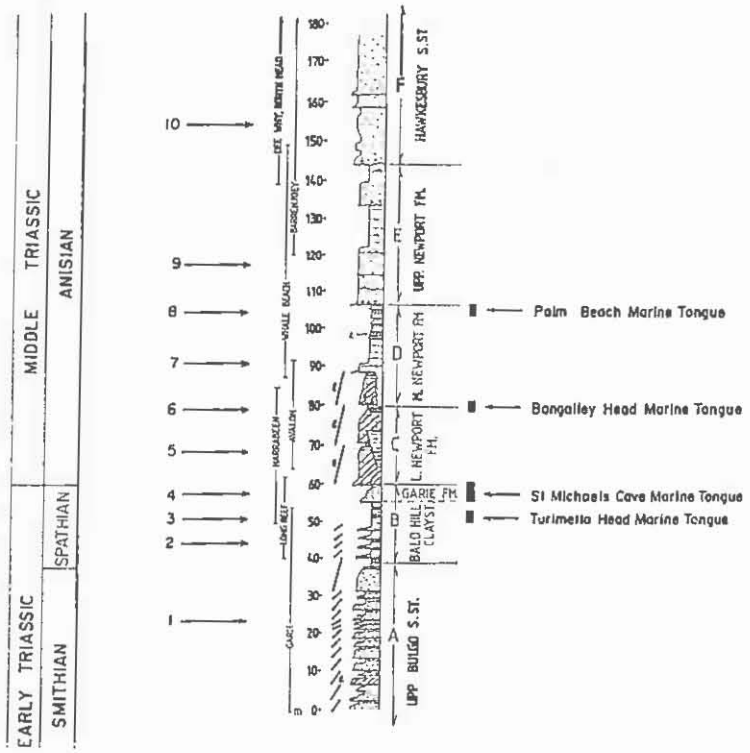

Figure 5. Stratigraphy of the Triassic rocks of the study area (from Cowan, 1985, fig. 2.1) showing stratigraphic position and extent of the four marine tongues. (Time slices 1 - 10 depicted in the palaeogeographic reconstructions of Figure 7).

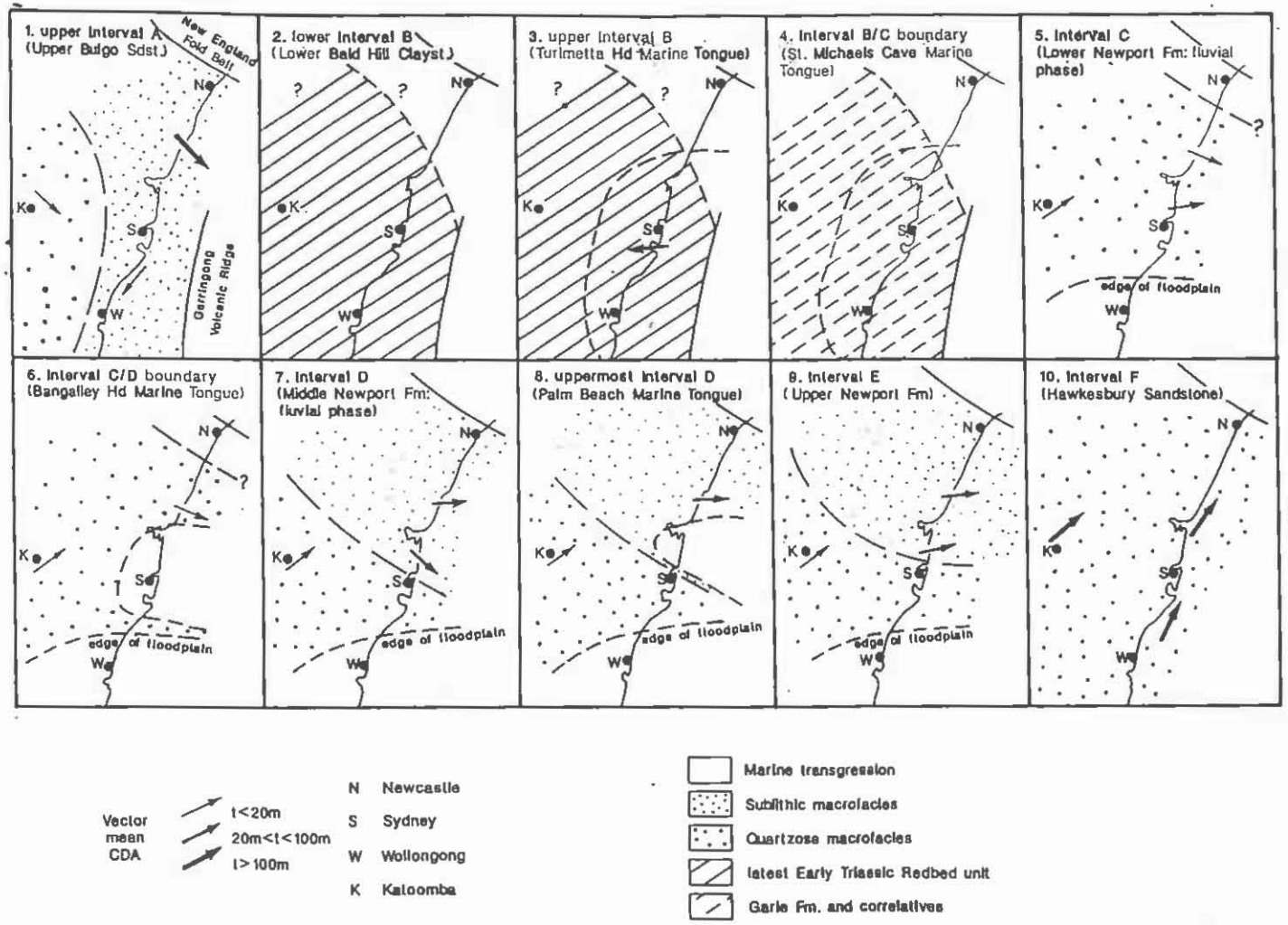

Figure 6. Latest Early and early Middle Triassic development of the central-eastern Sydney Basin in respect of 10 time slices defined stratigraphically in Figure 5.

SOUTHERN NEWNES PLATEAU COAL DEPOSITS – GEOLOGY, COAL RESOURCES & PROPOSALS FOR MINING

W. VLAHOVIC
Pacific Power

The Southern Newnes Plateau (SNP) is situated in the western Blue Mountains to the north of Lithgow and to the east of Cullen Bullen. The coal deposits in the area are contained in the Late Permian Illawarra Coal Measures on the western margin of the Sydney Basin. The coal measures are overlain by Triassic strata of the Narrabeen Group. The main coal resource occurs in the Cullen Bullen Subgroup towards the base of the Illawarra Coal Measures.

Colliery holdings occur in the south and west, where mines currently operate and are proposed to extract these resources.

In 1991, Pacific Power announced new long term coal supply contracts for Mt Piper and Wallerawang Power Stations. Of the total contract tonnage supplied to these power stations, some 84% will be sourced from the Southern Newnes Plateau.

Exploration History

Shallow non-cored drilling was conducted by the Joint Coal Board in about 1949, there was little active sub-surface exploration in the area until the late 1960's when Wallerawang Colliery put down the Wancol Lithgow (WL) series of reconnaissance bores. The WL bores were drilled at spacings of several kilometres.

Authorisation Nos. 104 and 142, (A.104, A.142) to prospect for coal were granted to Pacific Power on 20th September, 1977 and 20th December, 1980 respectively. A.142 has recently been relinquished (Figure 1).

Following a review of the coal potential of the Western Coalfield in 1974, Pacific Power commenced coal exploration drilling in 1975, initially concentrating on the areas of Lithgow seam potential in the western parts of the Southern Newnes Plateau. This drilling, which constituted the first series of Pacific Power bores, continued almost uninterrupted until 1981, by which time bores Elecom Lithgow Newnes (ELN) 1 - 61 had been completed. Following a Government decision to proceed with the Birds Rock export coal project, drilling of the Katoomba and Lithgow seam resources in the southeastern parts of the SNP commenced immediately.

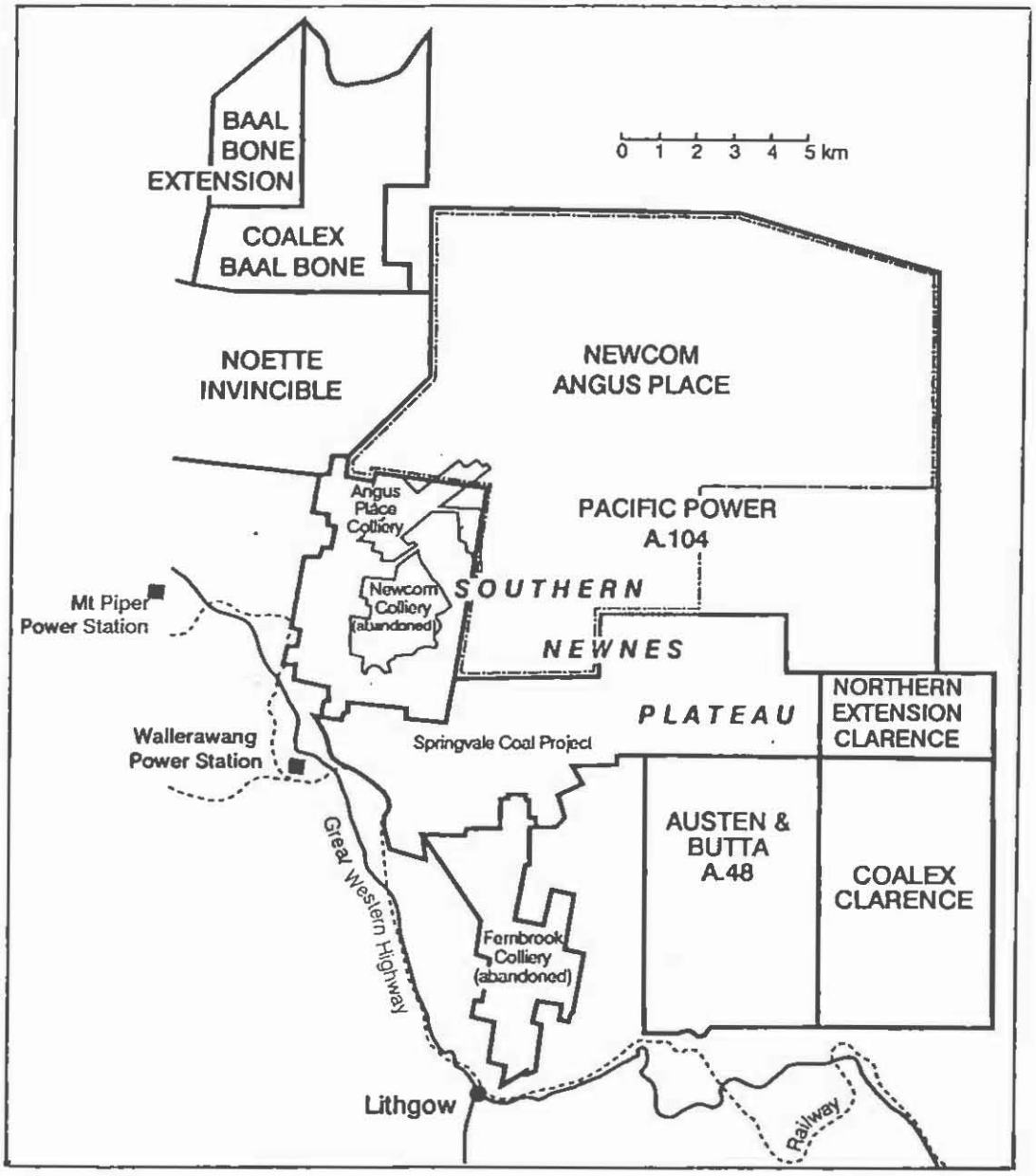

FIGURE 1. Southern Newnes Plateau Location Plan

This programme, which consisted of bores Elecom Birds Rocks (EBR) 1-25, was completed in 1981. A total of 17 of the EBR series bores was drilled within the SNP area. The Birds Rock proposal was abandoned in 1981.

The bores in the former Fernbrook Colliery, consisting of the State Coal Mine North Hermitage and Coalex North Hermitage series were drilled in 1978/79, in general these bores tested the Lithgow seam only.

The second series of ELN bores, which consisted of 14 holes, ELN 62-75 was drilled in 1984/85 and was designed mainly to test areas of Middle River and Irondale seam development. ELN 76 was added to the programme to obtain washability data on the Lithgow seam in the SNP area. This was the first cored bore drilled at the larger HQ/diameter and has been adopted as a reference bore for the area.

A third series of 11 ELN bores, ELN 77-87 was drilled in 1989/90. These bores were drilled at HQ size. The bores were geophysically logged and geomechanically tested. Coal seam gas testing undertaken by Pacific Power in the area has yielded essentially zero desorbable gas. Hydraulic fracture testing conducted by Strata-Tek Pty Ltd was undertaken in 1990 to define in situ stress conditions. The testing was performed in bores ELN 79R and ELN 82, results indicated that the horizontal stress field in the SNP can be defined as:

σ_2 = 12 - 16 MPa (mean 13.9 MPa)
σ_1 = 18 - 26.7 MPa (mean 227 MPa) Orientation of σ_1 is EW to SE-NW.

In 1990, Pacific Power engaged Seamgas Enterprises Pty Ltd to undertake permeability testing of the seams in bore ELN 84, utilising an In-situ Inc Hermit 1000 data logger.

Structure

The SNP area is situated on the stable western margin of the Permian-Triassic Sydney Basin. Overall dip is 1 in 50 (1°8') to the east-northeast. This has been modified by a very gently synclinal structure which trends easterly. Structure contours appear fairly regular and do not indicate the presence of major faults. However bore density is not sufficient to locate and define faults with low throws which may be present. Normal faulting with an estimated throw of a few metres was intersected in the lower part of the Middle River seam in EBR 11 and high angle strata in the order of 40° was intersected in the Lithgow seam in ELN 62. No igneous intrusions have been encountered.

A number of major lineament zones are present which may impact on mining conditions. A CSIRO assessment of lineaments has involved the recognition of regional joint sets at directions of about 70° and 160° and north-south and north-northeast to south-southwest "anomalous" zones which have historically been connected with bad mining conditions. Three such zones may affect Lithgow seam mining in the SNP area.

The nature of these zones at the Lithgow seam horizon is uncertain, but they may be associated with an increase in joint frequency, faulting and in some cases higher stresses. The presence of subvertical joints is recorded in many of the bore logs and is clearly evident in the cliff faces of the dissected plateau areas. The jointing at the surface generally produces large blocky structures in the sandstone. At the Lithgow seam horizon, the jointing is usually closer spaced and its frequency and the number of sets intersecting will have a considerable impact on the Lithgow seam roof stability and resultant mining conditions.

W. VLAHOVIC

General Geology

The Shoalhaven Group, which consists of the Megalong Conglomerate and overlying Berry Siltstone, has not been reached in bores in the SNP area. The stratigraphically deepest bore (EBR 15) penetrated some 23 m below the Lithgow seam into sandstone, minor coal and then 10 m of bioturbated mudstone of the Nile Subgroup. ELN 78, in the centre of the area, intersected 4 m of sandstone (Marrangaroo Conglomerate) and 2 m of bioturbated mudstone (Nile Subgroup).

The coal measure sequence from the top of the uppermost seam (be it Katoomba, Woodford or Middle River) to the base of the Lithgow seam is remarkably consistent in thickness. In the Fernbrook area, the thickness of this interval varies from 93-100 m; in Coal Lease 239 it varies from 110-120 m; and in the far east it varies from 120-130 m.

The Lithgow seam is present throughout the area. However, it is split in the Fernbrook area along a northwesterly trending line known locally as the "convergence". To the southwest of the line, the seam is split by the Blackmans Flat Conglomerate; the upper split is known as the Lidsdale seam and the lower split retains the name Lithgow seam.

The Katoomba, Woodford and Irondale seams are persistent, albeit thin, throughout the area. The Middle River seam is ubiquitous and consists of up to 15 m of coal and bands.

The Angus Place Sandstone with the underlying argillaceous Baal Bone Formation form a persistent marker horizon of considerable value in correlation in the SNP. The unit consists of a fine to very fine grained fining downwards sandstone which is readily identifiable. It is about 3 to 6 m thick, reaching a maximum recorded thickness of approximately 12 m.

The Baal Bone Formation consists mainly of claystones, mudstones and some minor sandstones. It shows a general thickening from the south-west, where it is just over 20 m thick, to the north and north-east where it reaches a thickness of 30.3 m.

The upper boundary of the Illawarra Coal Measures is in most places the Katoomba seam. In a few places it appears to be the Middle River or Woodford seam.

The Triassic Narrabeen Group sequence consists of the basal Caley Formation and the overlying Grose Sandstone and Burralow Formation. The upper formations have been eroded. The Grose Sandstone includes the Mt York Claystone Member which is a significant market horizon. The main seams in descending order in the SNP area are as follows:

. Katoomba seam
. Woodford seam
. Middle River seam
. Irondale seam
. Lithgow seam.

The Katoomba seam occurs at the top of the Illawarra Coal Measures and generally consists of dull coal and few bands; however several bands appear in the seam in the Fernbrook area. The seam is best developed in the far east where it attains a thickness of 2.21 m and 16.7% ash (7% moisture basis). It thins to the north and west and is less than 1.5 m thick over all but the easternmost parts of the area. The seam is mined at Clarence Colliery to the east.

The Woodford seam occurs about 2-4 m below the Katoomba seam and from 1-7 m above the Middle River seam. It appears to be present over all but the westernmost parts of the SNP area and consists of from 20 cm to 1.1 m of carbonaceous claystone and coal.

The Middle River seam occurs about from 4 m to 12 m below the Katoomba seam. It consists of a sequence of coal and mainly argillaceous sediments, although in some parts of the area sandstone is present at one or more horizons.

The geological thickness of the Middle River seam ranges from 9 m to 18 m. The seam essentially consists of an upper coal section and a basal coaly section separated by carbonaceous mudstone, claystone sandstone and other coal intervals. The upper section may prove to have some limited mining potential in those areas where the selected section exceeds 2.0 m. However, in many areas the roof and floor strata both consist of claystone and the seam has not been shown to be an economically feasible mining prospect in the Western Coalfield to date.

The Irondale seam occurs about 75 m to 85 m below the Middle River seam. It is a thin seam which contains a higher proportion of bright coal than the other major seams. It contains a few thin claystone bands; one in the lower part of the seam is widespread and consistent throughout the area. The seam varies irregularly in thickness from 40 cm to 1.49 m and is generally around 1 m thick throughout the area. Ash content varies from 8% to 33%. There does not appear to be a potentially mineable section within the SNP area.

The Lithgow seam is the most important of the seam of the Illawarra Coal Measures in the SNP area. It occurs near the base of the measures and is about 20 m to 25 m below the Irondale seam. The working sections occur at the base of the geological seam. The seam is split in the far southwestern part of the SNP area in the former Fernbrook Colliery along the "convergence".

Most of the SNP area lies to the east of the convergence. The geological thickness of the combined Lithgow seam is remarkably uniform across the area, varying from 7 m to 8 m. The combined seam contains two main tuffaceous claystone markers. It can be divided at the top of the second claystone marker into an upper (non-economic) and lower (mineable) section. The upper section is typically banded and stony.

West of the convergence line the combined Lithgow seam splits rapidly to produce discrete Lidsdale and Lithgow seams in the south west. The Lidsdale seam is less than 1.5 m thick in this area; however a 2.1 m thick seam at 19.1% ash was intersected in the abandoned Newcom Colliery.

The Lithgow seam varies from 1.3 m at the western boundary of Fernbrook Colliery to 2.5 m at the convergence. It is the seam with the most potential for mining in this area in the immediate future and was mined by longwall immediately prior to the closure of the Fernbrook pit in December, 1986.

Heavy roof conditions can be expected in a zone immediately to the west of the convergence of the Lithgow and Lidsdale seams. The intervening wedge of sandstone and overlying mudstone thickens rapidly westwards away from the convergence line.

Lithgow Seam Working Sections

The Lithgow seam working sections occur in the lower part of the seam. To the east of the convergence, the working sections are the same as those mined at the Angus Place Colliery in the north west of the SNP and identify by Pacific Power and Newcom Collieries Pty Ltd personnel in the borecore of ELN 76. (At the time it was proposed that the area would be mined by Newcom as part of the Kariwara Project.)

The sections have been correlated in detail throughout the SNP area, based on the identification of characteristic stone bands and comparison of seam brightness profiles.

The three potential mining sections identified in this area are respectively known as LW1 (Longwall 1 Section), LWS (Longwall Working Section), LW2 (Longwall 2 Section) and DH (Development Heading Section). (Figure 2)

The LWS section extends from the floor of the seam to the base of a light brown coloured claystone (second claystone marker). The LWS section has been mined by longwall at Angus Place Colliery in the past.

The LW1 section differs from the LWS section only in that the claystone marker band at the top is included in the section. The LW1 section is generally 0.2 m to 0.3 m thicker than the LWS.

The LW2 section has the same floor as the LWS and extends to the base of a thin light brown claystone band which persists throughout the area and is about 0.05 m to 0.10 m thick. The LW2 section is generally 0.7 m thinner than the LWS.

The thinnest Lithgow seam section is the DH. It extends from the seam floor to include a thin claystone band, generally less than 0.05 m thick, about 0.6 m below the LW2 section.

To the west of the convergence line, the LT (Lithgow Section) has been identified as the main working section. This has the same floor as the LWS and extends to the base of the sandstone interval (Blackmans Flat Conglomerate) which splits the Lithgow seam. This section has been mined by longwall in Fernbrook Colliery.

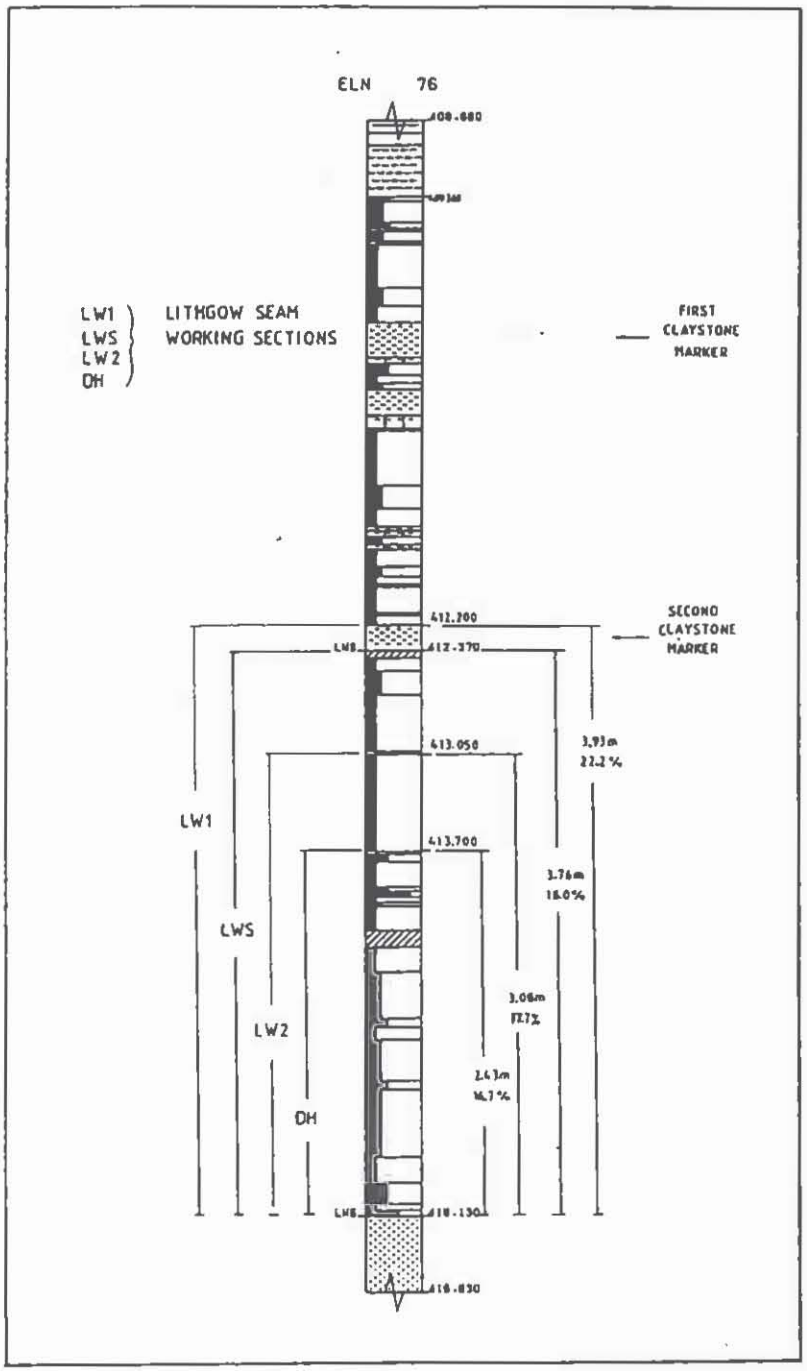

FIGURE 2. Southern Newnes Plateau, Lithgow Seam Working Sections

Proposals For Mining

A joint Working Group was set up in 1985 consisting of representatives from Coalex and Pacific Power to consider options for the transfer of coal reserves in the SNP between the two parties. The results of an exchange agreement resulted in the rationalisation of coal reserves ensuring future expansion opportunity for

the operating mines, Angus Place Colliery and Clarence Colliery and allowing from the calling of tenders for contract mining of a portion of the SNP.

The Clutha/Samsung consortium were successful in their tender to develop the Springvale mine to supply Mt Piper Power Station. The contract was awarded on 20th November, 1990 for a 20 year period to supply 2.0 Mtpa. The Springvale proposal in the SNP will extract the Lithgow seam (LW2 Section) by longwall mining techniques. The raw coal quality in the early years of development is expected to exceed 24%, coal will need to be washed to meet contract requirements.

Angus Place Colliery operated by Newcom Collieries Pty Ltd is expanding its operations in the SNP following its successful bid for a 15 year, 2.2 Mtpa coal supply contract to Mt Piper and Wallerawang Power Stations. Coal is produced from the Lithgow seam using a longwall and continuous miners. Mining conditions vary from good areas under shallow cover to extremely difficult areas beneath escarpments, the influence of lineaments and shallow dipping shear zones. Mine production yields consistent product ash within power station contract requirements.

Transfer of Katoomba seam coal reserves contained in Authorisations 104 and 142 held by Pacific Power has given Coalex Pty Ltd, owners of Clarence Colliery access to about 40 million tonnes of insitu resources. This will enable future northern expansion of Clarence Colliery into the SNP. The mine produces a thermal export product using bord and pillar mining techniques, with proposals to expand production by introduction of a longwall unit.

References

VLAHOVIC, W., WEBER, C.R., BOCKING, M.A., BEMBRICK, J., 1989: Southern Newnes Plateau Geology and Coal Seams - Report to Accompany Specification No. 4026. Vol. 1 and 2. Electricity Commission of N.S.W. Report No. PD 020/89.

WEBER, C.R., BARTO, C.L., 1987: An Assessment of the Geological Conditions and Coal Reserves in Fernbrook Colliery. Electricity Commission of N.S.W. Report No. DE 317.

CRAPP,C.E.,1985:A Report on the Geology of the Coal Resources of Authorisations 104,142 Lithgow- Newnes Area. Electricity Commission of N.S.W. Report No. DE 239.

SINCLAIR KNIGHT AND PARTNERS PTY LTD, 1992: Springvale Coal Project Environmental Impact Statement.

DETECTION OF ABANDONED MINE WORKINGS WITH RADIOWAVE METHODS

R.J. WHITELEY & P.R. FAMELI
Coffey Partners International Pty Ltd

Abstract:

Radiowave electromagnetic (EM) methods operating in the frequency range of 1 to 5MHz and using mobile sources and receivers are a new engineering geophysical technique. At these frequencies subsurface variations in relative dielectric constant are of more importance than those in electrical conductivity which are exploited by conventional EM induction methods. Experience has shown that relative dielectric contrasts within the earth are substantial, particularly when human action such as underground mining or pollution with organic contaminants has altered natural conditions.

One particular radiowave system (GRC-2) operating at 1.5 MHz has been under development in Ukraine for a number of years. This highly-tuned device uses a null-coupled loop arrangement and is relatively insensitive to surrounding metal objects, which adversely effect EM induction methods, and to shallow conductive zones which limit the penetration of Ground Probing Radar methods. The GRC-2 system sucessfully detected abandoned underground workings occurring at shallow depth at two locations in its first application within the Newcastle Coalfields.

Introduction

Electromagnetic (EM) methods which measure earth responses to time varying fields transmitted through closed loops of insulated wire (induction methods) or from antenna (Ground Probing Radar) are well known. The mathematical theory which provides the basis for these methods is derived from Maxwell's equations and is contained within the Helmoltz equation. In the case of a continuous EM source this may be written (Kaufman and Keller, 1983, p.1-3),

$$\nabla^2 \underline{A} + K^2 \underline{A} = 0$$

where $\underline{A}$ represents the required vector potential or function from which it can be derived. The complex parameter which controls this equation is K, the wavenumber i.e.

$$K^2 = i\sigma\mu\omega^2\epsilon \qquad (1.0)$$

where σ, μ, ϵ and $\omega$are electrical conductivity, magnetic permeability, dielectric permittivity and frequency in radians. The first term in the wavenumber equation is the diffusion term which represents the contribution to the overall response from conduction currents. The second term, the propagation term, represents the effect of displacement currents. Clearly the relative contribution of each of these terms to the measured EM response at a site depends on source frequency. Most conventional EM surveys are carried out either in the induction or low frequency (audio) range from about 50 Hz to 15 kHz or in the radar or high frequency (VHF to UHF) range from 80 to 1,000 Mhz.

In the low frequency range the propagation term in Eqn. 1.0 is close to zero and the response of EM induction systems is governed mainly by subsurface conductivity variations. These can be considerable, typically ranging over three to five orders of magnitude, with large conductivity contrasts between soils and rocks (Whiteley, 1983). A group of frequency domain EM (FEM) instruments operating in this range known as Terrain Conductivity Meters (e.g EM31 and EM34 manufactured by Geonics Ltd.) have been designed to operate effectively at low induction numbers (McNeill, 1980) in which field measurements are linearly related to aparent electrical conductivity. These instruments have been reasonably successful for many shallow engineering end environmental studies. However, they suffer a number of limitations mainly due to a sensitivity to surrounding metal objects and powerlines, limited depth of investigation, inherently low vertical resolution due to a limited range of operational frequencies and poor calibration where the low induction number condition is violated.

Ground Probing Radar (GPR) operates in the high frequency range where the conduction term in Eqn. 1.0 is usually ignored in interpretation and dielectric permittivity becomes to dominant earth parameter influencing responses. Relative dielectric permittivities of soil earth materials are listed on Table 1 (from Whiteley and Jewell, 1992) and show substantial variations. The magnitudes of dielectric constant are strongly dependent on moisture content and porosity (if fully saturated) with little direct relationship to electrical conductivity or salinity (Olhoeft, 1986). Unfortunately GPR suffers a major drawback. In highly conductive materials such as wet soils with a high clay content, subsurface penetration of GPR systems may be reduced to depths of less than 1m. This severely limits the application GPR to the detection of underground workings and has led to many erroneous interpretations (e.g. Whiteley and Jewell, 1992).

EM Studies of Old Coal Workings

Abandoned mine workings at shallow depth pose a significant hazard to urban development through the danger of collapse of undermined and stress-released earth. For over 130 years Newcastle, Australia has been the centre of major underground coal mining and, as a result, engineering construction on substantial areas of land where old workings within about 25m of the present land surface can be hazardous and expensive. Residential development may also be restricted.

Even though old mine plans are in existence they are rarely reliable, particularly on the scale of a single dwelling foundation. Consequently the need exists for a method which can screen such areas for cavities as grid drilling is expensive and rarely more than 10 to 20% effective.

In 1989, limited trials of a variety of conventional EM methods which have successfully used in metallic mineral exploration (e.g. Whiteley, 1981) and the GPR method were carried out over old coal mine workings in the Newcastle area. Hatherly and Won (1990) reported that GPR method penetrated only 3 to 4 m into the earth and could not directly detect the workings which occurred at between 14 and 33 m. However, the EM methods were more useful.

The VLF-EM method (EM16-R) using the remote transmitter at NW Cape which operates at 22 kHz appeared to respond to subsurface features indicative of collapse in the old workings at shallower depth (14 m) but not to the deep workings at 33 m depth. Interpretation was complicated by the irregular topographic variations resulting from slumping over the shallow workings. The Controlled Source Audio-Magnetotelluric (CSAMT) method which operates at a range of frequencies from almost DC to 12 kHz provided more encouraging results over the deeper workings with narrow resistive anomalies at regular intervals interpreted to represent remnant coal pillars with intervening broader conductive areas indicative of collapsed and water-filled workings. A limited SIROTEM survey was completed in the same area (Whiteley, unpub.) and anomalies believed to be associated with old workings were identified. Unfortunately, these data were later found to be adversely affected by the presence of rusted metal objects which were strewn over the land surface. As a result the performance of the SIROTEM method was uncertain.

Radiowave methods operating in the intermediate frequency range of about 30 kHz to 5 MHz are a recent development. One such system (Radio Imaging Method, RIM) designed to operate underground or between boreholes in the 50 to 500 kHz has had some success for the prediction of coal seam disruptions prior to mining over distances of several hundred metres (Thomson, 1991). In this region both conductivity and dielectric constant influence system responses and quantitative interpretation of the data obtained has proved complex.

The GRC-2 Radiowave System

The GRC-2 system has been under active development for a number of years at the Kiev Institute, Ukraine specifically for engineering and environmental problems such as the detection of underground cavities. This system operates at about 1.5 MHz which reduces the effective depth of investigation to about 50 to 70m in rock and about 30m when soil and weathered rock are present. Also at this frequency the response of the system is dominated by dielectric property variations and surrounding metals which adversely affect induction methods exhibit little influence nor do conductive soils which severely attenuate GPR signals.

The GRC-2 is similar in appearance to most frequency domain EM systems and comprises separate transmitter and receiver units each connected to specially designed screened loop antenna approximately 0.5m diameter. The transmitter radiates an EM field, whose intensity may be varied, at an ultra-stable frequency of 1.5Mhz. The receiver is also ultra-stable and is tuned to the transmitter frequency. This provides a system which highly selective, much more so than normal EM equipment, and highly discriminatory to external sources of noise.

The loops are mounted on individual tripods which are accurately maintained at a constant spacing, about 70% of the required depth of investigation, during the profiling. The transmitter loop is levelled in the vertical plane and is aligned with the receiver which is levelled in the horizontal plane. This null-coupled configuration further increases the sensitivity of the GRC-2 system to any significant lateral variations in dielectric constant within the subsurface. As the device is operating in a "pure anomaly" mode (Chetaev, 1956) signal intensities (Hz) at the receiver loop vary only when a buried heterogeneity is traversed. The EM anomalies produced by the GRC-2 device are controlled largely by the nature of the subsurface heterogeneity.

As with most other EM systems GRC-2 profiles using the prechosen loop spacing are normally completed orthogonal to the suspected strike of subsurface heterogeneities and it is not uncommon for detailed studies to be completed using station spacings of 0.5 to 1.0m.

Interpretation of GRC-2 Responses.

In the frequency range of about 1 to 5 Mhz any subsurface heterogeneity giving rise to a relative dielectric contrast causes an oscillating electric dipole to be formed. This, in turn, radiates a secondary magnetic field to the receiver coil on the surface. The intensity of the vertical component is influenced by a number of factors which are described below but is largely controlled by the magnitude of the dielectric contrast.

For example, in natural ground with a moisture content of 10% typical dielectric constants Eg = 20 (Table 1) could be expected. If a localised air-filled void (Ea = 1), within the investigation depth of the GRC-2 system, is traversed then Ea/Eg = 0.05 (< 1) and a decrease in the vertical magnetic field intensity (Hz) would be registered. If the void is water-filled (Ew=81) then Ew/Eg = 5 (>1) and an increase in the vertical magnetic field intensity would be registered. Fig. 2 (from Zaderigolova, 1986) shows typical GRC-2 Radiowave anomalies over just such features which were subsequently confirmed by drilling.

The form of the radiowave anomalies over subsurface features is governed by a variety of factors which may be expressed generally as, i.e.

$$H_z = \frac{Mx}{4\pi} G_m V_n D_n f(z)$$

where

H_z - measured vertical magnetic intensity
M_x - magnetic moment of the transmitter loop
G_m - geometric parameters of the GRC-2 system
V_n - geometric parameters of the subsurface heterogeneity
D_n - physical property magnitudes (i.e. conductivity and dielectric constant) and their contrast
$f(z)$ - depth function

The functions V_n, D_n, f_z are quite different for different forms of heterogeneity and interpretation curves are available for different simplified models, however, at the shallow depths involved location of the heterogeneity frequently suffices for follow-up by drilling.

Field Trials in the Newcastle Coalfields

Fig. 2 shows a plan of old mine workings near Maitland over which a borehole (BH 4) was drilled supposedly over an old drive with the objective of proving its existence. Unfortunately, BH 4 intersected a coal pillar and an intact coal seam at 15 m depth. This hole was tested with surface-to-borehole seismic (Whiteley and Love, 1992) which showed the presence of low velocity zones on either side of the hole in an east-west direction indicative of undermined and collapsed ground. The average seismic velocities within these zones (900 m/s) are less than the P-wave velocity in water indicating significant fractured roof rock above the water-table.

In Fig. 3 the final seismic model obtained and a GRC-2 radiowave profile in the same direction are shown. This profile shows prominent anomalies with a narrow region of low vertical magnetic field intensity over the unworked pillar at BH 4 and adjacent high values associated with the abandoned workings. The high field values demonstrate that the major cavities are water-filled. Further low field intensity anomalies which occur on either side of the are believed due to other coal pillars or unworked ground.

Fig. 4 shows radiowave profiles at an undermined sites in the Charlestown area where linear topographic depressions have been created by coal mining at depths of about 10 m. Again, as at the Maitland site, prominent high field intensity anomalies occur over the projected intersection of these linear features indicating that the significant cavities are water-filled.

Conclusions

The GRC-2 Radiowave system which responds to relative dielectric contrasts has demonstrated the ability to detect abandoned and flooded coal mine workings occurring at shallow depth in the Newcastle area. This new method permits rapid screening of areas which may have been undermined to shallow depth and may be applied in urban areas as it is not adversely affected by surrounding metallic objects, powerlines and conductive soils which limit the application of other electrical and electromagnetic geophysical methods. It is expected that the

GRC-2 system will be increasingly used in geotechnical studies to detect underground cavities occurring in the upper 30 m of the earth.

Table 1	Relative Dielectric Constant of Shallow Materials (from Whiteley and Jewell, 1992)
Figure 1	GRC-2 Radiowave Profiles over Air and Water Filled Cavities.
Figure 2	Plan of Old Mine Workings and BH4 near Maitland.
Figure 3	GRC-2 Radiowave Profile and Seismic Model in EW Direction, BH4.
Figure 4	GRC-2 radiowave profiles in the Charlestown area.

References

Chetaev, D.M. 1956 A Theorem of Electrical Exploration (in Russia) Izv. Akd. Nauk. USSR Ser. Geofiz, 6, 794-799.

Haltherly, P. and Won, G. 1990, Geophysical Detection of Old Mine Workings. Proc. 24th Symposium on Advances in the Study of the Sydney Basin, 23-25 March, 1990, 91-96.

Kaufman, A.A. and Keller, G.V. 1983 Frequency and Transient Soundings. Elsevier, NY 685p.

McNeill, J.D. 1980, Electromagnetic Terrain Conductivity Measurements at Low Induction Numbers. Geonics Ltd. Canada, TN-6.

Olhoeft, G.R. 1986, Direct Detection of Hydrocarbon and organic Chemicals with Ground Penetrating Radar and Complete Resistivity. Proc. National Water Well Assn. Conf. on Petroleum Hydrocarbons and Organic Chemicals in Groundwater. Nov. 12-14, 1986, Houston, Texas, 1-22.

Thomson, 5. 1991, Practial Applications of the RIM Techniques from boreholes. Proc. 25th Symposium, on Advances in the Study of the Sydney Basin, Newcastle, April, 1991.

Whiteley, R.J. 1983, Recent Developments in the Application Geophysics to Geotechnical Engineering in In-situ Testing for Geotechnical Investigations. A.A. Bakema, Rotterdam, Ch.7,87-110.

Whiteley, R.J. and Jewell, C.M. 1992, Geophysical Techniques in Contaminated Lands Assessment - Do They Deliver? Exploration Geophysics, 23.

Whiteley, R.J. 1981, Geophysical Case Study of the Woodlawn Orebody, NSW. Australia. Pergamon, Oxford. 586p.

Whiteley, R.J. and Love, A. 1992, Site Uniformity Borehole Seismic (SUBS^c) Testing in Undermined Areas. Proc. 26th Newcastle Symposium on Advances in the Sydney of the Sydney Basin 3-5 April, 1992, 110-118.

Zaderigolova, 1986, The Application of the Radiowave Method for Evaluation and Forecasting of Stability of Nuclear Power Station Facilities being Construction in Karst Environments.

ACKNOWLEDGEMENT

The authors are grateful the Geotronik (Australia) Pty. Ltd. for the loan of GRC-2 radiowave system for the field trials and to Mr. Chris Francis of the RTA, Newcastle Division for assisting at the Charleston site.

TABLE 1
RELATIVE DIELECTRIC PERMITTIVITY OF SHALLOW MATERIALS

MATERIAL	RELATIVE DIELECTRIC PERMITTIVITY
Air	1
Fresh Water	81
Sea Water	81
Sand (dry)	4
Sand (3-5% water)	10-30
Sand (6-30% kerosene)	3
Clay	10
Soil (dry to 15% water)	4-29
Soil	30-50
Sandstone	6
Shale	7
Basalt	8
Granite	7

NOTE: Unless otherwise stated, materials are saturated with fresh water.

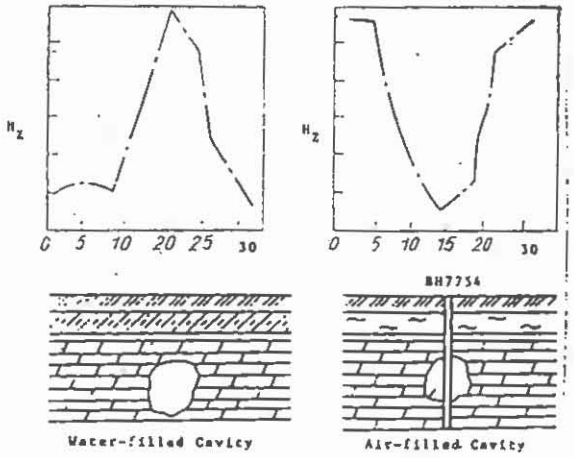

FIGURE 1

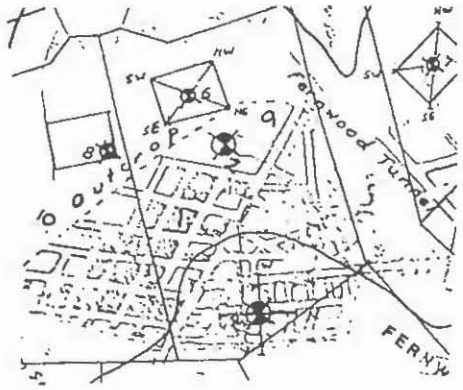

FIGURE 2

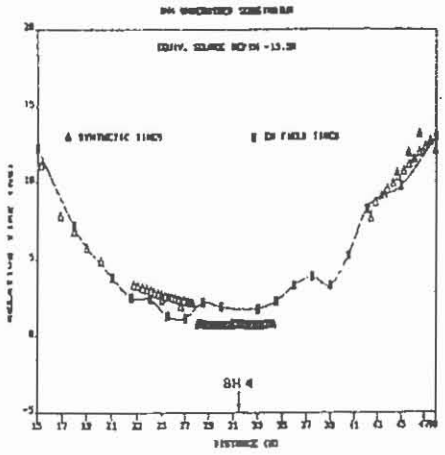

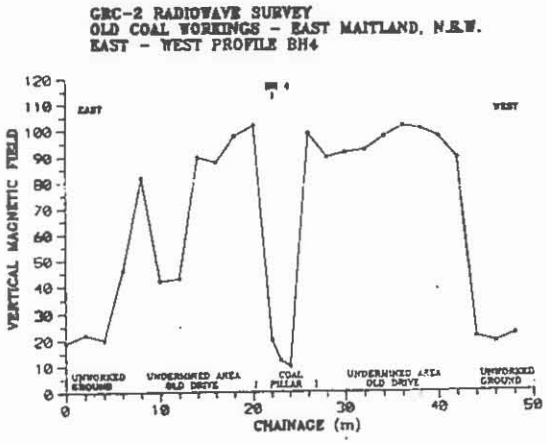

EAST-WEST PROFILE
COMPUTER MODEL DERIVED FROM DOWNHOLE SEISMIC TESTING

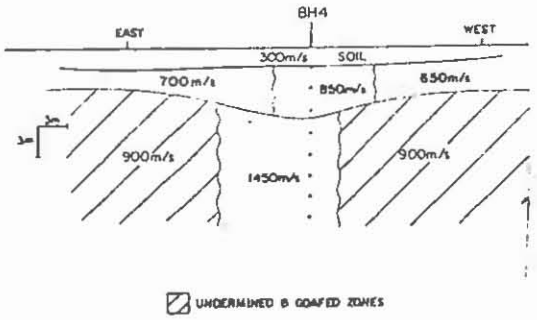

FIGURE 3

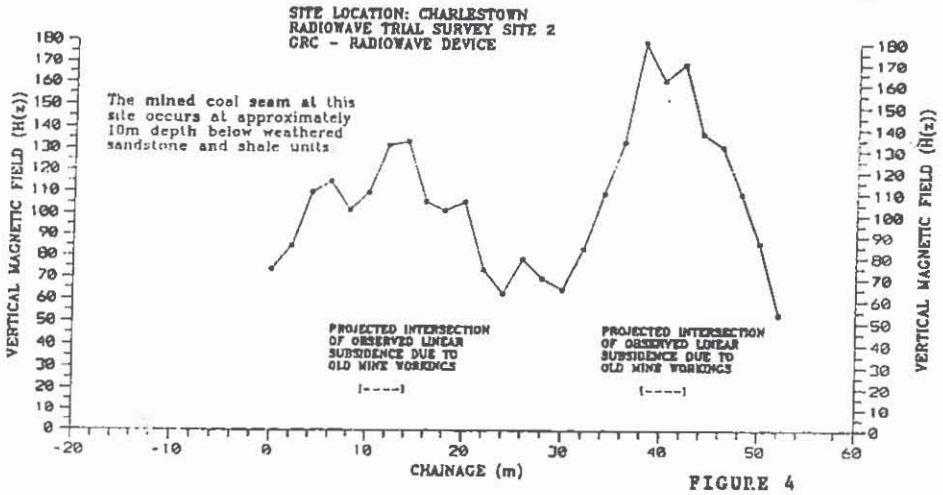

FIGURE 4

DESIGNING FOR SUBSIDENCE, PILLAR STABILITY & FLOOR HEAVE WITH LOW STRENGTH CLAYSTONE FLOORS

R.W. SEEDSMAN[1] & N. GORDON[2]
[1] Coffey Partners International Pty Ltd
[2] ACIRL Ltd

INTRODUCTION

The Awaba, Booragul, and Mannering Park Tuffs are composed of 'claystones' with highly variable properties. The Tuffs vary in thickness and the degree of cementation and are also unevenly distributed (especially the low strength varieties). Some of the 'claystones' are highly silicified and chert-like in appearance. Such material is of high strength and modulus and will not be considered further in this paper. Other 'claystones' are noticeably very weak - they can be readily scratched with a fingernail and slake/disperse on immersion in water. These latter materials appear to be developed around the Southern Lake Macquarie area are associated with roof and floor instability during underground coal mining and also anomalous surface subsidence.

Extensive laboratory testing has suggested that the low strength claystones can be considered as over-consolidated clays with low short-term (undrained) strength and deformation properties and even lower long-term (drained) properties.

PRACTICAL CONSTRAINTS TO THE DESIGN METHOD

Before seeking an engineering solution to an operational problem, recognition of the practical constraints to the solution must be made. In this context, it must be recognised that the claystones are highly variable, sporadically distributed, with limited borehole data available. Given these constraints to geological knowledge, only simple engineering analyses can be justified. However, the subsidence issue is highly politicised and there is an expectation that the mining industry should be able to move accurately predict subsidence. In addition, the current market conditions are very tight with resultant pressures to reduce mining costs.

It was decided that foundation engineering concepts could have the potential to be successfully applied to the various claystone related issues. The perceived advantages of this approach were the availability of simple analytical methods, reduced costs in developing design methods, and readier acceptance of the results.

PILLAR SETTLEMENT AND SUBSIDENCE

For the ratios of pillar width to claystone thickness commonly seen, pillar settlement into a claystone floor is given approximately as:

$$S = \Delta q \, h/E$$

where
- S = settlement
- Δq = change in average pillar stress, and
- h = claystone thickness
- E = elastic modulus

Fortunately, q is simple to calculate by tributary area concepts as extraction is by panel and pillar usually under massive conglomerate roof which does not cave.

Figure 1 gives the calculated pillar settlement for a range of claystone thicknesses and moduli for the case of 60% extraction at 200 m depth. Note that Seedsman & Mallett (1988) measured an undrained modulus of 1100 MPa and a drained modulus of 200 MPa. The calculated settlement for an undrained modulus of 1100 MPa compare well with measured short-term pillar settlements of 10-37 mm in 3 collieries around Lake Macquarie (Seedsman & Gordon 1991).

Of particular significance in Figure 1 are the very high pillar settlements calculated for drained modulus values of 200 MPa. It is postulated that long term pillar settlement into thick claystone will be reflected in a measurable increase in surface subsidence. Whilst this has not been definitively established, support for this postulate comes from the analysis of subsidence data. Figure 2 shows the classic straight line segment obtained from Taylors $\sqrt{\text{time}}$ method of analysising consolidation data when applied to some anomalous subsidence data.

CLAYSTONE FAILURE

If the imposed stresses are sufficiently high, failure of the claystone may be induced. Bearing capacity theory can be used to analyse such an occurrence. Pillars can be considered as surface footings and for the case of short-term failure (undrained) the failure stress (qmax) is given by:

$$qmax = \frac{UCS}{2} \times N$$

where
- UCS = unconfined compressive strength
- N = bearing capacity factor connected for layer thickness, footing shape, inclination etc

For thin clay layers in comparison to pillar width, N is given by:

$$N = \Pi + 1 + B/2h \quad (\text{for } B/h > 8)$$

where
- B = pillar width
- h = layer thickness

Figure 3 gives the required claystone thickness (h) for failure for the case of a 25 m wide pillar and a range of pillar stresses and claystone strengths. For depths of about 200 m, 60% extraction, and claystone strengths of 4 MPa, claystone horizons thicker than about 5 m would fail.

CLAYSTONE FLOORS

Possibility of Pillar Failure

One implication of the failure of claystone horizons may be the destruction of the integrity of the pillar itself. Claystone failure will result in the lateral extrusion of the clay. Such extrusion will induce tensile stresses within the enclosing coal/rock and may induce failure. This would be particularly the case for cleated coal. Two aspects of such a model need to be considered. Firstly, the mechanism will be active in the short-term; over time drained conditions will develop, the bearing capacity of the claystone increase, and the conditions become more stable. Secondly, failure should progress only until the resultant thickness of the layer decreases such that the calculated failure stress is equal to the average pillar stress.

Floor Heave

For the cases examined by Seedsman and Gordon (1991), floor heave was seen to develop with claystone thicknesses of 300 mm and strengths of 10-20 MPa. Such observations are not consistent with the mechanism discussed above. Further consideration of the nature of floor heave and the distribution of stresses across a pillar has led to the formulation of the model seen in Figure 4. In this model claystone failure is restricted to the rib zone only - say 1-2 m in width. This has the effect of significantly reducing the aspect ratio (B/h), reducing N and so reducing the failure stress. The applied stress can be taken as the average pillar stress.

Floor heave can also be caused by the simple swelling of claystone in the roadway. In this case the shape of the heave is distinctive - being relatively flat compared to the inverted V shape seen with most heave. A constant heave rate of about 0.5 mm/day over about 1 year was measured at one local colliery. Such a rate would be calculated from a drainage path length of 30 cm and a Cv of 0.01 m^2/day. Yet another mechanism of floor heave relates to the extrusion of claystone referred to earlier.

APPLICATION

A number of simple engineering analyses are available to predict mining conditions in the presence of claystones. Pillar settlement and subsidence can be analysed using elastic theory while pillar stability and floor heave can be analysed using bearing capacity concepts.

As in all geotechnical engineering, the design is only as good as the quality of the geological data. The availability of design methods means that focus now needs to be placed on the description and assessment of the claystone. Future logging of claystone must describe the thickness, strength and deformation properties of claystones - not only of the overall units but also bands within it. Figure 3 gives guidance as to the required resolution in terms of banding thickness and strength.

Testing of thin units of claystone may be difficult. Wherever possible, water content should be measured so that a data base of UCS, modulus and water content relationships can be developed as shown in Figure 5.

CONCLUSIONS

It is concluded that an internally consistent geotechnical model and simple design methods are available for claystones. The model and method are based on well established foundation engineering concepts and can be used to predict subsidence, pillar stability and floor heave.

Routine use is recommended to verify and improve the methods. Future logging of the claystones needs to describe thickness and strength variations in more detail.

ACKNOWLEDGMENTS

Work on claystones of the Newcastle Coal Measures has been funded by NERDDC. The work described above was conducted while the author was employed by ACIRL.

REFERENCES

Seedsman and Mallett 1988: Claystones of the Newcastle Coal Measures. Final report to NERDDC, Project 902.

Seedsman and Gordon 1991: Methods to optimise mining operations affected by weak claystone materials. Final report to NERDDC, Project 1440.

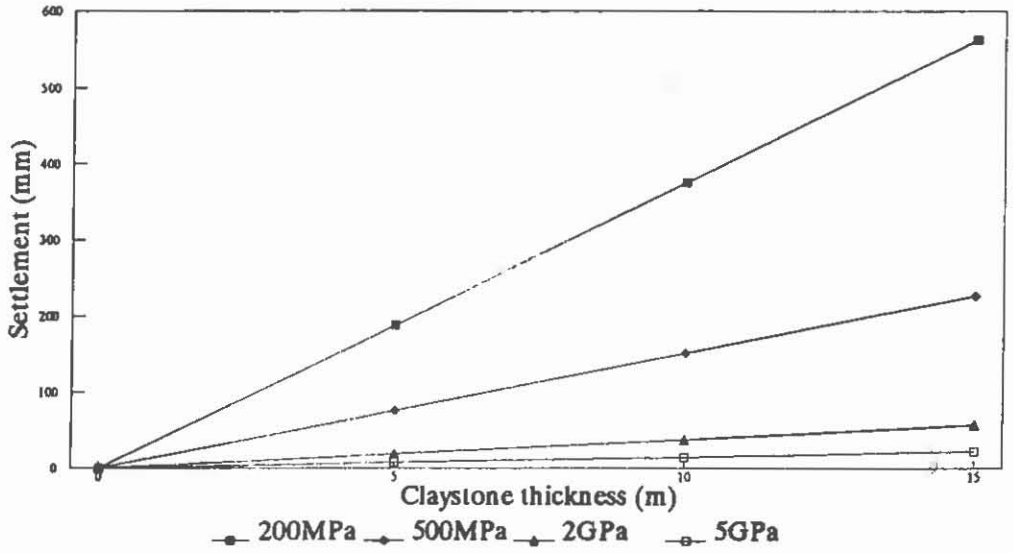

FIGURE 1 Pillar settlement as a function of claystone thickness and for 4 values of modulus

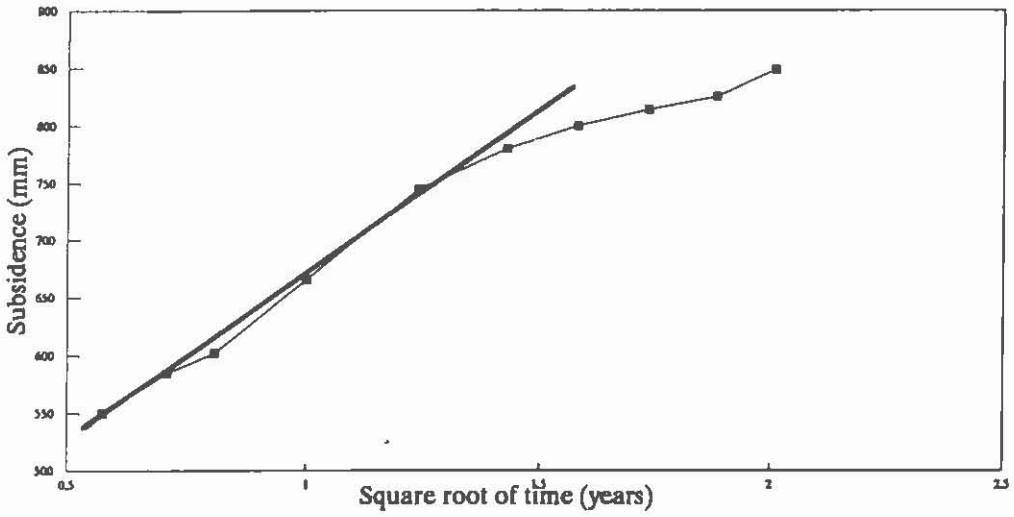

FIGURE 2 Anomalous subsidence data plotted are a 1 dimensional consolidation test

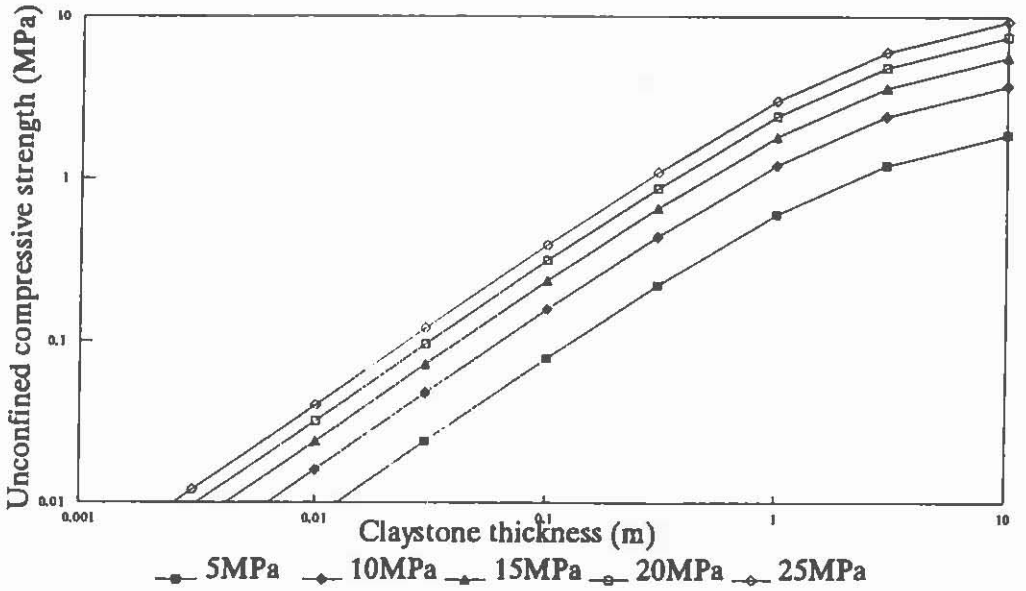

FIGURE 3 Claystone strength for bearing capacity failure as a function of thickness for a range of average pillar stresses

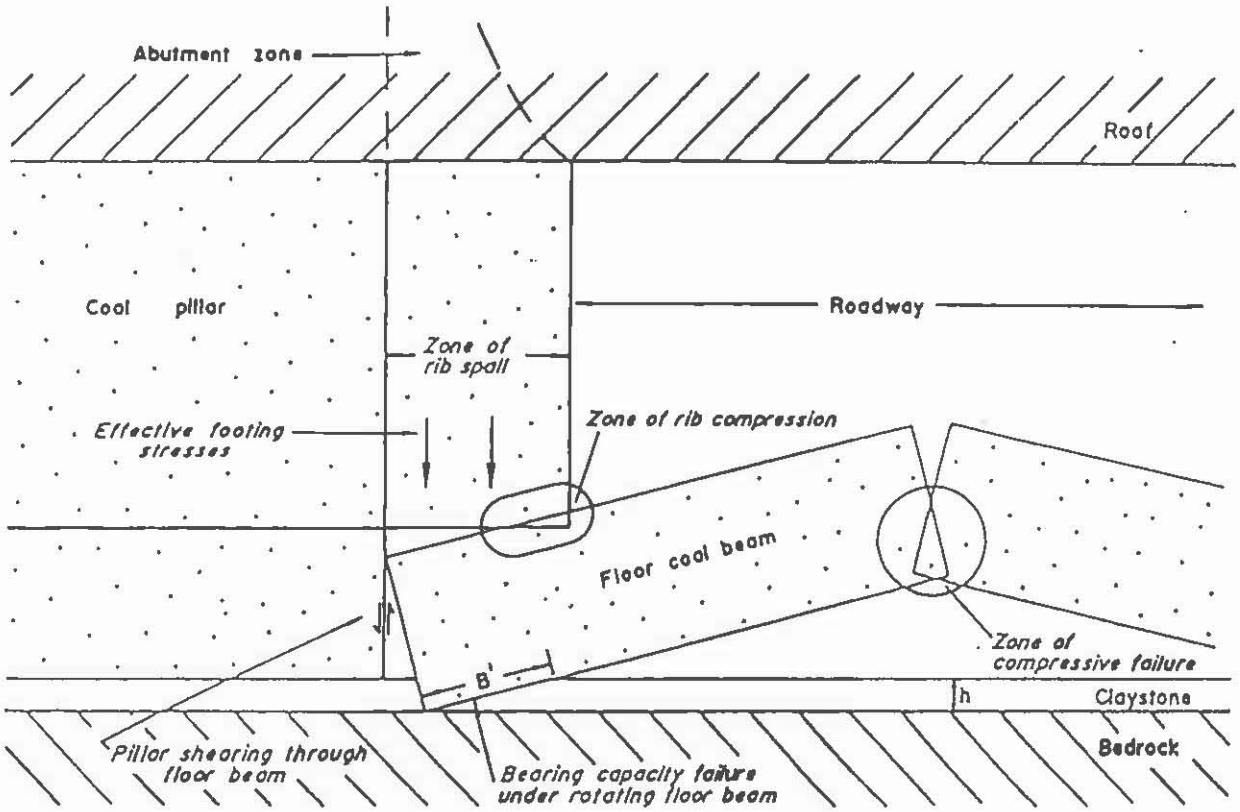

FIGURE 4 Model for floor heave and rib failure

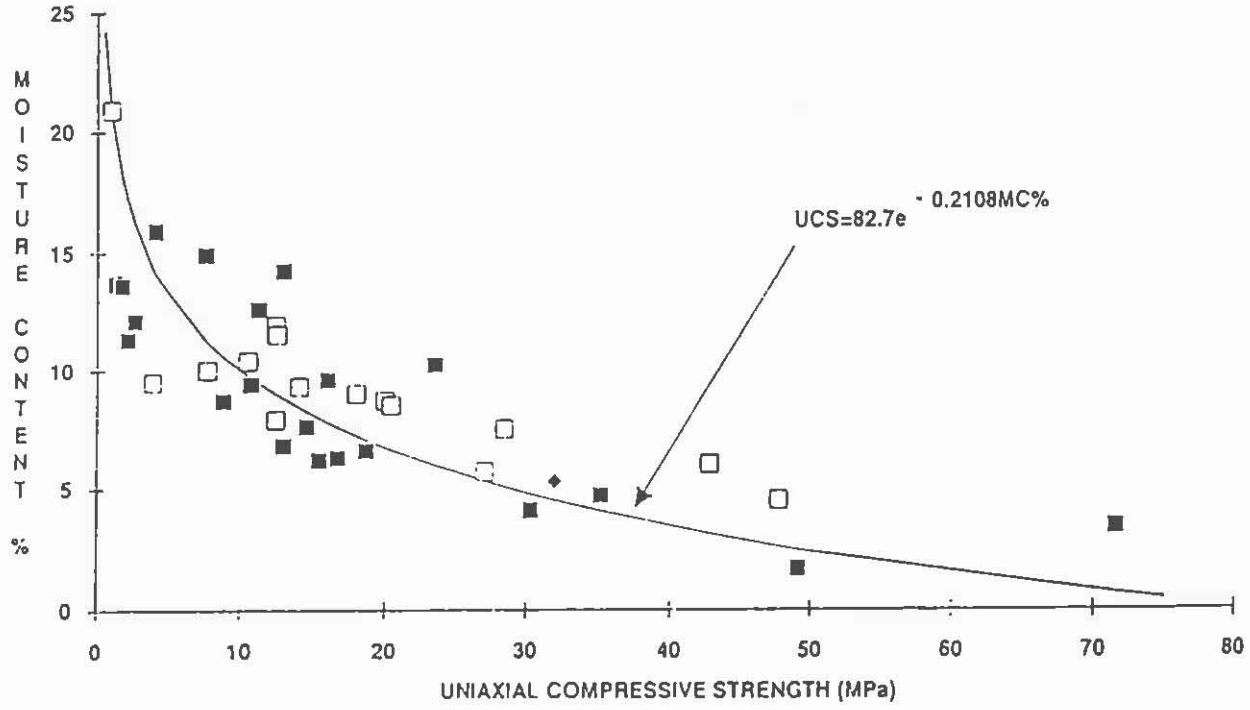

FIGURE 5 Correlation between moisture content and unconfined compressive strength

A COMPARISON OF EXPLOSIVE & NON-EXPLOSIVE SEISMIC SOURCES IN AN IN SEAM SEISMIC BOREHOLE TO BOREHOLE SURVEY

A.R. NEWLAND[1], G.R. POOLE[2] & C.R. HOFFMANN[3]
[1] BHP Engineering
[2] BHP Steel Division Collieries
[3] BHP Research

SUMMARY

During 1992 an In Seam Seismic transmission survey was conducted in the Hunter Valley which used the "Boomer" non explosive seismic source and an explosive seismic source. This enabled a comparison to be made between the two types of seismic source in a coal measure sequence. The effective "boomer" range in a coal measure sequence was shown to be 200 to 250 metres.

THE "BOOMER" SOURCE

The boomer is an electromagnetically driven seismic source consisting of a triggered capacitor bank which discharges electricity through a flat coil. Eddy currents are produced in a copper plate held against the coil by a neoprene sealing jacket and by water pressure. The magnetic fields interact so that the plate is rapidly repelled from the coil, creating a pressure pulse in the fluid in the borehole. The design objectives were to produce a seismic source which would not damage the borehole, require little or no maintenance, be capable of repetitive firing to enable data stacking. Initial development of the "Boomer" took place at Macquarie University with further development being undertaken at BHP Research Newcastle. Currently the "Boomer" has a depth limit of 200 metres with an input of 2000 joules and an output of 1000 joules at the source. The drop between input and output is due to cable losses with the capacitor banks being on the surface. The Mk 2 "Boomer" currently under construction will have downhole capacitor banks to solve this problem of cable losses allowing operation to depths of 1000 metres.

THE EXPLOSIVE SOURCE

Instantaneous submarine No 8 detonators were used as the explosive source. These were electrically fired using a Beethoven Shot exploder.

A R NEWLAND G R POOLE C R HOFFMANN

THE VSP SONDE

The (VSP) Vertical Seismic Profiling Sonde is a clamping XYZ geophone which digitises the received seismic data downhole before sending the data up a standard four conductor logging cable to be recorded by the field control unit. The downhole digitisers can sample at rates from 0.0625 millisecond to 2 milliseconds, data length from 1 to 8K and gain from 26 to 66dB. Digitising the data downhole has many advantages such as maximising the recorded signal-to-noise ratio and minimising the effects of background electrical noise the data. The VSP detector and the attached seismic data recording system were designed and manufactured by BHP Research Newcastle.

THE ISS SURVEY

The ISS survey was conducted between two exploration boreholes spaced 152 metres apart.

The "Boomer" was placed mid seam in the target coal seam in one borehole while the VSP detector was clamped in the middle of the same seam in the adjacent borehole.

The "Boomer" was fired every eight seconds sixty-four times to stack the seismic data. This improves the signal to noise ratio so that useable data is obtained.

A single detonator was fired in the same position as the "Boomer" to enable a close comparison to be made between the explosive and "Boomer" data.

The data was processed using the BHP Research developed seismic processing software on a 486 PC.

The raw trace plots (Figure 1 for the "Boomer", Figure 3 for the detonator) show that the signal amplitude of the "boomer" data is 30 times smaller than the detonator in the X and Z components and 12 times smaller than the detonator in the Y component. This difference in the amplitudes of the data reflects the relative size of the energy output of the "Boomer" and the detonator.

The frequency spectra plots (Figure 2 for the "Boomer", Figure 4 for the detonator) show that the detonator shot has more high frequency data than the boomer. This can be partly explained by the attenuation of the smaller energy "boomer" by comparison with the detonator source.

CONCLUSION

The recent ISS borehole to borehole survey conducted in a coal measure sequence in the Hunter Valley show that the "Boomer" non explosive seismic source is a successful seismic source which can be used in closely spaced exploration boreholes. The preferable sites to use the "Boomer" in its present form would be where there are site restrictions on the use of shotfiring.The next stage of the "boomer" currently under construction with downhole capacitors will have a depth capability of 600 metres and output of 3000 joules which will improve its range.

ACKNOWLEDGMENTS

The "Boomer" trial survey was conducted as part of a National Energy Research Development and Demonstration Council Project No 1608 "Development of a Non Explosive Seismic Source for the Coal Industry".

REFERENCES

TAYTON J W and HOFFMANN C R 1992: Development of a Borehole Boomer Seismic Source
University of Sydney Geophysics Consortium Conference September 1992.

TAYTON J W SMITH P D VOZOFF K and LEUNG L 1991:
Seismic Source for Deep Borehole Operation
NERDDP Report No 1441.

NON EXPLOSIVE SEISMIC SOURCE

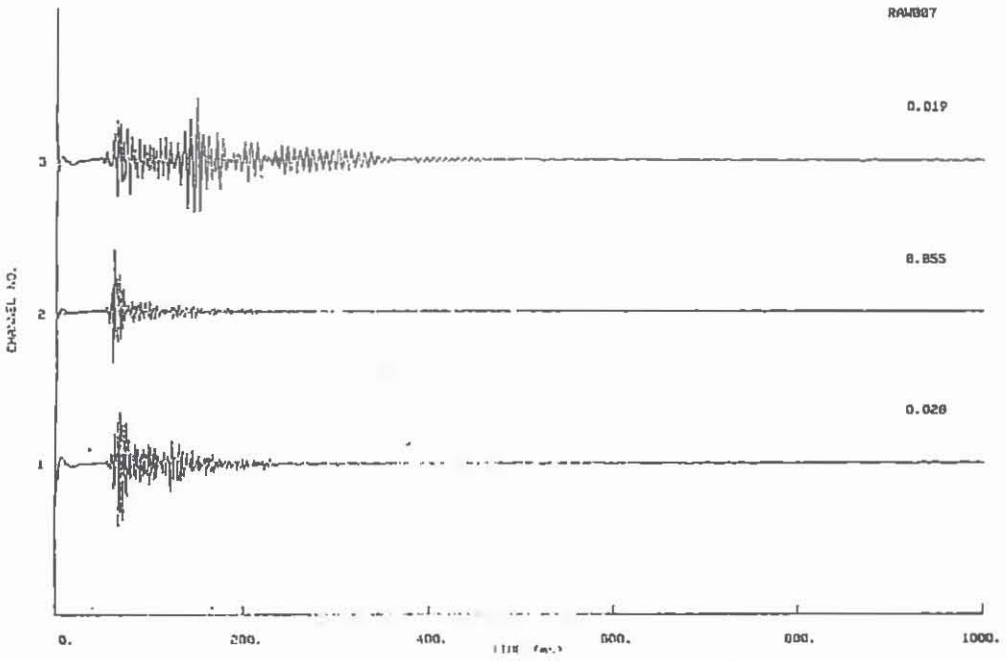

FIGURE 1

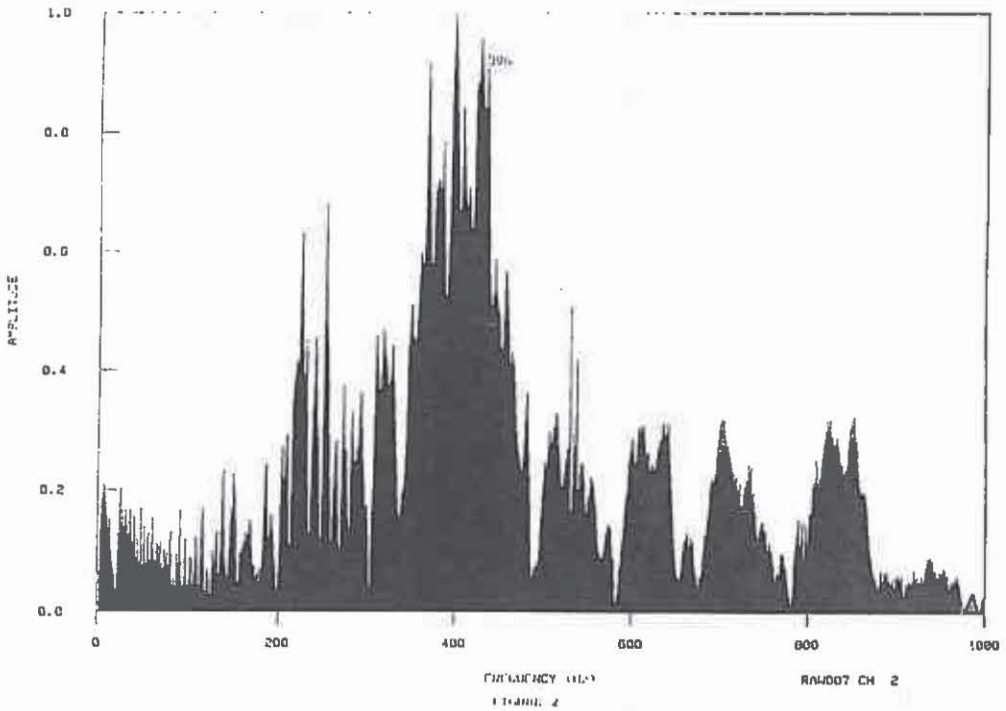

FIGURE 2

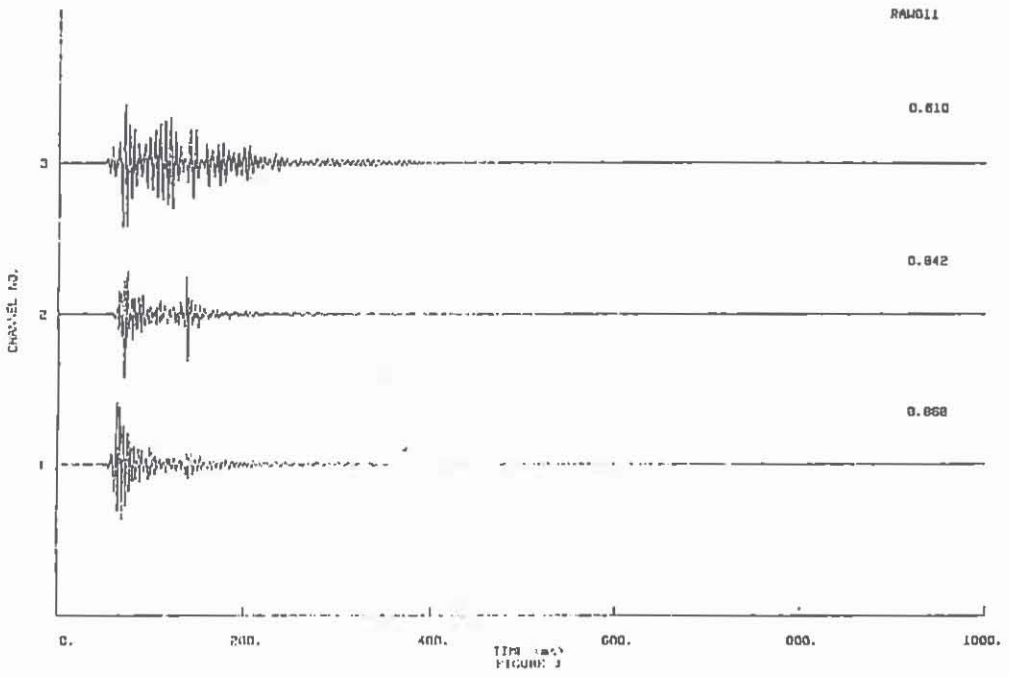

FIGURE 3

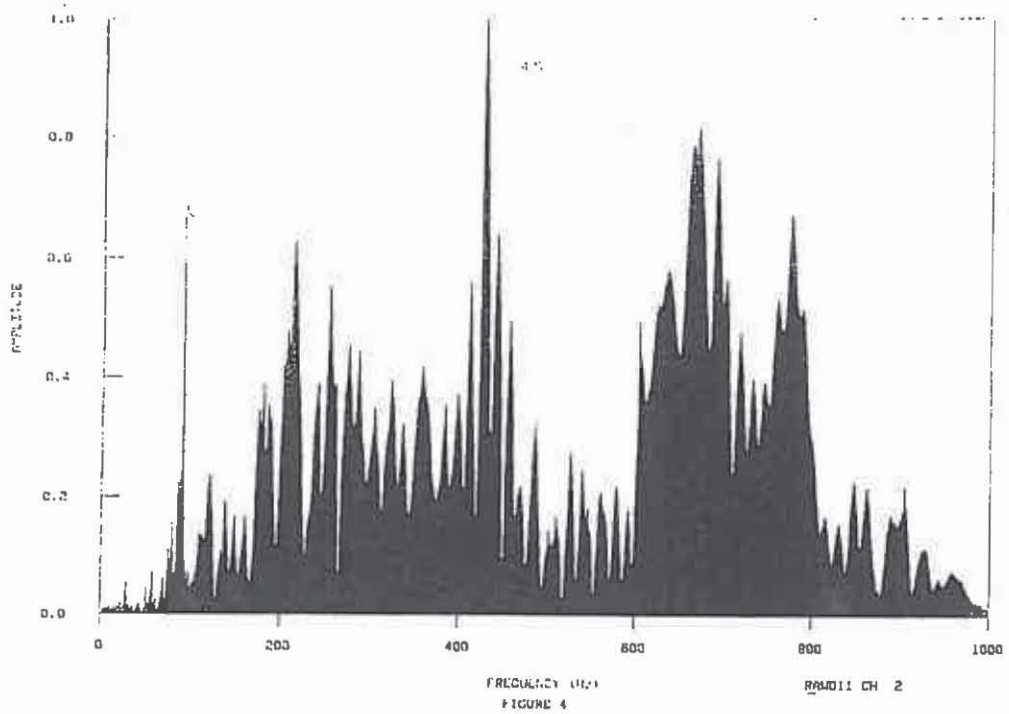

FIGURE 4

FRACTURE HISTORY OF THE COAL CLIFF SANDSTONE AT COALCLIFF, NSW

H. MEMARIAN
University of Wollongong

SUMMARY

A 10 m thick quartz lithic sandstone over a coastal platform at Coalcliff, NSW, has undergone 3 stages of brittle deformation. Three sets of mapped systematic joints, strike N, NNE and NE, are the result of the first stage of deformation. They are of extension origin and formed from tectonic stresses during burial. In the second stage the NNE and NE joint sets were recracked and moved dextrally and sinistrally respectively. The third stage involved opening of the faults and formation of non-systematic joints due to unloading, weathering and surficial movement. Comparison of the direction of the maximum horizontal stress responsible for each deformation episode reveal that σ_1 was swinging between N to NE since the initiation of fracturing, which is comparable to the reported contemporary σ_1 for the southeastern Sydney Basin.

INTRODUCTION

The surficial study of joints and other fractures in the southeastern part of Sydney Basin has been mostly based on Landsat imaginary and air-photo interpretation (Bowman, 1974; Mauger et al., 1984). The results of these studies usually reflect fracturing of Hawkesbury Sandstone, which covers most of this region. Similar studies in underground coal mines have been generally limited to some coal seems and their adjacent roof and floor strata.

This paper reports the results of a study of the southern member of a twin coastal platforms at Coalcliff, 35 km south of Sydney. The studied platform is in the Coal Cliff Sandstone. This unit which is around 10 m thick, consists of a homogeneous, medium to coarse grained lithic sandstone with a number of pebbly bands and a few beds of grey shale and brown clay ironstone. Brown clay ironstone (siderite claystone) generally occur in beds usually less than 5 cm in thickness. These beds usually grade into grey shale at the base and are sharply overlain by either additional shale or by sandstone (Ward, 1971). Coal Cliff Sandstone disconformably overlies the coal of Bulli Seam, and forms the basal formation of the Narrabeen Group.

JOINTING OF ROCK

An enlarged airphotograph (almost 1:250) was used for preparing the base map and tracing the longer open joints, which in turn were used as references for field mapping of the smaller fractures and related features. Three distinctive sets of fractures were measured in this platform, which for the sake of convenience, are called the N, NNE, and NE sets. All of the systematic joints are vertical, and normally straight. Among these, the N joints (178-180°) are less frequent and limited to the southern edge of the platform. The NNE joints strike 5-15° with a mean direction of 10° and the NE joints strike between 35-50°, with a mean direction of 45°.

The systematic joints are generally rectangular in shape, with their height normally bounded by the upper and lower limits of a single layer. The length of joints are generally several times their height. Thin ironstone and shale beds, a few centimetre in thickness, act as mechanical boundaries and arrest the vertical propagation of joints to neighbouring sandstone beds. The thin ironstone beds are themselves jointed. Most of the joints were originally filled with calcite which indicate that joints formed and filled below the water table. In general, the infilling indicates that the joints were filled with fluids at the time of fracturing, although the infilled minerals themselves may have crystallized from other fluids flowing through the fracture system later (Wheeler & Holland, 1978). In most parts of the platform, especially in fractures with wider openings, subhedral crystals of calcite cover the fracture wall and indicate that the fracture was open at depth (Lorenz & Finley, 1991).

RECRACKING

Both NNE and NE joints were recracked and slipped laterally, in a subsequent event and produced what are called faulted joints (Zhao & Johnson, 1991). This movement was dextral for NNE and sinistral for NE fractures. Recracking normally took place along the previous infilled and closed joints, but when a propagating front reached the end of an existing joint, it continued and fractured intact rock.

The recracking of rock and development of faulted joints, also gave birth to a new set of fractures, which are developed normally at the tip, and sometimes at the sides of existing NNE and NE joints. These fractures are straight to curved, and compared to the parent joints, they are very short (few centimetres to less than a metre), and strike between 20-30°. The direction of secondary fractures, in respect to the parent joints, reveal the sense of lateral movement (Fig. 1).

ORIGIN

Joints are kinematically puzzling structures and their interpretation has generated controversy. In many instance the origin of an identical set of joints is suggested to be either extensional or shear by different authors (e.g. Engelder, 1982; Scheidegger, 1982).

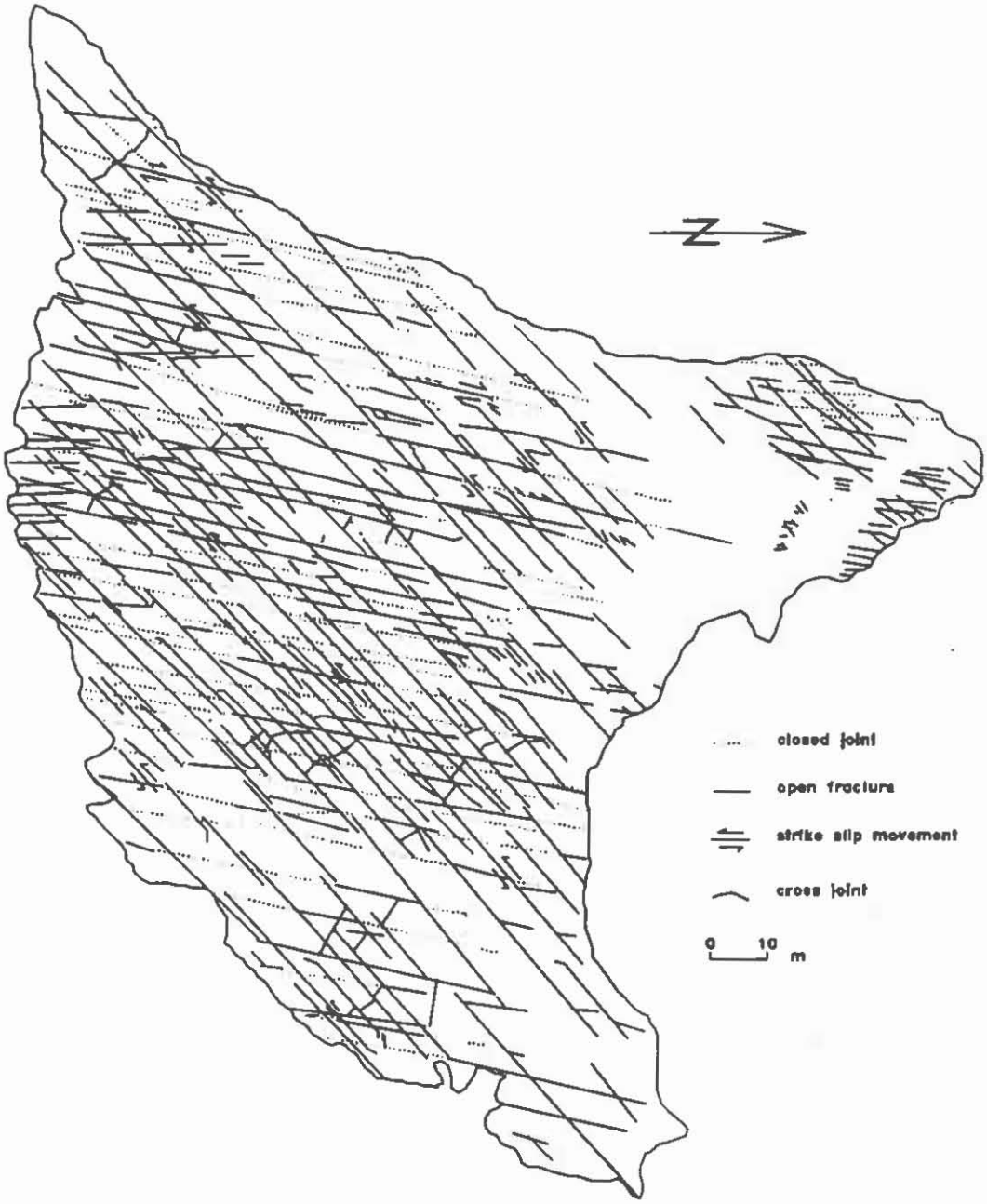

Fig. 1 Fracture pattern of Coal Cliff Sandstone at Coalcliff, NSW.

No surface markings are visible on joints of this platform, perhaps due to the subsequent lateral movements along the joints. It should be noted that in other exposures, to the south, joints with almost identical geometrical characteristics, show distinctive surface markings and plume structures. Both at mesoscopic and microscopic scales, no original lateral movements are visible in the infilled and closed parts of the joints. All of the existing shear displacements along the joints

postdated formation of joints. The dihedral angle (2θ) between conjugate joints is another criteria differentiating between shear and extension joints. Assuming a ϕ angle of 30° for the rock, Hancock (1985) suggests that shear joints should have 2θ of more than 60°, whereas in this case the dihedral angle between NNE and NE joints is around 35°. It is concluded that all of the systematic joints are propagated originally in extension form (mode I).

RELATIVE AGE

Two joint sets, namely A and B can have three possible age relations. Set A is younger than set B, set B is younger than set A, and finally both sets have the same age. In the latter case all of the members of two sets might have exactly the same age, i.e. propagate simultaneously, or they might initiate alternatively. Cross cutting relations, and other characteristics of the joints, suggests that N joints were the first extension fractures developed.

The cross cutting relations traced from the enlarged air photograph suggests that set NNE is younger than set NE, simply because a larger number of NNE fractures terminate against NE ones (solid lines in Fig. 1). Closer inspection reveals that this conclusion is not correct and that the traced parts are only the open segments of fractures, which are themselves the result of subsequent recracking. Geometrical relations mapped from thin ironstone layers, which have not suffered from subsequent recracking, and overprinting data collected from neighbouring platforms, suggest that the NNE joints are most probably older than NE ones.

SEQUENCES OF BRITTLE DEFORMATION

To obtain the sequences of stress fields responsible for present fracture pattern, one must know the direction of propagation of joints in a deviatoric stress field and be able to date the formation of joint sets relative to each other (Engelder & Geiser, 1980). The deformation history of the Coal Cliff Sandstone in the studied platform is ordered chronologically in stages.

1. Formation of extension joints: The three sets of extension joints (namely N, NNE and NE) are the result of the first stage of brittle deformation in this platform, which in turn is divided into three sub-stage, each responsible for propagation of one extension set. The N joints were the first brittle structure that formed in the original intact rock. Joints filled with calcite crystals soon after propagation and the rock became intact, almost the same as it was before deformation.

Joints NNE and NE display more or less similar characters, which suggests some relation between them. They even might have propagated simultaneously. Zhao and Johnson (1991, 1992) reported alternative formation of segments of joints belonging to two separate sets. It is often difficult to determine the age relationships between several interfering joint sets (Hancock, 1985). The lack of frequent original butting of the members of two sets against each other and also the absence of mutual interaction between the members of these two sets, are

among the reasons that reduce the possibility of alternative formation of these joints. Geometrical relations between closed joints in thin layers of ironstone, which did not suffer from subsequent lateral movements, suggest a younger age for the NE joint set.

For the Upper Devonian rocks of Appalachian Plateau of New York state, Engelder and Geyser (1980) interpreted, outcrops containing two sets of extension joints as evidence for the rotation of the stress field responsible for the formation of each set. In the study area, during the formation of each set, all of its members were infilled with calcite, which in turn healed the rock, before the first member of the next set started to propagate. In this way, each set began to form in an intact rock, and therefore has no interaction with the previously healed joints.

The formation of extension joints starts early in the history of a basin and continues through uplift and unloading (Engelder, 1985). For stratified rocks, Bahat (1991) recognises three major classes of joints namely burial, syntectonic and uplift and a minor class which he related to a post uplift phase. In the southeastern Sydney Basin, where the folds and faults are claimed to be syndepositional (Hanlon, 1956; Branagan, 1970; Bunny, 1972; Bowman, 1974; Wilson, 1975; Sherwin & Holms, 1986), the burial and syntectonic phases of Bahat (1991), would seem to be identical and the three existing sets of extension joints are classified as burial-syntectonic joints.

2. Formation of Faulted joints: After the formation of three sets of extension joints, σ_1 activated in a 25°- 30° direction. The stress from this direction, reactivated the two sets of NNE and NE joints as a conjugate fracture system. These shear stresses caused a dextral movement on NNE and a sinistral movement on NE joints. This deformation is visible all over the platform, and all of the open segments of the existing fractures are the result of it (Fig. 1).

The mean direction of secondary cracks which propagated generally at the end and sometimes from the sides of the existing joints, strikes around 30° (Fig. 1), which is the presumed direction of σ_1. In some parts of southeastern Sydney Basin, more than one substage leading to the formation of faulted joints are mappable. In Austinmer, some 8 km to the south of the studied platform, at least two deformations, which manifest in two phase of lateral movement, are readily recognisable.

3. Formation of cross joints and jointed faults: The next phase of deformation in this platform is signified by a series of relatively short, curved and open fractures. These nonsystematic fractures arrest when they reach the open segments of the existing faulted joints (Fig.1). These fractures are cross joints in the sense of Hodgson (1961). The general direction of these fractures are almost perpendicular to set NE, and it seems that they were initiated as the stress relief fractures, due to unloading. These can be classified as uplift fractures.

Most of the faulted segments of sets NNE and NE are presently open, sometimes as wide as 30 cm. This phenomena apparently contradicts the assumed shear movement along faulted joints. These openings are partly due to a later unloading,

which initiated the cross joints and in some places due to a very recent and slight seaward movement of the sandstone. Lateral spreading and toppling are more pronounced around the edges of the platform. It should be noted that the openings in part are surficial and very recent. These are due to the weathering and also the action of wave and water, which cover parts of this platform at high tides. Weathering and other recent processes are also responsible for the initiation of some small nonsystematic cracks.

STRESS FIELD

The direction of the major principal stress (σ_1), was parallel to each extension set during its propagation. It can be concluded that σ_1 was swinging between north and northeast from the beginning of the brittle deformation in this platform . This is more or less similar to the contemporary major horizontal stress, frequently reported to be northeasterly in the southeastern part of Sydney Basin (Worotnicki & Denham, 1976; Shepherd & Huntington, 1981; Gray, 1982).

The stress fields discussed here, assumed to be the local manifestation of far field stress due to the combination of local and regional folding, faulting, unloading and some other unknown factors. The study is under way in the neighbouring platforms to disclose the possible local and regional relationships.

CONCLUSIONS

1. All of the joints in this platform are propagated originally in extension form (mode I).

2. Three stages of brittle deformation affected the rock platform. In the first stage three sets of extension joints were propagated. The N joint set was the first, followed by the NNE and the NE joint sets. Subsequently, in the second stage segments of some joints were reactivated as faults and secondary fractures formed. In the last stage the recracked fractures were opened.

3. All of the extension joints were formed during a burial-syntectonic phase. The formation of faulted joints is related to a later tectonic phase. Cross joints and jointed faults are the result of a combination of unloading (uplift) and some very recent phenomena like weathering and wave action.

4. The σ_1 responsible for the formation of the extension joints and faulted joints was swinging between N to NE, which is almost identical with the prevailing contemporary maximum horizontal stress, reported for the southeastern part of Sydney Basin.

ACKNOWLEDGEMENT

I am most grateful to C.L. Fergusson of the Department of Geology, Wollongong University, for his careful reviewing and invaluable comments. Also thanks to M.M. Faiz for his assistance with formating the text and the figure.

REFERENCES

Bahat, D., 1991. Tectonophractography. Springer Verlag, 345 pp.

Bowman, H.N., 1974. Geology of the Wollongong, Kiama, and Robertson, 1:50,000 Sheets (9029-11, 9028-I & IV), Geological Survey of New South Wales.

Branagan, D.F. & Packham, G.H., 1970. Field geology of New South Wales, 2nd ed., Science Press, Sydney.

Bunny, M.R., 1972. Geology and coal resources of the Southern Catchment Coal Reserve, Southern Sydney Basin, New South Wales. Geological Survey of New South Wales, Bulletin, 22, 146 pp.

Egelder, T., Geiser, P., 1980. On the use of regional joint sets as trajectories of paleostress fields during the development of the Appalacian Plateau. Journal of Geophysical Research, 85, 6319-6341.

Engelder, T., 1982. Reply to a comment by A.E. Scheidegger on "is there a genetic relationship between selected regional joints and contemporary stress within the lithosphere of North America?", by T. Engelder. Tectonics, 1, 465-470.

Engelder, T., 1985. Loading paths to joint propagation during a tectonic cycle: An example from the Appalachian Plateau, USA. Journal of Structural Geology, 7, 459-476.

Gray, N.M., 1982. Direction of Stress, southern Sydney Basin, Geological Society of Australia, Journal, 29, 277-284.

Hancock, P.L., 1985. Brittle microtectonics: Principals and practice, Journal of Structural Geology, 7, 437-457.

Hanlon, F.N., 1956. Geology of the Southern Coalfield, Illawarra District. New South Wales Department of Mines, Annual Report for 1952, 95-104.

Hodgson, R.A., 1961. Regional study of jointing in Comb Ridge- Navajo Mountain area, Arizona and Utah. American Association of Petroleum Geologists, Bulletin, 45, 11-38.

Lorenz, J.C., & Finley, S.J., 1991. Regional fractures II: Fracturing of Mesaverde Reservoirs in Piceance Basin, Colorado. American Association of Petroleum Geologists, 75, 1737-1757.

Mauger, A.J., Creasey, J.W. & Huntington, J.F., 1984. The use of pre-development data for mine design: Sydney Basin fracture pattern analysis. CSIRO Division of Mineral Physics, NSW, Australia.

Scheidegger, A.C., 1982. Comments on " is there a genetic relationship between selected regional joints and contemporary stress within the lithosphere of North America?" by T. Engelder, Tectonics, 1, 463-464.

Shepherd, J., Huntington, J.F., 1981. Geological fracture mapping in coalfields and the stress fields of the Sydney Basin. Geological Society of Australia, Journal, 28, 299-309.

Sherwin, L. & Holmes, G.G. (Eds.), 1986. Geology of the Wollongong and Port Hacking 1:100,000 sheets 9029, 9129. 179 pp., Geological Survey of New South Wales.

Ward, C.R., 1971. Mesozoic Sedimentation and structure in the southern part of the Sydney Basin, the Narrabeen Group, PhD thesis, University of New South Wales, 2 Vols.

Wheeler, R.L. & Holland, S.M., 1978. Style element of systematic joints: An analytic procedure with a field example. In: Third international Conference on New Basement Tectonics, Proceedings, pp 393-404.

Wilson, R.G., 1975. Southern Coalfield. In Travis D.M. & King K.eds., Economic Geology of Australia and Papua New Guinea, pp. 206-218. Australasian Institute of Mining and Metallurgy, Monograph 6, Coal.

Worotnicki, G. & Denham, D., 1976. The state of stress in the upper part of the Earth's crust in Australia according to measurements in mines and tunnels and from seismic observations. Symposium on the Investigation of Stress in Rock. International Society of Rock Mechanics, 71-82.

Zhao, G., Johnson, A.M., 1991. Sequential and incremental formation of conjugate sets of faults. Journal of Structural Geology, 13, 887- 895.

A BOX FULL OF SQUIGGLY LINES

P. WOOTTON
IMS Pty Ltd, Maitland

INTRODUCTION

Geophysical logging of boreholes in coal exploration and mine development is today a routine function. Much data in both detail and quantitatives nature are generated. However lithogical interpretation and the preparation of data for geological and mine planning modelling systems remains a tedious and time consuming procedure.

Current systems that operate on geophysical logs mirror manual interpretation methodologies. A geologial log either from core or chip samples must first exist. Rock unit boundaries are adjusted by picking appropriate points on the down hole curves on a computer graphic screen. A system developed by IMS called C-LOG interprets rock types directly from geophysical log data either in the field as part of direct output from the logging unit or from data provided to a project or off site office facility.

The system has been tested on geophysical log data from the Singleton Super-Group and Greta Coal Measures in the Hunter Valley, the Illawarra Coal Measures in the Western Coalfield of the Sydney Basin, the Black Jack Coal Measures of the Gunnedah Basin, the Rangal Coal Measures in the Central Bowen Basin and iron ore deposits in the Pilbarra region.

PAUL WOOTTON

SYSTEM OVERVEIW

Logging data from three major logging companies has been used and consistant lithogical interpretations have been achieved. In so doing varying formats in the "LAS" data files, caliper and density were standardised in format and converted to consistant units. In addition when there are several files of down hole data for the one hole, (eg. detail logs over specific intervals or measurement of additional parameters) one standard file containing all data is generated.

The system utilises user generated specification files to accommodate variations in geological and drilling conditions and geophysical logging tool calibration problems.

A great advantage of this approach is that the raw down hole files are significantly reduced in size, eg: typical bores of 200 metres depth are of the order of one Megabyte size but the interpreted output files for such bores are of the order of forty kilobytes.

All specification and output files are in ASCII format allowing veiwing, editing and printing functions on the data and specifications. These files can be directly loaded into geological data bases and modelling systems. In fact complete data bases for coal resource evaluation projects have been developed from C-LOG files.

Output files include data fields with interpreted rock types, strength, thickness, depth and averages of all logged parameters.

Features include : -

Mixed rock types including ratios calculated to user nominated minimum interbed thickness.

Ranking of coal unit quality based on relative density to provide coal seam profiles.

A BOX FULL OF SQUIGGLY LINES

Tagging of coal units above a user defined minimum thickness.

Rock strength classifiction based on sonic logs when available.

Hard copy bore log text reports and graphic logs can be generated directly for field reporting immediately following the completion of each bore hole. Samlples of graphic output are shown in figures 1 and 2. These examples demonstrate comparisons between geologists logs, raw down hole geophysical data and synthetic lithological logs with interpreted and corrected traces.

FUTURE DEVELOPMENT

To date most sedimentary rock types are identified by the system, however on-going work is preceding in the defining parameters to define conglomerates and refining delineation of igneous intrusions and cindered and heat affected coal. Further evaluation of geophysical log data for application in geotechnical and ground water studies is on going. Advice and test data are welcome from any contributing persons or groups.

ACKNOWLEDGEMENTS

In the development and testing of this system I am most grateful for the input and support of the Dennis Stevens of Geoscience Assocs.(Aust), Ian Poppit of Coalex, Gary Salter of Bayswater Colliery Company, and Leigh McPherson of IMS.

PAUL WOOTTON

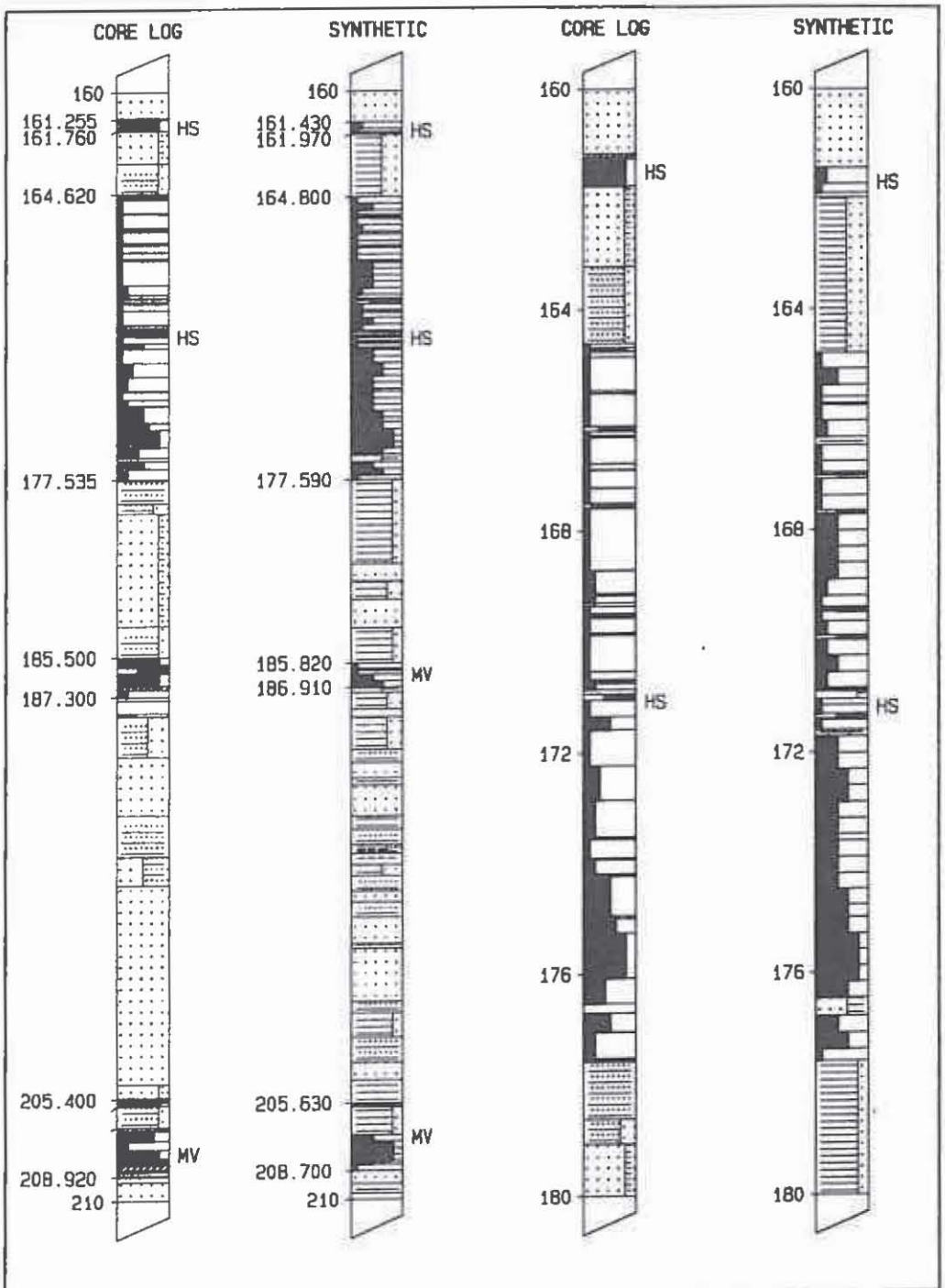

SCALE 1: 250/100		COMPARISON OF GEOLOGIST CORE LOG (LEFT) AND SYNTHETIC LITHOLOGY FROM C-LOG (RIGHT)	
DRN.	DATE - 21-02-1993		
TRD.			
FILE No.		I M S PTY LIMITED	FIGURE No.1
REV.	DATE	APPD. DATE	

A BOX FULL OF SQUIGGLY LINES

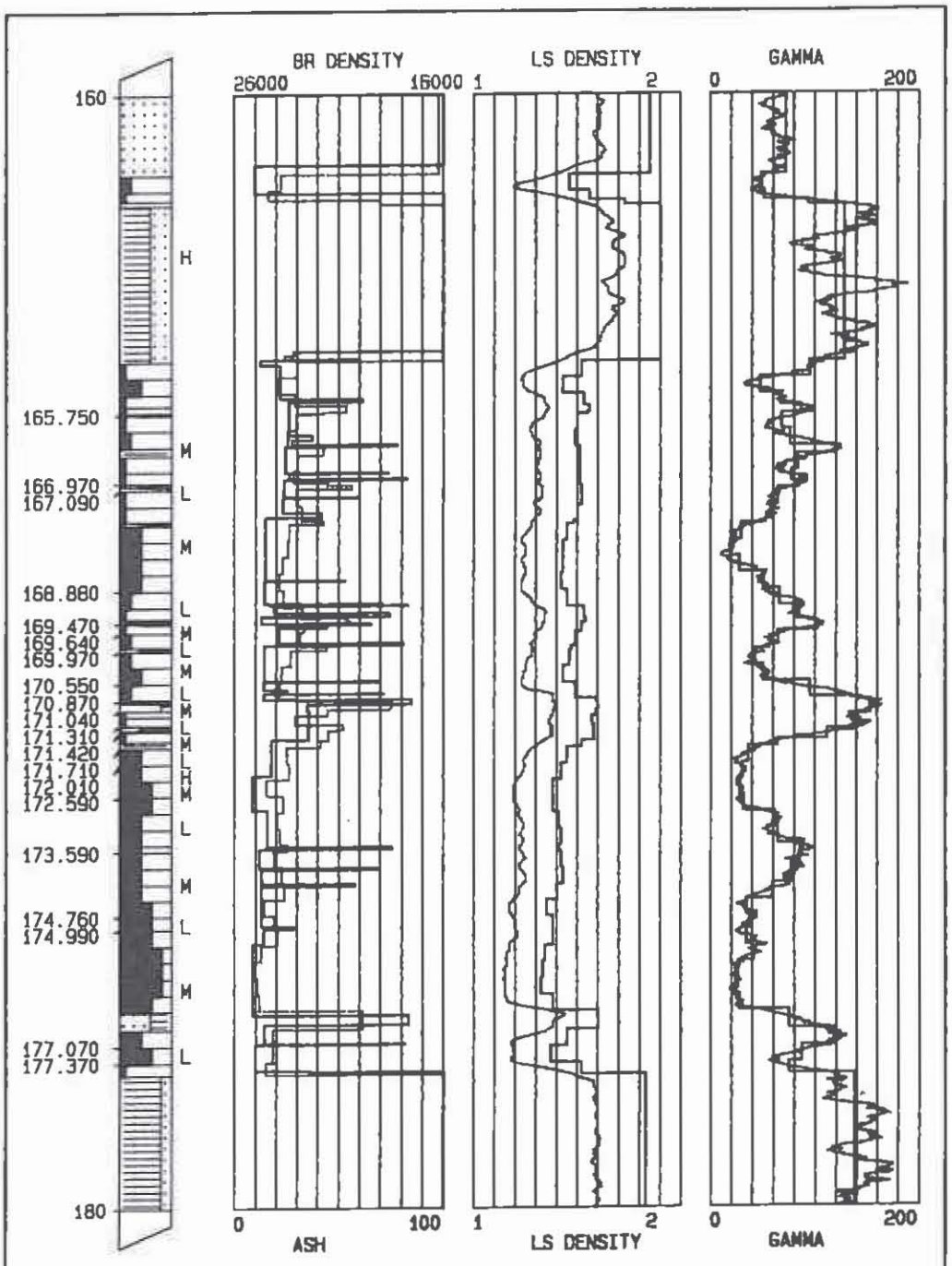

SCALE 1: 100		SYNTHETIC COAL SEAM LOG WITH STRENGTH INDICES ASH% COMPARED TO BED RESOLUTION DENSITY RAW (LIGHT) AND INTERPRETED (DARK) DATA TRACES	
DRN.	DATE - 21-02-1993		
TRD.			
FILE No.		I M S PTY LIMITED	FIGURE No.2
REV.	DATE	APPD.	DATE

STRIKE-SLIP DEFORMATION AT KANGAROO TOPS, SOUTHERN NEW ENGLAND OROGEN: 10KM OF SINISTRAL DISPLACEMENT RECORDED ON THE YARROWITCH FAULT

M. VICKERS
University of Sydney

ABSTRACT

The Yarrowitch fault records at least 10 km of sinistral strike-slip movement at Kangaroo Tops, in the southern New England orogen. Several elements of the New England orogen are deformed, including the Weraerai, Djungati and Anaiwan terranes, as well as lower Permian Manning Group sedimentary rocks. This map-scale structure demonstrates that sinistral strike-slip faulting has been active since emplacement of the Gwydir superterrane onto the Gondwana margin in the late Paleozoic.

INTRODUCTION

New England is a complex collage of Paleozoic terranes (Cawood and Leitch, 1984; Fergusson et al., 1987; Flood and Aitchison, 1988 Aitchison 1988, 1989, 1990; Aitchison, Flood and Spiller, 1992; Aitchison *et al.*, 1992) emplaced onto the Gondwana margin in the Late Paleozoic. Serpentinised and attenuated Early Cambrian ophiolite (Weraerai terrane of Flood and Aitchison, 1988) and the regionally significant Peel-Manning-Nowendoc fault system separates the two major, distinctly different elements of New England. The Gwydir superterrane (Fergusson *et al.*, 1987) lies east and north of the ophiolite and the Gamilaroi terrane (Flood and Aitchison, 1988) lies to the west and southwest (Fig. 1).

The Gamilaroi terrane has elements consistent with an interpretation that it originated within an intra-oceanic island arc (Aitchison and Flood, *in press*). This terrane cannot be demonstrably tied to the Gondwana margin until the appearance of sediments containing distinctive Gondwana-derived quartzite clasts, above a major unconformity and facies change in the Uppermost Devonian (Flood and Aitchison, 1992).

Gwydir superterrane in this area, comprises elements derived from ocean floor (Djungati terrane: Flood and Aitchison, 1988), as well as mixed ocean floor and volcanic arc sediments (Anaiwan terrane: Flood and Aitchison, 1988). Pebbles of distinctive red chert derived from the Djungati terrane occur in the lower Permian Manning Group, along with volcanic pebbles derived from the Gamilaroi terrane and its overlap sequence (Mayer, 1972; Vickers and Aitchison, 1992). This clastic detritus provides the oldest unambiguous evidence for constraints on the timing of the juxtaposition of the Gwydir superterrane and the Gondwana margin.

Emplacement of the Gwydir superterrane by sinistral strike-slip motion along the Peel-Manning fault system has been proposed by several workers (Corbett, 1976; Cawood, 1982; Cawood and Leitch, 1984; Leitch, 1988; Leitch and Skillbeck,

1991; Collins, 1992), based mainly on sinistral microstructures within the Weraerai terrane (Corbett, 1976; Offler and Williams, 1985, 1987; Offler et al., 1989) or regional lithological groupings (Cawood, 1982; Leitch, 1988; Leitch and Skillbeck, 1991).

The Yarrowitch Fault records at least 10 km of sinistral strike-slip movement at Kangaroo Tops, in the southern part of the New England Orogen. Map-scale deformation structures include a large hook-shaped drag-fold. I propose that similar large-scale structures at Pigna Barney and Mt George may record an episode of sinistral crustal reorganisation that post-dates the assembly of the New England section of the Gondwana margin.

GEOLOGY AT KANGAROO TOPS.

The Oxley Metamorphics (Gunthorpe, 1970) are the structurally lowest rocks in this area (Fig. 2). They are a polydeformed quartzose blueschist-greenschist assemblage at textural zone (Bishop 1972) III or higher. Protolith material includes chert, basalt and sandstone interpreted (Flood and Aitchison, 1988) as metamorphosed equivalents of the Anaiwan terrane.

Serpentinites of the Weraerai terrane are faulted against and structurally overlie the Oxley metamorphics. Serpentinite with a scaly, schistose fabric encloses blocks of blueschist, greenschist, serpentinised harzburgite, dolerite and gabbro up to 250 m in size. These rocks are lithologically similar to Weraerai terrane dismembered ophiolites elsewhere in New England. Weraerai terrane rocks dip gently to steeply southwest.

Red cherts and greenstones tentatively assigned to the Djungati terrane occur as narrow fault slivers that structurally overlie Weraerai terrane serpentinites in some places. Greenstone protoliths are mafic sediments and basalts. Processing for radiolarians was unsuccessful, hence these cherts are included in the Djungati terrane on lithological grounds alone.

Lower Permian sediments of the Manning Group (Voisey, 1938, 1939, 1957; Mayer, 1972) are faulted against and structurally overlie Djungati terrane and Weraerai terrane rocks. Manning Group rocks consist of basal sub-angular conglomerates, stratigraphically overlain by sub-rounded conglomerates and then by a thick succession of diamictites and turbidite sandstones. The Manning Group is interpreted as having been deposited on a marine slope-apron by high density mass- and debris-flows (Vickers and Aitchison, 1992, 1993; Jenkins, 1992). In general, Manning Group rocks dip moderately to steeply southwest.

SINISTRAL DEFORMATION

At Kangaroo Tops, a large drag-fold (Fig. 2) with a near-vertical axis is delineated by serpentinites of the Weraerai terrane and Manning Group bedding traces. The drag-fold has been punctured by the steeply southwest-dipping Yarrowitch Fault. The fold limbs have been displaced 4 km in a sinistral sense, and Manning Group sediments are juxtaposed against the Oxley Metamorphics. Weraerai terrane serpentinites are progressively more attenuated near the fault. All tectonic contacts between lithological units are deformed.

Within the Manning Group, the fault is multi-stranded, nearly bedding-parallel and occupies a zone about a kilometre wide. It is <3 m wide where it separates the Manning Group and Oxley Metamorphics. Total sinistral displacement on the Yarrowitch Fault at Kangaroo Tops exceeds 10 km.

DISCUSSION

Sinistral strike-slip deformation is post Early Permian, as all lithological units in the area, and their tectonic contacts are deformed. The Manning Group provides provenance evidence for the juxtaposition of the Gwydir superterrane and the Gamilaroi terrane, so its deformation implies that a sinistral deformation regime was active after the emplacement of the Gwydir superterrane onto the Gondwana margin. This evidence, however, does not resolve the sense of that emplacement.

The near vertical attitude of the fault indicates that it has not been rotated around a horizontal axis to any significant extent since the inception of sinistral deformation. It is proposed that the many kilometres of dominantly dip-slip, Late Permian (253-265 Ma) movement reported by Landenberger *et al.* (1993) on the same fault about 90 km north of Kangaroo Tops, occurred on a pre-existing, near vertical strike-slip structure and that this earlier phase of sinistral deformation is recorded at Kangaroo Tops.

Similar hook-shaped structures delineated by Weraerai terrane rocks occur at Pigna Barney and at Mt George (Fig 1). Northwest of Pigna Barney, (at Glenrock and Barry Stations), rocks of the Gamilaroi, Djungati, and Weraerai terranes as well as Manning Group rocks, appear to have been repeated (Gilligan *et al.*, 1987). It is proposed that this area is analagous to Kangaroo tops. Sinistral displacement of about 40 km may have occurred.

The hook-shaped structure at Kangaroo Tops demonstrates at map-scale that sinistral strike-slip deformation has occurred since emplacement of the Gwydir superterrane onto the Gondwana margin in the late Paleozoic.

ACKNOWLEDGEMENTS

Jonathan Aitchison is thanked for stimulating discussions. James Stratford and Sébastien Meffre commented on drafts of this manuscript. Thanks.

REFERENCES

AITCHISON, J. C., 1988. Late Paleozoic radiolarian ages from the Gwydir terrane, New England orogen, eastern Australia. *Geology* **16,** 793-795.

AITCHISON, J. C., 1989. Paleozoic radiolarians and lithotectonic terranes of the southern New England Orogen, eastern Australia. Unpublished Ph.D. thesis University of New England, Armidale.

AITCHISON, J. C., 1990. Significance of Devonian - Carboniferous radiolarians from accretionary terranes of the New England Orogen, eastern Australia. *Marine Micropaleontology*. **15,** 365-378.

AITCHISON J. C. & FLOOD, P. G., 1992. Early Permian transform margin development of the southern New England Orogen, eastern Australia (eastern Gondwana). *Tectonics.*

AITCHISON, J. C., and FLOOD, P. G., *in press*. Gamilaroi terrane: A rifted Devonian intra-oceanic island-arc assemblage, NSW, Australia. *Journal of the Geological Society of London.*

AITCHISON, J. C., FLOOD, P. G., and SPILLER, F. C. P., 1992. Tectonic setting and paleoenvironment of terranes in the southern New England orogen as constrained by radiolarian biostratigraphy. *Palaeogeography, Palaeoclimatology, Palaeoecology* **94,** 31-54.

AITCHISON, J. C., IRELAND, T. R., BLAKE, M. C, Jr., and FLOOD, P. G., 1992. 530 Ma zircon age for ophiolite from the New England orogen: Oldest rocks known from eastern Australia. *Geology*. **20,** 125-128.

BISHOP, D. G., 1972. Progressive metamorphism from prehnite-pumpellyite to greenschist facies in the Dansey Pass area, Otago, New Zealand. *Geological Society of America Bulletin.* **83,** 3177-98.

CAWOOD, P. A., 1982. Tectonic reconstruction of the New England Fold Belt in the Early Permian: an example of development at an oblique-slip margin. *In* P. G. Flood and B Runnegar (eds.), *New England Geology.* Department of Geology, University of New England and AHV Club. Armidale. NSW. pp. 25-34.

CAWOOD, P. A., and LEITCH, E. C., 1984. Accretion and Dispersal Tectonics in the Southern New England Fold Belt, Eastern Australia. *In* D. G. Howell (ed.), *Tectonostratigraphic Terranes of the Circum-Pacific Region.* Circum-Pacific Council for Energy and Mineral Resources Earth Science Series, Number 1. pp. 481-492.

COLLINS, W. J., 1992. Influence of the Peel Fault system on the evolution of the Sydney Basin. *In* C.F.K. Diessel (ed.), *Twenty-sixth Newcastle symposium on advances in the study of the Sydney Basin.* pp. 47-55. Department of Geology, the University of Newcastle, 2308.

CORBETT, G. J., 1976. A new fold structure in the Woolomin Beds suggesting a sinistral movement on the Peel Fault. *Journal of the Geological Society of Australia.* **23,** 401-406.

FERGUSSON, C. L., FLOOD, P. G., and CROSS, K. C., 1985. The Gwydir terrane: a Palaeozoic subduction complex in the southern New England Fold Belt of Eastern Australia. *In* E. C. Leitch (ed.), *Third Circum-Pacific Terrane Conference extended abstracts. Geological Society of Australia Abstracts.* **14:** 66-70.

FLOOD, P. G., and AITCHISON, J. C., 1988. Tectonostratigraphic terranes of the southern part of the New England Orogen. *In* J. D. Kleeman (ed.), *New England Orogen - Tectonics and Metallogenesis.* pp. 7-10. Department of Geology and Geophysics, University of New England, Armidale.

FLOOD, P. G., and AITCHISON, J. C., 1992. Late Devonian accretion of the Gamilaroi terrane to eastern Gondwana: Provenance linkage suggested by the first appearance of Lachlan Fold Belt-derived quartz arenite. *Australian Journal of Earth Sciences.* **39,** 539-544.

GILLIGAN, L. B., BROWNLOW, J. W., and CAMERON, R. G., 1987. *Tamworth-Hastings 1:250 000 Metallogenic Map.* NSW Geological Survey, Sydney.

GUNTHORPE, R. J., 1970. Plutonic and Metamorphic rocks of the Walcha-Nowendoc-Yarrowitch District, Northern New South Wales. Unpublished Ph.D. thesis, University of New England, Armidale.

JENKINS, R., 1992. A geologic and thermal history of the Manning Group. *In* C.F.K. Diessel (ed.), *Twenty-sixth Newcastle symposium on advances in the study of the Sydney Basin.* pp. 39-46. Department of Geology, the University of Newcastle, 2308.

LANDENBURGER, B. FARRELL, T. R. OFFLER, R. COLLINS, W. J., and WHITFORD, D. J., 1993. Tectonic Implications of Rb/Sr biotite ages from the Hillgrove Plutonic Suite. *In* P. G. Flood and J. C. Aitchison (eds.), *New England Orogen, eastern Australia.* pp. 353-358. Department of Geology and Geophysics, University of New England, Armidale NSW, 2351, Australia.

LEITCH, E. C., 1988. The Barnard Basin and the Early Permian development of the southern part of the New England Fold Belt. *In* J. D. Kleeman (ed.), *New England Orogen - Tectonics and Metallogenesis.* pp. 61-67. Department of Geology and Geophysics, University of New England, Armidale.

LEITCH, E. C., 1991. Early Permian volcanism and Early Permian facies belts at the base of the Gunnedah Basin, in the northern Sydney Basin and in the

southern part of the New England Fold Belt. *In* C.F.K. Diessel (ed.), *Twenty-fifth Newcastle symposium on advances in the study of the Sydney Basin.* pp. 59-66. Department of Geology, the University of Newcastle, 2308.

MAYER, W., 1972. Palaeozoic Sedimentary Rocks from Southern New England: a Sedimentological Evaluation. Unpublished Ph.D. thesis, University of New England, Armidale.

OFFLER, R., O'HANLEY, D. S., and LENNOX, P. G., 1989. Kinematic indicators in serpentinites - the Peel-Manning Fault system, a test case. *Geological Society of Australia. Specialist Group in Tectonics and Structural Geology. Abstracts* **24.** pp. 110-111.

OFFLER, R. and WILLIAMS, A., 1985. Evidence for Sinistral Movement on the Peel Fault System in Serpentinites, Glenrock Station, NSW. *In* E. C. Leitch *3rd Circum-Pacific terrane conference, Sydney, extended abstracts. Geological Society of Australia Abstracts* **14.** pp. 171-173.

OFFLER, R. and WILLIAMS, A., 1987. Evidence for Sinistral Movement on the Peel Fault System in Serpentinites, Glenrock Station, NSW. *In* E. C. Leitch and E. Scheibner (eds.) *Terrane accretion and orogenic belts.* Geodynamics Series, Vol. 19. American Geophysical Union. pp. 141-151

VICKERS, M. D. and AITCHISON, J. C., 1992. Lower Permian Manning Group: Tectonic implications of sedimentary architecture and provenance studies in the Nowendoc-Cooplacurripa area. *In* C.F.K. Diessel (ed.), *Twenty-sixth Newcastle symposium on advances in the study of the Sydney Basin.* pp. 31-38. Department of Geology, the University of Newcastle, 2308.

VICKERS, M. D. and AITCHISON, J. C., 1993. The Lower Permian Manning Group at Kangaroo Tops, southern New England Orogen: tectonic implications of basin studies. In P. G. Flood and J. C. Aitchison (eds.), *New England Orogen, eastern Australia.* pp. 309-314. Department of Geology and Geophysics, University of New England, Armidale NSW, 2351, Australia.

VOISEY, A. H., 1938. The Upper Palaeozoic rocks in the neighbourhood of Taree, NSW. *Proceedings of the Linnean Society of New South Wales.* **63,** 453-462.

VOISEY, A. H., 1939. The Upper Palaeozoic rocks between Mount George and Wingham, N. S. Wales. *Proceedings of the Linnean Society of New South Wales.* **64,** 242-254.

VOISEY, A. H., 1957. Further remarks on the sedimentary formations of New South Wales. *Journal and Proceedings of the Royal Society of New South Wales.* **91,** 165-188.

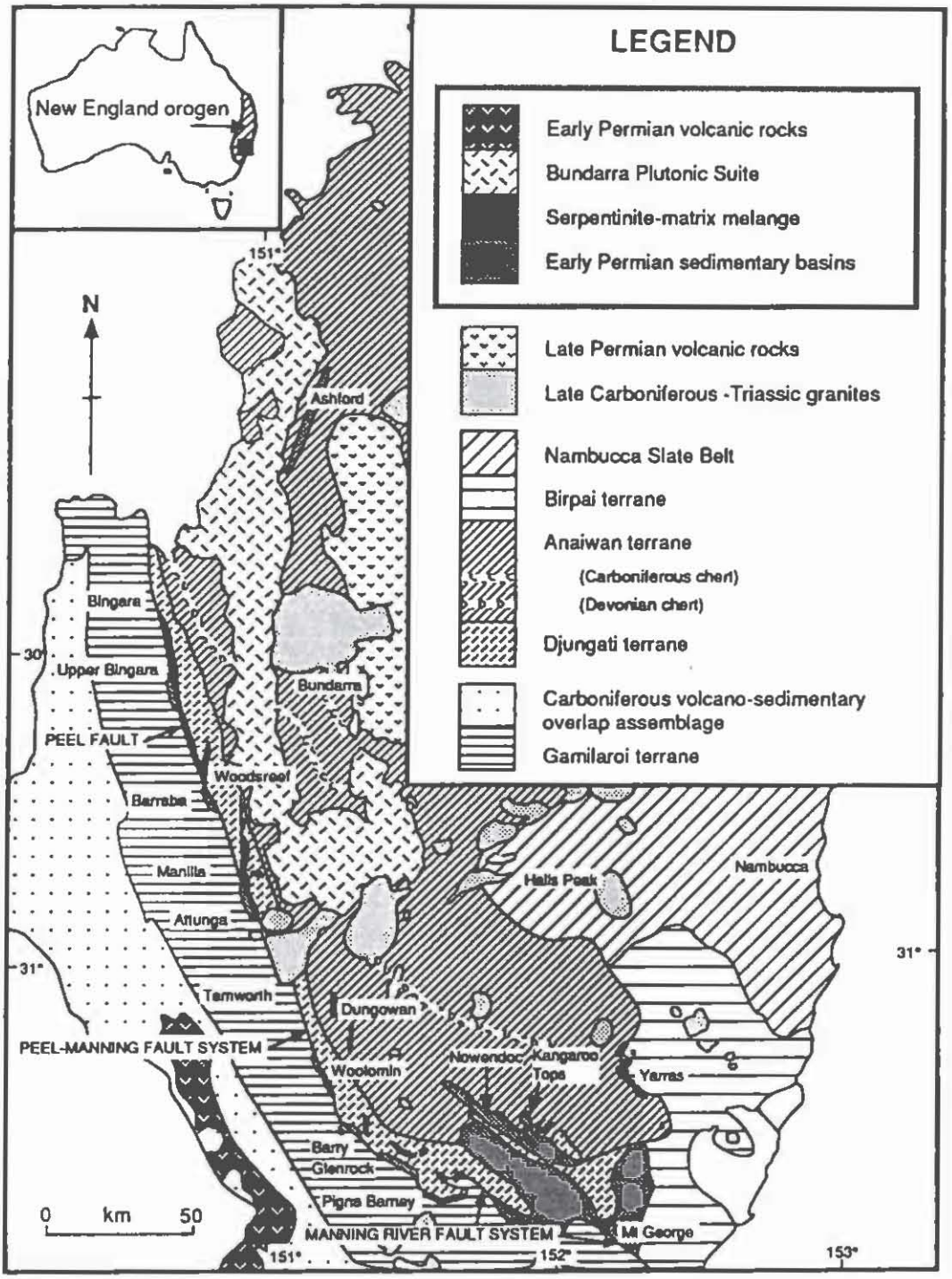

Fig. 1. Terrane map of the southern New England Orogen. (after Aitchison and Flood, 1992)

YARROWITCH FAULT: 10 km OF SINISTRAL DISPLACEMENT

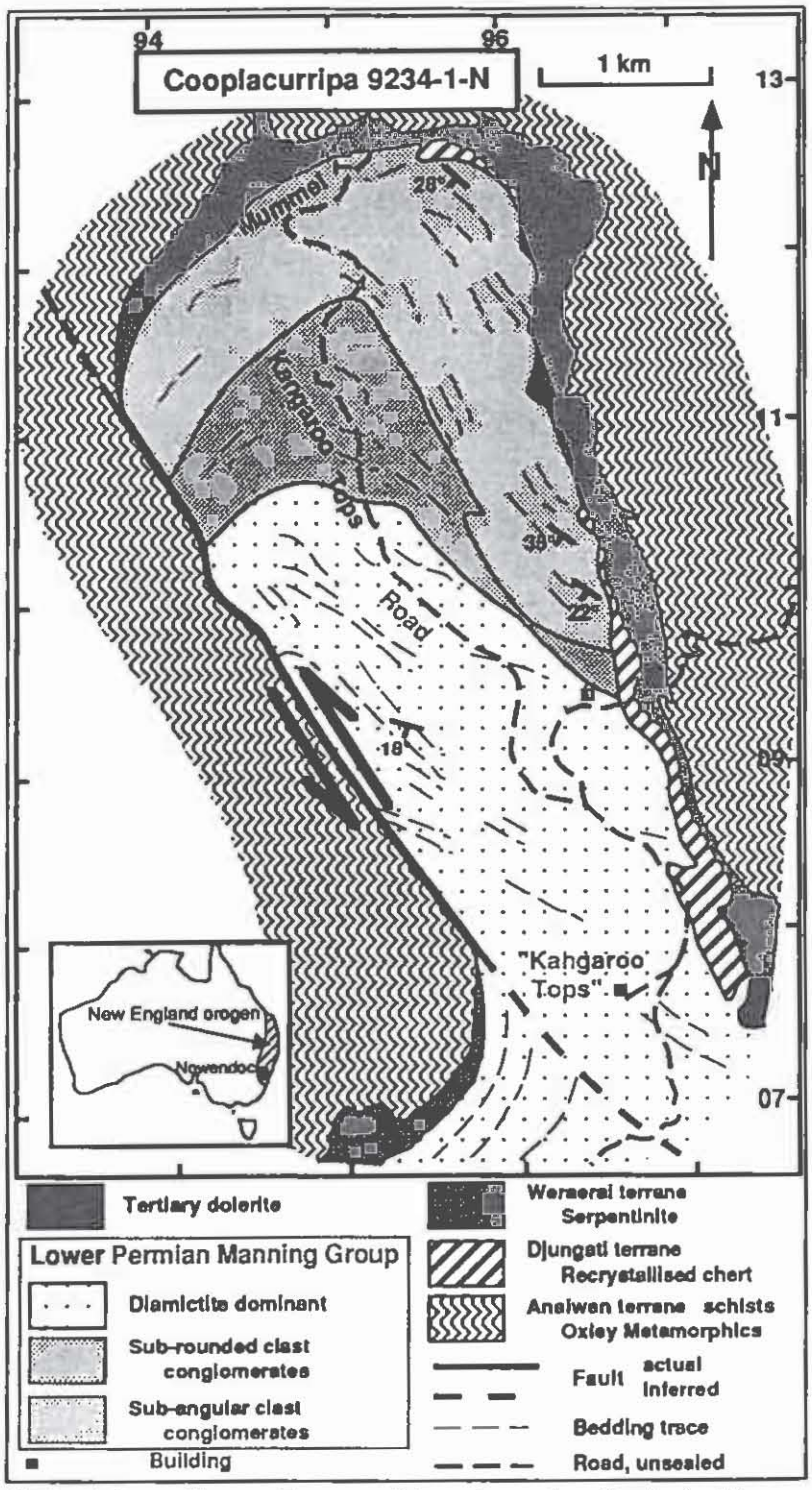

Fig. 2. Geology at Kangaroo Tops, east of Nowendoc, southern New England Orogen.

SALINITY VARIATIONS IN THE UPPER HUNTER

J. BEMBRICK
Pacific Power, Sydney

Salinity in the Hunter River recurs as a topical and emotive issue, particularly for irrigators during dry periods when river flow is low. At these times river utilisation in terms of water extraction and discharge of excess mine water tests the capacity of the river to support the range of activities now undertaken and there is conflict between user groups.

While major developments in the Upper Hunter have occurred over the last 20 years and have contributed to salinity of surface waters, catchment geology remains by far the largest contributor. Various authors have investigated the salinity associated with the individual geological units. Their findings have indicated that marine strata are associated with the most saline surface and groundwater sources. However there did not appear to be any studies which sought to quantify this contribution.

An investigation of the contribution of Maitland Group strata in the Muswellbrook area was undertaken by analysing spatial and temporal variations in salinity of surface waters for a small catchment (Antiene) above Lake Liddell. Hydrological data and water quality analyses were available from the Department of Water Resources and the catchment geology as mapped was mainly represented by Branxton Formation and Mulbring Siltstone. Analysis results mostly showed high salinity.

The dissolved salt load of the Antiene catchment was calculated to be 80 tonnes/km^2/year. The bulk of the load is carried at times of high flow. If this figure were representative of the Maitland Group in the Muswellbrook area then the contribution to dissolved load in the Hunter River at Singleton from the Maitland Group would be about 6%.

Variations in salinity associated with different parts of the Branxton Formation were noted and in general it appeared that there was a decrease upwards in the sequence. The Mulbring Siltstone was poorly represented in this catchment but limited data from an adjacent catchment indicated high sodium content in surface flows which may explain severe forms of erosion associated with this unit.

During the investigation several anomalies were recognised in previous mapping and include the location of the Hunter Thrust, extent of Mulbring Siltstone, presence of igneous dykes and several structural features not explained by current mapping.

BARRINGTON VOLCANO – REPEATED GEMSTONE ERUPTIONS (ZIRCON, SAPPHIRE & RUBY) AT THE EDGE OF THE SYDNEY BASIN

F.L. SUTHERLAND, B.J. BARRON & G.B. WEBB
The Australian Museum, Sydney

INTRODUCTION

The Barrington volcano, a large dissected basaltic shield, lies on the Sydney Basin margin, 80-150km north of Newcastle (Fig.1). The central part is enclosed by a scarp and outlying flow remnants are prominent to the south west (Pain, 1983). Radial drainage from the volcano has cut into the basalts and underlying Palaeozoic sediments and granites of the New England Orogen. Volcanic construction was placed at 53-54Ma (recalculated ages) on K-Ar dating of basalts (Wellman & McDougall, 1974), but with extra K-Ar dating Pain (1983) favoured basalt accumulation between 55-36Ma (early Eocene-early Oligocene).

Basalt exposures show over 27-33 flows, giving a minimum thickness of 350-430m, but are incompletely studied (Mason, 1982). Basal tholeiitic flows are overlain by alkali basalts. Ankaramites appear above 950m near Prospero Trig where one was dated at 37Ma and also overlie interbasaltic sediments at 1300m under the flows capping the main divide to the east.

Gem minerals (zircon, sapphire and ruby) are found in alluvials washing out of the volcanic sequence. Their distribution was sampled by A.W. Chubb of Gloucester, who found the ruby. Zircons and sapphires are common associates in east Australian basaltic gem fields, e.g. New England (Sutherland et al., 1993). Because ruby is rare, the Barrington rubies are described in detail here.

The zircons vary in type and their uranium contents provide a useful tool to explore the Barrington volcanism. Fission track dating yields thermally reset ages related to eruption and preliminary Pb/U isotopic (SHRIMP) dating gives their formation age (Sutherland & Kinny, 1990). The gemstones and their role in the evolution of Barrington volcano are described and outlined in this paper.

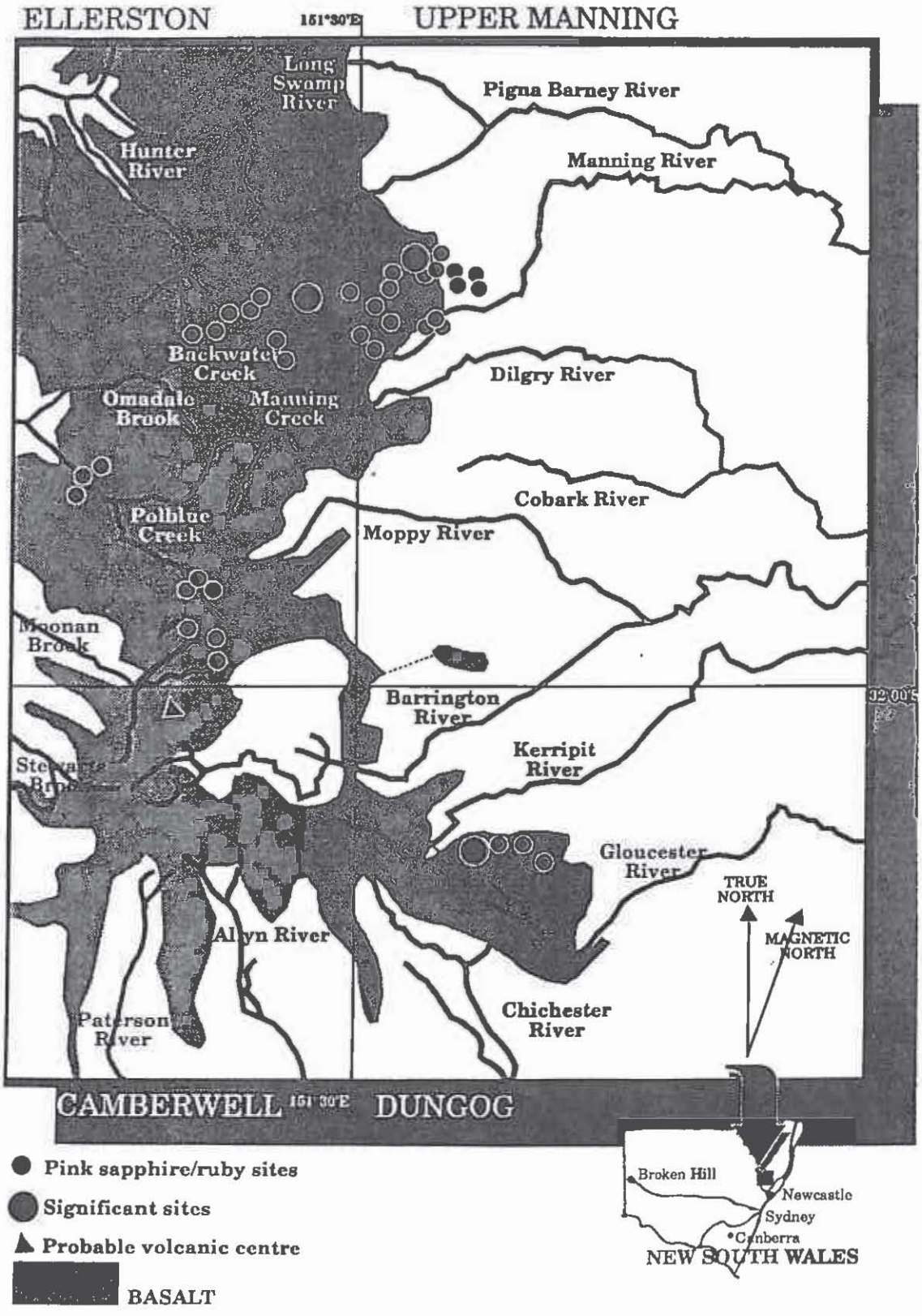

Fig.1. Distribution of basalts, gemstone sites and drainage, Barrington volcano.

BARRINGTON VOLCANO - REPEATED GEMSTONE ERUPTIONS

GEMSTONE SUITES

Heavy mineral sample sites yielding corundums and zircons are shown in Fig.1. Two bulk samples of alluvials in the Upper Manning River yielded 0.5-8% zircon and 0.4-0.7% corundum by weight. Blue, green and opaque corundum and pink, mauve and red corundum show similar amounts.

Zircon data

Zircons are white to pale and deep yellow, brown and orange. Crystals, mostly to 8mm across, show rounded to irregular shapes with corroded and worn surfaces. Some exhibit indentations from crystal intergrowths. Rare perfect crystals usually with pyramid and prism faces, indicate little transport from sources.

Three zircon groups were dated by fission track means (Table 1).

TABLE 1. Zircon Fission Track Data, Barrington Area

Grains	Ns	Ni	Na	Ratio	RHOs	RHOi	Age(Ma)	Uppm
Gummai (8522-113, orange grains)								
1	611	432	100	1.414	6.97E+06	4.93E+06	69.2±4.3	235
4	346	299	63	1.169	6.38E+06	5.45E+06	57.3±4.7	281
Gloucester Tops-Barrington Tops (GC192-3, pale fluorescent grains)								
10	789	951	95	0.855	1.320E+06	1.591E+06	43.8±2.6	72
Gloucester Tops-Barrington Tops (GC308-1, orange-red grains)								
3	206	155	75	1.320	4.063E+06	3.130E+06	38.0±4.2	254
4	150	157	75	0.961	3.480E+06	3.706E+06	27.7±3.3	300
1	271	433	50	0.626	8.613E+06	1.376E+07	18.0±1.5	1115
2	20	124	100	0.155	3.099E+05	1.971E+06	4.5±1.1	160

Determinations from Geotrack Reports (30, 192, 308) compiled by P.F. Green and I.R. Duddy. Standard (RHO D) and induced track (RHOi) densities were measured on external detector faces and fossil track densities (RHOs) on internal mineral surfaces. Ages were calculated using a Zeta of 87.9 (Gummai) and 87.7±0.75 (Gloucester Tops-Barrington Tops) for dosimeter glass U3. Ns is the number of spontaneous tracks, Ni the number of induced tracks and Na area of units of counted tracks. RHO D is 1.119E+06 (Gummai), 1.174E+06 (Gloucester Tops-Barrington Tops pale zircons) and 6.579E+05 (Gloucester Tops-Barrington Tops, orange-red zircons). Ages represent mean ages and U contents average values.

Orange zircons from Upper Manning River, below the basalt base, gave 57 and 69(?)M ages. Pale coloured zircons from higher levels through Barrington Tops and Gloucester Tops gave 43-44Ma. Orange-red zircons from this level gave 38-39, 27-28, 18(?) and 4-5(?)Ma. Reconnaissance Pb/U isotopic dating gave 56-60, 41-48 and 35-36Ma ages (F.L. Sutherland, P.D. Kinny & M. Fanning data). This confirms extended activity of the volcano and suggests several magmatic fractionation events. The zircon events bracket the 53-54, 43-44 and 36-37Ma basaltic events considered by Pain (1983). Some zircons show higher U (320-350ppm) and Th (250-330ppm) levels, approaching those of zircon inclusions in sapphires from New England basaltic activity (Coenraads et al., 1990).

Corundum-sapphire

Corroded and water worn crystals reach up to 8 carats in weight. Sapphires show typical colours and features as in other New South Wales basalt fields (MacNevin, 1972). Rare colour change sapphire occurs and probably owes its green to pink colour change to presence of iron in two oxidation states. One blue sapphire, a cut stone of 5.5 carats weight, contained a small ruby inclusion.

Ruby

Colours range from purple to pink red, grading into lavender pink, pale pink and yellow pink. Paler stones exhibit blue pink and yellow pink dichroism and red stones, orange red and purple red dichroism. Crystals mostly range to 6mm in size, but reach 3 carats in weight and cut stones can exceed one carat.

Crystals with recognisable faces suggest elongated rather than tabular forms. Many crystals show strong rounding, pitting or angular indentations, suggesting considerable corrosion and etching prior to alluvial transport. Conchoidal to subconchoidal fractures include old etched ones as well as fresh ones with vitreous lustre. The material is largely transparent and redder stones are more free of inclusions. Both mineral and fluid inclusions increase in paler and more yellow coloured stones.

The ruby shows stubby black opaque and small light coloured mineral inclusions, opaque cloudy drifts of mineral matter, long thin needles lying along three crystal directions, negative crystal inclusions, prevalent iron staining, healed fractures with liquid channels and droplets (feathers) and polysynthetic twin planes. The opaque inclusions are Cr spinel and spinel and the needles resemble exsolved boehmite (hydrous alumina) in Thai rubies (Gübelin and Koivula, 1986).

BARRINGTON VOLCANO - REPEATED GEMSTONE ERUPTIONS

The rubies fluoresce a strong red under longwave, but are inert under shortwave UV light. Testing with a spectroscope, the pale pinks showed Cr absorption bands in the red part of the spectrum. Darker reds also showed this, sometimes with absorption in the yellow green area, two lines in the blue and absorption in the violet. Some reds display the classic ruby spectrum.

Analyses of the ruby by electron microprobe shows an increase from 0.60wt% Cr_2O_3 in pinks to 1.42% in reds. Fe is present (0.44-0.75wt% 'FeO'), with Ti and Mg in very minor amounts. The main mineral inclusions are spinel, mostly Cr-bearing (up to 12wt% Cr_2O_3), see Fig 2, below.

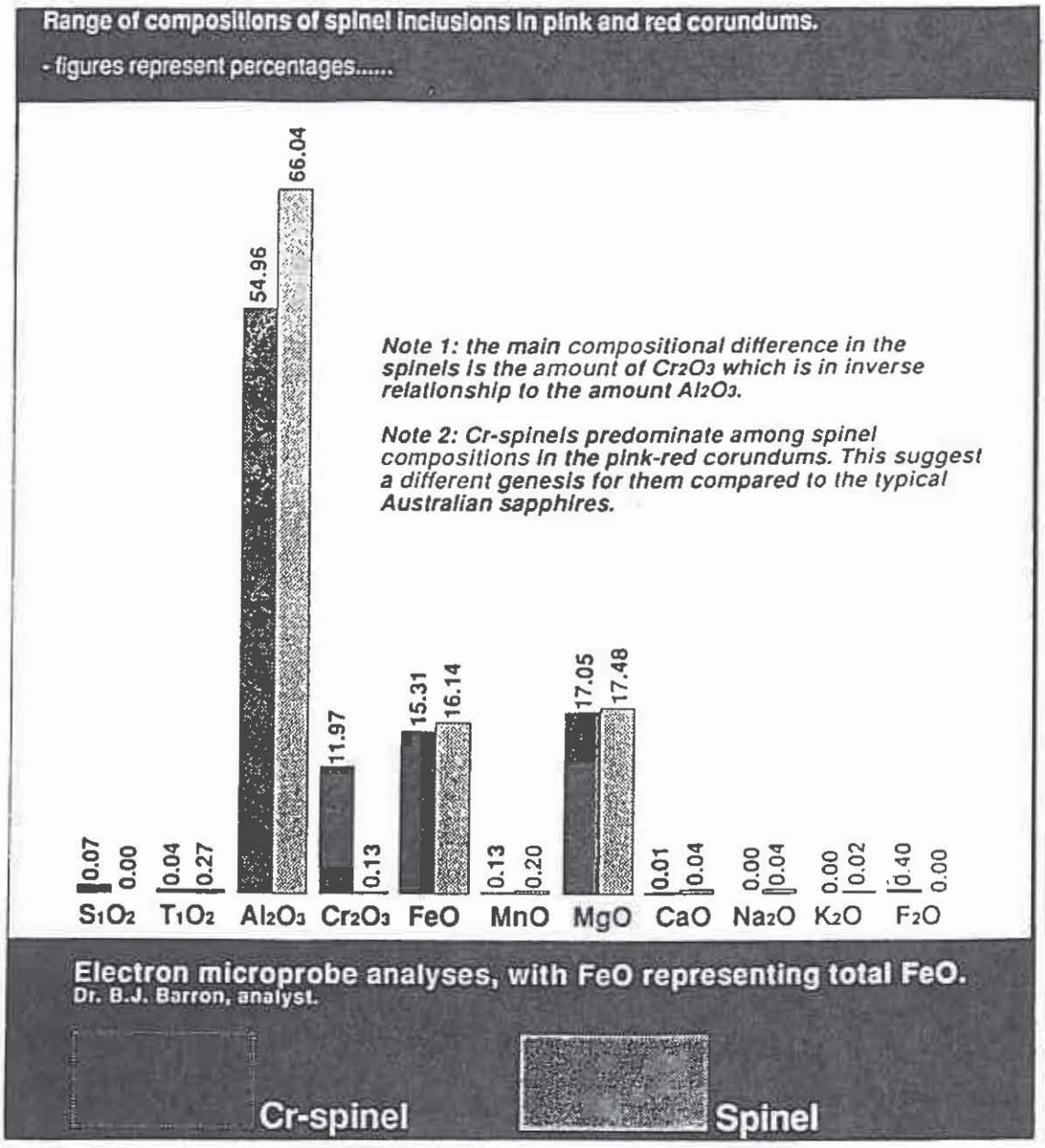

F.L. SUTHERLAND, B.J. BARRON and G.B. WEBB

GROWTH OF BARRINGTON GEM VOLCANO

Several periods of activity built up the basalt shield, with the main part erupting around 54Ma. Zircon formation is largely correlated with the alkaline activity. Primitive basalts are rare, but include basanite (authors' data) and the ankaramites suggest magmatic fractionation processes near the base of the crust (Mason, 1985). The zircons (and sapphire?) probably formed from end-stage magmatic evolution in these chambers, before expulsion in later eruptions. These may include pyroclastic events not readily seen in the poorly exposed and partly reworked sequences. The pale zircons largely correspond to activity around 43-44Ma.

Ankaramites seem to feature in the post-43Ma sequence and the general form of the shield was probably established by 36Ma. The upper levels of the volcano through Barrington Tops to Gloucester Tops were modified by some alkali basalt flows overlying leads carrying 27-28Ma zircons. Little addition to the shield since then, apart from possible minor events recorded in a few zircons, has led to its present form under post-Oligocene dissection.

The ruby is an enigmatic feature of the volcano and its inclusion in a sapphire provides a tenuous link with the magmatic activity. However, no mutual zoning of sapphire and ruby was observed. The Cr spinel inclusion suite differs from typical inclusion suites found in east Australian sapphires and the related high U and Th zircons. Both the ruby and pale, relatively low U zircons represent distinct eruptive features in the magmatic story at Barrington, which need further exploration.

DISCUSSION

The Barrington gem zircon suite indicates four significant and possibly up to seven eruptive episodes for the volcano, a more complex history than previously considered. The gem suites also suggest several episodes of basaltic fractionation into felsic magmas at depth. Thus, the volcano shows some characteristics linking it to the felsic activity of the migratory 'hotspot' central volcanoes in eastern Australia (Johnson et al., 1989). However, the activity was significantly older and in this respect resembles the multiple early Tertiary activity of the New England basaltic gem field. Activity in that field was linked to passage over a hotspot system associated with the North Tasman-Cato Trough spreading system (Sutherland & Kinny, 1991; Sutherland et al., 1993). Isotopically, Barrington basalts show $^{87}Sr/^{86}Sr$ (0.7031 to 0.7035) and ϵNd (+6 to +8). These ranges relate more closely to those of the older basalt fields of the Tasman margin than to values associated with the younger central volcano plume component (Sun, McDonough and Ewart, 1989).

BARRINGTON VOLCANO - REPEATED GEMSTONE ERUPTIONS

In a multiple hotspot model proposed by Sutherland (1991), repeated eruptions characterised the Australian margin as it passed over asthenospheric upwellings which arose along the Tasman spreading rift. Barrington volcano provides support for such a model, with the main eruptive phases around 54, 44, 37 and 28Ma diminishing in intensity with time.

Barrington volcano is one of several New South Wales basaltic gem fields that need further study to elucidate their petrological affinities.

ACKNOWLEDGEMENTS

A.W. Chubb of Gloucester supplied considerable information and material for this study. Fieldwork was assisted by J.E. Hingley and R.E. Pogson. The Australian Museum Trust provided funds for zircon dating. G. Ferguson supplied the figure graphics and S. Folwell typed the script.

REFERENCES

COENRAADS, R.R., SUTHERLAND, F.L. and KINNY, P.D., 1990: The origin of sapphires: U-Pb dating of zircon inclusions sheds new light. Min. Mag., 54, 113-122.

GÜBELIN, E.J. and KOIVULA, J.I., 1986: Photoatlas of Inclusions in Gemstones, ABC Edition, Zürich.

JOHNSON, R.W., compl. and ed. 1989: Intraplate Volcanism in eastern Australia and New Zealand. Cambridge Univ. Press, Cambridge.

MACNEVIN, A.A., 1972: Sapphires in the New England district, New South Wales. NSW Geol. Surv. Rec., 14, 19-35.

MASON, D.R., 1982: Stratigraphy of western parts of the Barrington Tops Tertiary volcanic field. In Flood, P.G. and Runnegar, B. (eds.). New England Geology A.H. Voisey Symposium, pp.133-139. Dept. Geol. Univ. New England & A.H.V. Club, Armidale NSW.

MASON, D.R., 1985. Polybaric crystallisation of clinopyroxene in ankaramites of the Barrington Tops Tertiary volcanic field, New South Wales. In Sutherland, F.L., Franklin B.J. and Waltho, A.E. (eds.) Volcanism in Eastern Australia with case histories from New South Wales Publ. Geol. Soc. Aust., NSW Div., 1, 87-105.

PAIN, C.F., 1983: Geomorphology of the Barrington Tops area, New South Wales. J. Geol. Soc. Aust., 30, 187-194.

SUN, S-S., McDONOUGH, W.F. and EWART A., 1989: Four component model for East Australian basalts. In Johnson, R.W. (compl. and ed.) Intraplate Volcanism in Eastern Australia and New Zealand, pp.333-347. Cambridge Univ. Press, Cambridge.

SUTHERLAND, F.L., POGSON, R.E. and HOLLIS, J.D., 1993: Growth of the central New England basaltic gemfields, New South Wales, based on zircon fission track dating. In Flood, P.G. and Aitchison, J.C. (eds.). New England Orogen, eastern Australia, 483-491. Dept. Geol. Geophys., Univ. New England, Armidale N.S.W.

SUTHERLAND, F.L. and KINNY, P.D., 1990: Ion probe U/Pb isotopic ages of gemmy zircons from eastern Australia, including Tasmania. Geol. Soc. Aust. Abstr. Ser., 25, 241-242.

SUTHERLAND, F.L., KINNY, P.D. and HOLLIS, J.D., 1991: Use of zircons to resolve origins of sapphires in east Australian gem fields - the mysterious case of the shuffling sapphire volcanoes. Geol. Soc. Aust. Abstr. Ser., 30, 227-228.

WELLMAN, P. and McDOUGALL, I. 1974. Potassium-argon ages on the Cainozoic volcanic rocks of New South Wales, J. Geol. Soc. Aust., 21, 247-272.

THE COX'S GAP INCIDENTS

D.F. BRANAGAN
The University of Sydney

INTRODUCTION

Cox's Gap is situated on the Sandy Hollow-Bylong Rd, 5kms south west of Kerabee, and nearly 20 kms west of Baerami (Fig.1). The Ulan-Sandy Hollow railway Tunnel cuts through the Cox's Gap ridge 2kms to the north. The passing motorist will notice, on climbing the Gap from the east (a vertical rise of 160m), that there appears to be a considerable amount of disturbance of the strata. This paper describes the disturbed zone and discusses the cause of the disturbance.

STRATIGRAPHY

The stratigraphy of the area consists of Permian coal measures overlain by Triassic Narrabeen Group sedimentary rocks. The Triassic succession is well-exposed on the road section descending west of Cox's Gap, and consists of a succession of coarse to medium-grained sandstones interspersed with red and grey shales, overlying a thin coal seam, sandstones, shales and cherts (Fig.2). The Narrabeen succession here is cut by several normal faults dipping north at 70 to 80^0, with displacements of 1 to 2m.

Apart from the road cutting mentioned above the coal measures are generally poorly-exposed, but shales, sandstones cherts and coal can be seen in the lower cuttings on the east side of the Gap, albeit often disturbed.

Towards the top of the eastern side of the pass, road cuttings expose a generally chaotic range of rocks, but mostly apparently belonging to the Narrabeen succession.

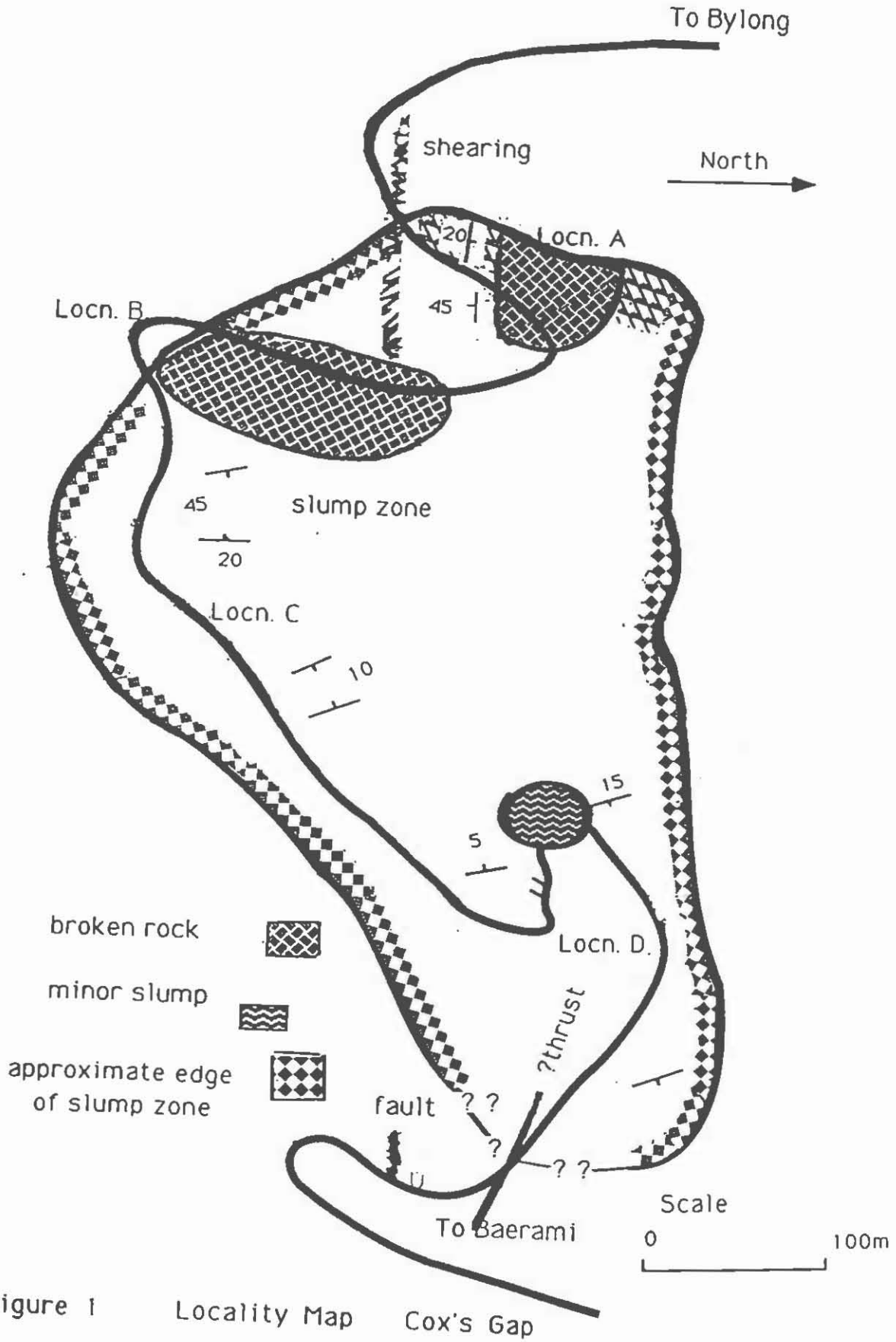

Figure 1 Locality Map Cox's Gap

COX'S GAP INCIDENTS

ZONE OF DISTURBANCE

The zone of disturbance extends from the base to the top of the road climb on the eastern side of the Gap, a distance along the road of 1.5kms, but a
direct distance, east-west of .7kms, and a maximum width of .4kms. The plan view (Fig.1) shows the areal extent of the zone of disturbance. The total dimension of the disturbance is probably .14kms^3, not a huge feature, but enough to cause headaches for any engineer.

What might be regarded as the "main exposure" -in the uppermost cutting on the east side of the gap (locn. A, Fig.1 & Fig.3)- consists of a zone of shattered conglomeratic sandstone blocks with varying orientations in a finer sandy matrix, blocks varying in size from 2m to a few centimetres diameter. Some of the blocks show internal faulting. There appear to have been two phases of cementation, one relatively old, and producing a firm rock, one more recent and soft.

The chaotic zone "grades" towards the southern end of the cutting into somewhat more regular sandstone beds. These consist of light-coloured beds dipping northerly at 10-15^0, with a few dips up to 20^0, but there are zones of broken rock both above and below. The northern end of the cutting consists of larger blocks of relatively horizontal sandstone and some stratigraphy can be delineated although the rock mass is quite fractured. This disturbed zone rests on unfractured sandstone beds dipping northerly at about 10^0.The erosional boundary between the disturbed and coherent units dips southerly at about 20^0. North beyond the cutting face the beds at the same level around the hillside appear to be horizontal and undisturbed. However downslope in the bush 100m, blocks of conglomerate dip downslope(easterly). Similarly, adjacent to the road within the curve below the main cutting, beds are not shattered but dip is southerly, generally 15-20^0, but dips up to 40^0 were observed.

On the next bend (locn.B, Fig.1), another shattered zone occurs, somewhat similar in character to that described in the "main exposure", but there is some evidence of vertical shearing and recementation of conglomerate as recorded at other sites (mainly in Hawkesbury Sandstone) in the Sydney Basin (Branagan,1985).

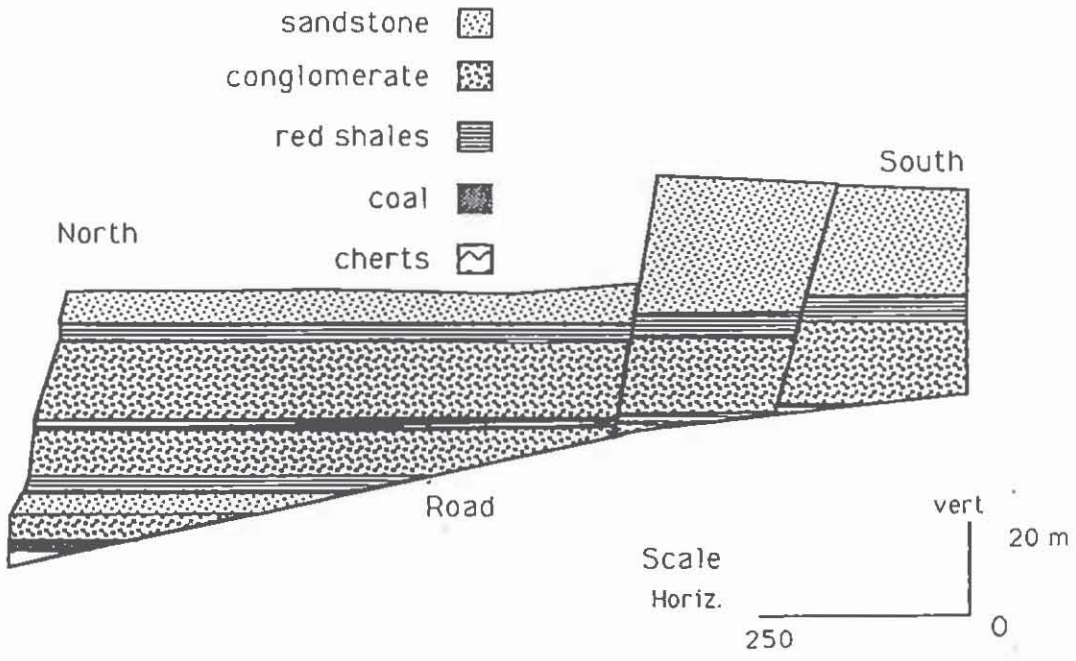

FIG. 2 Stratigraphic section, west side of Cox's Gap

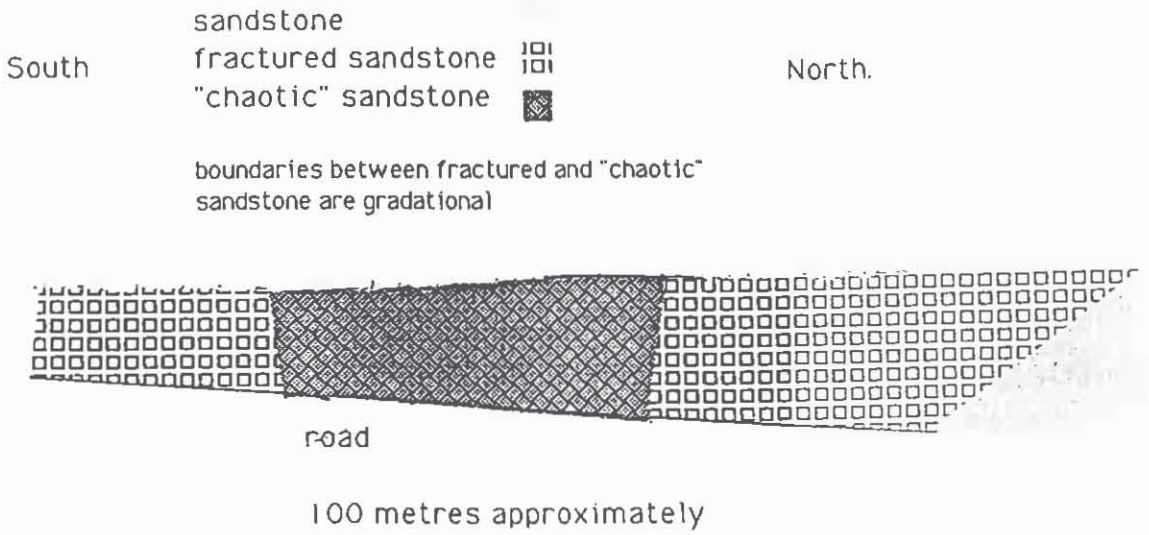

FIGURE 3. Road cutting at top of east climb to Cox's Gap

COX'S GAP INCIDENTS

Down slope from this corner along a relatively straight stretch of road (Locn.C, Fig.1) outcrop is patchy, but conglomerate, often in blocks, red shales and grey sandstones can be observed in places. Very broken conglomerate occurs over a distance of 350ms and dips of up to 60^0 (westerly, i.e. into the slope) can be observed. Over the next 150ms downhill dips within the broken material are up to 45^0, but towards the east. Over the next 200ms downhill, where bedding can be clearly observed it varies from horizontal to 10^0. However dip direction varies, sometimes towards the valley (WSW).

The second major area of disturbance is exposed around two bends at the base of the pass road (Locn.D, Fig.1). In this area there are several well-exposed faults in both Narrabeen and coal measure rocks. There are also rotated blocks. The boundary between the Triassic and the underlying Permian rocks is here quite irregular. Although this irregularity is partly caused by faulting it is mainly the result of slumping of Narrabeen Group rocks which overlap the coal measures (Locn.E, Fig.1)

From the above descriptions it is clear there are considerable differences in the degree and type of disturbance. The pattern can be discerned in a conceptual east-west cross-section from the base of the road climb to the top (Figs.4). This indicates that the disturbance is essentially shallow, and this point is emphasised by the relative thinness of the shattered rock in the highest road cutting. The zone is essentially a large slump, or rather a series of slumps, but there are some complications. One is the abundance of coarse sandstone units, which makes the correlation of material between disturbed zones quite difficult, and at times impossible.

THE CAUSE

The zone of disturbance appears to be the result of relatively recent slumping of a rock mass dominated by coarse sandstone, which was in several different conditions prior to slumping. These masses consisted of (a) coal measures in which there had been localised small scale faulting, possibly of several types (normal, thrusting and strike slip), at the foot of the pass, (b) Narrabeen Group sedimentary rocks showing irregular orientation of bedding because of the separation along joint and bedding planes and differential movement, including rotation, during slumping, and (c)

the shattered zone at the top of the pass. The apparently shattered zone at the top of the pass was probably an old "gully fill" of the type exposed in many parts of the Blue Mountains (Branagan, 1987), although it may also have been partly caused be shearing. There were possibly several movements involved in its final condition.

It is uncertain if the faulted and distorted coal measures at the base of the hill have been totally incorporated in the slump zone. A likely plane of failure in this area is the coal seam (now exposed in the road cuttings), but another slip plane may occur at valley floor level, and now hidden below alluvium. This could explain some of the distortions within the coal measures, and the variable topographic relations between the Triassic and Permian rocks in this area. [An irregular boundary between Triassic and Permian exposed at Growee on the Bylong-Rylstone road may be a similar type of slump/tectonic failure.]

The three different states of rock have almost certainly formed over a long period. The undisturbed rocks are of course Triassic or older. The faulting may be as old as Triassic, but could also have been caused by stresses set up in the area during intrusion by the numerous quite large igneous bodies in the region (possibly Mesozoic). The gully fill phenomenon may date from early Tertiary, as it does not seem to be related to the present geomorphology. The major slumping event was probably prehistoric, but later minor movements occurred, and there have been some falls and slight slips since the present road was constructed.

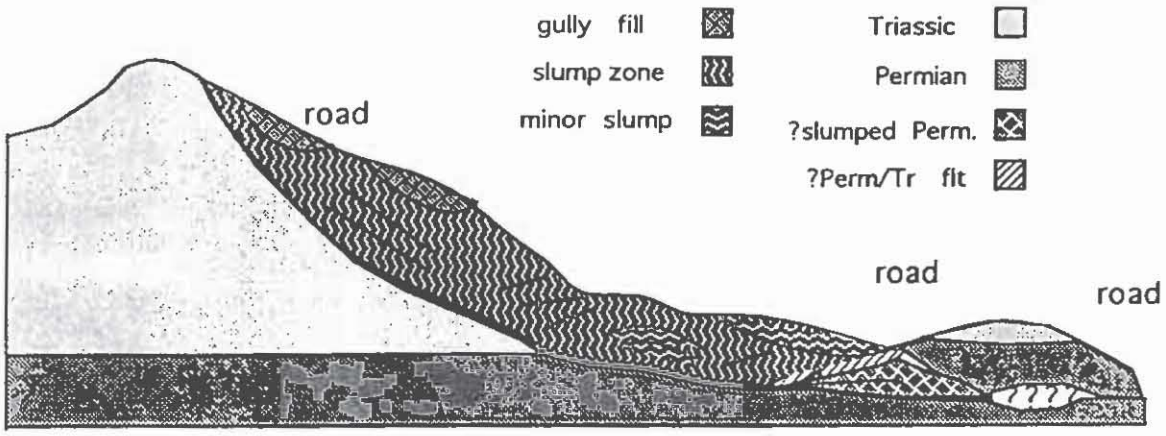

FIG. 4 Conceptual cross-section at Cox's Gap

REFERENCES

Branagan, D.F., 1985: An overview of the geology of the Sydney region. In P.J.N. Pells (editor) Engineering Geology of the Sydney Region, Balkema, Rotterdam, 3-46.

Branagan, D.F., 1987: Gully Fill deposits in the Blue Mountains. Adv. Stud. Syd. Bas., 21st Newcastle Symp., Proc., 171-177.

THE USEFULNESS OF PETROGRAPHIC, CHEMICAL & COMBUSTION INDICES & CHAR CHARACTER IN PREDICTING BURN-OFF FOR AUSTRALIAN COALS

J.G. BAILEY
University of Newcastle

INTRODUCTION

In this study, many characteristics relating to a set of 7 whole coals and their char residues from pyrolysis and combustion were recorded with the aim of relating the burn-off or combustion efficiency of the coals to some simple measurable characteristic(s) of the coal or char. It was also envisaged that by quantifying char types, particularly for those coals which leave high levels of unburnt carbon, the char parameters which affect combustion reactivity may be more fully understood.

Indices of Burn-off Performance

In many previous studies relating to char reactivity, emphasis has been placed on the reaction rates of coals or chars in the early stages of devolatilisation or volatiles combustion. In this study emphasis is placed on the unburnt carbon levels at later stages of combustion, and the way in which they reflect the nature of the remaining char.

Four parameters have been selected for comparison of the overall burning behaviour of each coal. The percentage of unburnt carbon remaining at 1300° C after combustion in the laboratory drop-tube furnace is regarded as the principal parameter of combustion performance. This figure should not, however, be regarded as the sole burn-off indicator because for some groups of coals, the unburnt carbon figures at 1300° C are subject to experimental errors as large as their differences. In Figure 1 the order of burn-off of the seven whole coals changes more than once between 900° C and 1300° C. The percentages of unburnt carbon at 900° C and 1000° C are therefore also assessed as combustion efficiency parameters. Burn-off levels obtained in the laboratory drop-tube furnace cannot be directly extrapolated to those in an industrial situation, where turbulence and other configurational factors alter particle trajectories and oxygen levels in the furnace. Nevertheless, the significance of these laboratory-based parameters is considered while taking into account their limitations.

An additional parameter relating to the earlier stages of burn-off is defined as the rate of change of burn-off with temperature at 900° C. This is measured as the tangent to the burn-off versus temperature curve for each coal shown in Figure 1. A shallow slope represents little change in burn-off level with temperature at 900° C. The parameter is expressed as $\Delta U/T_{900}$, in units of % change in burn-off/ °C.

The four combustion parameters are correlated against other properties for the whole coals in an attempt to find those characteristics which most influence burning rate and level of unburnt carbon, and the correlation coefficients are shown in Table 1.

Combustion Parameters

The good correlation between $\Delta U/T_{900}$ and unburnt carbon at 900° C ($R^2=0.90$) implies that coals which have burnt out almost completely by 900° C, can improve little from this temperature onwards, while those achieving only low burn-off by 900°C are reacting more rapidly at this stage. This suggests that coals with low $\Delta U/T_{900}$ probably begin with lower carbon contents, and/or ignite at lower temperatures and burn away substantially before reaching 900° C, i.e. are more reactive.

Comparison of unburnt carbon level at 900° C with that at 1000° C and 1300° C shows that while the correlation coefficients diminish as temperature increases, this parameter still provides the best prediction of burn-off at high temperature. Unburnt carbon at 900° C could be used to differentiate between the performance of sub-bituminous and high volatile bituminous coals, between some high volatile bituminous coals, and between these and medium volatile bituminous coal at 1000°C and 1300°C.

Unburnt carbon levels at 1000° C may be used to predict those at 1300° C only at the coal rank stage level ($R^2=0.77$). The parameter $\Delta U/T_{900}$ may enable some predictive ranking within the high volatile bituminous coals with respect to unburnt carbon at 1000° C, but not at 1300° C.

Coal Parameters

Coal rank allows prediction of $\Delta U/T_{900}$ and unburnt carbon level at 1000° C to the level of distinguishing between the sub-bituminous and high volatile bituminous coals, between two groups of high volatile bituminous coals, and between those and the medium volatile bituminous coal. Rank can be used for predicting distinctly different burn-off at 1300° C only for the sub-bituminous, high volatile and medium volatile bituminous coal groups.

Fuel ratio is most closely correlated with $\Delta U/T_{900}$, indicating that a high burn-off rate at 900° C is more likely in coals with higher carbon and lower volatile matter contents, i.e. generally higher rank coals. With respect to the prediction of burn-off performance at higher temperature, fuel ratio is able to differentiate only between sub-bituminous coals and high volatile and medium volatile bituminous coals.

Figure 1 % Burn-off of whole coals against temperature at 50% excess air.

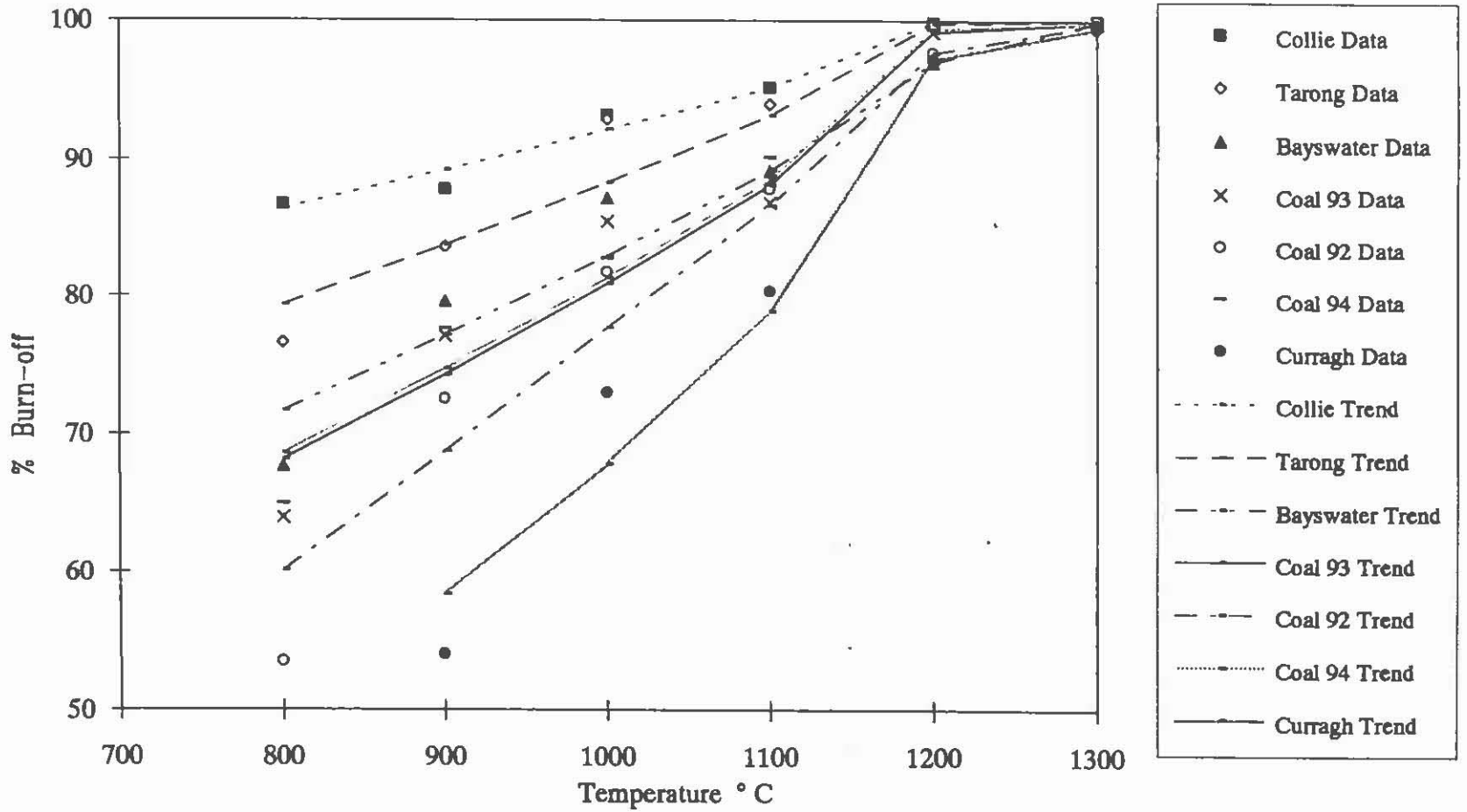

Table 1 Regression coefficients for various coal and char parameters against $\Delta U/T_{900}$ (% carbon burn-off $°C^{-1}$), unburnt carbon level at 1000° C (%) and unburnt carbon level at 1300° C (%).

	Correlation Parameter	Against $\Delta U/T_{900}$		Against Unburnt C at 1000°C		Against Unburnt C at 1300°C	
		r_{xy}	$S_{y.x}$ *	r_{xy}	$S_{y.x}$*	r_{xy}	$S_{y.x}$*
1.	Unburnt C at 900°C	0.95	0.014	0.96	4.1	0.93	0.22
2.	Unburnt C at 1000°C	0.96	0.013	-	-	0.88	0.28
3.	Unburnt C at 1300°C	0.86	0.023	0.88	6.8	-	-
4.	Coal Rank	0.94	0.016	0.88	6.9	0.84	0.50
5.	Fuel Ratio	0.86	0.023	0.82	8.3	0.82	0.34
6.	FTIR Aromaticity	0.93	0.017	0.76	4.6	0.76	0.32
7.	Inertinite Macerals	0.47	0.04	0.58	11.7	0.61	0.47
8.	Inertinite-rich Microlithotypes	-	-	0.51	12.4	0.60	0.48
9.	Infusible Inertinite^	-	-	0.68	10.6	0.76	0.39
10.	Infusible and Partly Fusible Inertinite^	-	-	0.57	11.9	0.71	0.42
11.	Dense char - combustion at 1150/1200° C	-	-	0.29	13.9	0.35	0.56
12.	Dense and thick-walled char - combustion at 1000° C	-	-	0.34	13.6	0.63	0.47
13.	Dense and thick-walled char - combustion at 1150/1200° C	-	-	0.63	11.3	0.77	0.38
14.	Dense and thick-walled char - pyrolysis at 900/1000° C	-	-	0.54	12.2	0.62	0.47
15.	Dense and thick-walled char - pyrolysis at 1050/1100° C	-	-	0.68	10.6	0.75	0.39
16.	Dense and thick-walled char - pyrolysis at 1500° C	0.81	0.026	0.80	8.7	0.88	0.28

* Standard Error of Estimate

^ Calculated according to Diessel, 1986

PREDICTION OF UNBURNT CARBON

Aromaticity measured by FTIR is able to predict $\Delta U/T_{900}$, unburnt carbon at 1000° C and unburnt carbon at 1300° C to the rank stage level, with some differentiation possible between high volatile bituminous coals. This means that coals with high aromaticity (higher rank, inertinite-rich etc.) have higher rates of burn-off with temperature at 900° C, and higher levels of unburnt carbon at both higher temperatures.

Petrographic Content

Correlations 7-10 in Table 1 show that petrographic character alone is not a useful predictor of coal burn-off performance at 1000° or 1300° C. Neither inertinite maceral content nor inertite-rich microlithotype content are able to estimate performance except to distinguish between sub-bituminous and medium volatile bituminous coal.

Contents of infusible and partly fusible inertinite (Diessel, 1986), and of infusible inertinite alone have slightly higher correlation coefficients with high temperature burn-off. It is noteworthy that the content of infusible inertinite alone is the most reliable predictor of this group of petrographic parameters, and that the correlation between content of infusible inertinite and unburnt carbon improves for higher temperature burn-off, i.e. at higher burn-off level. These observations merely reflect the presence at low temperature of relics of more reactive coal particles, which are more completely consumed at higher temperature leaving only the least reactive particles in the residue.

Table 2 Percentages of fusible, partly fusible and infusible inertinite (Diessel, 1986) in whole coals, and totals of possible low reactivity combinations.

Component	Collie	Tarong	Bayswater	Coal 93	Coal 92	Coal 94	Curragh
1. Fusible Inertinite	5.3	7.5	5.1	4.3	15.4	4.4	5.8
2. Partly Fusible Inertinite	20.7	7.3	8.1	2.0	13.0	4.2	20.2
3. Infusible Inertinite	10.3	7.3	25.7	7.7	26.5	8.7	28.7
4. Minerals	4.6	16.9	18.5	9.7	4.8	7.5	8.0
5. Sum of 3. and 4.	14.9	24.2	44.2	17.4	31.3	16.2	36.7
6. Sum of 2., 3. and 4.	35.6	31.5	52.3	19.4	44.3	20.4	56.9
7. Sum of 2. and 3.	31.0	14.6	33.8	9.7	39.5	12.9	48.9

Totals of unfused and partly fused char shown at the base of Table 2 show two distinct groupings, namely the sub-bituminous and high vitrinite coals, and the higher inertinite coals, which form separate clusters at high temperature on the burn-off curves of Figure 1. Coal 92, Curragh and Bayswater have the highest actual percentages of infusible inertinite (25-29%), while the other four coals have only between 7 and 10%. This factor alone satisfactorily accounts for the arrangement of the coals into two groups

with respect to levels of dense char in high temperature residues (Table 3): a low density group with 17-20% (Collie, Tarong, Coal 93, Coal 94), and a high density group with 37-40% dense char (Bayswater, Coal 92, Curragh). This type of clustering also occurs in the burn-off results seen at 1200° C in Figure 1.

Char Type

A number of alternative char treatments and char groups were assessed to find which most closely represented the burn-off performance of the coals at high temperature. Combustion studies (Jones et al., 1985; Oka et al., 1985; Bailey, 1992) indicate that char burning rate is decreased by increased wall thickness in spherical and network chars and by increased anisotropic texture, and that unfused chars have lower burning rates than more porous lacy chars and *cenospheres*.

The dominant char types in high temperature combustion residue and flyash are the particles which are ultimately the most difficult to burn. Their characteristics should provide some indication of those char qualities detrimental to rapid burn-off.

A discussion of the flyash types found after full-scale combustion of the samples is necessarily limited to only those four coals which are currently used as power station feedstock. Char *fragments* are the most numerous particles in all samples but Collie, and *tenuisphere, solid* and *inertoid* chars are also very common on a volume basis. On a mass basis, *solid* and *inertoid* chars contribute most mass (over 50%) to the unburnt carbon in flyash, with another 23-28% contributed by *mixed porous, mesospheres* and *mixed dense. Fragments* range from 7-13% by mass in all but Collie flyash, which is dominated by a spherical *tenuinetwork* with highly vesicular, filamentous, isotropic walls. This char type is typical of low rank coal, also dominating high temperature char from Australian brown coals (G. Mackay, pers. comm.).

In Table 3 the mass proportions of char types in high temperature (1200° C) combustion residue produced in the laboratory drop-tube furnace show a dominance of *inertoid* and *solid* chars in all the bituminous coals. These chars were shown by Bailey (1992) to be derived from inertinite particles. The sub-bituminous coals have the greater part of their mass in *inertoid* particles and *tenuinetwork* particles. While all coals have between 36 and 63% of *inertoid* and *solid* chars by mass, the remaining 64-37% consists of *tenuinetworks* (Collie, Tarong, Coal 94), *tenuispheres* (Coal 94), *fragments, crassinetworks* (Curragh, Collie) and *mesospheres* (Collie, Bayswater, Coal 93, Coal 94). These char types may be totally or partly derived from vitrinite (Bailey, 1992), so inertinite is not implicated as the sole source of the char types remaining in residue at high burn-off.

Table 3 Char types in combustion char at 1150/1200°C (% mass basis).

Char Type	Collie	Tarong	Bayswater	Coal 93	Coal 92	Coal 94	Curragh
tenuisphere	3.2	1.5	0.3	3.9	1.0	8.1	3.3
tenuinetwork	24.2	25.8	8.7	9.8	4.0	18.1	7.3
skeletal	0.5	0	2.7	6.4	5.0	6.5	2.1
fragment	7.1	12.3	5.3	13.2	6.7	6.8	0.3
crassisphere	0.7	0.5	0	0.7	0.3	1.1	3.3
crassinetwork	9.5	0	2.6	0.6	0	0.4	8.5
mesosphere	10.0	0	4.7	7.4	1.4	5.0	0
mixed	0.7	0	0.4	0	5.5	4.1	12.2
inertoid	32.0	42.6	45.2	21.1	27.2	22.4	21.6
solid	4.4	10.2	17.4	34.5	35.9	21.3	27.4
fusinoid	7.7	7.0	12.7	2.5	13.1	6.3	14.1
Unfused + partly fused char	44.8	59.8	75.7	58.1	81.7	54.1	75.3

The first char group examined as an indicator of burn-off was dense combustion char (less than 50% porosity) obtained at the highest available temperature, about 1200° C. As shown in Table 1 this char group was found to have very poor predictive ability. The correlation was improved by using the total of dense char and thick-walled char produced at 1000° C, and further improved by using the total of dense and thick-walled char produced at 1150/1200°C, but the predictive value of these char totals was still far below that for other coal parameters. Dense and thick-walled chars include the types *crassisphere, crassinetwork, mesosphere, mixed dense, inertoid, solid* and *fusinoid.* The correlations between the three groups of combustion chars listed above and unburnt carbon level improve at higher combustion temperature, i.e. at higher burn-off.

The weakness of the correlations between these combustion char groups and burn-off probably lies in the inability to take into account the material which has already burned to completion, so that although all three flyash samples from Tarong, Bayswater and Curragh coals contain 53-60% *solid* and *inertoid* chars by mass (Bailey, 1992), this disguises their very different unburnt carbon levels.

Use of char pyrolysed in the absence of oxygen overcomes the problem of complete disappearance of a large proportion of the original particles. The total of dense and thick-walled char types formed during pyrolysis at 1050/1100°C is a more reliable predictor of burn-off performance than combustion char, and the total of dense and thick-walled chars pyrolysed at 1500° C may be used to predict unburnt carbon at 1300° C with greater reliability than rank, fuel ratio, FTIR aromaticity, and infusible inertinite content. The correlation between the total dense and thick-walled chars and unburnt carbon also improves at higher burn-off. Only unburnt carbon at 900° C gives a more reliable estimate of performance.

J.G.BAILEY

OVERALL VIEW OF BURN-OFF OF WHOLE COALS

In Figure 1 the overall trends of the whole coal burn-off curves indicate a strong influence due to coal rank at temperatures up to about 1100° C. The two sub-bituminous coals surpass all others in performance, largely due to high volatile matter content and early ignition. The high volatile bituminous coals have intermediate burn-off levels and the medium volatile bituminous coal has poorer performance at all temperatures. The correlations between rank and burn-off level in Table 1 are good, but are not adequate to distinguish between the four high volatile bituminous coals at high temperature.

The performance of the high volatile bituminous coals is influenced by type (petrographic composition) as well as rank. At 900° C, Bayswater has higher burn-off (lower rank), followed by Coals 93 and 94 (high vitrinite) and trailed by Coal 92 (high inertinite). The coals change burn-off order at 1000° C, and at 1200° C, where the order is still discernible, they fall in two groups, the high vitrinite coals approaching the sub-bituminous coals at about 99% burn-off, and the higher inertinite coals grouped with Curragh medium volatile coal at about 97% burn-off.

Although rank is a strong indicator of final burn-off level, there are significant deviations from rank-dominated burn-off behaviour within this series of samples. Indices which take "type" as well as rank into consideration in the form of chemical parameters such as aromaticity and infusible inertinite determined by fluorescence microscopy refine and improve predictive ability within a particular rank group of coals. The proportion of low reactivity or low fusibility char morphotypes produced by a coal is obviously related to both rank and type characteristics and provides a method of not only predicting the level of unburnt carbon at high temperature but also of explaining its failure to burn in terms of char shape, pore accessibility and carbon chemistry.

REFERENCES

Bailey, J.G., 1992. The origin of unburnt combustibles in coal. Ph.D. thesis, University of Newcastle, NSW. Unpubl.

Diessel, C.F.K., 1986. Fusible and non-fusible components of coal. Aust. Coal Sci. 2, Proc., pp. 327-332.

Jones, R.B., Morley, C. and McCourt, C.B., 1985. Maceral effects on the morphology and combustion of coal char. International Conference on Coal Science, 1985, Proc., pp. 669-672.

Oka, N., Murayma, T., Matsuoka, H., Yamada, T., Shinozaki, S., Shibaoka, M. and Thomas, C.G., 1987. The influence of rank and maceral composition on ignition and char burnout of pulverised coal. Fuel. Proc. Tech., 15:213-224.

MINERAL MATTER ... ASH ... WHAT'S THE DIFFERENCE?

R.H. SANDERS[1] & D. BUTEL[2]
[1] Quality Coal Consulting Pty Ltd, Carrington
[2] SGS Aust Pty Ltd, Carrington

SUMMARY

A study was carried out to determine the effect of additions of increasing proportions of certain minerals, mostly found naturally in coal seams and in their contained stone bands, on the proximate analysis of a "pure coal" sample. The aim of the study was to demonstrate quantitatively, and graphically, the contribution made to a coal's volatile matter value when mineral matter decomposes to ash. The mineral matter to ash ratio of the range of minerals tested was also to be demonstrated.

The analyses of the mineral additives, and their mixtures with coal, were carried out according to Australian Standard AS 1038 - 1989 "Methods For the Analysis and Testing of Coal and Coke, Part 3, Proximate Analysis of Coal".

The test results for the two clays (bentonite and kaolinite), and the silica (sand) were generally as anticipated, with the former yielding volatiles consistent with their water of hydration contents, and the latter being inert except for a small amount of carbonate contamination. The pyrite sample yielded the predicted ash, while its volatile matter yield was lower than expected for the pure mineral and gave decreasingly lower values for the calculated $V_{o,dmmf}$ of the mixtures. This behaviour will be further investigated.

Although the $MgCO_3$ mixtures yielded the predicted amounts of ash and volatiles, samples containing large proportions of $CaCO_3$ needed to be ashed to constant mass, and not to a constant incineration time (as is normal practice), and yielded well below the predicted amount of mineral volatiles (CO_2), even when the heating time was increased two-fold and then three-fold. There was evidence, however, that the yield of *coal* volatile matter was increased at these prolonged, non-Standard, heating times. The "siderite" sample was found to contain little Fe and was not able to be evaluated. All carbonate minerals will be the subject of further testing.

BACKGROUND

When coal is *burned* the moisture is driven off, all of the organic component consumed with the production of heat, and the inorganic (mineral) component decomposed and oxidised to ash residue, with the evolution of inert gases. When coal is heated in the *absence* of air to produce coke, moisture is driven off, together with the organic volatiles and the gases from the decomposition of the minerals, leaving a solid residue comprising fused organic carbon ("coke") and inorganic ash.

In both situations, the inorganic or mineral fraction is reduced in mass, with the evolution of gas. The amount of gas produced varies with the "inertness" of the mineral.

FIGURE 1
Schematic Representation of the Make-up of Coal

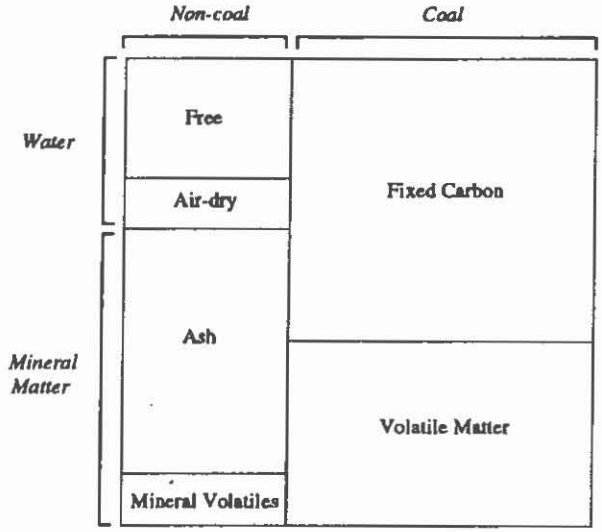

Figure 1 shows a schematic representation of the fundamental make-up of coal. The organic or coal matter component can be thought of as made up, on heating, of a gaseous "volatile matter" phase and a solid "fixed carbon" phase. The mineral matter, as explained above, is made up of ash and "mineral volatiles" components.

The fundamental laboratory analysis of coal is given by the "proximate analysis", which is done on coal which is air-dry, and determines empirically the amounts of moisture, ash and volatile matter, with the amount of fixed carbon being given by difference. As can be seen from Figure 1, the volatile matter reported in this way includes the component contributed by the decomposition of the mineral matter to ash.

LABORATORY TESTWORK

The Laboratory Analysis Methods

The proximate analyses used are in this study are described in Australian Standard AS 1038 Part 3 "Methods for the analysis and testing of coal and coke - proximate analysis of coal". The individual analyses are described below. All use an analysis sample, ground to pass 212 μm and allowed to attain equilibrium with the laboratory atmosphere. Moisture is determined from the loss of mass at 105°C under nitrogen; ash is the residue remaining after incineration at 815°C, with air, until constant in mass; volatile matter is the mass lost, corrected for moisture, when heated out of contact with air at 900°C for 7 minutes; fixed carbon is 100 minus moisture, ash and volatile matter.

The Samples Studied

Coal: This was a sample of Hunter Valley coal, previously separated in organic liquids at a relative density of 1.25. Its proximate analysis is given in Table 1.

Bentonite: The sample was obtained from a bulk consignment. Bentonite was chosen for the study as its principal constituent is montmorillonite, a common "swelling clay" associated with coal.

Montmorillonite is in turn a phyllosilicate, a hydrous aluminosilicate with a layered atomic structure containing exchangeable cations and a variable number of water molecules between the layers. Its ability to take in water molecules gives it its swelling property. An alteration product of volcanic ashes, its published relative density is 2.0 to 2.7, depending on the water content. Analyses of the bentonite are given in Table 1.

TABLE 1
Basic Analyses of The Minerals and Coal Used in the Study

	% M_{ad}	% A_d	% V_d	% *1 "FC"	RD_d	CO_2	*2% MM/A	*Theoretical* % A_d	% V_d
Bentonite	10.7	94.1	6.0	-0.1	2.68	0.99	1.06		
Calcite	0.1	62.5	8.0	29.5	2.86		1.60	56.0	44.0
Coal	3.0	2.2	41.9	55.9	1.30	0.20	(1.1)		
"Siderite"	0.6	66.1	31.7	0.2	2.93		1.51	70.0	38.0
Kaolinite	0.6	88.5	12.0	-0.5	2.74	0.07	1.13		
Magnesite	2.0	45.3	55.8	-1.1	2.35		2.21	47.8	52.2
Pyrite	0.4	67.8	23.0	9.2	5.15	0.28	1.47	66.7	
Silica	0.3	97.8	2.3	-0.1	2.77	2.06	1.02		

*1 "FC" = 100 - A_d - V_d *2 = 100/Ad for minerals

Kaolinite: The sample used was AR grade kaolin. Kaolinite is also a clay mineral commonly associated with coal, often as pellets, bands, cleat fillings and as thin bands in higher ash coal plies. It is formed from the decomposition of other aluminosilicates, especially the feldspars. It has a published relative density of 2.6. See Table 1.

Calcite (Calcium Carbonate, $CaCO_3$): The sample used was an AR grade reagent. Calcite is a common mineral associated with coal, often as veins and infilling cleats in vitrain. It is soft, with a Moh's hardness of 3, and has a published density of 2.71.

Based on the assumption that $CaCO_3$ decomposes completely during both laboratory determinations, it should yield 56% of ash (CaO or "quicklime") and 44% of volatile matter. However, as shown in Table 1, the study showed a higher ash (even to constant mass) and much lower volatile matter. Because of the low V result for the first analyses of the pure mineral and mixtures, a second AR grade sample was used. This confirmed the validity of the initial (higher A, lower V) results.

Magnesite (Magnesium Carbonate, $MgCO_3$): The sample used was an AR grade reagent. Magnesite is not common in coal although dolomite, a mineral intermediate between calcite and magnesite, and dolomite-ankerites (containing some iron by substitution) have been found to be common (Patterson et al, 1992). Magnesite, with a published relative density of 3.01, and a high theoretical volatility, was included in this study to give further information on the decomposition of carbonates during ash and volatile matter analyses.

Based on the assumption that $MgCO_3$ decomposes completely during both the ash and volatile matter laboratory determinations, it should yield 47.8% of ash and 52.2% of volatile matter. As shown in Table 1, the study achieved results close to these.

Siderite (Ferrous Carbonate, $FeCO_3$): The sample used was a donated geological specimen, in the form of a brown-coloured nodular aggregate. Siderite commonly occurs in coal (" ubiquitous to the Sydney Basin coal seams " - Patterson et al, 1992), often in

nodular form, varying from small, dispersed pellets to massive football sized aggregates. Calcite and siderite form a continuous series, with the mineral of intermediate composition being ankerite, $CaFe(CO_3)_2$. Siderite has a published relative density of 3.96, decreasing with increasing calcium content.

Based on the assumption that $FeCO_3$ decomposes completely during both the ash and volatile matter laboratory determinations, to form Fe_2O_3 and CO_2 during the former and FeO and CO_2 during the latter test, it should yield 70% of ash and 38% of volatile matter. However, as shown in Table 1, the study gave results which were low for volatile matter and very low for relative density. These analyses, given in Table 1, prompted an ash analysis of the sample which showed it to contain only 6% as Fe_2O_3, with the majority of the ash, 67%, being CaO. Thus the sample was, in fact, a contaminated calcite-ankerite. Because of publication deadlines, there was no time to acquire another sample of siderite. This will, however, form part of the continuing study.

Pyrite (Iron Sulphide, FeS_2): The sample used was a geological specimen, in the form of a massive crystalline aggregate. Pyrite commonly occurs in coal, often as infillings in cleats, and has a published relative density of 5.01.

Based on the assumption that FeS_2 oxidises completely during the laboratory determination of ash, to form Fe_2O_3, it should yield 66.7% of ash. A value close to this was achieved, as shown in Figure 1. The decomposition products from the volatile matter determination are not known and will be studied further.

Silica (Quartz, SiO_2): The sample used was beach sand. Quartz is common in coal and its associated stone bands, typically as angular grains. It has a published density of 2.65. It was included in this study as an "inert" mineral, with an expected mineral matter to ash ratio of 1. As shown in Table 1 the sample yielded, in fact, some volatile matter, in the form of CO_2. This is thought to derive from minor calcareous contamination.

The Mixtures

Mixtures were prepared for each mineral, containing 0, 20, 40, 60 and 80 percent by mass of the mineral, on an air-dry basis.

RESULTS

General

Corrections were made, to the analyses of the mixtures, for the ash value (2.2% dry), and assumed mineral volatile matter content (0.2% dry) of the coal component, that is the coal was assumed to be "pure".

The $V_{m,d}$ values for the mixtures in Tables 2, 3 and 4 are obtained by factoring the value obtained for the pure mineral by the proportion of mineral contained in the dry mixture. Low values for the pure mineral (such as for $CaCO_3$) produce inflated values for the $V_{o,d}$ (which is by difference), and hence for the $V_{o,dmmf}$, of the mixtures.

Linear regression analyses were carried out, for each mineral, on $V_{t,d}$ against A_d. From these were derived values for the MM/A ratio, the intercept V_t value (that is the value for V_{dmmf}), and the value for V_m of the pure mineral.

The Clays

Brown et al (1965) give the following typical properties for the two clays tested, with the values in brackets those obtained during this study for M_{ad} (air-dry moisture) and V_d (volatile matter, dry) respectively.

Clay	SiO_2/Al_2O_3	M_{ad}%	W_h% *
Montmorillonite	2.7	14.8 (10.7)	7.5 (6.0)
Kaolinite	1.2	0.6 (0.6)	12.2 (12.0)

* Water of hydration (800°C).

The above table shows that the bentonite probably contains 70% to 80% of montmorillonite. The results for the bentonite / coal, and kaolinite / coal, mixtures are summarised in Table 2. The near-zero "FC" values in Table 1, and the linearity of the plot in Figure 2, confirm the predictable behaviour of clays during the proximate analysis.

TABLE 2
Analyses of the Mixtures of Clays and Coal

. . . . . Bentonite / Coal					. . . . . Kaolinite / Coal				
A_d	$V_{t,d}$	$V_{m,d}$	$V_{o,d}$	$V_{o,dmmf}$	A_d	$V_{t,d}$	$V_{m,d}$	$V_{o,d}$	$V_{o,dmmf}$
0.0	41.9	0.0	41.9	41.9	0.0	41.9	0.0	41.9	41.9
19.6	34.7	1.1	33.6	41.5	19.4	35.1	2.5	32.6	41.2
37.4	27.4	2.3	25.1	41.0	37.2	28.9	5.0	23.9	40.9
55.2	20.5	3.6	16.9	41.6	54.5	24.3	7.4	16.9	44.3
74.7	13.0	4.8	8.2	41.8	71.8	17.8	9.8	8.0	44.4
94.1	6.0	6.0	0.0		88.5	12.0	12.0	0.0	

Where $_d$ = dry, $_t$ = total, $_m$ = mineral, $_o$ = organic, $_{dmmf}$ = dry, mineral matter-free.

Derived by linear regression: Bentonite $V_{o,dmmf}$ = 41.9%; V_t(pure) = 5.6%; MM/A = 1.06
Kaolinite $V_{o,dmmf}$ = 41.8%; V_t(pure) = 12.6%; MM/A = 1.14

The Carbonates

General: Choudhury and Ganguly (1978) tested mixtures separately containing up to 30% each of calcite, magnesite and siderite with Indian coals having volatile matter contents of 19 to 37%. They found that the calcite and magnesite in the mixtures decomposed completely during the normal volatile matter determination (at 900°C), as evidenced by testing the residue with acid. The results could be corrected for the carbon dioxide from these carbonates to yield a constant value, equal to the organic volatile matter content. They found, however, that results similarly corrected for siderite showed a steady increase of the organic volatile matter content with increasing siderite content. They deduced that the FeO produced during the test was reduced to elemental iron by the coal's fixed carbon, reducing the mass of residue and thereby inflating the volatile matter value, which is determined by difference of the starting mass and residue.

It was hoped to test this conclusion during the current study. This was not achieved (i) because of the unsuitable "siderite" sample and (ii) because total decomposition did not occur for either the "siderite" or (especially) the calcite during the volatile matter test, even when the heating times were increased three-fold. Note that the Indian study did not use mixtures containing more than 30% of the carbonate in coal.

The results from this study, for calcite / coal, "siderite" / coal, and magnesite / coal, are summarised in Table 3.

FIGURE 2
Plots of Total Volatile Matter Against Ash for All Mixtures

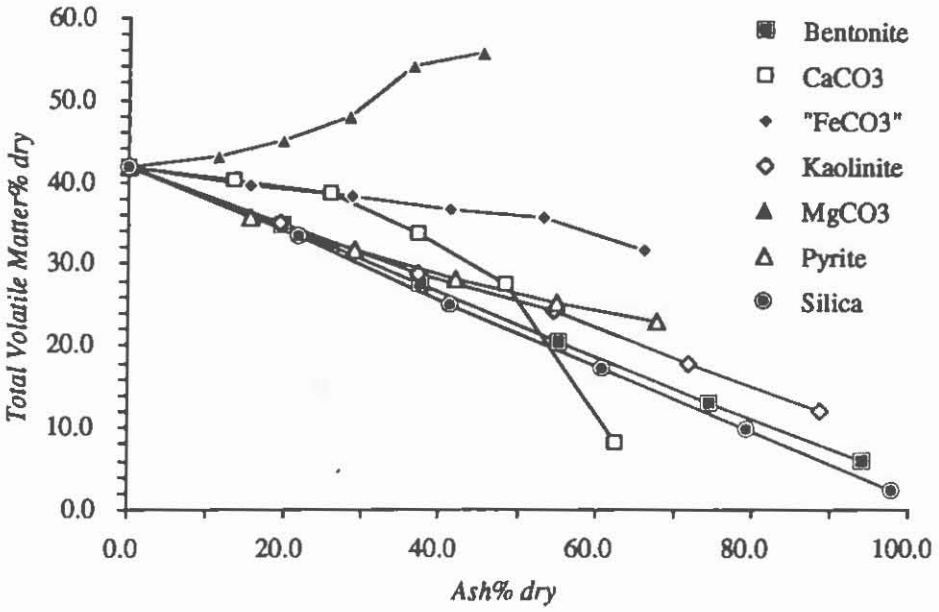

Calcite: Figure 3 shows the plots of V_d against A_d for the $CaCO_3$ / coal mixtures, for heating times of 7 (Standard), 14 and 21 minutes. It shows that the standard heating time was inadequate to decompose the $CaCO_3$, a fact substantiated by the effervescence of the residue with acid. 14 minutes was adequate to achieve decomposition for mixtures of up to about 50% only, and even after 21 minutes decomposition was still incomplete for mixtures containing more than 60% $CaCO_3$. Importantly, there was evidence that heating for longer than the standard time gave non-standard (high) coal volatile matter results.

FIGURE 3
Variation of Volatile Matter With Heating Times, Calcite / Coal Mixtures

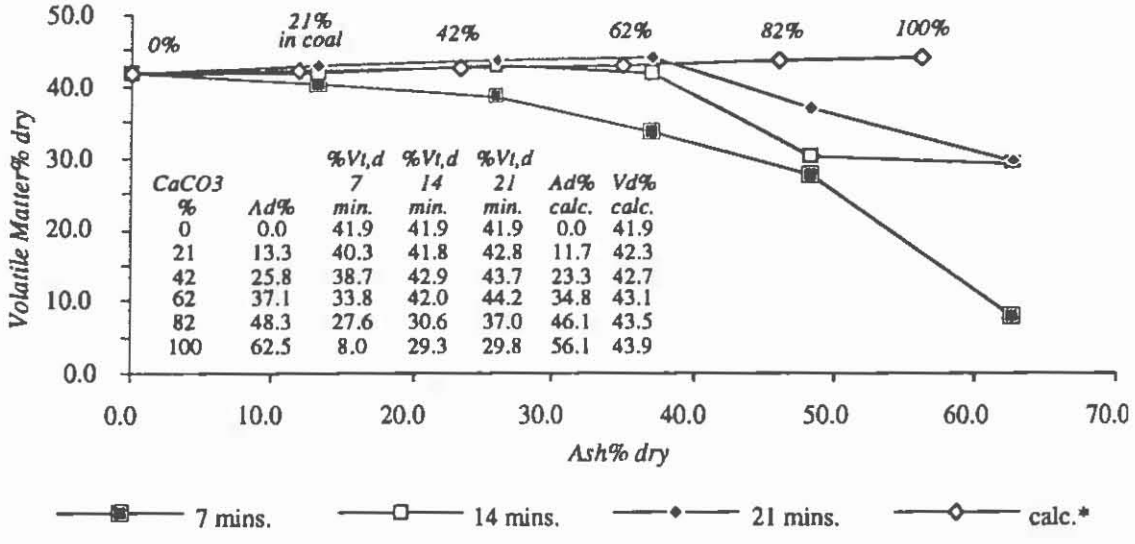

CaCO3 %	Ad%	%Vt,d 7 min.	%Vt,d 14 min.	%Vt,d 21 min.	Ad% calc.	Vd% calc.
0	0.0	41.9	41.9	41.9	0.0	41.9
21	13.3	40.3	41.8	42.8	11.7	42.3
42	25.8	38.7	42.9	43.7	23.3	42.7
62	37.1	33.8	42.0	44.2	34.8	43.1
82	48.3	27.6	30.6	37.0	46.1	43.5
100	62.5	8.0	29.3	29.8	56.1	43.9

The full range of calcite / coal mixtures was put in an ash muffle between rows of coal samples containing over 5% of sulphur. Contrary to expectation the ash values obtained were closely similar to those obtained without the high sulphur samples present, indicating that no fixation of the sulphur gases by the calcium oxide, to form calcium sulphate, had occurred.

Siderite: As explained, the sample was not sufficiently pure to proceed fully with the experiment. However, it is interesting to note that the sample gave volatile matter yields much closer to those expected than did the $CaCO_3$ sample (see Figure 2).

Magnesite: This pure sample decomposed as expected, unlike the calcite. Of interest, however, is the shape of the line in Figure 2, which has a curvature indicating incomplete decomposition in the 20, 40 and 60 percent mixtures, and a higher than expected result for the mixture containing 80%. This latter anomaly was confirmed by repeat analysis. Also, when all mixtures were re-analysed using a heating time of 21 minutes, the 20, 40 and 60 percent values increased by about 1.5%, to give a better fit, but the value for the 80% mixture was again high.

Ashing the $MgCO_3$ mixtures to constant mass, rather than constant time, gave no appreciable change to the ash values.

TABLE 3
Analyses of the Mixtures of Carbonates and Coal

. . . . . Calcite / Coal					. . . . . Magnesite / Coal				
A_d	$V_{t,d}$	$V_{m,d}$	$V_{o,d}$	$V_{o,dmmf}$	A_d	$V_{t,d}$	$V_{m,d}$	$V_{o,d}$	$V_{o,dmmf}$
0.0	41.9	0.0	41.9	41.9	0.0	41.9	0.0	41.9	41.9
13.3	40.3	1.7	38.6	48.8	11.3	43.1	11.5	31.6	39.8
25.8	38.7	3.3	35.4	60.5	19.7	45.0	22.9	22.1	37.5
37.1	33.8	5.0	28.8	75.9	28.2	47.8	34.3	13.5	35.0
48.3	27.6	6.6	21.0	117.8	36.4	54.2	45.7	8.5	47.0
62.5	8.0	8.0	0.0		45.3	55.8	55.8	0.0	

Where $_d$ = dry, $_t$ = total, $_m$ = mineral, $_o$ = organic, dmmf = dry, mineral matter-free.

Derived by linear regression: Calcite* $V_{o,dmmf}$ = N/A; V_t(pure) = N/A; MM/A = N/A
Magnesite $V_{o,dmmf}$ = 40.1%; V_t(pure) = 55.1%; MM/A = 2.23
* values not applicable because plot not a straight line.

The Others

The results for pyrite / coal, and silica / coal, mixtures are summarised in Table 4, and shown in Figure 2.

The volatile matter results for pyrite are interesting in that corrections to $V_{t,d}$, which are based on the volatile matter of pure FeS_2, result in values for $V_{o,dmmf}$ which steadily *decrease* for mixtures containing up to 80% of pyrite in coal. This is directly opposite to the experience of Choudhury and Ganguly (1978), as explained above, for mixtures of $FeCO_3$ and coal. A similar mechanism, the reduction of FeO by the fixed carbon in the coal, to yield a *higher* $V_{o,dmmf}$, might have been expected for the pyrite.

TABLE 4
Analyses of the Mixtures of Pyrite/Coal, Silica/Coal

Pyrite / Coal					Silica / Coal				
A_d	$V_{t,d}$	$V_{m,d}$	$V_{o,d}$	$V_{o,dmmf}$	A_d	$V_{t,d}$	$V_{m,d}$	$V_{o,d}$	$V_{o,dmmf}$
0.0	41.9	0.0	41.9	41.9	0.0	41.9	0.0	41.9	41.9
15.4	35.7	4.8	30.9	39.0	21.6	33.3	0.5	32.8	41.5
29.0	31.9	9.5	22.4	38.2	41.2	25.1	1.0	24.1	41.3
41.9	28.3	14.2	14.1	36.9	60.7	17.3	1.4	15.9	41.7
55.0	25.3	18.9	6.4	35.9	79.4	9.7	1.9	7.8	43.7
67.8	23.0	23.0	0.0		97.8	2.3	2.3	0.0	

Where $_d$ = dry, $_t$ = total, $_m$ = mineral, $_o$ = organic, $_{dmmf}$ = dry, mineral matter-free.

Derived by linear regression: Pyrite* $V_{o,dmmf} = 40.6\%$; $V_t(\text{pure}) = 18.0\%$; MM/A = 1.22
Silica $V_{o,dmmf} = 41.9\%$; $V_t(\text{pure}) = 2.3\%$; MM/A = 1.02
* derived values influenced by the distinct curvature of the plot.

CONCLUSIONS

1 Clays in coal lose their water of hydration during both the standard ash and volatile matter tests, giving predictable ash yields and volatile matter contributions.

2 Coals containing high proportions of calcium carbonate require additional ashing time to avoid high results.

3 Coals containing high proportions of calcium carbonate do not appear to completely decompose during a standard volatile matter test, giving low results.

4 Further study is needed to determine the behaviour of pure siderite during the proximate analysis of coal.

5 Further study is needed to properly understand the decomposition of pyrite and, to a lesser extent magnesite, during the standard volatile matter test.

REFERENCES

BERRY, L. G., and MASON, B., 1959: Mineralogy - Concepts, Descriptions, Determinations, W. H. Freeman and Co.

BROWN, N. A., et al, 1965: Mineral Matter in N.S.W. Coke-making Coals: Composition, Determination and Effects, Jour. Inst. Fuel, May, 198-206.

CHOUDHURY, S. S., 1978: Effect of Carbonate Minerals on Volatile Matter Of Coals, Fuel, v. 57, March, 175-178.

NAYAK, R., V., et al, 1987: Mineral Matter in Coal - Origin, Identification, High-Temperature Transformation, and Boiler Erosion, Jour. Coal Qual., April, 37-39.

PATTERSON, J. H., et al, 1992: The Composition of Carbonate Minerals in Coal Measures of The Sydney Basin, Adv. Stud. Syd. Bas., 26th Newcastle Symp., Proc., 72-79.

STANDARDS AUSTRALIA, 1989: AS 1038, Methods For the Analysis and Testing of Coal and Coke, Part 3, Proximate Analysis of Coal.

STANDARDS AUSTRALIA, 1983: AS 1038, Methods For the Analysis and Testing of Coal and Coke, Part 21, Determination of the Relative Density and Apparent Relative Density of Hard Coal.

WARD, C., 1978: Mineral Matter in Australian Bituminous Coals, Australas. Inst. Min. Metall., Proc., N° 267, Sept., 11-17.

MAGMA-MIXING IN GRANITOIDS OF THE LACHLAN FOLD BELT : BASEMENT ROCKS OF THE SYDNEY BASIN

S. KEAY
University of Newcastle

INTRODUCTION

Recently obtained seismic profiles suggest that Lachlan Orogen rocks extend beneath the Sydney Basin, continuing below at least part of the Tamworth Belt and may abut New England Orogen rocks along the Peel Fault (Korsch et al., 1993). The Lachlan Fold Belt (LFB) forms the basement of the Sydney Basin and has acted as an important sediment source, yet the mechanism by which this extensive orogenic belt has formed is still a matter for debate. Granitoids are an important feature of the LFB, comprising 20% of the total exposed area of Palaeozoic rocks of the belt which is up to 750km wide (White & Chappell, 1983). The intrusion of these Siluro-Devonian granitoids into Early Paleozoic metasedimentary rocks occurred within a relatively short time span from 420 to 390 Ma (Williams et al., 1988). Investigations into the origin of mafic enclaves contained in the Tuross Head Tonalite, part of the 390Ma Moruya Batholith, at Bingie Bingie Point on the New South

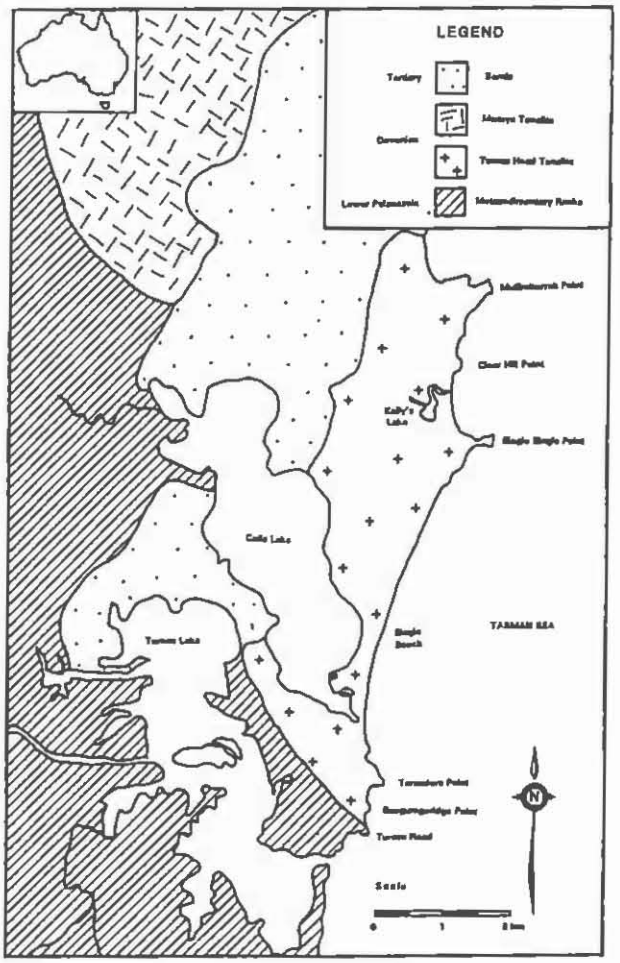

Figure 1 The southeastern section of Moruya Batholith (adapted from Griffin et al., 1978).

Wales south coast (Fig.1), suggest that magma mixing processes are an important consideration in theories of orogenesis.

The geochemical and mineralogical variations of LFB granitoids and their inclusions have been explained by two main theories, restite unmixing (White & Chappell, 1977) and magma mixing (Gray, 1984). The origin of enclaves at Bingie Bingie Point has also been ascribed to these two theories, with Griffin et al. (1978) supporting the restite model and Vernon et al. (1988) proposing magma mixing and mingling processes. These models have different implications for the Paleozoic evolution of the LFB. To explain the geochemistry of LFB granitoids and enclaves, the restite model requires the presence of Proterozoic basement terranes to act as source rocks (Chappell et al., 1988), while a mixing model requires mixing between juvenile crust and basaltic mantle material (Gray, 1990). Information from enclaves at Bingie Bingie Point tests these two divergent theories.

Figure 2

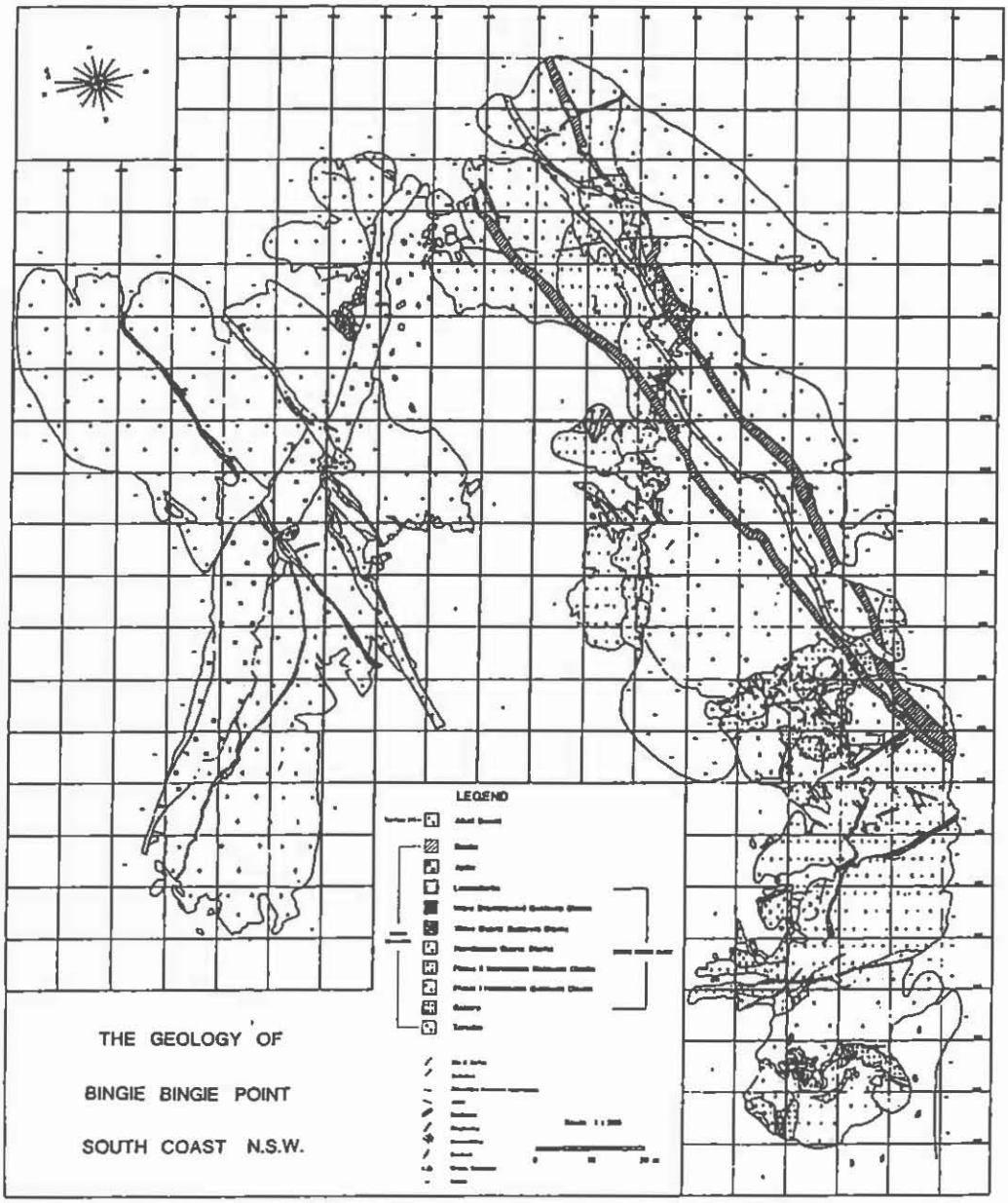

MAGMA-MIXING IN GRANITOIDS OF THE LACHLAN FOLD BELT

THE GEOLOGY OF BINGIE BINGIE POINT

Two distinct suites of rocks occur at Bingie Bingie Point (Fig. 2), the Tuross Head Tonalite, which forms part of the Moruya Suite and encloses a variety of gabbroic diorite rocks, which form the Bingie Bingie Suite (Griffin et al., 1978). The Tuross Head Tonalite pluton is part of the Moruya Batholith which intrudes a deformed sequence of conformable Ordovician metasedimentary units including the Wagonga beds (Brown, 1928). These rocks are cut by an array of microdiorite dykes, along with aplite and later dacite and basaltic dykes.

As less than 0.1% of rocks in the Lachlan Fold Belt are gabbroic (White & Chappell, 1983), Bingie Bingie Point provides a unique opportunity to study the character of a gabbroic diorite, which appears to have intruded synchronously with a tonalite. The order of intrusion of the rocks in the vicinity of Bingie Bingie Point has undergone revision in recent years, with the recognition that age relationships of the tonalite and diorite masses were ambiguous (Vernon et al., 1988; O'Sullivan, 1990). Earlier workers (Brown, 1928; Griffin et al., 1978) suggested that the diorite bodies were intruded first and later engulfed by the Tuross Head Tonalite. While the diorite is included and veined by the tonalite, it appears chilled against the tonalite and often "pillows" into the tonalite mass forming ovoid shaped inclusions with crenulate margins. This suggests that the diorite was magmatic at the time it interacted with the tonalite magma resulting in magma mingling and the reversal of apparent age relationships (Walker & Skelhorn, 1966). The term magma "mingling" implies that the magmas retain their original identities, while magma "mixing" is an extension of this process which results in the formation of hybrid rocks.

A number of dyke rocks also display ambiguous age relationships, resulting from variations in emplacement and cooling times. The composition of the dykes is microtonalite and microdiorite, as well as mingled magma dykes which occur in the area surrounding the Point and consist of pillows of microdiorite in a microtonalite host. These dykes are interpreted as late-stage intrusions related to the main tonalite and diorite bodies, and have chemistries which place them as members of the Moruya and Bingie Bingie Suites. While most dykes show knife-sharp contacts with their hosts, some appear to have intruded prior to 70% crystallisation of the tonalite at a stage when the tonalite could still behave magmatically (van der Molen & Paterson, 1979) and have formed pinch & swell, chocolate tablet boudinage and flame structures. The other igneous rocks at the Point display relatively straightforward cross-cutting relationships, resulting in the order of intrusion shown in Fig. 2.

The Tuross Head Tonalite contains numerous mafic inclusions of quartz diorite composition, known as microgranitoid enclaves (Vernon, 1983), which are fine-grained with an igneous texture. The origin of microgranitoid enclaves is currently a contentious issue with important implications for granitoid genesis. There are five main theories for the origin of these enclaves including that they represent; 1. reworked wall-rock xenoliths, 2. fragments of chilled margins produced by thermal or pressure quenching, 3. autoliths derived from the host magma by differentiation,

accumulation or liquid immiscibility, 4. modified restite (refractory residue from the source), 5. globules or fragments of mafic or hybrid magma. These diverse theories have been discussed by several workers (eg. Barbarin & Didier, 1991) and discovering the method by which enclaves are formed is essential information in understanding the evolution of the granitoid host.

THE ORIGIN OF ENCLAVES

Field Relationships

Enclaves in the Tuross Head Tonalite occur in a variety of shapes and sizes, ranging from rounded to angular, less than 2cm to greater than 1m. Generally, enclaves are elliptical and less than 10cm long, displaying sharp contacts with the tonalite and occasionally showing fine-grained, perhaps chilled, margins up to 5mm wide. Many enclaves appear elongate, with aspect ratios ranging from 1:1 to 1:40 but displaying no microstructural evidence of having undergone solid state deformation, indicating that the enclaves were magmatic at the time of incorporation in the tonalite. These observations discount the possibility that the enclaves are reworked xenoliths of wall-rock, as these could not behave magmatically. At Bingie Bingie Point enclaves make up to 6% of the volume of the tonalite according to point counts, but at nearby Tarandore Point the density of enclaves increases to 60% with proximity to a large felsic diorite body. At the contact between the tonalite and the diorite at this point, enclaves can be seen literally peeling away from the diorite mass. This automatically suggests that the magma mingling theory of enclave genesis should be accepted, but what other evidence of magma-magma interaction exists?

Textural Relationships

Many of the features attributed to enclaves are ambiguous when interpreted, this is especially true of petrography. Although the mineralogy of the enclaves is similar to that of their host tonalites, consisting mainly of plagioclase (50%) along with roughly equal proportions of hornblende, biotite and quartz, the textures of the enclaves are characteristically pseudo-doleritic (Vernon, 1983) with frequent ophitic textures developed. This texture is also common to the microdiorite dykes. Both enclaves, diorites and tonalites display textures indicative of the variations in temperature and chemistry which would accompany mixing and mingling between a more felsic and more mafic magma. Alone these textures could be attributed to other processes, but combined they form a "textural assemblage" (Hibbard, 1991) which is strong evidence of magma-magma interactions. Such features evident in the enclaves include; xenocrystic quartz, poikilitic quartz and biotite, subophitic hornblende, acicular apatite, mafic clots and both boxy and spongy cellular plagioclase, often containing magmatic inclusions and rimmed by more sodic plagioclase. For a more detailed discussion of the formation of these textures the reader is referred to Hibbard (1991).

Geochemistry

The interpretation of the geochemistry of the enclaves and their relationship to the tonalites and diorites at Bingie Bingie Point is also open to different interpretations. Both restite unmixing (Chappell et al., 1987), fractionation (Wall et al., 1987) and

two component magma mixing between a mafic and felsic end-member (Wilson, 1989), will produce straight line trends on Harker variation diagrams, unfortunately neither the diorites, or the enclaves fall along such trends (Fig. 3). According to the restite model, this suggests that there is a discontinuity between not only the tonalite and diorite, but also the enclaves. The tonalite (60-67% SiO_2) defines a generally tight linear array on major oxide variation diagrams, while the enclaves (51-60% SiO_2) exhibit a scatter of data points away from this trend, and the diorites (48-56% SiO_2) plot as an array of points which generally fall along a line drawn between diorite hornblende and plagioclase compositions, suggesting the scatter of points is due to fractionation of these minerals.

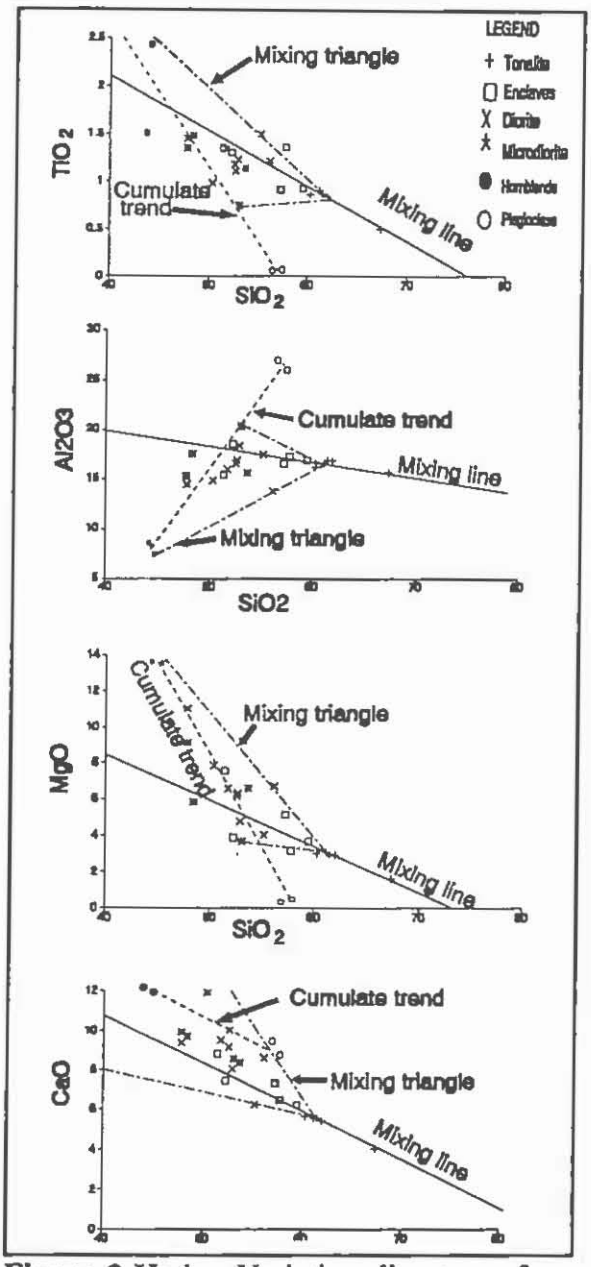

Figure 3 Harker Variation diagrams of TiO_2, Al_2O_3, MgO and CaO.

By accounting for fractionation and accumulation in the diorites to produce a range of mafic end-member compositions, the trends shown on the chemical variation diagrams can be explained in terms of multi-component magma mixing. Mixing this range of diorites with members of the Moruya Suite would form a "mixing triangle" enclosing intermediate hybrids produced within the triangle of possible end-member compositions. Significantly, most of the enclaves, along with some felsic diorites plot within these so-called "mixing triangles" for most major and trace element compositions. The diversity of enclave compositions which plot away from the trend of the tonalites is impossible to reconcile with any model of enclave genesis which relies exclusively on the enclaves being an internal product of the host tonalite. This discounts not only the restite model, which requires that the enclaves are refractory material from the source of the tonalite, but also any model which involves auto-segregation from the tonalite host such as accumulation, liquid immiscibility or thermal/pressure quench models. Old theories die hard however, and it has been suggested that two types of enclaves occur in the Tuross Head Tonalite, one produced by magma mingling and the other restite (Chen et al., 1991).

If this were the case, then this study has shown that these two apparent types of enclaves are indistinguishable on mineralogical, textural, morphological and geochemical grounds.

DISCUSSION

Magma-magma interactions are gaining increasing acceptance as the process responsible for generating enclaves in granitoids, and also as an important petrological process involved in generating a range of granitoid compositions (eg. Reid et al., 1983; Didier, 1987). The occurrence of microgranitoid enclaves and mafic-felsic rock associations such as those visible at Bingie Bingie Point, highlight the significance of hybridisation processes in the genesis of calc-alkaline granitoids (Eichelberger, 1980). Mafic magmas play a fundamental role in the formation of calc-alkaline granitoids, providing the heat necessary for melting the lower crust. These primitive magmas must invariably mix to some extent with the melts they produce and so will influence melt composition. Magma mixing can thus act as a significant differentiation process and must be taken into account when considering models of granitoid evolution, especially for the LFB where the occurrence of magma mixing processes can be established.

CONCLUSION

The geology at Bingie Bingie Point has implications not only for the genesis of enclaves in granitoids of the LFB, but also for the genesis of the granitoids themselves. The range of field relationships and textures visible in rocks at Bingie Bingie Point can be attributed to a combination of mixing and mingling between melts of similar composition. This resulted in modest undercooling of the diorite and heating of the tonalite, producing changes in the temperature of both magmas, resulting in the formation of characteristic textural assemblages. Two main sources are inferred for the generation of the rock-types at Bingie Bingie Point, involving melting of the continental crust to form granitoid magmas (the Moruya Suite) with the heat for melting provided by mantle-derived magmas (the Bingie Bingie Suite) which pooled at the base of the crust and mixed to form intermediate compositions (enclaves and felsic diorites) which mingled with the Moruya Suite at emplacement level. The involvement of mantle magmas in the genesis of the granitoids makes the involvement of Proterozoic basement source rocks unnecessary in models of granitoid evolution for the LFB.

ACKNOWLEDGMENTS

The work presented in this paper comprises part of the author's BSc (Hons) thesis completed under the supervision of Dr Bill Collins and submitted in November, 1992 to the Geology Department, University of Newcastle. The author was funded by a scholarship in geomorphology from ANSTO through the University of Newcastle Geography Department. Hope Nesmith-Ruming constructed Figure 3.

REFERENCES

BARBARIN, B. and DIDIER, J., 1991: Review of the main hypotheses proposed for the genesis and evolution of mafic microgranular enclaves, in J. Didier & B. Barbarin (eds) Enclaves and Granite Petrology, Elsevier, London, 367-373.

BROWN, I.A., 1928: The geology of the south coast of New South Wales: Part 1. The Palaeozoic geology of the Moruya district, Proceedings Linnean Society N.S.W., 53, 151-192.

CHAPPELL, B.W., WHITE, A.J.R. and HINE, R., 1988: Granite provinces and basement terranes in the Lachlan Fold Belt, southeastern Australia, Australian Journal of Earth Sciences, 35, 505-521.

CHAPPELL, B.W., WHITE, A.J.R. and WYBORN, D., 1987: The importance of residual source material (restite) in granite petrogenesis, Journal of Petrology, 28(6), 1111-1138.

CHEN, Y., CHAPPELL, B.W. and WHITE, A.J.R., 1991: Mafic enclaves of some I-type granites of the Palaeozoic Lachlan fold belt, southeastern Australia, in J. Didier & B. Barbarin (eds) Enclaves and Granite Petrology, Elsevier, London 113-124.

DIDIER, J., 1987: Contribution of enclave studies to the understanding of origin and evolution of granitic magmas, Geologische Rundschau, 76 (1), 41-50.

EICHELBERGER, J.C., 1980: Vesiculation of mafic magma during replenishment of silicic magma reservoirs, Nature, 288, 446-450.

GRAY, C.M., 1984: An isotopic mixing model for the origin of granitic rocks in southeastern Australia, Earth and Planetary Science Letters, 70, 47-60.

GRAY, C.M., 1990: A strontium isotopic traverse across the granitic rocks of southeastern Australia: Petrogenetic and tectonic implications, Australian Journal of Earth Sciences, 37, 331-349.

GRIFFIN, T.J., WHITE, A.J.R. and CHAPPELL, B.W., 1978: The Moruya batholith and geochemical contrasts between the Moruya and Jindabyne suites, Journal Geological Society of Australia, 25(4), 235-247.

HIBBARD, M.J., 1991: Textural anatomy of twelve magma-mixed granitoid systems, in J. Didier & B. Barbarin (eds) Enclaves and Granite Petrology, Elsevier, London, 431-444.

KORSCH, R.J., WAKE-DYSTER, K.D. and JOHNSTONE, D.W., 1993: The Gunnedah Basin - New England Orogen deep seismic reflection profile:

implications for New England tectonics, *in* P.G. Flood & J.C. Aitchison (eds) New England Orogen, eastern Australia, Department of Geology & Geophysics, University of New England, Armidale, 85-100.

O'SULLIVAN, D.N., 1990: The geology of the Tuross plutonic complex north of Coila Lake, N.S.W., B.Sc.(Hons) Thesis, Geology Department, University of Sydney, N.S.W.

REID, J.B., EVANS, O.C. and FATES, D.G., 1983: Magma mixing in granitic rocks of the central Sierra Nevada, California, Earth and Planetary Science Letters, 66, 243-261.

VAN DER MOLEN, I. and PATERSON, M.S., 1979: Experimental deformation of partially melted granite, Contributions to Mineralogy and Petrology, 70, 299-318.

VERNON, R.H., 1983: Restite, xenoliths and microgranitoid enclaves in granites, Journal of the Proceedings of the Royal Society of N.S.W., 116, 77-103.

VERNON, R.H., ETHERIDGE, M.A. and WALL, V.J., 1988: Shape and microstructure of microgranitoid enclaves: indicators of magma mingling and flow, Lithos, 22, 1-11.

WALKER, G.P.L. and SKELHORN, R.R., 1966: Some associations of acid and basic igneous rocks, Earth-Science Reviews, 2, 93-109.

WALL, V.J., CLEMENS, J.D. and CLARKE, D.B., 1987: Models for granitoid evolution and source compositions, Journal of Geology, 95(6), 731-749.

WHITE, A.J.R. and CHAPPELL, B.W. (1977) Ultrametamorphism and granitoid genesis, *in* D.H. Green (editor), Experimental Petrology Related to Extreme Metamorphism, Tectonophysics, 43, 7-22.

WHITE, A.J.R. and CHAPPELL, B.W., 1983: Granitoid types and their distribution in the Lachlan Fold Belt, southeastern Australia, Geological Society of America Memoir, 159, 21-34.

WILLIAMS, I.S., CHEN, Y., CHAPPELL, B.W. and COMPSTON, W., 1988: Dating the sources of Bega Batholith granites by ion microprobe, Geological Society of Australia Abstracts, 21, 424.

WILSON, M., 1989: Igneous Petrogenesis: a global tectonic approach, Harper Collins Academic, London p.258.

A FLUORESCENCE LASER MICROPROBE FOR COAL ASSESSMENT

J.R. WILMSHURST & R.W.T. WILKINS
CSIRO Division of Exploration Geoscience

SUMMARY

An instrument has been developed for measuring the fluorescence of coal macerals and for studying the fusibility of macerals *in-situ* as defined in Wilkins et al. (1993a, b), it is also well suited to the examination of other fossil organic matter. The instrument is best described as a scanning laser-excited fluorescence microprobe, capable of measuring the fluorescence intensity of macerals at the μm scale, and with a higher source power, of fusing compliant macerals.

INTRODUCTION

While the fluorescence properties of fossil organic matter has aroused not inconsiderable interest as an organic petrology tool (e.g. Crelling, 1983; Ottenjahn, 1988; Teichmuller and Wolf, 1977) and as a probe of chemical composition, (e.g. Davis et al., 1990; Landis et al., 1987a, 1987b; Lin et al., 1986; Lin, 1988), the impetus for the present project came from the work of Diessel et al. (1986a, 1986b, 1987) and Ng et al. (1987) together with subsequent work from the Newcastle School. In short, Diessel's NERDDC study demonstrated that fluorescence intensity offers advantage over reflectance in estimating the extent of fusibility of a coal; it was shown that the thermo-plastic properties of the macerals correlate with fluorescence intensity across maceral-type boundaries and that, accordingly, fluorescence measurements offered a better petrographic means of estimating the coking properties of a coal than reflectance alone.

Meantimes in the CSIRO laboratories, Wilkins et al. (1990, 1991a, 1991b) in studying petroleum source rocks, concluded that cw visible lasers are useful and appropriate fluorescence excitation sources well suited to the task of the measurement of the fluorescence of macerals, with target areas down to 2 μm diameter. The relatively high power density provided by a laser allows meaningful results to be obtained readily for even the least fluorescent inertinitic macerals. With an automated scanning stage fitted to the CSIRO laser Raman microprobe, it was demonstrated that areal

fluorescence data could readily be obtained from petrographically prepared coal specimens (Wilmshurst et al. 1991).

This latter work suggested that relatively simple instrumentation could be constructed which would allow the rapid collection of fluorescence data for the maceral populations of a coal, such data might then be applied in evaluation of the coking properties (following Diessel). The scanning capability of such an instrument might also be used for mapping the areal distribution of the macerals and their internal variability. The proposition to construct the instrument was supported by a NERDDC grant.

INSTRUMENTATION

The instrumentation package that has been developed is modular and consists of laser, microscope, photometers, instrumentation computer and control software; the physical components are assembled on a custom optical bench. A brief description of the assemblage follows.

The fluorescence excitation laser which we have chosen is a small air cooled argon ion laser capable of delivering powers of some 20 mW. While a level of only1 mW is required for fluorescence work, 10 mw or more is necessary for micro-fusion determinations as defined by Wilkins et al. (1992, 1993). The 488 nm (blue) laser line is used for routine work.

The microscope consists of a modular reflected light instrument which has been somewhat modified to accept both laser and white light illumination sources. In normal use, ultra long working distance objectives are employed to minimise contamination of the front lens by errant organic matter. A RGB video camera and photometers are fitted to the microscope, the former is used both for direct observation and for preparation of digital images.

An automated scanning stage is used which has travel in the x and y directions of 25 mm with step size of 0.25 μm.

The fluorescence photometer is non-dispersive and uses precision band-pass filters for wavelength selection. Measurements are made at 620 nm. The sensing element is a photomultiplier, operated in photon counting mode to allow for the low fluorescence of the inertinitic macerals. A second photometer (silicon photo-diode based) can be used for simultaneous "reflectance" measurement.

The control and data presentation software has been written for the express application and hence can be modified incrementally as required.

FLUORESCENCE LASER MICROPROBE

In application, the new fluorescence microprobe produces fluorescence intensity and alteration data which are quantitatively similar to those which are obtained on the laser Raman microprobe. Most significantly however, there is a sensitivity gain of some 80 to 100 times over that instrument. This gain in sensitivity allows fluorescence data to be acquired within 100 ms or less, an important factor where an individual data set may contain rather more than 1000 entries.

APPLICATION

The microprobe has been used to produce single point fluorescence and fluorescence alteration intensity data and to record fluorescence data for both line and area scans of coal grain and block mounts. A protocol has also been developed for acquiring and analysing fluorescence/micro-fusion data for coking coal evaluation as discussed in Wilkins et al. (1993a, b) and Wilmshurst et al. (1992)

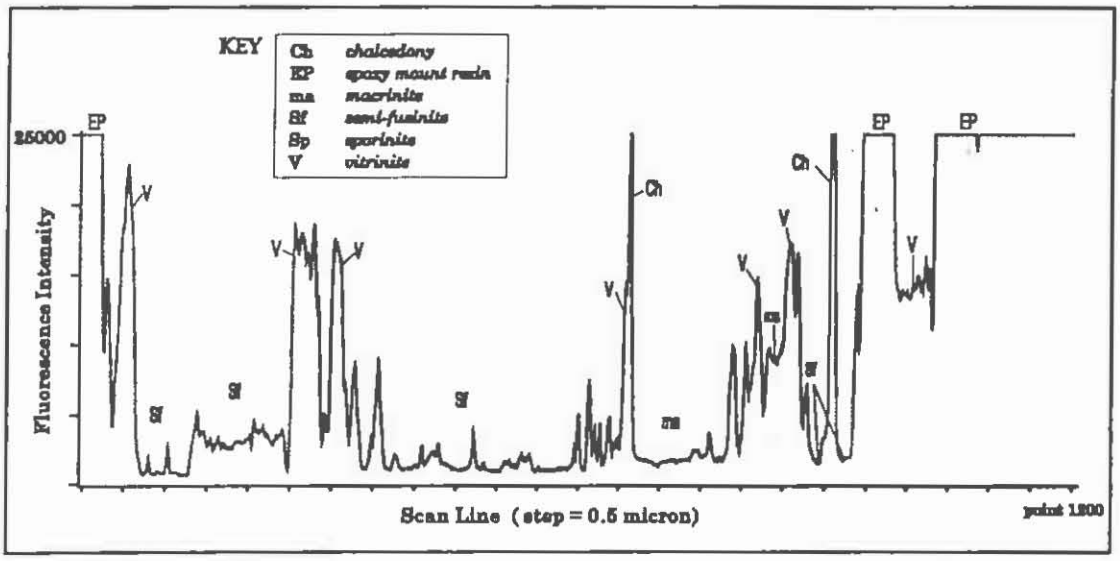

Figure 1. Fluorescence line-scan across a grain of Bulli reference coal, showing the fluorescence response of the maceral types.

For the purpose of coking evaluation, the data are perhaps best presented in statistical summary, and this will be dealt with elsewhere, but graphic visualisation can be a powerful tool for presenting the maceral distributional data for both linear and areal scan-modes. Thus the results of fluorescence area scans are routinely presented as false color images or maps on screen and as hard copy, but such cannot be conveniently reproduced here in either color or gray scale. However line scans may be shown as a simple graph of intensity against distance to show the maceral relationships.

Such a scan across a predominently inertinitic grain of a Bulli reference coal (Diessel, 1991) is shown in Figure 1. In this illustration, 1201 points were measured along a 600 μm line at 0.5 μm spacing. The maceral types are indicated on the figure.

We believe that the fluorescence microprobe will prove to be an important petrographic tool for studying and evaluating coals and other fossil organic matter.

REFERENCES

CRELLING, J.C. 1983. Current uses of fluorescence microscopy in coal petrology. J. Microscopy. 132, 251-256.

DAVIS, A, RATHBONE, R.F, LIN. R and QUICK, J.C. 1990. Observations concerning the nature of maceral fluorescence alteration with time. Organic Geochemistry 16, 897-906.

DIESSEL, C.F.K, McHUGH, E. and BROWN K., 1986a. Coal Characterisation by Vitrinite and Inertinite Fluorescence. NERDDC End of Grant Report 658pp.

DIESSEL, C.F.K, McHUGH, E., 1986b. Fluoreszintensitat und Reflexionsvermogen von Vitriniten und Inertiniten zur Kennzeichnung des Verkokungsverhaltens. Gluckauf Forschungshefte 47, 60-70.

DIESSEL, C.F.K, and WOLFF-FISCHER, E. 1987. On the relationship between reflectance, and fluorescence and fusibility of inertinite in Ruhr coals. in Moulijn, J.A. (ed) 1987 International Conference on Coal Science, Elsevier, Amsterdam. p901-906.

DIESSEL, C.F.K. 1991. The 1991 ICCP ring analysis - an interesting comparison of two coals and their cokes. Advances in the Study of the Sydney Basin. 25th Newcastle Symposium. p251-260

LANDIS, C.R., CRELLING, J.R., SULLIVAN, G.W., PLEIL, M.W. and BORST, W.L. 1987a. Results of laser induced fluorescence of organic materials. Organic Geochemistry . 11, 423.

LANDIS, C.R., SULLIVAN, G.W., PLEIL, M.W., BORST, W.L. and CRELLING, J.C. 1987b. Pulsed laser fluorescence microscopy of coal macerals and dispersed organic matter. FUEL 66, 984-991.

LIN, R. 1988. The chemistry of coal maceral fluorescence: with special reference to the huminite/vitrinite group. Ph.D. Dissertation, The Pennsylvania State University.

LIN, R., DAVIS, A., BENSLEY, D.F., and DERBYSHIRE, F.J. 1986. Vitrinite secondary fluorescence: its chemistry and relation to the development of a mobile phase and thermoplasticity in coal. International Journal of Coal Geology. 6, 215-228.

NG, N., et al. 1987. Coking coal characterisation by etching and fluorescence techniques. NERDDC End of Grant Report. 679

OTTENJAHN, K. 1988. Fluorescence alteration and its value for studies of maturation and bituminisation. Organic Geochemistry 12, 309-321.

TEICHMULLER, M. and WOLF, M. 1977. Application of fluorescence microscopy in coal petrology and oil exploration. J. Microscopy. 109, 49-73.

WILKINS, R.W.T., WILMSHURST, J.R., Hladky, G., ELLACOTT, M.V., and BUCKINGHAM, C.P. 1990. Laser micro-Raman spectroscopy: a new tool for petroleum exploration. NERDDP End of Project Report EG 90/910 pp87.

WILKINS, R.W.T., WILMSHURST, J.R., HLADKY, G., ELLACOTT, M.V., and BUCKINGHAM, C.P. 1991a. Fluorescence alteration: a maceral insensitive thermal maturity technique. NERDDP End of Project Report pp77.

WILKINS, R.W.T., ZHONG, N., ELLACOTT, M.V., and BUCKINGHAM, C.P. 1991b. The suppression of vitrinite reflectance in the Greta and Pelton coals: a fluorescence alteration study. Advances in the study of the Sydney Basin. 25th Newcastle Symposium p234-236.

WILKINS, R.W.T., WILMSHURST, J.R., and BUCKINGHAM, C.P. 1993a. Fusibility imaging of coking coal: a direct calibration by laser micropyrolysis. (NERDDP) End of Project Report. 1614.

WILKINS, R.W.T., WILMSHURST, J.R. and BUCKINGHAM, C.P. 1993b. The use of lasers for the fusibility assessment of coals. This Volume.

WILMSHURST, J.R., DIESSEL, C.F.K., WILKINS, R.W.T, and ELLACOTT, M.V. 1991. A new instrumental method for the assessment of coking coal.. Advances in the study of the Sydney Basin. 25th Newcastle Symposium. p234-236.

WILMSHURST, J.R., DIESSEL, C.F.K., WILKINS, R.W.T, and ELLACOTT, M.V. 1992. Progress in the fusibility imaging of coal. Proceedings of the 5th Australian Coal Science Conference. Australian Institute of Energy, Melbourne.p366-367.

THE USE OF SMALL LASERS FOR THE FUSIBILITY ASSESSMENT OF COALS

R.W.T. WILKINS, J.R. WILMSHURST & C.P. BUCKINGHAM
CSIRO Division of Exploration Geoscience

INTRODUCTION

A measure of the fusibility of macerals may be obtained conveniently from the fusion trace developed by moving a focussed laser beam across a polished surface of coal. The technique was introduced by C. D. A. Coin and K. D. Hall in the BHP Central Research Laboratories, Wallsend, N.S.W. (Coin and Hall, 1989; Hall and Coin, 1989), using a 750 μm beam from a YAG laser yielding 0.9 W of infrared radiation. A 50 μm beam of infrared radiation from a CO_2 laser was also used successfully but the beam had low stability. In this form of the technique the polished block was vertically mounted on a dropping stage which was allowed to fall at a constant rate across the beam. To inhibit actual burning of the sample, a jet of nitrogen was directed onto the sample surface at the focus of the laser. Their method of assessment of fusibility involved determining the continuity of inertinite bands across the fusion trace. Despite the acquisition of results which compared very favourably with those obtained by the coal/coke mass balance approach of Diessel and Wolff-Fischer (1987), the technique possessed some severe disadvantages. Because the infrared beam at focus was so wide, coal grains in conventional particulate blocks were often narrower than the beam so that there was no unheated coal adjacent to the laser trace. Although this problem could be overcome by the use of solid blocks of coal, this introduced sampling problems. Furthermore, the variability in the depth of the coal grains beneath the surface sometimes resulted in complete burn through. Another undesirable feature of the technique was the relatively expensive laser required. For best observation of the fusion trace the surface had to be repolished before the assessment of fusibility of the macerals.

The technique can be improved by the use of visible laser radiation. At the focal point of a laser beam, the beam diameter is controlled by the diffraction limit which is a function of the wavelength of light. The diameter of the beam at focus is given by

$$d = 4 \lambda f / \pi D$$

where λ is the wavelength of the light, f is the focal length of the lens and D is the diameter of the laser beam before entering the lens (Long, 1977). This means that if a small focal point is required, there is an advantage in using visible rather than infrared radiation. The second advantage is that with the higher light flux at the focus of a smaller diameter beam, a laser of much lower power could be used with equal efficiency and considerable savings in cost.

EXPERIMENTAL

We have carried out experiments with both red and blue radiation from respectively a Coherent Innova-90 krypton ion laser delivering 100 mW of 647 nm radiation, and an Omnichrome 532 air cooled argon ion laser delivering a maximum of 25 mW of 488 nm radiation. Initial experiments used an experimental arrangement similar to that of Coin and Hall (1989), but this was abandoned when it was found that a laser beam directed through long distance objectives on the microscope of the DILOR Microdil-28 laser Raman microprobe in the CSIRO Division of Exploration Geoscience, coupled with programmed horizontal translation of the sample on a positioning stage produced a fine fusion trace. It was found that by careful control of experimental conditions fusion traces as fine as 2 μm could be readily obtained using blue radiation. However, a 4 μm trace formed with a laser power of 1 mW at the coal surface was found to be optimum, because it contains more useful textural information which is clearly visible without repolishing the surface. Fine fusion traces could also be obtained using the red laser radiation but the depth of the fused layer appeared to be deeper, and repolishing of the surface would be desirable. Examples of fusion traces developed using both blue and red radiation are shown in Fig. 1.

In routine examination of coals, the blue laser radiation focussed through a 50x ultra long working distance objective is moved across the surface in 4 μm steps with 100 ms rest times so that several scans can be made across the surface of the petrographic block in a few minutes. Under the chosen experimental conditions, fusion rather than pyrolysis seems to be the main response to the rapid movement of the laser across the sample, but the appearance of copious bubbles in the fusion product of some vitrinites attests to micropyrolysis reactions taking place. Under the conditions we have chosen, there seems to be no discernible difference in the marks produced by the laser whether the irradiation is carried out in an air or a nitrogen atmosphere.

LASERS FOR THE FUSIBILITY ASSESSMENT OF COALS.

INTERPRETATION

Our method of fusibility assessment is based on textural characteristics, and their degree of development, in the fusion trace itself, without any repolishing of the coal surface. With the block mounted on the positioning stage, using an 80x ultra long distance objective, the fusion traces are examined in reflected light and classified into fusible, partially fusible and infusible categories using scanning/point counting software created for the task. The criteria used were simple although it must be borne in mind that there is no natural boundary between the fusibility categories, and the distinctions are not always clear.

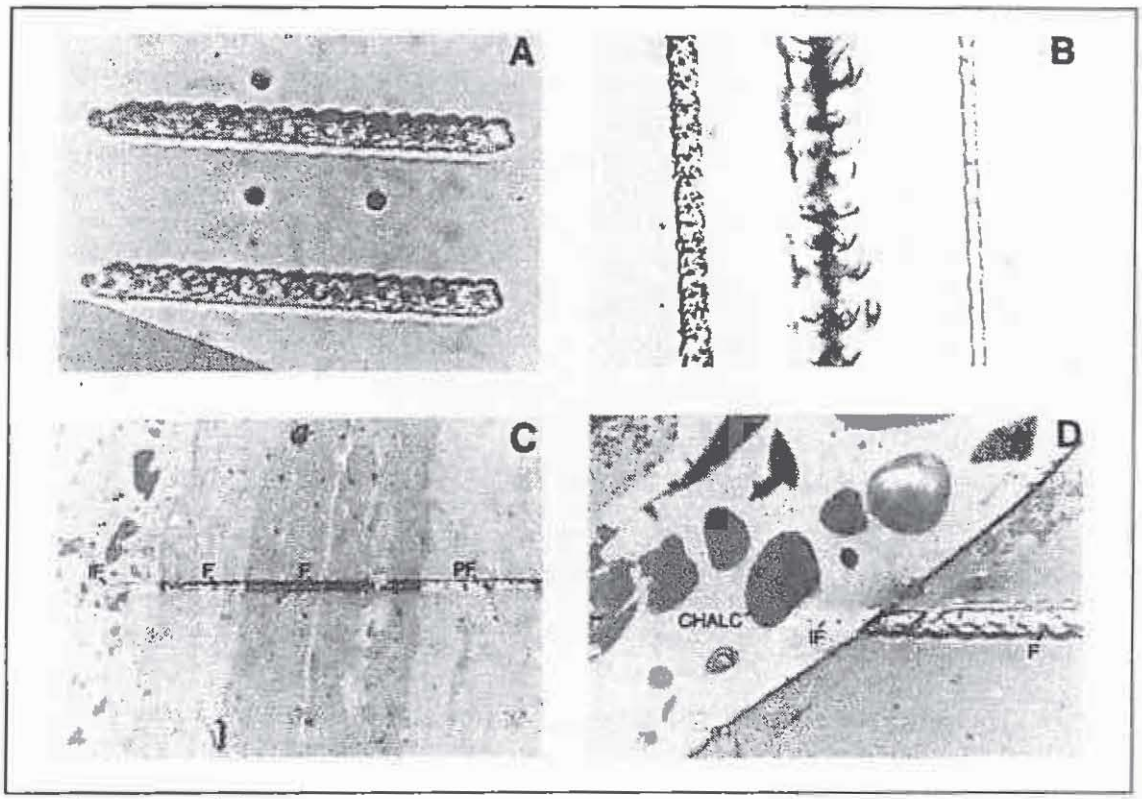

Fig. 1 Laser fusion traces :
(A) Comparison of "burn" marks left by single pulses (black spots) with laser fusion traces (initiated from the left). West Wallsend telovitrinite, 488 nm radiation.
(B) Comparison of 2 μm and 4 μm laser fusion traces using 488 nm radiation, with a 647 nm laser fusion trace (centre). Moura telovitrinite.
(C) A comparison of the appearance of a 4 μm 488 nm laser fusion trace on a vitrinite band (dark, central) and three semifusinite bands. Tower coal.
(D) Comparison of a 4 μm 488 nm laser fusion trace on vitrinite (right) with semifusinite (left) which is infusible . The cell lumens of the semifusinite are filled with chalcedony (CHALC) which is not marked by the laser beam. Wongawilli coal. F = fusible, IF = infusible, PF = partially fusible

The fusion trace on liptinites is black and easily distinguished as fusible. For vitrinites and inertinites, if a strongly marked boundary is observed on each side of the fusion trace, the maceral is classified as fusible. If only one boundary is well defined, the maceral was classified as partially fusible. If fusion was not visible, or if neither boundary of the maceral is well defined even though the trace of the laser beam can be seen by a reflectance enhancement, the maceral was classified as infusible. Minerals are readily distinguished. Sulphides were identified by their extreme reflectance, and silica and clays by moderate reflectance and lack of any trace of fusion by the laser beam.

The fusion traces contain information not only upon the quantity, but also on the quality of the fusible product. The fusion traces developed on telovitrinite in high volatile bituminous coals have a dark appearance with irregular surface markings due to the abundance of small bubbles which have in part broken through the surface, Fig. 1A. In coals of higher rank, bubbles are rarely developed in the fusion traces of telovitrinite and a regularly repeating pattern of sculpture is characteristic, Fig 1B (left of field). The laser fusion traces on telovitrinite of sub-bituminous coals are very poorly developed and typically consist of a series of equally spaced "burn" holes along the path of stepwise movement of the sample across the focussed laser beam. This observation is in accord with the known poor caking properties of such coals.

CONCLUSION

Combined with total fluorograms which are obtained by use of a laser fluorescence microprobe (Wilmshurst and Wilkins, 1993a), laser fusion offers a rapid and powerful means of petrographic assessment of the fusibility properties of coals which complements methods based on bulk samples. Further details on the methodology of these techniques is given in the CRD and D Program Final reports on these projects (Wilmshurst and Wilkins, 1993b; Wilkins et al. 1993).

REFERENCES

COIN, C.D.A. and HALL, K.N. 1989. Rapid laser micropyrolysis of coal to assess the fusibility characteristics of the inertinite group of macerals. In Thomas, C.G. and Strachan, M.G. (eds.) Proceedings of the Macerals '89 Symposium. CSIRO Division of Coal Technology 7.1-7.12.

DIESSEL, C.F.K. and WOLFF-FISCHER, E. 1987. Coal and coke petrographic investigations into the fusibility of Carboniferous and Permian coking coals. International Journal of Coal Geology 9, 87-108.

HALL, K.N. and COIN, C.D.A. 1989. Laser micro-pyrolysis of coals to determine the fusibility characteristics of the inertinite group of coal macerals. BHP Central Research Laboratories, Report CRL/R/15.89 1-32.

WILKINS, R.W.T. WILMSHURST, J.R. and BUCKINGHAM, C.P. 1993. Fusibility imaging of coking coal : A direct calibration by laser micropyrolysis. (NERDDP) End of Project Report 1614

WILMSHURST, J. R. and WILKINS, R. W. T. 1993a. A fluorescence based microprobe for coal assessment. This volume.

WILMSHURST, J. R. and WILKINS, R. W. T. 1993b. A practical instrument for assessing coking coals. (NERDDP) End of Project Report 1596

INTEGRATED FLUORESCENCE ALTERATION & REFLECTANCE STUDY OF VOLADOR-1, GIPPSLAND BASIN, VICTORIA

M.V. ELLACOTT & R.W.T. WILKINS
CSIRO Division of Exploration Geoscience

INTRODUCTION

The fluorescence alteration of multiple macerals (FAMM) technique (Wilkins et al., 1992a) was introduced as an objective multi-parameter thermal maturity tool for use in petroleum exploration. It is closely related to the vitrinite reflectance technique and it has been shown to be a powerful tool for correcting for the effect of suppression of vitrinite reflectance (Wilkins et al., 1992b).

The FAMM technique is calibrated in terms of equivalent vitrinite reflectance on data derived from a suite of reference Permian coals from eastern Australia. It is of particular interest to test if this calibration can be applied to organic matter of different age which has originated from a distinctly different flora (Thomas, 1982).

VOLADOR-1: LOCATION AND SAMPLE SELECTION

Volador-1 is located in the deepest part of the Gippsland Basin between the coast of eastern Victoria and a ridge extending from the Mornington Peninsula to Flinders Island called the Bassian Rise (Fig. 1). The well provides an excellent test for the FAMM technique because of the relatively simple depositional history of the Late Cretaceous Latrobe Group, documented thermal histories and source rock evaluation, and availability of side wall core samples containing mostly coaly material in which telovitrinite can be unequivocally identified. The ten available samples from 3550 - 4527 m consisted of seven side wall cores (SWC) and three ditch cuttings from within the fluviatile facies of the Latrobe Group. The location of the samples and the well stratigraphy are shown in Fig. 2. Geology, structure and hydrocarbon potential of the Gippsland Basin are described in Threfall et al. (1976), Brown (1986), Hegarty et al. (1986) and Thompson (1986). Specific descriptions of the geology, source rocks and hydrocarbon potential for Volador-1 are given in Stainforth (1984) and Clark and Thomas (1988).

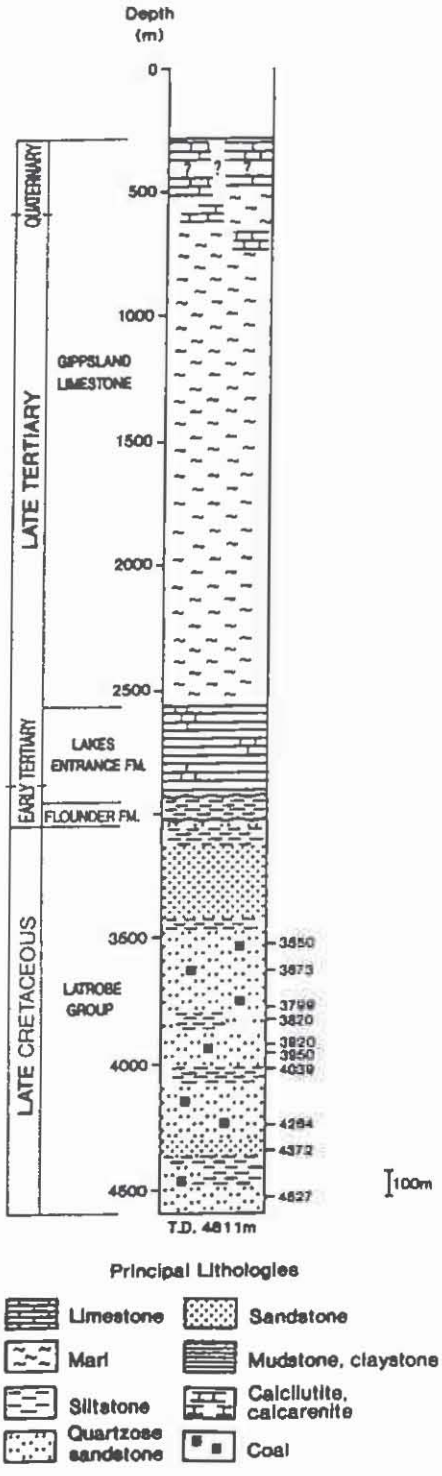

Fig. 1. Location map for Volador-1.

THERMAL MATURITY ASSESSMENT BY FLUORESCENCE ALTERATION ANALYSIS

The results of FAMM analysis of Volador-1 samples are presented in the form of standard fluorescence alteration diagrams in Fig. 3. In each diagram the abcissa is the fluorescence intensity measured at 700 s under standard conditions (Wilkins, 1992a), and the ordinate is the ratio of the final to the initial fluorescence intensity. Each point represents fluorescence alteration measurements on a single maceral grain and the scatter of data results from the range of inertinite, vitrinite and liptinite macerals randomly selected to define the characteristic parabolic multi-maceral curve for each sample. The sub-vertical or "J" curve on each diagram, represents the curve of best fit to the average telovitrinite fluorescence alteration data for the Permian reference coals. In each diagram, data from visually identified telovitrinites are represented by a filled circle. It should be noted that the multi-maceral curves

Fig. 2. Stratigraphy and sample locations for Volador-1. (Based on information supplied by B. Thomas, pers. comm., Shell Development Australia Pty Ltd.).

FLUORESCENCE ALTERATION AND REFLECTANCE, VOLADOR-1

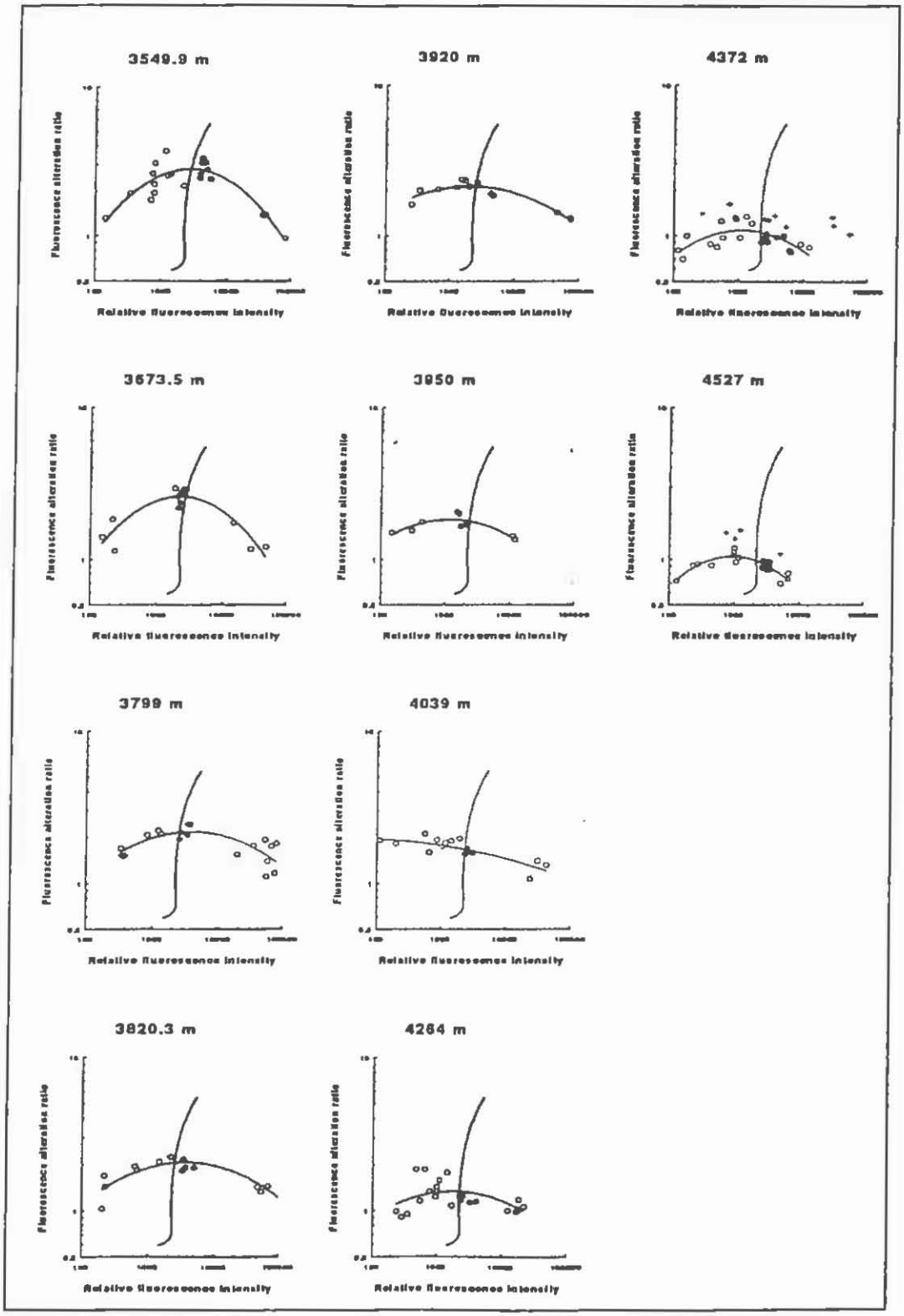

Fig. 3. Fluorescence alteration diagrams for Volador-1 samples. • Telovitrinite, o inertinite and liptinite, + cavings.

generally intersect the "J" curve at a lower position as the depth of the sample increases.

In Fig. 4 the averaged telovitrinite data for each sample is plotted separately on a fluorescence alteration diagram. For Permian coals, hydrogen-rich (perhydrous) vitrinites plot in the field to the right, and hydrogen-poor (subhydrous) vitrinites plot to the left of the "J" curve. The amount of scatter of the telovitrinite data around the "J" curve is not unusual even for Permian coals and this suggests that the "J" curve appropriate to Late Cretaceous coals is very close to that defined by "normal" Permian coals. In Table 1, the equivalent vitrinite reflectance for each sample has been determined from the intersection of the multi-maceral curve with the "J" curve using the Permian coal calibration given in Wilkins et al. (1992a).

An interesting feature of Fig. 3 is the notable increase in the scatter of data in samples from 4264 m and below. The samples above this level are all SWC and those from 4264 m and below are all ditch cuttings. The results from 4372 m are shown in more detail in Fig. 5. Two populations of macerals may be distinguished in this sample, the indigenous population through which the parabolic line of best fit has been constructed, and a second population marked by crosses which has a lower equivalent reflectance. This is typical of the pattern resulting from cavings contamination. Anomalously low reflectance resulting from cavings is readily distinguished from suppression of vitrinite reflectance associated with hydrogen-rich organic matter, evidenced by the telovitrinite population plotting in the perhydrous vitrinite field of the fluorescence alteration diagram. In the case of the 4372 m and the 4527 m samples, the telovitrinites have a slight perhydrous character which must be corrected for, even after the contribution from cavings has been eliminated.

THERMAL MATURITY ASSESSMENT BY CONVENTIONAL VITRINITE REFLECTANCE

Mean random vitrinite reflectance ($\bar{R}r\%$, polarizer removed, no stage rotation) was measured according to the procedure recommended in Australian Standard AS 2486 (1989). This is Ting's (1978) mean average vitrinite reflectance. The measured telovitrinite reflectance results and brief petrographic descriptions are listed in Table 1, and histograms and statistics are shown in Fig. 6.

The organic matter in the samples consists of banded telovitrinite in coal, coal partings in shale, dispersed organic matter (DOM) in shale or siltstone, and heavily fissured coal fragments resembling pseudovitrinite (Stach et al, 1975) with reflectance values consistently higher than those of vitrinite in the banded coals and shales. A breakdown of the reflectance populations by coal type is given in Table 1 and the populations distinguished are also indicated on the histograms (Fig. 6). Measured reflectance values for Volador-1 samples increase steadily from $\bar{R}r\% = 0.58$ at 3549.9 m to 0.84 at 3950 m, thereafter increasing slightly to 0.87% at 4264 m and remaining at that level to 4527 m.

FLUORESCENCE ALTERATION AND REFLECTANCE, VOLADOR-1

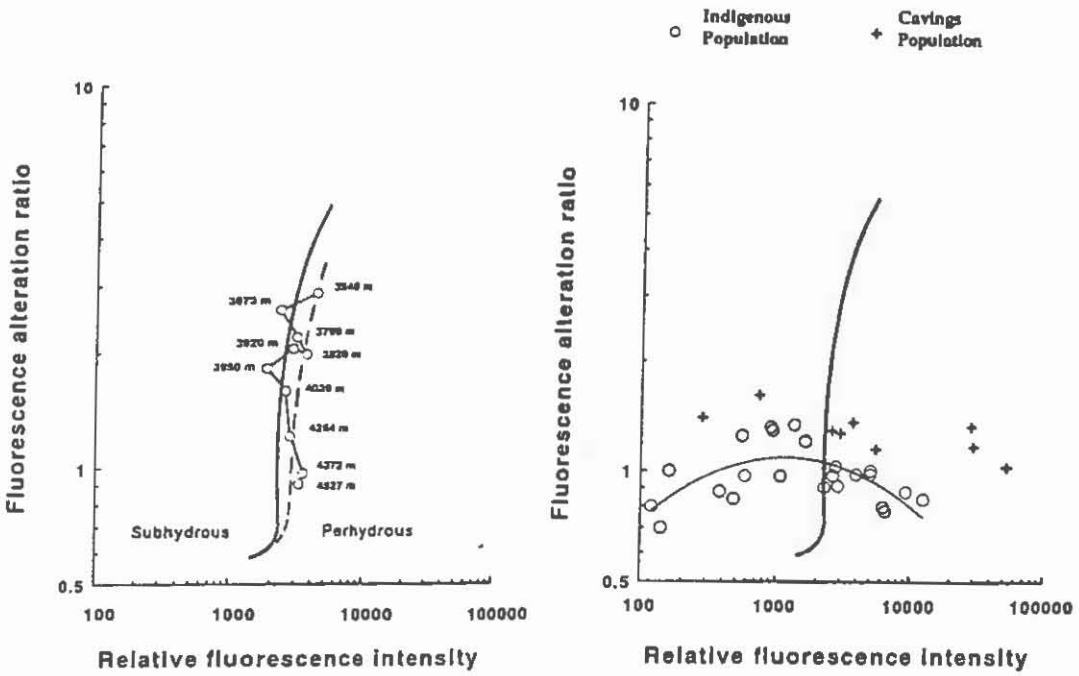

Fig. 4, (Left). Fluorescence alteration diagram showing the variation with depth of average telovitrinite fluorescence alteration data. The displaced curve (broken line) represents a Late Cretaceous "normal" vitrinite line (see text).

Fig. 5, (Right) Enlarged fluorescence alteration diagram for the 4372 m sample, illustrating the use of FAMM analysis in discriminating between indigenous and cavings populations.

Table 1

Depth (m)	Sample Type	Equivalent Reflectance (%)	Mean Average Reflectance ($\bar{R}r\%$)	Petrographic Description
3549.9	SWC	0.56	0.58	Banded coal (telocollinite).
3673.5	SWC	0.58	0.69	Coal partings and DOM in shale ($\bar{R}r\% \sim 0.62\%$), heavily fissured coal fragments (pseudovitrinite?).
3799.0	SWC	0.64	0.68	Inertinite rich banded coal.
3820.3	SWC	0.66	0.70	Banded coal.
3920.0	SWC	0.65	0.80	Two vitrinite populations derived from: (a) banded coal ($\bar{R}r\% \sim 0.71$) and (b) heavily fissured coal fragments ($\bar{R}r\% \sim 0.90$).
3950.0	SWC	0.70	0.84	Coal partings and DOM in shale ($\bar{R}r\% \sim 0.79$), coal fragments.
4039.0	SWC	0.73	0.83	Heavily fissured coal fragments, some banded coal.
4264.0	CTS	0.83	0.87	Coal fragments.
4372.0	CTS	0.90	0.87	Two vitrinite populations derived from: (a) coal partings in shale, DOM in siltstone, coal fragments ($\bar{R}r\% \sim 0.87$) and (b) cavings ($\bar{R}r\% \sim 0.77$).
4527.0	CTS	0.91	0.87	Two vitrinite populations derived from: (a) coal partings in shale, coal fragments ($\bar{R}r\% \sim 0.87$) and (b) cavings ($\bar{R}r\% \sim 0.76$).

Table 1. Measured and equivalent reflectance values and brief petrographic descriptions for the samples studied. SWC side wall core, CTS cuttings

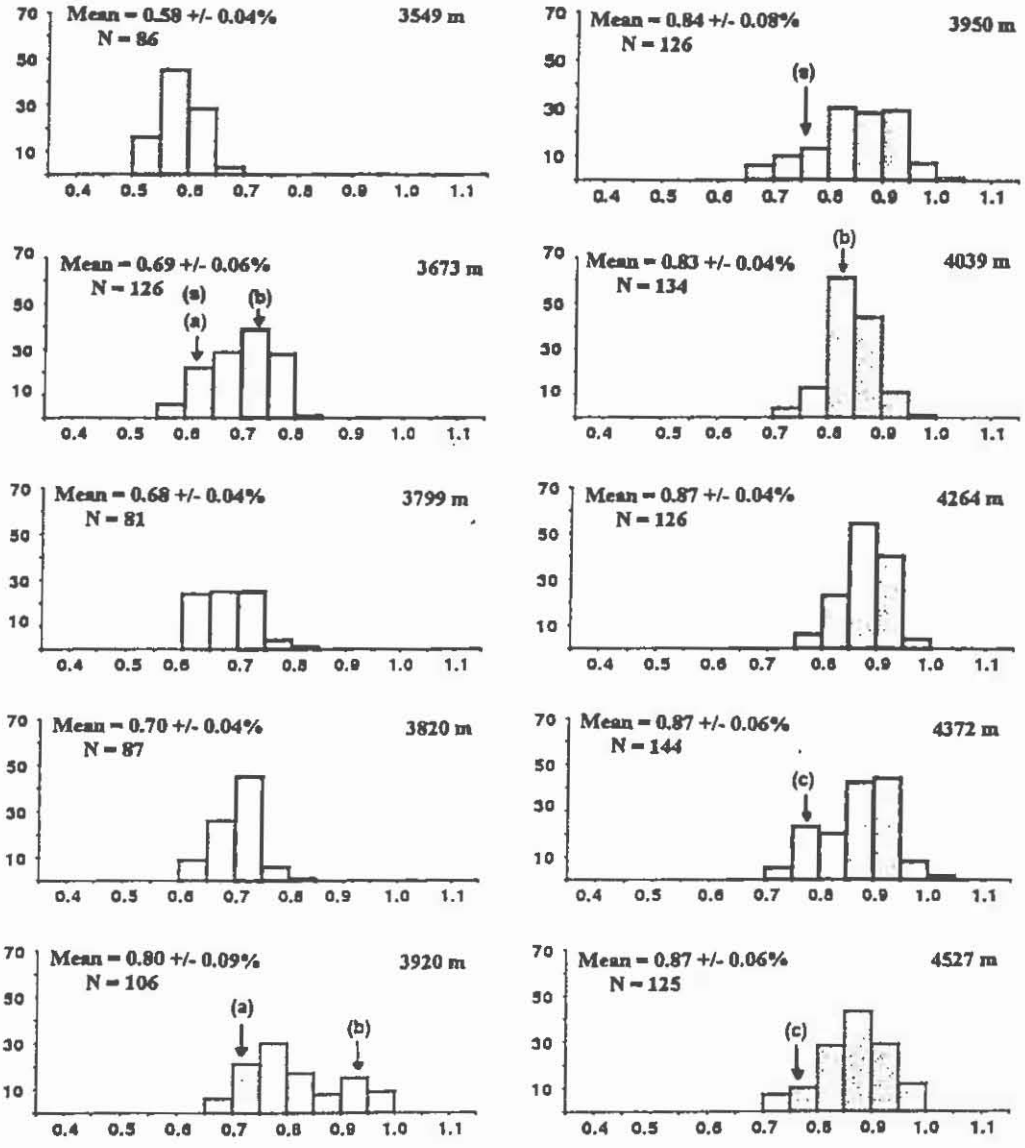

Fig. 6. Reflectance histograms for telovitrinite in the Volador-1 samples. In the diagram, abscissa = random reflectance (Rr%); ordinate = number of observations. The mean reflectance value indicated is based on the total telovitrinite populations in the sample: (a) banded vitrinite, (b) heavily fissured "pseudovitrinite", (c) cavings, (s) shale (see Table 1).

INTEGRATION OF RESULTS

Depth is plotted against vitrinite reflectance for the two sets of maturity data in Fig. 7. Linear regression analysis shows a higher correlation of depth with equivalent vitrinite reflectance ($r^2 = 0.97$) than with directly measured vitrinite reflectance ($r^2 = 0.78$). For the 3673 m and 3950 m samples, the Rr% values are strongly biased towards the higher reflectance "pseudovitrinite" population which is dominant in these samples. Although the "pseudovitrinite" population in the 3920 m

sample is subordinate, the difference between the means of the two vitrinite populations is large so the mean reflectance also shows some bias. Because of the inverse relationship between reflectance and fluorescence intensity of macerals, the high reflectance values of these samples are consistent with their anomalously low fluorescence and subhydrous character.

On the other hand, the higher values of equivalent vitrinite reflectance relative to measured reflectance for the 4372 m and 4527 m samples is consistent with their distinctly perhydrous nature revealed by the fluorescence alteration diagrams. The complete data set suggest that the best interpretation of the data would be obtained if the "normal" vitrinite line for these Late Cretaceous coals was displaced slightly to the right of the Permian line as shown in Fig. 4. This would provide a better explanation of the considerably enhanced reflectance of the 3673 m and 3950 m samples. It is important to note that this slight displacement of position of the "normal" vitrinite line for the Late Cretaceous will not change the values of equivalent vitrinite reflectance compared to those determined from the equivalent Permian line - it merely assists the explanation of measured reflectance anomalies.

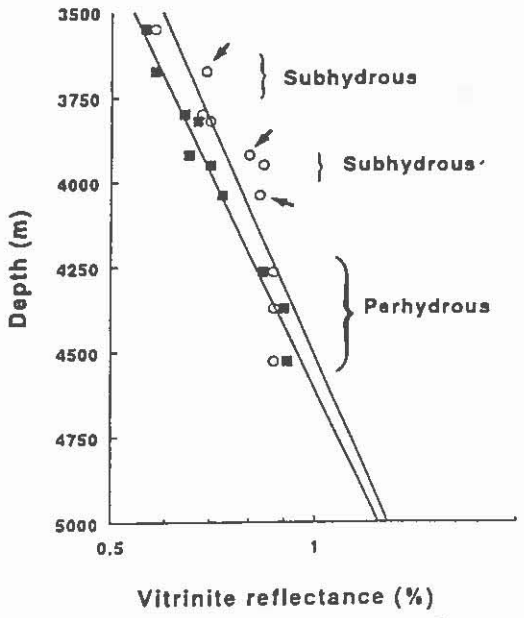

Fig. 7. Plot showing the vitrinite reflectance /depth trends for both measured and equivalent reflectance data. Subhydrous and perhydrous vitrinite data is indicated on the diagram. → Measured results influenced by higher reflecting "pseudovitrinite".

ACKNOWLEDGEMENTS

We would like to thank Bruce Thomas for suggesting the project and supplying samples and background information, Carol Buckingham for her assistance with the generation of the diagrams, Paul Marvig for sample preparation, Michelle Smyth and Neil Sherwood for their comments on the petrography of the samples and Nigel Russell for his earlier (unpublished) reflectance analysis of the Volador-1 samples.

REFERENCES

BROWN, B.R., 1986: Offshore Gippsland Silver Jubilee. IN: Glenie, R.C., (Ed), Second South-eastern Australia Oil Exploration Symposium. PESA Victorian and Tasmanian Branch Symposium, Melbourne, 1985, 29-56.

CLARK A.B.S. and THOMAS, B.M., 1988: The intra-Latrobe play: A case history from the Basker/Manta Block (Vic/P19), Gippsland Basin. APEA J., 28, 100-112.

HEGARTY, K.A., DUDDY, I.R., GREEN, P.F., GLEADOW, A.J.W., FRASER, I. and WEISSEL, J.K., 1986: Regional evaluation of the tectonic and thermal history of the Gippsland Basin. IN: Glenie, R.C., (Ed), Second South-eastern Australia Oil Exploration Symposium. PESA Victorian and Tasmanian Branch Symposium, Melbourne, 1985, 65-74.

STACH, E., MACKOWSKY, M.-TH., TAYLOR, G.H., CHANDRA, D., TEICHMULLER, M. and TEICHMULLER, R., 1975: Stach's Textbook of Coal Petrology second edition, Gebrueder Borntraeger, Berlin, Stuttgart, 535p.

STAINFORTH, J.G., 1984: Gippsland hydrocarbons - A perspective from the basin edge. APEA J., 24, 91-100.

STANDARDS ASSOCIATION OF AUSTRALIA, 1989: Methods for microscopical determination of the reflectance of coal macerals, Australian Standard 2486 - 1989, 4-12.

THOMAS, B.M., 1982: Land plant source rocks for oil and their significance in Australian basins, APEA J., 22, 164-178.

THOMPSON, B.R., 1985: The Gippsland Basin, development and stratigraphy. IN: Glenie, R.C., (Ed), Second South-eastern Australia Oil Exploration Symposium. PESA Victorian and Tasmanian Branch Symposium, Melbourne, 1985, 57-64.

THREFALL,W.F., BROWN, R.B. and GRIFFITH, B.R., 1976: Gippsland Basin, offshore: IN: Leslie, R.B., Evans, H.J. and Knight, C.L., (Eds), Economic Geology of Australia and Papua New Guinea, Monograph Series, 7, Parkville, 1971, 41-67.

TING, F.T.C., 1978: Petrographic techniques in coal analyses. IN: Karr, C.(Ed), Analytical Methods for Coal and Coal Products, Vol 1., Academic Press, New York, 3-26.

WILKINS, R.W.T., WILMSHURST, J.R., RUSSELL, N.J., HLADKY G., ELLACOTT, M.V., and BUCKINGHAM, C.P., 1992a: Fluorescence alteration and the suppression of vitrinite reflectance. Org. Geochem., 18, 629-640.

WILKINS, R.W.T., WILMSHURST, J.R., HLADKY, G., ELLACOTT, M.V. and BUCKINGHAM, C.P., 1992b: The suppression of vitrinite reflectance in some North West Shelf wells: Barrow-1, Jupiter-1 and Flamingo-1. APEA J., 32, 300-311.

THE DETERMINATION OF MARINE INFLUENCES ON THE GRETA & PELTON SEAMS BY THE USE OF SELECTED PALAEO-ENVIRONMENTAL INDICATORS

D.K. STEVENSON
University of Newcastle

INTRODUCTION

The aim of this study was to determine the extent and timing of marine influences on the Greta and Pelton Seams in the Ellalong-Pelton-Quorrobolong area of New South Wales, by the use of selected palaeo-environmental indicators. Within this context, particular emphasis has been placed on the lateral and vertical distribution of sulphur, and telovitrinite fluorescence intensity.

Data were gathered principally from bore core and underground strip samples. The Greta and Pelton Seams were chosen for this study because of their high sulphur contents and close proximity to marine sediments.

The study area, which comprises an area of 80 km^2, is located approximately 50 km by road west of Newcastle, New South Wales (Figure 1). It encompasses the Pelton and Ellalong Collieries, which are the last two coal mining operations within the South Maitland Coalfield that are extracting coal from the Greta Seam.

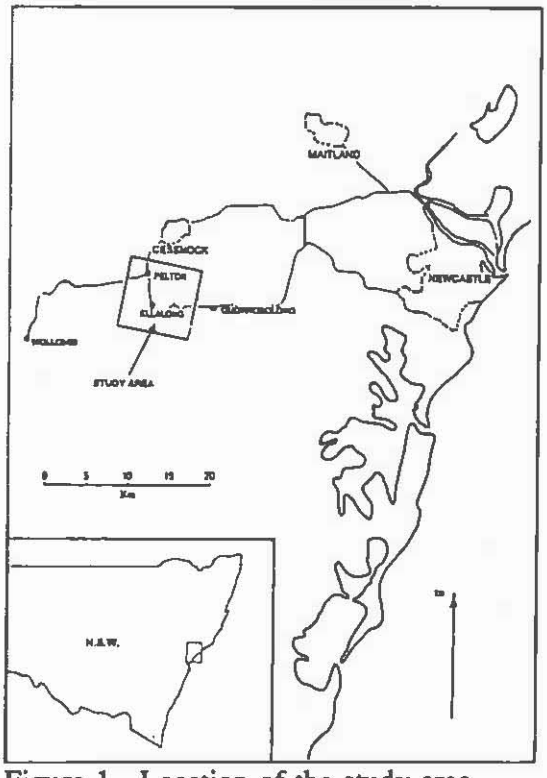

Figure 1. Location of the study area.

PALAEO-ENVIRONMENTAL INDICATORS

Coal will attain certain chemical and petrographic signatures which are dependent on the chemical and biological conditions that were present during peat formation and early diagenesis. When recognition of these signatures is coupled with an analysis of the interseam sediments, an accurate interpretation of the type of peat forming palaeo-environment is possible.

Sulphur

During organic matter decomposition under anaerobic conditions, sulphate species in the surrounding water are reduced to H_2S by bacteria. The H_2S can then form compounds with the abundant organic material, or it can react with Fe^{2+} to form iron sulphides. Initially unstable monosulphides form; however, in the presence of adequate concentrations of sulphur they are transformed into pyrite during early diagenesis (Berner *et al.* 1979). The pyrite typically occurs as

framboidal masses of minute octahedral crystals (Cohen *et al.* 1984). The sulphate-reducing bacteria can only survive and reproduce if the pH and Eh are within a certain range. The amount of sulphur produced is therefore dependent on the pH, Eh, and sulphate concentration, and in the case of pyrite, the amount of Fe^{2+} present during deposition and later during early diagenesis.

In marine environments the pH is generally between about 6 and 8, the Eh is sufficiently low in all but the top few decimetres, sulphate is in abundance, and there are usually sufficient quantities of Fe^{2+} present. This leads to vigorous bacterial action and the subsequent formation of high levels of sulphur.

In fresh-water peat, the pH, Eh, and sulphate content tend to remain low and relatively constant. This reduces bacterial action to a very low level and therefore retards sulphur production. The sulphur concentration in fresh-water peats is thus primarily dependent on the sulphur originally fixed in the plant material. The result is a relatively uniform sulphur content at all levels in the peat.

Peat formed in brackish environments shows the greatest variation in form and distribution of sulphur. Conditions may vary from fresh-water during high rainfall and flooding, to marine during droughts or severe storms that inundate the peat-land with sea-water. An increased marine influence will cause a slight raising of the pH and increased sulphate availability, that may result in increased sulphur formation.

The origin of sulphur in coal can be obscured by post-depositional enrichment of sulphur. Fresh-water peat that is influenced by post-depositional marine conditions may be indistinguishable from saline peats. The influence can be in the form of a gradual change to saline conditions, temporary inundation of the peat-lands by sea-water during storms, or the sudden and total termination of peat-forming conditions by drowning the peat in sea-water in the course of a marine transgression. In each example, elevations in pH and increased levels of sulphate will result in an enrichment in sulphur. Pyrite can also precipitate along cleat planes and in void spaces during coalification, but it is commonly recognised as epigenetic in form.

Vitrinite Fluorescence

When organic compounds are subjected to high levels of short wave radiation, electrons in the atoms can be promoted from their ground state to higher energy levels. The resultant excited energy state is unstable, so the electron drops back to its more stable ground state, and in doing so releases a quantum of energy in the form of a photon of longer wavelength than the excitation energy. As the energy released is quantised, only photons within a certain frequency spectrum will be emitted. This frequency spectrum, which is characteristic of the emitting molecule or atom, extends into the visible light spectrum, with the result that the organic compound exhibits fluorescence (Robert 1981). The part of a molecule which contains easily excitable electrons is called a fluorophore by Lin and Davis (1988), or a chromophore by Bertrand *et al.* (1986), and with increased concentration of these species fluorescence intensity increases. Liptinite, vitrinite, and inertinite, in that order, contain decreasing numbers of fluorophores, and consequently show decreasing levels of fluorescence intensity.

In vitrinite macerals, the fluorophore content, and therefore the intensity of fluorescence, is related to the original plant matter and how it is modified during biochemical and physicochemical coalification. The plant constituents, including lipids, cellulose, and lignin, depolymerise during the biochemical stage. The nuclei produced then recombine to form organic geopolymers during the physicochemical stage, which results in the formation of a condensed aromatic network and an aliphatic-rich mobile phase (Diessel in press). The aliphatic-rich phase contains a higher concentration of fluorophores, and therefore, vitrinite macerals with higher aliphatic to aromatic ratios display higher fluorescence intensities (Bertrand *et al.* 1986).

During humification and peatification vitrinite precursors can be enriched in aliphatic compounds by the addition of bacteria-derived lipids and liptinite decomposition products.

Increasing pH promotes bacterial activity and liptinite decomposition, and results in an increase in vitrinite fluorescence intensity. It is for this reason that vitrinite fluorescence intensity can be used as an indication of the degree of marine influence that the peat swamp was subjected to during peat deposition and early diagenesis.

In this study measurements were carried out by a Carl Zeiss Universal Microscope using a wide spectrum incident blue light and measuring the fluorescence intensity at 650 nm.

RESULTS FROM THE GRETA SEAM

Sulphur

Total, pyritic, and organic sulphur have been arbitrarily grouped into low, medium, and high values (Table 1). This terminology is used irrespective of whether it relates to the full-seam or to individual plies.

Table 1. Sulphur terminology used in this study

	TOTAL SULPHUR %	PYRITIC SULPHUR %	ORGANIC SULPHUR %
LOW	< 1.25	≤ 0.1	< 0.9
MEDIUM	1.25 - 2.0	0.1 - 1.0	0.9 - 1.0
HIGH	> 2.0	> 1.0	> 1.0

Figure 2. (full seam) indicates two extensive high-sulphur areas which both trend in an approximately northwest-southeast direction. They are separated by a low-sulphur region that trends southward from the northwest corner of the study area towards Ellalong Colliery. Other low-sulphur areas occur on the northern and southeastern boundaries of the study area. The remainder of the study area comprises medium-sulphur coals and isolated regions of both high- and low-sulphur coals. In all areas sulphur values change rapidly over a small distance along an approximately southwest to northeast traverse.

The concentration range of the pyritic and organic sulphur forms in the low-, medium-, and high-sulphur areas, indicates that the entire region has been subjected to varying degrees of marine influence. Even samples containing low sulphur contents have values that are much higher than would be expected from coals that are derived from fresh-water peat-forming environments. The main contributing factor in elevated sulphur concentrations is pyrite, which on average shows a six-fold increase in content between low- and high-sulphur areas. It should also be noted that microscopy carried out on raw coal samples has shown that almost all of the pyrite is framboidal and therefore syngenetic.

The low-, medium-, and high-sulphur areas can be distinguished from one another by vertical trends in total, pyritic, and organic sulphur. The difference between examples of low- and high-sulphur samples (Figure 3) is very distinctive; however, there is no abrupt change between low- and medium-, and medium- and high-sulphur samples.

Although most samples do show differing patterns of sulphur distribution, a number of general observations do apply:

All samples

1. There is no relationship between sulphur levels in the clay bands and their adjoining coal plies.
2. Some plies have sulphur concentrations that are low enough to have been formed in

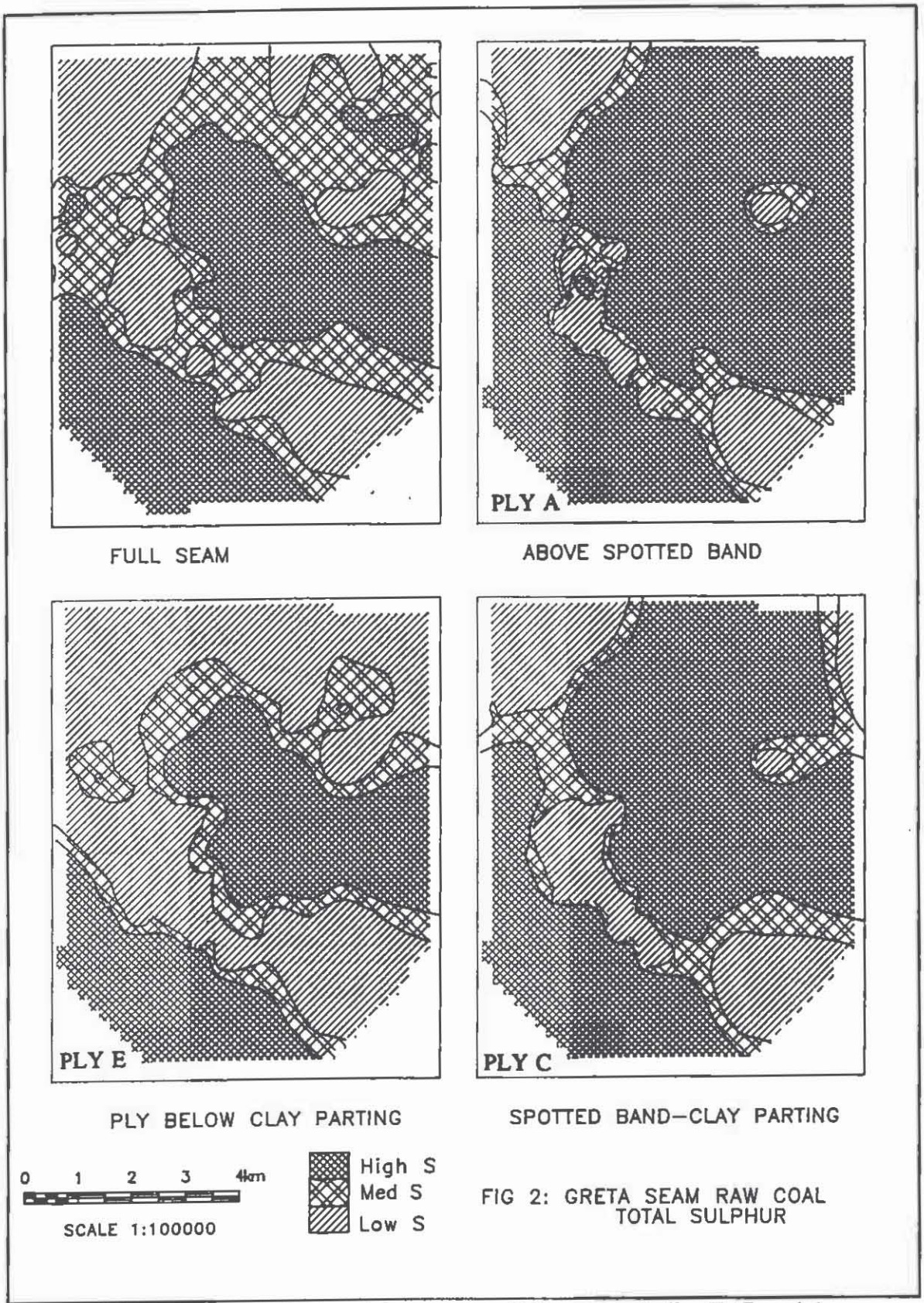

Figure 2. The lateral variation in sulphur content: Full seam and plies E, C, and A.

water with very low salinity levels.

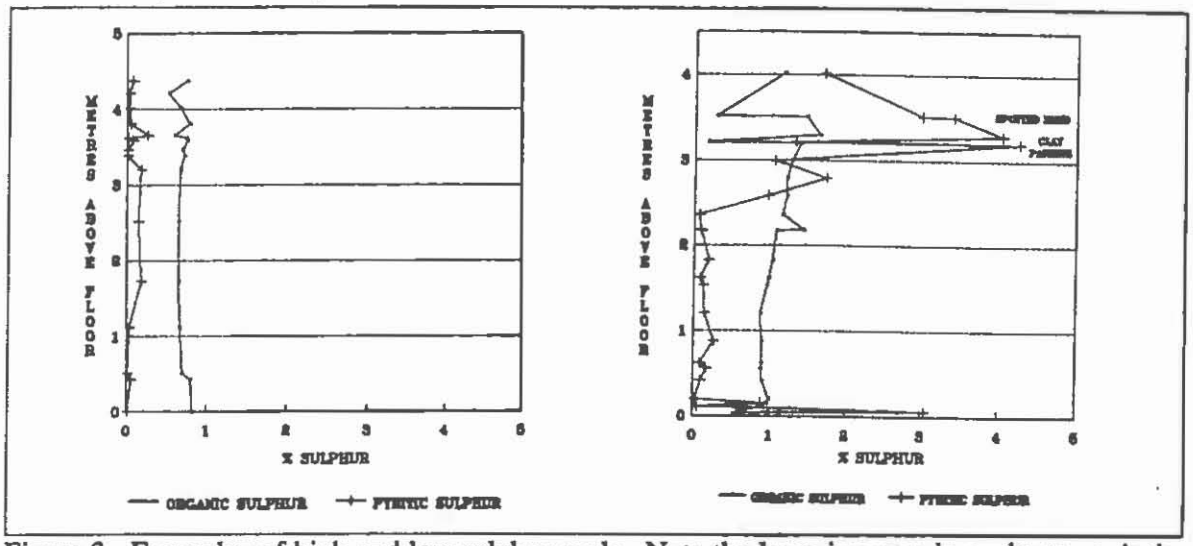

Figure 3. Examples of high and low sulphur coals. Note the large increase in pyrite towards the top of the seam.

Low-sulphur coal

1. Pyrite content is low to medium, with occasional increases in concentration in the top and bottom plies.
2. Organic sulphur content is mostly low, and almost always increases in concentration in the top and bottom plies.
3. The average total sulphur content is generally highest below the Clay Parting.

Medium-sulphur coal

1. Pyrite content is generally low to medium with high pyrite contents often occurring at the base and middle of the seam. All samples show increasing pyrite levels in the top plies.
2. Organic sulphur content is mostly low, with the occasional medium concentration at mid-seam and upper parts of the seam. Organic sulphur generally increases in concentration in both the top and bottom plies.

High-sulphur coal

1. High concentrations of pyrite commonly occur in the lower and mid levels of the seam, and always occur in the upper-most plies.
2. Organic sulphur content is mostly low to medium, with high concentrations usually occurring in the upper-most plies.
3. A permanent high sulphur content, caused mainly by high pyrite levels, is attained below the Clay Parting in all samples.

It can be seen that the primary control on total sulphur content is the presence of isolated high pyrite content plies, or the level within the seam at which the coal begins to be permanently affected by high pyrite concentrations.

The pyrite content can be increased by either an increasing marine influence that is contemporaneous with peat formation, or by marine water diffusing down into the peat after peat deposition. In the study area the Greta Seam attains a thickness of up to 8.0 m, and as a compaction ratio of approximately 8:1 occurs between peat and coal, the depth to which elevated pyrite

concentrations occurred was as much as 64 m. The downward diffusion of marine water can explain the "brassy tops", but it does not explain the occurrence of isolated high pyrite plies surrounded by in some cases several metres of low-sulphur coal. Therefore, it is unlikely that the increased sulphur levels are solely related to the diffusion of marine water down into the peat after deposition. The presence of medium to high concentrations of pyrite throughout and below the Greta Seam indicates that the peat was influenced by marine conditions right from the start, with high pyrite levels in the top plies showing that in the later stages of peat formation this marine influence increased.

The increasing marine influence hypothesis is also indicated by the lateral variation in total sulphur content between Plies E, C, and A (Figure 2). In the upward succession from Ply E to Ply A, the area affected by high sulphur levels increases, but in all plies the highest levels are still found in a northwest-southeasterly trending zone, and in the southwest corner of the study area. This is the pattern of sulphur distribution that would be expected if marine water entered the peat swamp from the south and east, and due to increasing water levels spread out laterally over time.

The variation in lateral sulphur distribution between Plies E, C, and A, as well as the presence of isolated high-pyrite plies in the lower parts of medium- and high-sulphur area samples indicate that these areas were always influenced by marine conditions to a greater extent than low-sulphur areas. The peat-swamp was generally mildly brackish, with regions that were to become medium- and high-sulphur areas affected by occurrences such as king tides or storms that increased salinity levels. During the subsequent marine transgression increasing water levels caused the lateral spreading of marine conditions.

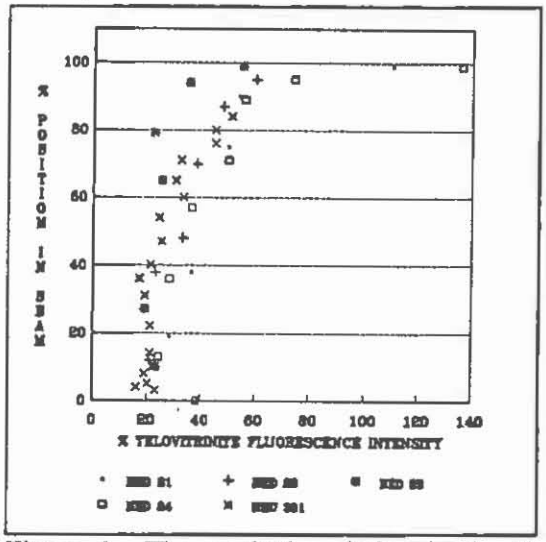

Figure 4. The vertical variation in the % telovitrinite fluorescence intensity within the Greta Seam.

Telovitrinite Fluorescence

The results for telovitrinite fluorescence intensity are presented in Figure 4. In all samples the general trend is for an increase in intensity from around 20 % just above the base of the seam to between 55 and 136 % at the top of the seam. Samples NED 23, 24, and NEU 381 show an increase in the intensity at the bottom of the seam.

The almost continuous increase in fluorescence intensity from just above the seam floor to the top of the seam, indicates a rising pH throughout the life of the peat swamp. The extremely high fluorescence intensities at the top of the seam indicate that the pH probably attained a level close to neutrality towards the end of peat-forming conditions. The most likely means of producing a steadily increasing pH over time, followed by a rapid increase in pH towards the close of peat-forming conditions, is by an increasing marine influence. The increase in the fluorescence intensity at the base of the seam can be the result of increased pH due to the presence of inorganic sediments, or that the peat swamp was subjected to an initially high marine influence at the commencement of peat formation.

RESULTS FROM THE PELTON SEAM

Sulphur

The vertical variation in total, organic, and pyritic sulphur is shown in Figure 5. The pyrite is primarily in the framboidal form and is usually associated with telovitrinite. The framboids also tend to be regularly spaced.

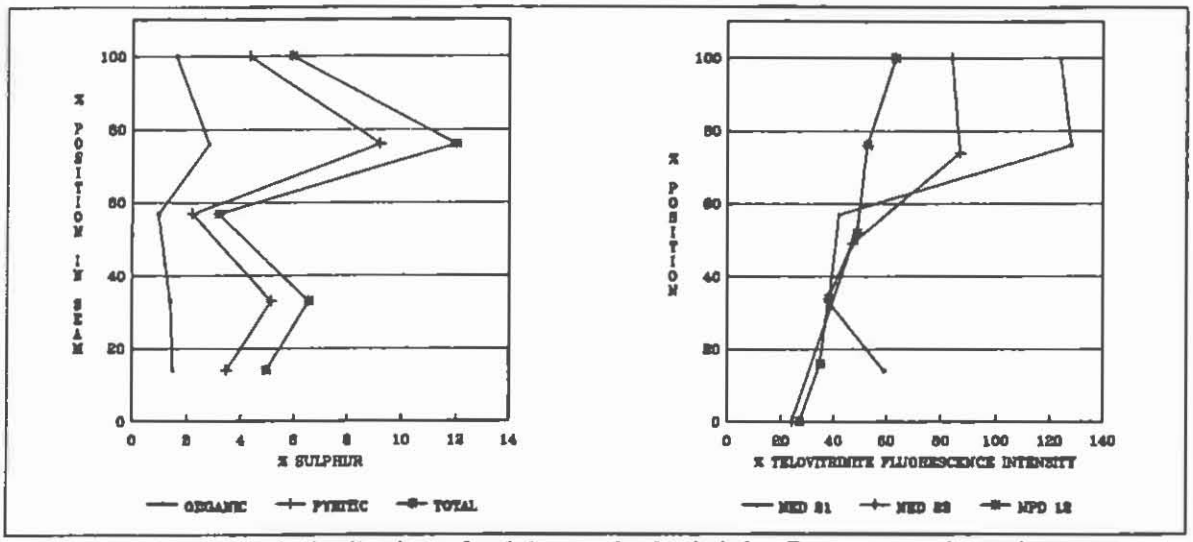

Figure 5. The vertical distribution of sulphur and telovitrinite fluorescence intensity.

The range of organic and pyritic sulphur contents of 0.96 to 2.8 % and 2.21 to 9.2 % respectively indicate a strong marine influence. The framboidal form of the pyrite and its regular spacing, indicates that pyrite formation was syngenetic and associated with bacteria that primarily resided in the cell lumens of the telovitrinite precursors.

The small seam thickness of only 420 mm in NED 21, means that the peat was between about 3 to 4 m thick at this location. This compares in size to many of the peats that are currently being studied. This as well as the presence of fossils immediately above the Pelton Seam in NED 21 indicate that the diffusion of marine water into the peat swamp would have occurred. This of course does not imply that the swamp was not under an increasing marine influence during peat formation.

Telovitrinite Fluorescence

Results for NED 21, NED 23, and NPD 12 show an increase in telovitrinite fluorescence intensity towards the top of the seam (Figure 5). Several coal lenses situated up to 3 m below the Pelton Seam have fluorescence intensities up to 26 %.

This clearly indicates an increase in bacterial activity due to an increase in pH. Single samples from NED 22 and NED 24 also have a high fluorescence intensity indicating increased bacterial activity. An increasing marine influence contemporaneous with peat accumulation is the most likely cause of increased bacterial activity, but because of the thickness of the peat swamp (only 3 to 4 m), inundation of a fresh-water swamp with marine water cannot be discounted. The decrease in fluorescence intensity in NED 21 Plies 2 and 3 may be related to a lack of readings. Both plies have a low telovitrinite content, that is characterised by their small size and clay filled cell lumens.

CONCLUSIONS

The above discussion indicates that the Greta peat swamp was under a marine influence from the very start of peat formation and that this influence increased over time. The almost simultaneous increase in sulphur content and telovitrinite fluorescence intensity (Figure 7) indicates that the pH of the peat swamp increased, and that this increase in pH was accompanied by an increase in sulphate at the same time. The lateral sulphur distribution between Plies A, C, and E indicates that marine conditions spread out over the peat swamp and progressively affected a larger area.

The vertical variation in fluorescence and sulphur distribution below and within the Pelton Seam indicates an increasing pH gradient. This evidence, as well as the close proximity of the Branxton Formation, indicates that marine influences were present before, during, and after deposition of the Pelton peat swamp. The general trend, however, is for an increasing marine influence from below the Pelton Seam. The presence of marine fossils immediately overlying the Pelton Seam in some locations may indicate that peat formation was terminated by marine water inundating the peat swamp.

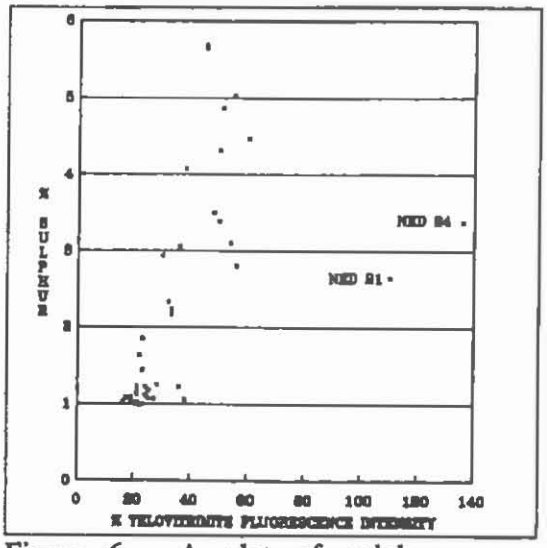

Figure 6. A plot of sulphur versus fluorescence within the Greta Seam.

One theory that has been put forward in the past, states that marine water migrated down from the Branxton Formation during diagenesis. If this was the case the sulphur content and telovitrinite fluorescence intensity at most levels within the Pelton Seam would be higher than in the Greta Seam. This is clearly not the case. Sulphur and fluorescence levels in the upper-most plies of the Greta Seam are usually higher than in the lower-most plies of the Pelton Seam. This indicates that the upper parts of the Greta swamp were subjected to higher pH and sulphate levels than in the lower parts of the Pelton Seam.

The Greta and Pelton Seams were subjected to a permanent and increasing marine influence during their formation. Coal property characteristics were attained contemporaneously with peat formation, although the Pelton Seam would almost certainly have been subjected to the downward diffusion of sulphate into the peat after peat-forming conditions ceased.

ACKNOWLEDGMENTS

The Author wishes to thank the management and staff of the Newcastle Wallsend Coal Company, in particular Mr. Russell Rigby, for their help in carrying out this study.

BIBLIOGRAPHY

BERNER R.A., BALDWIN T. & HOLDREN J.R. 1979. Authigenic iron sulfides as paleosalinity indicators. Journal of Sedimentary Petrology 49, 1345-1350.

BERTRAND P., PITTION J-L. & BERNAUD C. 1986. Fluorescence of sedimentary organic matter in relation to its chemical composition. Organic Geochemistry 10, 641-647.

COHEN A.D., SPACKMAN W. & DOLSEN P. 1984. Occurrence and distribution of sulphur in peat forming environments of southern Florida. International Journal of Coal Geology 4, 73-96.

DIESSEL C.F.K. In press. Coal-bearing depositional systems.

LIN R. & DAVIS A. 1988. A fluorogeochemical model for coal macerals. Organic Geochemistry 12, 363-374.

ROBERT P. 1981. Classification of organic matter by means of fluorescence; application to hydrocarbon source rocks. International Journal of Coal Geology 1, 101-137.

THE USE OF DISPERSED ORGANIC MATTER IN THE INVESTIGATION OF HYDROTHERMAL FLUIDS WITHIN THE COPELAND GOLDFIELDS

J.G. GIBSON
University of Newcastle

ABSTRACT

Reflectance of dispersed organic matter (DOM) in the Upper Devonian rocks of the Bowman Beds at Copeland has been used in an attempt to determine if the thermal yield from mineralising hydrothermal fluids reached sufficient intensity to cause a hydrothermal overprint of the burial metamorphism registered within the area. It was found that within the kilometric and metric scale there is an overprint consistent with the hypothesis.

INTRODUCTION

The Copeland Gold District is a small slate-belt type goldfield that lies 10km west of Gloucester and 125km north of Newcastle, producing 163kg alluvial and 1,954kg primary gold between the years of 1876 and 1956. The Copeland gold deposits are contained within the Bowman Beds of the Tamworth Group, within the Tamworth Belt the southern extremity of the New England Fold Belt. (Grids applied to maps are the Australian Map Grid (U.T.M.) Grid zones 56J and 56H. Bearing are corrected to Grid North.)

METHOD

DOM particles frequent the finer grained rocks within the area, particularly those which have been deposited in quiet and anaerobic conditions. The DOM particles consist primarily of botanical debris, although occasionally particles of zoological nature are recorded. This botanical debris is primarily of terrestrial origin, therefore containing the same macerals and undergoing coalification in a similar manner to coal.

Samples from 39 stations were selected from an area covering 12 km^2 of this part of the Barrington Gold Field (Figure 1) in a semi-systematic manner, as systematic collecting of specimens on a regular grid pattern was impractical due to the difficult terrane and lack of suitable outcrop.

As weathering is one of the conditions that can affect DOM particles, causing a drop in reflectivity, samples were deemed weathered and generally rejected, if all or most of the diagenetic pyrite had been altered to limonite ± secondary hematite. Some weathered samples were included when, on close examination, particles showed no signs of deterioration and had an appropriately narrow standard deviation of readings.

JOHN GIBSON

Organic Petrology

The most commonly used petrological parameter for the measure of coalification, is the percentage of light reflected from a polished surface of the maceral under investigation, the maceral generally being vitrinite and viewed in an oil medium. The percentage of light reflected from vitrinite increases with coalification, and this property has been used to determine coal rank (Stach *et al*, 1975).

The study of DOM particles as a palaeo-thermometer or metamorphic indicator, has been extended to oil investigations and used in regional geological studies, e.g. Héroux *et al.* (1979), investigations of metamorphic terrains, e.g. Diessel & Offler (1975) and Âkai (1983, 1991) who correlated illite crystallinity, chlorite crystallinity, diagenetic clay minerals, vitrinite reflectance, conodont colour alteration index, metabasite mineral facies and temperature to the diagenetic zone, anchizone, and epizone. Vitrinite reflectance has been calibrated as a geothermometer by Barker & Pawlewicz (1986) and refined by Barker & Goldstein (1990), resulting in the equation:

$$T_{peak} = \text{lm}\ (R_{mvo} + 1.26 :- 0.00811 \qquad (1)$$

Random reflectance of vitrinite has been used exclusively in determinations for this study.

Most vitrinite particles encountered are under 0.02mm in diameter, therefore according to Australian standard As 2856-1986 they are detrovitrinite or more specifically, the maceral vitrodetrinite. In general they are recognised by their irregular outline, structureless internal nature and present the narrowest spread of reflectance readings.

Inertinite which is the most prevalent maceral present in the area consists mainly of inertodetrinite and micrinite, both consisting of fragmented cell walls. The differentiation between the two macerals is one of size, inertodetrinite ranging from 0.03 to 0.002mm and micrinite being under 0.002mm in size.

Sclerotinite which consists of fungal remains is so rarely encountered that it is of no statistical significance, even in the unlikely occurrence of being misread and included as vitrinite.

A minium of 40 measurements per sample were made using a Photomicroscope III largely in accordance with Australian Standard AS 2486 - 1989.

RESULTS

Regional Scale Survey

The DOM particles encountered are basically of terrestrial origin, being dominated by maceral groups vitrinite and inertinite, and minor amounts of liptinite. Some kerogen type I is present in the form of marine algae, but the high rank obtained makes positive identification difficult.

COPELAND GOLDFIELD

The reflectance of DOM particles has the advantages of being more ubiquitous than metamorphic minerals in metamorphic zones, and once registering maximum metamorphic conditions, are unaffected by most retrograde metamorphic reactions. A regional study of reflectance was made and Equation 1 was used to convert these readings to temperature, and an isogeothermal was drawn map drawn (Figure 2). Using these isotherms, the metamorphic classifications of Arkai (1991) can be applied i.e., diagenesis being completed at 250°C, the anchizone spans the temperature range of 250 to 350°C, with the epizone extending beyond 350°C.

Within the Copeland Gold District (Gibson & Seccombe 1993), diagenetic to lower epizonal metamorphism is evident, in the form of burial metamorphism. The concept of burial metamorphism is further reinforced when the southern plunge of 16° of the major F_1 fold axis is considered (Figure 1). This plunging component should expose successively older facies in a northerly direction. The isotherms do have a north/south elongated aspect similar to the general geology.

Lowest epizone grade rocks occur in three places accompanied by the close proximity of gold mines (Figure 2). The first two areas of epizonal rocks occurring adjacent to the crest of the major F_1 fold axis, while a third occurs within a zone of shearing adjacent to the Boonara Fault, a splay of the Manning Fault System. A simplistic explanation of the first two zones is the unroofing of the rocks along the crestal zone of the southern plunging anticline, but this explanation does not explain the high temperature node adjacent to the Boonara Fault.

Local Scale Survey

A survey was undertaken over an area of 3x4 km to ascertain if DOM particles register geothermal fluctuations on a local scale (Figure 4). The area chosen is that part of the Barrington Goldfield which had been the major producer of lode gold (Figure 1), with the survey being conducted along the beds of three major drainage systems within the area, Copeland Creek, Duffer's Creek and Craddock's Creek. Stations were more closely spaced than was possible on a regional scale, with fresh rock available, (containing diagenetic pyrite), and DOM particles are plentiful.

The reflectance readings from this survey were not converted to temperature because of the high reflectivity of DOM particles within the area, 4.15% (331°C) to 5.16% (358°C). The reflectance values of vitrinite increase exponentially to rises in temperature, and therefore in these high reflectance areas more precision is gained contouring by isoreflectance lines.

When viewed in detail, the picture changes from a simple burial metamorphic model, with the appearance of an area of low reflectance sandwiched between two areas of high reflectance. These areas of high reflectance equate to the areas of higher palaeo-"terrestrial heat flow" of Sharma (1986), and are generally auriferous within the area studied. The low reflectance belt, which strikes roughly 103° cuts across the F_1 fold axis at an angle of approximately 60° suggesting that peak metamorphic temperatures were reached in these areas after folding. Graphs were drawn (Figure 4) to test the concept that

these high temperatures arise from burial metamorphism. The first graph plotted the percentage of reflectance from vitrinite against the elevation of the sample site relative to a datum consisting of a 250m thick vulcanoclastic unit (Figure 3-A). If peak metamorphic temperatures were attained within the area before folding, then there should be a correlation between depth and reflectance relative to the datum. The graph shows Pearson's product-moment co-efficient of linear correlation (r) of 0.07, indicating no correlation between depth and reflectance and therefore temperature by inference.

The second diagram illustrated in Figure 3-B percentage of reflectance from vitrinite is plotted against the hight above sea level. This was compiled to test the assumption that peak metamorphic temperatures were the product of burial metamorphism but attained after folding and hence should show a correlation relative to the present vertical profile. Once again $r = 0.10$ indicating no correlation. These results suggest that the burial metamorphic temperatures within the area have been overprinted.

A third graph was compiled (Figure 3-C), that plotted the percentage of reflectance against the horizontal distance measured normal to a base-line A - B (Figure 3) drawn through the centre of the area of low reflectance. This would test the hypothesis that heat flowed laterally from the areas of increased vitrinite reflectivity into the areas of low reflectance. In this case there was a statistically significant correlation of $r = 0.81$, with $r^2 = 0.66$ indicating that 66% of the total variance is accounted for by the reflectance versus horizontal distance. A Student's t-test of r, indicated that r is statistically highly significant, relating to a horizontal geothermal heat flow of 27°C per 1000m.

Considering that these data have been gathered from a wide horizontal plane, not a vertical profile, the following conclusions can be drawn:

1) The areas of higher reflectivity have received a higher heat flow, than those areas surrounding them.
2) A lateral dissipation of this excess thermal flux has occurred probably by conduction.
3) The thermal flux occurred after the maximum burial metamorphic temperatures were attained, overprinting the latter.

To ascertain the heat flow normal to vein systems, two sets of samples were collected in sandstone from the active Bromley Mine at a distance of up to 1 metre away from the vein. The graph of the percentage of vitrinite reflectance versus distance from the vein is shown in Figure 3-D, indicating a statistically significant drop in reflectance from 5.5% to 5.2%, which is directly related to the heat flow away from the vein at a rate of 8°C per metre. The metric gradient is two orders of magnitude greater than the kilometric gradient (27°C per 1000m) indicating an expediential fall in temperature in a direction normal to the vein.

CONCLUSIONS

Burial metamorphism has been overprinted within the area of investigation by a later thermal event which is evidenced by two areas of elevated vitrinite reflectance

between an area of low reflectance. The excess heat from the areas of high heat flow appears to have permeated into the area of low temperature, probably by conduction. A decline in temperature normal to the mineralized veins is inferred from a fall in vitrinite reflectance which is two orders of magnitude above that of the general rate of horizontal vitrinite reflectance decline, and it is suggested that hot fluids flowing through these fractures has caused a hydrothermal overprint in the Copeland area.

REFERENCES

ARKAI P., 1983. Very low- and low-grade Alpine regional metamorphism of the Palaeozoic and Mesozoic formations of the Bükkium, NE-Hungary. *Atica Geologica Hungarica*, **Vol. 26**, pp 83-101.

ARKAI P., 1991. Chlorite crystallinity: an empirical approach and correlation with illite crystallinity, coal rank, and mineral facies as exemplified by Palaeozoic and Mesozoic rocks of northeast Hungary. *Journal of Metamorphic Geology*, **Vol, 9**, pp 723-734.

BARKER C.E. & M.J. PAWLEWICZ M.J., 1986. The correlation of vitrinite reflectance with maximum temperature in humic organic matter. In (Ed. G.Buntebarth and L. Stegena) Lectures in the Earth Sciences **Vol. 5**, Paleogeothermics, Springer-Verlag, Berlin, pp 79-93.

BARKER C.E. & GOLDSTEIN R.H., 1990. Fluid-inclusion technique for determining maximum temperature in calcite and its comparison to the vitrinite reflectance geothermometer. *Geology*, **Vol 18**, pp 1003-1006.

DIESSEL C.F.K. & OFFLER R., 1975. Change in physical properties of coalified and graphitised phytoclasts with grade of metamorphism. *Neues Jahrbuch Für Mineralogie und Monatshefte* **H 1**, pp 11-26.

GIBSON J.H., & SECCOMBE P.K., 1993. A geological synthesis of the Copeland gold district, southern New England Fold Belt. In (ed. P.Flood and J. Aitchison) New England Orogen, eastern Australia, University of New England, Armidale N.S.W. Australia. pp 467-478.

HÉROUX Y., CHAGNON A., & BERTRAND R., 1979. Compilation and correlation of major thermal maturation indicators. American Association of Petroleum Geologists Bulletin, **Vol. 63**, pp 2128-2144.

STACH E., MACKOWSKY M.T., TEICHMULLER M. & R., TAYLOR G.H., & CHANDRA D., 1975. Stach's Textbook of Coal Petrology. Borntraeger, Berlin.

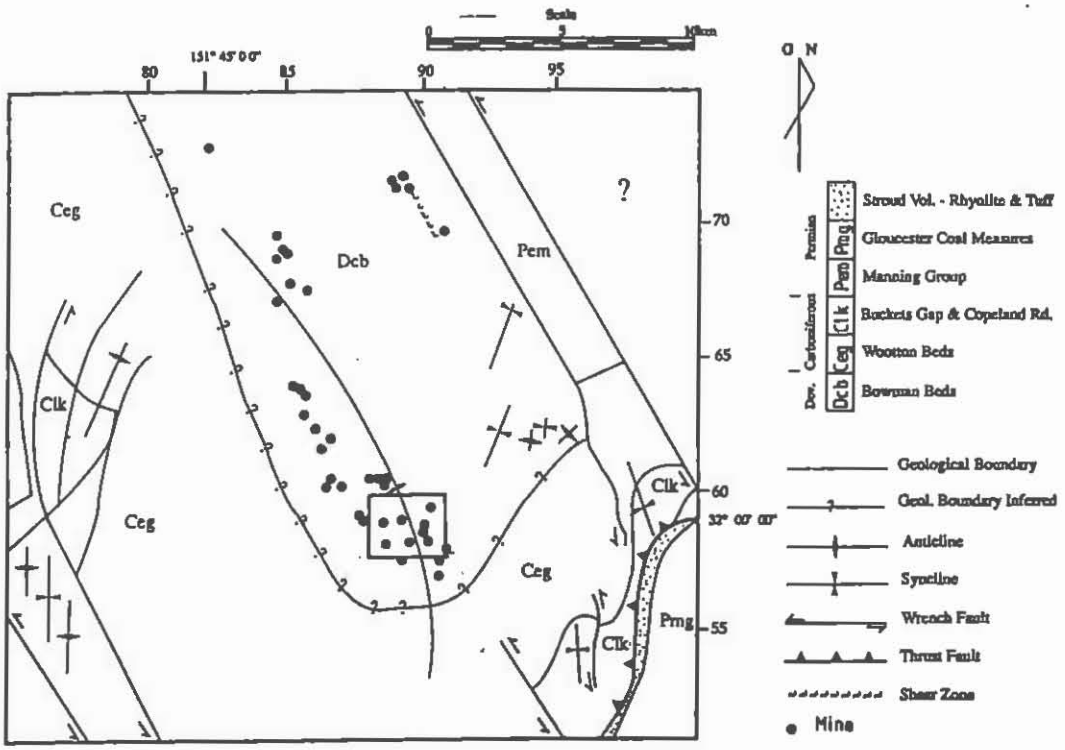

Figure 1 Geological map of part of the Barrington Goldfield, the Copeland area (marked rectangle) was the most productive area, and area under investigation.

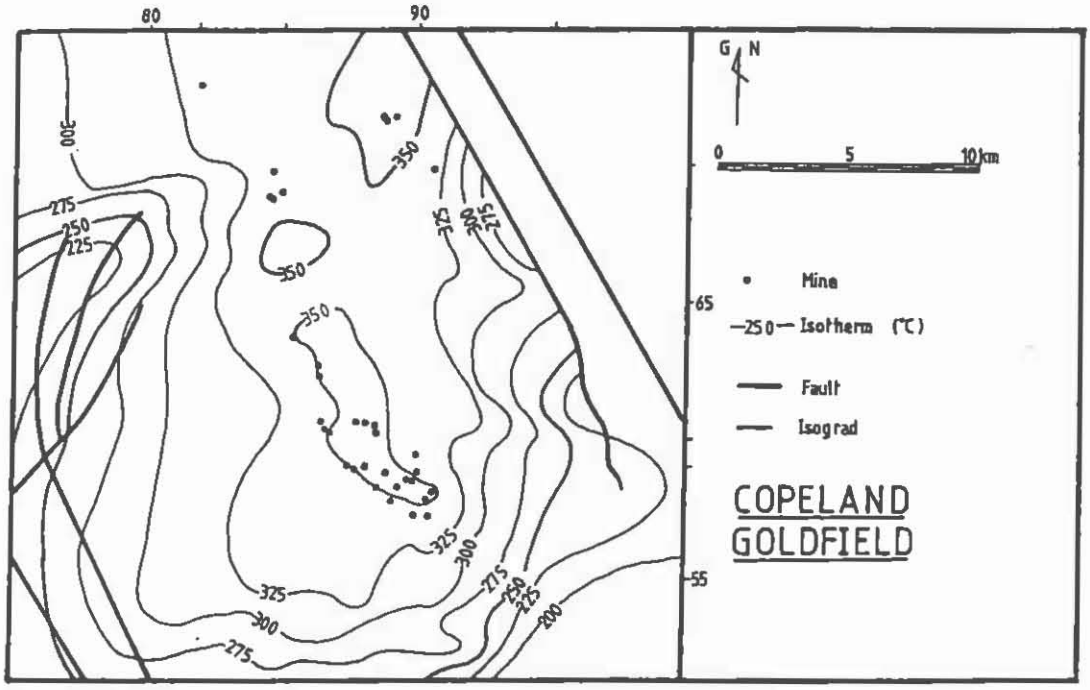

Figure 2 Isothermal map of part of the Barrington Goldfield, the area covered in Figure 1.

COPELAND GOLDFIELD

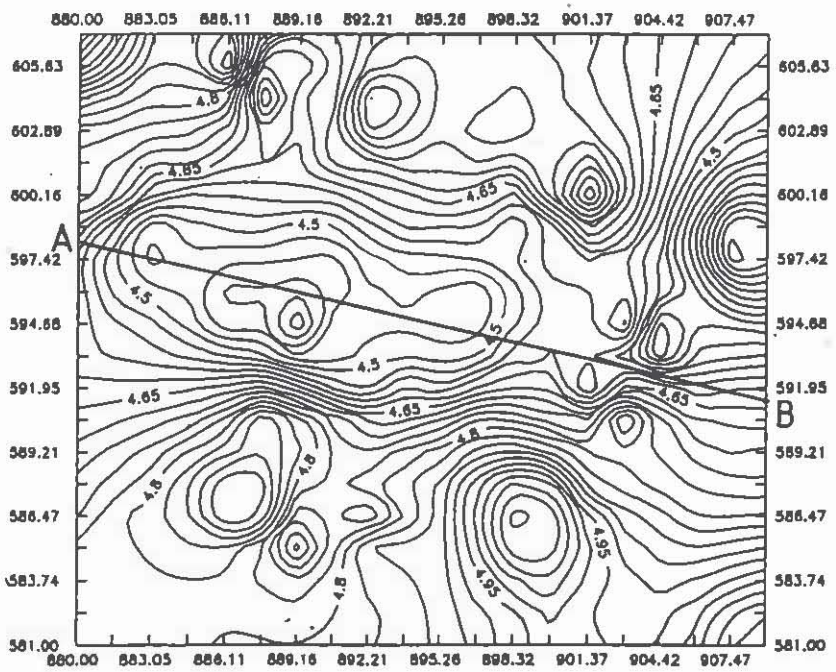

Figure 3 Isoreflectance map of the Copeland area (rectangle in Figure 1). The line A B, marking the centre of the palaeo-thermal low.

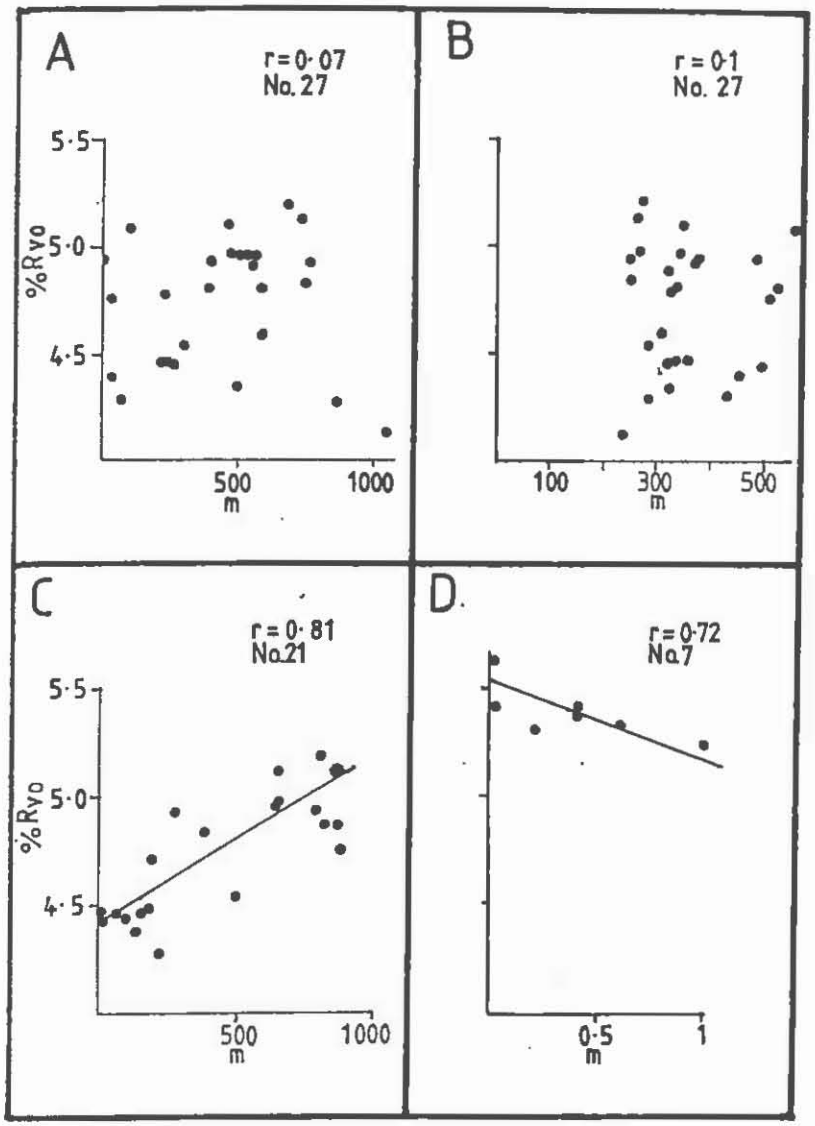

Figure 4
Diagrams of distance versus reflectance. **A** is a graph of reflectance versus height above a thick vulcanoclastic unit, drawn to test the scenario that peak burial metamorphic temperatures were attained prior to folding, and therefore reflectance values should follow strata attitudes. The low correlation coefficient indicates that there is no correlation in this plot. **B** is a diagram of reflectance versus height above sea level, to test the scenario that peak burial metamorphism was attained post folding, but r = 0.10 once again indicated that there is no correlation. **C**, a diagram of horizontal distance normal to the line A B in Figure 2, versus reflectance. The correlation figure , r = 0.82, indicates there is a significant correlation, suggesting a horizontal overprint of burial metamorphism. **D** represents distance versus reflectance away from the vein of the Bromley Mine. This graph shows a geologically significant correlation of r = 0.72.

ORGANIC MATURATION IN THE EARLY PERMIAN MANNING GROUP

R. JENKINS
University of Newcastle

INTRODUCTION

What has the Manning Group to do with the Sydney Basin? The Manning Group can be correlated, in terms of age, with the basal Dalwood Group in the Sydney Basin. This paper investigates the organic maturation (coalification) of dispersed organic matter in the Manning Group by measuring vitrinite reflectance and compares this to maturation in the Sydney Basin, in order to suggest a common tectonic link.

The bulk of the Manning Group (Mayer 1972; Jenkins 1992; Vickers & Aitchison 1992) consists of the Giro Diamictite (pebbly mudstone), which contains fossil assemblages equivalent to the Lyons group in Western Australia (Briggs 1987) and can be indirectly correlated both locally with an unnamed glaciogene unit below the Lochinvar Formation at Cranky Corner (Kemp et al. 1977) and elsewhere at the base of the Sydney Basin (McMinn 1983). The incoming of *Eurydesma sp.* occurs at the top of the Lochinvar Formation (McClung 1973) and is also present in the Glory Vale Conglomerate which overlies the Giro Diamictite (DJC Briggs pers comm 1993). The Colraine Mudstone, which overlies the Glory Vale Conglomerate, contains equivalent fauna to the Farley Formation in the Sydney Basin and these units are of similar lithotype.

VITRINITE REFLECTANCE

A regional study of vitrinite reflectance in the Manning Group (Jenkins 1992) showed an overall correlation with stratigraphic younging (figure 1) and with inorganic metamorphic mineral assemblages. This suggests that coalification occurred as a response to burial metamorphism. Thus it may be possible to establish a thermal gradient for the Manning Group and hence establish a more accurate thickness for the Group as well as constrain the tectonic setting in which deposition took place.

To test this, three detailed sampling traverses were made through the

Wards Creek Beds at the base of the Manning Group, where good bedding is present, in contrast with elsewhere. The traverses were along Wild Cattle and Jacky Barker Creeks to the south, and the Cooplacurripa River to the east, of Nowendoc (figures 1&2). Random reflectance (oil) measurements were made on polished blocks cut normal to bedding with 30 to 50 measurements per sample. The data was processed according to Barker and Goldstein (1990) to obtain peak metamorphic temperatures. As well, maximum and minimum reflectance in plane light was measured on a small number of samples to assess the degree of tectonic stress imposed in the rocks.

RESULTS

The Wild Cattle Creek area showed a consistent increase in coalification with increasing depth. Linear regression (figure 3) gives a thermal gradient of 36°C/km with a correlation coefficient (r) of 0.87.

Ductile and brittle deformation in the Jacky Barker Creek area is more complex than initial traversing indicated and it is not possible to estimate a thermal gradient from the current data set. Field mapping, however, suggests that this section is stratigraphically equivalent to the Wild Cattle Creek section and the similarity in degree of coalification tends to confirm this.

In the Cooplacurripa River area the organic matter in 17 of the 22 samples collected was far too degraded to be measurable, as evidenced by its inability to take a polish, opalescent mottling and severe post-diagenetic volume loss. The remaining five samples were also strongly altered and the reflectances measured are probably less, and less reliable, than those that could be gained from unaltered material. Reflectances were around 2.1-2.5%, yielding peak metamorphic temperatures of 250-270°C. The poor preservation of the organic matter in this area appears to be a function of the metamorphic grade. These rocks are noticeably less indurated than those from the other areas and consequently would have experienced longer periods of oxidation. Also, higher degrees of coalification, as seen in the other two areas, appear to render the organic matter less susceptible to weathering.

DISCUSSION

Of the three sections sampled in detail, only the Wild Cattle Creek area has yielded data that can be interpreted in terms of a thermal gradient. Before this can be applied however, certain criteria have to be met:

1) that a horizontal thermal gradient was present at the time of coalification,

2) that syn-deposition deformation has not occurred,
3) that post-tectonic coalification has not occurred and
4) that post-coalification tectonism has not disrupted the sequences over which the measurements were taken.

In the absence of further detailed sections in the Manning Group, a horizontal thermal gradient is difficult to confirm. Given, however, the apparent correlation between the Jacky Barker and Wild Cattle Creek sections, and the absence of any known igneous activity that would seriously affect the thermal profile, a horizontal thermal gradient is assumed.

Tilting of recently deposited sediment towards the basin margin by up to 10° in extensional settings is known elsewhere in the world (eg Paton 1992) and this may have occurred in the Manning Group. The effect of this, in any single block of sediment, would result in an apparent lowering of the thermal gradient. In a somewhat analogous fashion, tectonic thickening, by thrust faulting, if undetected, would also result in an apparent lowering of the measured thermal gradient.

Post tectonic coalification has in the past been considered a significant factor in maturation studies, due to the apparently slow rate of coalification (eg Diessel 1973). More recent studies, however, have shown that time is a much less critical factor in coalification than temperature and may be regarded in most cases as insignificant (see Hillier & Marshall 1992 for review). For this reason, and the absence of any significant post-depositional igneous activity in the area, post tectonic coalification is not considered significant in the Manning Group.

The critical factors here are whether syn-depositional deformation and/or post coalification thickening have affected the Manning Group. Both are likely to have done so, considering the depositional setting and later tectonic history (Jenkins unpublished data). The Manning Group, therefore, is considered to have been exposed to a high geothermal gradient, at least in its lower 1-2 km. This is supported by studies of vitrinite bireflectance measurements, as the degree of anisotrophy in vitrinite is controlled by pressure (Gerolymatos unpublished data). The low bireflectance of samples from the Manning Group indicate that coalification occurred under conditions of low tectonic stress and lithostatic pressure.

COMPARISON WITH THE SYDNEY BASIN

Vitrinite reflectances from the upper part of the Manning Group are equivalent to those obtained from deep bores in the Dalwood Group in the Sydney Basin (Esso Howes Swamp #1 Bore; Diessel 1973). Thermal gradients calculated from this and other bores in the Sydney Basin, based on the graphical data (depth vs. maximum reflectance) in Diessel (1973) yield the

following results: Esso Howes Swamp (1600-2600 m) 54°C/km; AOG Dural S (2000-3000 m) 32°C/km; Alkane Terrigal (900-1900 m) 77°C/km. Geothermal gradients in the range 40-50°C/km have previously been proposed for the Sydney Basin (Middleton & Bennett 1980).

CONCLUSIONS

The Manning Group has been exposed to a high geothermal gradient of at least 36°C/km. This indicates that the 9 km thickness proposed by Mayer (1972) was overestimated, and a thickness of about 5 km is probably more realistic. The high geothermal gradient also helps constrain the tectonic setting during deposition.

An extensional model for the Manning Group now seems well established (Jenkins 1992; Vickers & Aitchison 1992), however there is debate as to whether extension was accomplished by strike-slip (pull-apart basin) or orthogonal (rift basin) movements. Strike-slip basins generally have low thermal gradients (Christie-Blick & Biddle 1985) as a response to heating by the adjacent crust, whereas rift basins develop high gradients, due to the thinning of the continental lithosphere (McKenzie 1978). The data presented here suggest that rifting is the controlling influence in the development of the Manning Group. The high geothermal gradient in the Sydney Basin (albeit to what extent this has been influenced by Tertiary igneous activity) suggests that this basin was also initiated by rifting.

REFERENCES

Barker CE & Goldstein RH 1990. Fluid inclusion technique for determining maximum temperature in calcite and its comparison to the vitrinite reflectance geothermometer. Geology 18, 1003-1006

Briggs DJC 1987. Permian productid zones of NSW. Symposium proceedings: Advances in the study of the Sydney Basin 21, 135-142

Christie-Blick N & Biddle KT 1985. Deformation and Basin formation along strike-slip faults. in KT Biddle & N Christie-Blick eds. Strike-slip deformation, basin formation and sedimentation. Society of economic paleontologists and mineralogists Special Publication 37,1-34

Diessel CFK 1975. Coalification trends in the Sydney Basin. in KSW Campbell ed. Gondwana Geology ANU press 295-309

Kemp EM, Balme BE, Helby RJ, Kyle RA, Playford G & Price PL 1977. Carboniferous and Permian palynostratigraphy in Australia and Antarctica: a review. BMR Journal of Geology and Geophysics 2, 177-280

Hillier S & Marshall JEA 1992. Organic maturation, thermal history and hydrocarbon generation in the Orcadian Basin, Scotland. Journal of the Geological Society; London 149, 491-501

Jenkins R 1992. A geologic and thermal history of the Manning Group. Symposium proceedings: Advances in the study of the Sydney Basin 26, 39-46

McClung G 1973. Permian biostratigraphy of the northern Sydney Basin. in Herbert C & Helby R 1980. A guide to the Sydney Basin. GSNSW-BMR bull. 26, 360-375

McKenzie D 1987. Some remarks on the development of sedimentary basins. Earth and Planetary Science Letters 40, 25-32

McMinn A 1983. Permo-Carboniferous palynology of a sample from McDonalds Creek, Mudgee district. Geological Survey of New South Wales DMR unpublished palynology report 83/14

Middleton MF & Bennett 1980. Post-depositional tectonics of the Sydney Basin from vitrinite reflectance. Symposium proceedings: Advances in the study of the Sydney Basin 14, 10-11

Paton S 1992. Active normal faulting, drainage patterns and sedimentation in southwestern Turkey. Journal of the Geological Society; London 149, 1031-1044

Vickers MD & Aitchison JC 1992. Lower Permian Manning Group: tectonic implications of sedimentary architecture & provenance studies in the Nowendoc-Cooplacurripa area. Symposium proceedings: Advances in the study of the Sydney Basin 26, 31-38

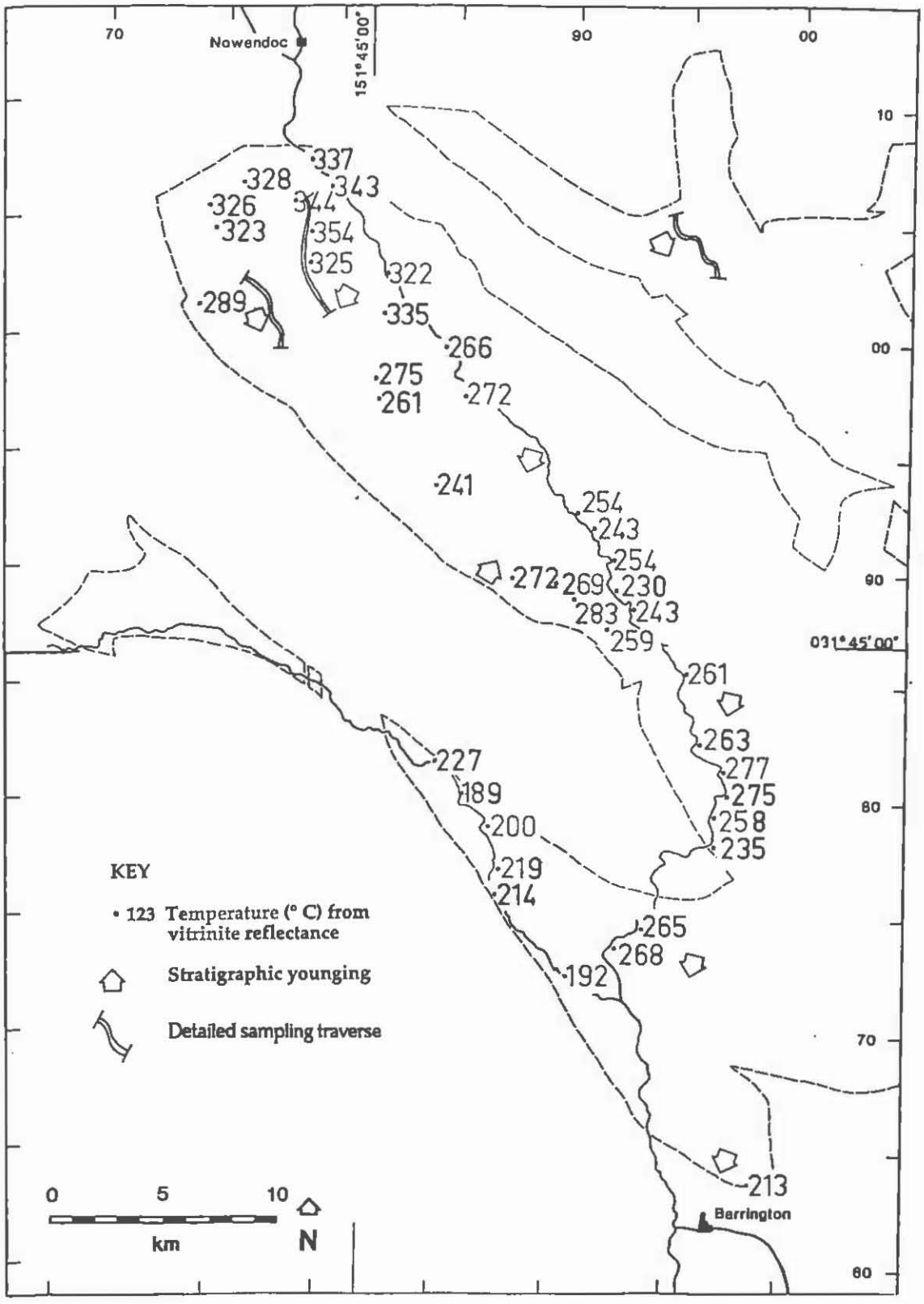

Figure 1. Peak metamorphic temperatures in the Manning Group from vitrinite reflectance. Marginal numbers refer to the Australian Map Grid.

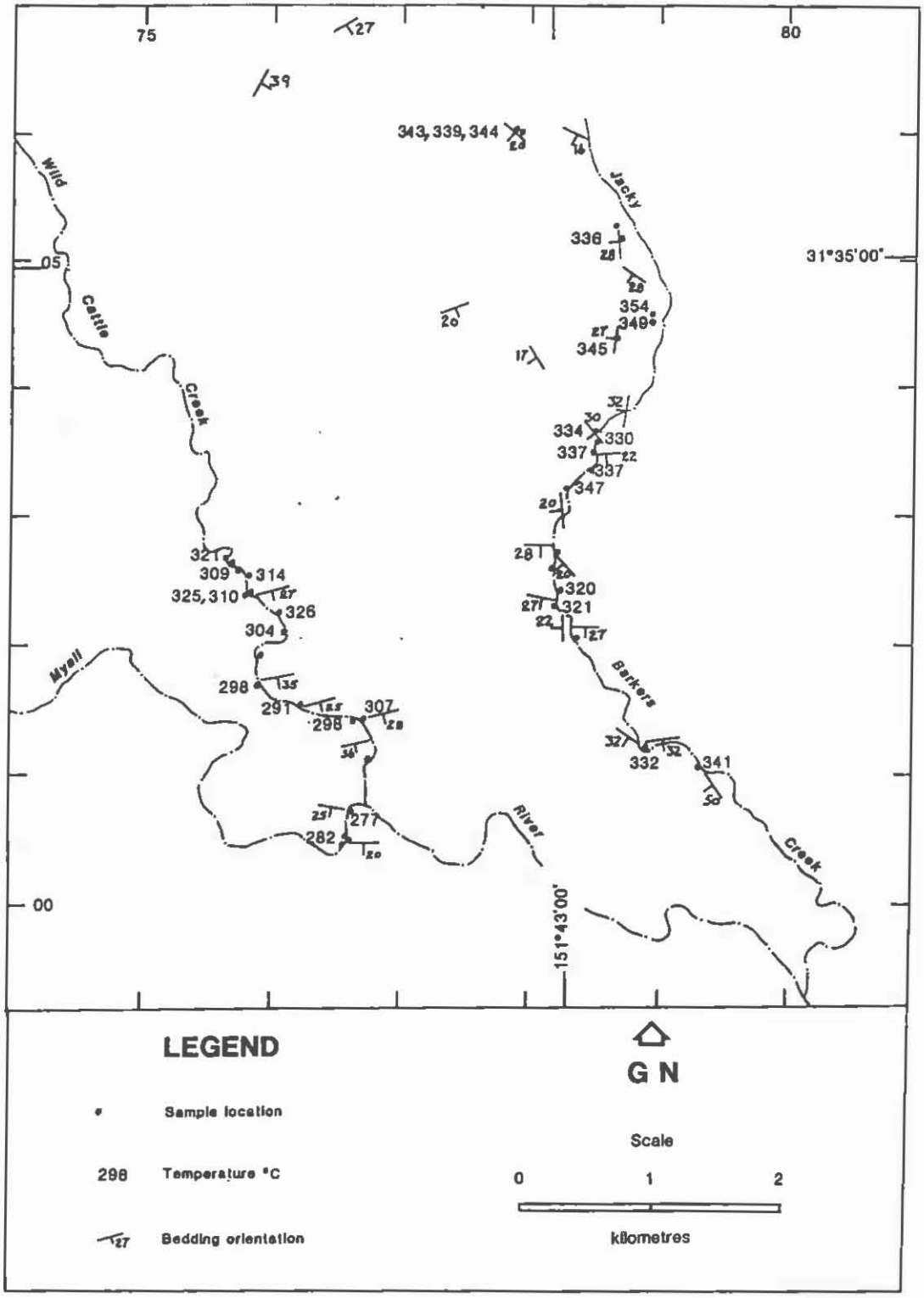

Figure 2. Peak metamorphic temperatures from vitrinite reflectance in the Jacky Barkers-Wild Cattle Creek area. Marginal numbers refer to the Australian Map Grid.

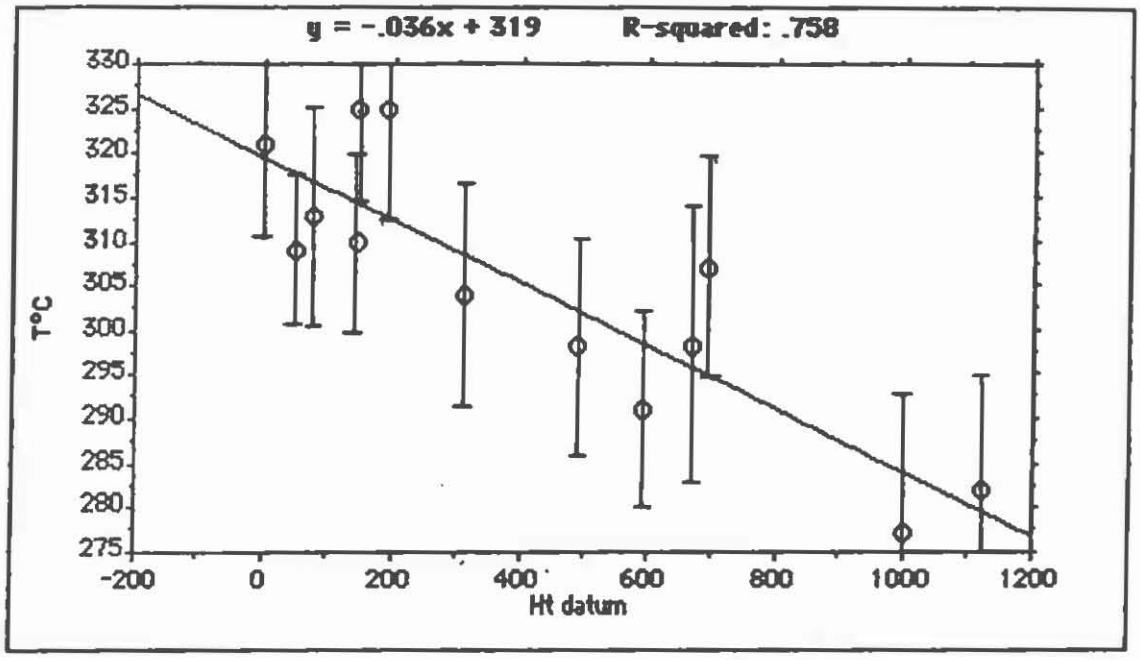

Figure 3. Correlation of temperatures from vitrinite reflectance vs. stratigraphic thickness from the Wild Cattle Creek area. Two sigma error intervals shown.

TWO KILOMETRES OF POST-PERMIAN SEDIMENT – DID IT EXIST?

M.M. FAIZ & A.C. HUTTON
University of Wollongong

INTRODUCTION

In a keynote address to this symposium in 1983, Branagan (1983a) stated that from "the earliest days of the study of the Sydney Basin workers have been fascinated with questions such as how big, how much, what direction, how hot, how cold, how old, as they attempted to study the present and past characters of the basin and to predict future trends." Not only were these questions intriguing to the early workers but some of them are still pertinent and puzzle present-day researchers. One such question is 'how much sediment was deposited after Permian Illawarra Coal Measures?', or in modern day parlance, what depth of cover has been removed from the Sydney Basin during the Jurassic to Recent time interval? Approaches to solving this vexing problem have varied.

One of the earliest, if not the earliest, publication pertinent to the 'how much cover has been removed?' question was that of Mitchell who estimated the volume of eroded material from the Blue Mountains. Of the solution given, Branagan commented that it "could only have been of theoretical value, and perhaps of aesthetic interest".

The rank, and variations in rank, of coal in the Permian Illawarra Coal Measures has been one of the enigmas of the Sydney Basin and is closely linked to the 'how much' question by some researchers. The rank enigma has been attacked by hard rock specialists as well as sedimentologists and coal petrographers, many of whom use vitrinite reflectance data to assess coalification rates and coal rank from which an estimated cover needed to produce the observed rank is calculated; other researchers examine heat flow, heat source and geothermal gradient data.

An early paper relating to heat flow and geothermal gradients was that of Rae *et al.* (1899) who measured the temperatures in the Birthday Shaft at Balmain; this paper gave a range of mean values from 69.875 °F (21 °C) at a depth of 606 ft (185 m) to 78.812 °F (26 °C) at a depth of 1449 ft (442 m) which gives a calculated geothermal gradient of 19.45 °C per kilometre. Papers by Dulhunty *et al.* (1950) and Facer *et al. (1980)* have given heat source and heat flow data for the igneous rocks along the edges, and for windows near the edges, of the basin. For the latter paper, it was presumed that the "data would provide background information for detailed investigation of the thermal setting of the Sydney Basin - *to assist in understanding the rank of the Permian coal (and variations in its rank) within the basin.* "

Explanations for the apparently elevated coal ranks in terms of "an eroded section" hypotheses give various estimated values for the cover thicknesses and as Branagan stated (1983b), some authors postulated a cover of up to 2 km over the presently exposed surface. Branagan did not accept this value and stated that the maximum cover was considerably less than 1 km. Dulhunty *et al.* (1950) also concluded that "In general, however, it appears that rank variation in the Central Eastern Coalfield is not a simple consequence of depth of burial, and cannot be related to folding or other tectonic disturbances in the coal measure".

Various authors have presented vitrinite reflectance profiles and have hypothesised as to the cause of the shape and gradients of the profiles. This paper commenced as one of *those* studies in that optical petrographic techniques were being used to characterise coal type and rank of various seams in the Southern Coalfield in order to assess those properties that influence gas storage capabilities of coal. The variations in coal rank in deep bore holes were also utilised to investigate the thermal and gas generation history of the region. The study left the rails and digressed into a 'how much cover' papers when we used the WinBury thermal modelling program to plot the geothermal history and consequently to determine a coalification model for the southern Sydney Basin.

ORGANIC PETROGRAPHY

Maceral Analyses

A summary of the maceral composition of various coal seams shows (Table 1) that the coals of the southern Sydney Basin are dominantly composed of vitrinite and inertinite with minor amounts of liptinite (< 3 %).

Vitrinite Reflectance

Mean maximum reflectance ($R_v$max) values for the Bulli and Balgownie seams are similar and range from approximately 1% in the west and south to >1.4% towards the northeast. $R_v$max values for the Wongawilli seam also show similar lateral variations to those of the Bulli and Balgownie seams but are approximately 0.1 to 0.2% higher than the Bulli seam.

Lateral variations in $R_v$max of all the coal seams indicate a general increase in rank towards the northeast and east of the study area. Localised increases in $R_v$max values seen in the data are mainly related to igneous intrusions (for example, Kemira and Appin areas). Such increases in $R_v$max are localised and commonly encompass a radius of less than a few hundred metres suggesting dykes.

To study the vertical rank variations in detail and to model the thermal history of the region, vitrinite reflectances were measured in coals as well as dispersed vitrinite in clastic lithologies in deep bore holes. The vertical $R_v$max profiles of these holes show increases in reflectance with depth and gradients range between 0.69 and 1.78% per kilometre.

THERMAL MODELLING

Tectonic History

Understanding the depositional and tectonic history of the Sydney Basin is vital to understanding rank and coalification models for the basin. Both aspects of the history of

the basin have been discussed previously by various authors such as Conolly and Ferm, 1971; Mayne *et. al.*, 1974; Herbert, 1980; Middleton and Schimdt, 1982 and Branagan, 1983b.

A summary of the details suggest that the basin initiated as a foreland basin with a basement comprising Ordovician, Silurian and Devonian metamorphic rocks and Devono-Carboniferous intrusive rocks. Deposition and subsidence in the southern Sydney Basin sequence commenced in the Permian and continued into the Early Jurassic with a possible hiatus in the Late Triassic (Herbert, 1980). Stable conditions, probably with minor erosion, prevailed from Late Jurassic (150 ma) until the Late Cretaceous (100 ma). This was followed by a major uplift and erosion with the commencement of sea-floor spreading in the Tasman Sea (Falvey, 1974; Middleton and Schmidt, 1982).

Geothermal Gradients and Palaeotemperatures.

Heat flow measurements, based on near-surface radioactivity, given by Saas *et. al.*, indicate a present day geothermal gradient for the Sydney Basin of approximately 24 ^{0}C/km. The geothermal gradient determined from the temperature log for Moonshine-7 drill hole shows a geothermal gradient of 27 ^{0}C/km. This approximates a present day heat flow value of 1.2 HFU (one heat flow unit being 10^{-6} cal $cm^{-2}s^{-1}$), a value that is consistent with the continental average.

Very high heat flows, thought to correspond to the most significant thermal event that occurred in the southern Sydney Basin, were probably present at the onset of Tasman sea-floor spreading in the Late Cretaceous. Therefore, it is reasonable to believe that the sedimentary succession of the study area was subjected to its highest temperatures during this period of its history. In this case it is assumed that this high thermal event commenced shortly before the continental break-up and lasted for approximately 10 million years (B. Jones, *pers. comm.*). Fluid inclusion studies of the Narrabeen Group (Eadington *et al.*, 1991) indicated that the maximum palaeoheat flow of the southern Sydney Basin reached 2.1 HFU.

COALIFICATION MODEL

An estimation of the thermal history prior to this period, and back to the Late Permian, is extremely difficult to predict using $R_v$max values because the present $R_v$max values are mainly determined by the highest temperature attained by organic matter in the Late Cretaceous. Prior coalification events would have been obscured by this later event. In an attempt to overcome some of these problems, the coalification history of the study area was modelled using the WinBury thermal modelling computer program.

WinBury Thermal Modelling Program

The basic aim of thermal modelling is to calibrate the observed maturity levels ($R_v$max values) to modelled values (Fig. 1), without violation of the basic geological and physical concepts. The kinetic method given by Sweeney and Burnham (1990) was used to model the $R_v$max values in this study. In order to obtain the best fit of the modelled and observed maturity levels the two most important variables are palaeoheat flow and thickness of cover or thickness of the eroded section (for the latter is was further assumed that most of the erosion has been since the Late Cretaceous).

The first step when using the WinBury program is to accurately model the geohistory of the basin to produce a curve for subsidence and sediment accumulation through time;

the best fits, corrections to present stratigraphic thickness, such as using decompaction, palaeobathymetry and absolute sea-level fluctuations, have to be made. Decompaction to obtain is a correction of the present-day thicknesses to account for the progressive loss of porosity with depth of burial. The phenomenological model describing the porosity-depth relationship as proposed by Falvey and Middleton (1981) is used in the WinBury program; this model assumes that the incremental change in porosity is proportional to the load and porosity which in turn is also a function of lithology.

Palaeobathymetry or the palaeowater depth is estimated from benthic microfossils or sedimentary facies. Fluctuations in absolute sea levels are used for the calculation of tectonic basement position. The default values of the program (based on age) were used in this study.

In this paper, input data for the reconstruction of geohistory consisted of depths and ages of formation tops, lithologies, porosities and depth of water at time of deposition of each formation. The formation depths and lithologies of each unit was determined from lithological well logs and the palaeowater depths were estimated from the sedimentary facies. Because reliable data for conductivity, porosity and density are lacking, the default values of the program, which are based on the lithological composition of each unit, were used.

A second major step in thermal history modelling is the estimation of the thickness of eroded sections and palaeoheat flows. Estimation of these two parameters is achieved by the calibration of calculated vitrinite reflectance data against the observed data. Vitrinite reflectance values can be calculated either using the TTI (Time-temperature index of Lopatin, 1971) or a kinetic method such as of Burnham and Sweeny (1990). Lopatin's TTI method is simply based on the assumption that the reaction rate doubles every 10°C rise in temperature over the entire range from 50 to 250°C. The Sweeney and Burnham method is based on the assumption that vitrinite reflectance evolution follows the Arrehnius equation.

The Burnham and Sweeney model is based on activation energies representing chemical reactions; it is assumed to be more accurate than the Lopatin's TTI method for any heating rate. Therefore, in this study the kinetic method of Sweeney and Burnham was used because of its versatility.

A very important factor is the lithology of the missing section. Lithology influences conductivity and hence the temperature to which rocks are exposed which in turn influences the rank of coals and the maturity of dispersed organic matter. For example, where the missing section is assumed to be predominantly, or only sandstone, (which has a thermal conductivity = 6.1 W/mK) 2750 m of missing section is required for Bootleg 8 well (BL-8) to produce the required reflectance values. In contrast, if it is assumed that the lithology was shale, or predominantly shale, (with a thermal conductivity = 1.9 W/mK) the required thickness of the missing section for the same hole is only 1175 m.

An assumed shale/predominantly shale lithology is a useful hypothesis if the missing section was additional Wianamatta Shale. Furthermore, erosion of an approximately 1200 m section would have been much easier if the lithology was shale rather than sandstone. As to whether the Wianamatta Shale was much thicker than it is now, is difficult to determine. Thus alternatives need to be considered.

It has been suggested that the Triassic section was much thicker than it is at present

?POST-PERMIAN SEDIMENT

and if this was so, the missing section may have been similar lithologically to the Triassic section in the southern Sydney Basin where the shale:sand ratio is approximately 60:40 (based on BL-8). Therefore, it would be reasonable to use this proportion of shale:sand as the missing "lithology" when modelling rather than only sandstone or shale. The thermal conductivity of this "lithology" is calculated to be 3.2 W/mk. The calculated thickness for the missing section comprising 60% shale and 40% sandstone in BL-8 is 1600 m (Table 2).

DISCUSSION

The concept of an eroded cover for the present surface to the Sydney Basin has been debated at length. Middleton and Bennett (1980) used a coalification model, based on geothermal gradients of 40 to 50 °C, to argue for an eroded thickness in excess of 2 km in the central coastal region of the basin if uplift coincided with Tasman Sea opening 70 to 80 million years ago. The calculated thickness of eroded cover decreased to 1 km near the margins of the basin although it was as thick as 1.5 km near the northeastern margin. Branagan (1980) stated that the reported cover thickness values that had been published ranged between 500 and 1700 m but rejected the idea of a thick cover, suggesting that ideas on reflectance may need to be re-examined.

Falvey and Middleton (1981) modelled vitrinite reflectance using the Lopatin model and gave an overburden thickness of 600 m; this calculation assumed that the overburden existed between 220 and 80 Ma B.P. and palaeotemperatures remained high and constant.

Branagan (1983b) reviewed the data of Crawford *et. al.* (1980), who discussed the origin and erosion of diatremes, and concluded that diatremes in the northern part of the southern Sydney Basin had been eroded by up to 1400 m, that is, the cover had been 1400 m. This figure agrees well with the values obtained in this study if the missing section is presumed to be a shale-dominated sequence.

In his paper, Branagan reported that a fission track estimate indicated the cover was 950 m thick. Branagan concluded that the evidence for a "now-vanished very thick Jurassic-Cretaceous cover was poor and inconsistent. At most, if there was a Triassic cover it was less than 1 km and was largely deposited during the Triassic". Furthermore, the rank of the Sydney Basin coals could be explained largely as a result of heat flow.

Previous thermal modelling conducted by Middleton and Schmidt (1982) indicated that the thickness of the missing section in the southern Sydney Basin was in excess of 2700 m. This work was based on a quantitative model for the evolution of $R_v$max values as a function of time and temperature. Such a model does not take into consideration important parameters such as lithology, conductivity and compaction. The values obtained by Middleton and Schmidt closely agree with the values obtained using the WinBury program if the lithology of the missing section was sandstone only. However a section of sandstone 2700 m thick would be extremely difficult to erode due to the hardness of such a section; and it might be expected that some remnants of sandstone are likely to be part of the present day topography.

When additional drill hole data have been analysed, it will be possible to construct a contour map showing the loss of cover for the southern Sydney Basin. For the two drill holes examined to date, BL-1 and BL-8, the thickness of the missing section (assuming a shale to sandstone ratio of 60:40) is 1400 m and 1600 m respectively.

Maximum palaeoheat flows varied from 2.0 HFU in the north and west up to 2.5 HFU towards the east. Such high values towards the east is to be expected as it has been interpreted that the present coastline represents a rift margin. In this context palaeoheat flow values even higher than 2.5 HFU probably existed further east. Given these high heat flow values and using data from the WinBury program, it is predicted that the Illawarra Coal Measures, in some localities, was probably buried to depths of up to 2400 m of sediment (as at BL-8) before the uplift in the Middle Cretaceous.

ACKNOWLEDGEMENTS

We wish to acknowledge the cooperation of International Oil Pty Ltd (formeerly AGL Petroleum Pty Ltd) for permission to use data for drill holes Moonshine 7, Bootleg 1 and Bootleg 8.

REFERENCES

Branagan, D., 1980: Blowing their cover. *Adv. Stud. Syd. Bas., 14th Newcastle Symp., Proc.*, 25-26.

Branagan, D., 1983a: Summing up the Sydney Basin. *Adv. Stud. Syd. Bas., 17th Newcastle Symp., Proc.*, Keynote Address, 24-25

Branagan, D., 1983b: The Sydney basin and its vanished sequence. *J. Geol. Soc. Aust.*, 30(1), 75-84.

Conolly, J.R. and Ferm, J.C., 1971: Permo-Triassic sedimentation patterns, Sydney Basin, Australia. *Am. Assoc. Pet. Geol. Bull.*, 55, 2018-2032.

Crawford, E.A., Herbert, C., Taylor, G., Helby, R., Morgan, R. and Ferguson, J. 1980: Diatremes of the Sydney Basin, *Geol. Surv. N.S.W. Bull.*, 26, 294-323.

Dulhunty, J.A., Hiner, N. and Penrose, I., 1950: Rank variations in the Central Eastern Coalfields of New South Wales. *J. Roy. Soc. N.S.W.*, 84, 99-106.

Eadington, P.J., Hamilton, P.J. and Bai G.P., 1991: Fluid history analysis - A new concept for prospect evaluation. *APEA J.*, 31(1), 282-294.

Facer, R.A., Cook, A.C. and Beck, A.E., 1980: Thermal properties an coal rank in rocks and coal seams of the southern Sydney Basin, NSW: a palaeogeothermal explanation of coalification. *Int. J. Coal Geol.*, 1, 1-17.

Falvey, D. A. and Middleton, M.F., 1981: Passive continental margins: evidence for a prebreakup deep crustal metamorphic subsidence mechanism. *Oceanologica Acta*, 4, 1-14.

Herbert, C., 1980: Depositional development of the Sydney Basin, *Geol. Surv. NSW. Bull.*, 26, 10-52.

Lopatin, N.V., 1971: Temperature and geologic time as a factor in coalification: *Akademiya Nauk SSSR Izvestiya, Seriya Geologicheskaya*, 3, 95-106.

Mayne S.J.E., Nicholas, A.L., Bigg-Wither, Rasidi, J.S. and Raine, M.J., 1974: Geology

of the Sydney Basin - A review. *Bull. Bur. Miner. Resour. Geol. Geophys. Aust.*, 149, 229 pp.

Middleton, M.F. and Bennett, A.J.R., 1980: Post-depositional tectonics of the Sydney Basin from vitrinite reflectance. *Adv. Stud. Syd. Bas., 14th Newcastle Symp., Proc.*, 10-11.

Middleton, M.F. and Schmidt, P.W., 1982: Paleothermometry of the Sydney Basin. *J. Geophys. Res.*, 87, B5351-59.

Rae, J.L.C., Pittman, E.F. and David, T.W.E., 1899: Records of rock temperatures at Sydney Harbour Colliery, Birthday Shaft, Balmain, Sydney. *J. Roy. Soc. N.S.W.*, 33, 211-219.

Sweeney, J.J. and Burnham, A.K., 1990: Evaluation of a simple model of vitrinite reflectance based on chemical kinetics. *AAPG Bull.*, 74, 1559-1570.

Table 1. Maceral Compositions for Selected Seams, Southern Coalfield

Seam	Percentage							
	Mean	Range	Mean	Range	Mean	Range	Mean	Range
Bulli	42.1	17.0-66.7	1.0	<0.1-6.3	50.7	27.1-72.3	6.9	2.6-37.1
Balgownie	35.6	16.9-56.4	0.1	<0.1-0.6	54.2	28.6-72.3	10.1	5.4-26.8
Cape Horn	54.3	45.6-64.9	<0.1	<0.1-0.1	37.7	30.1-49.4	8.0	4.6-11.4
Wongawilli	52.3	31.9-80.8	<0.1	<0.1-0.2	13.6	1.6-22.4	34.1	17.7-60.1

Table 2. Modelled Heat Flow Data and Thicknesses of Missing Section

Well	Heat Flow (HFU)	-- Thickness of Missing Section --- 100% Sand	100% Shale	Shale:Sand 60:40
BL-1	2.5	2550	1150	1400
BL-8	2.0	2600	1175	1600

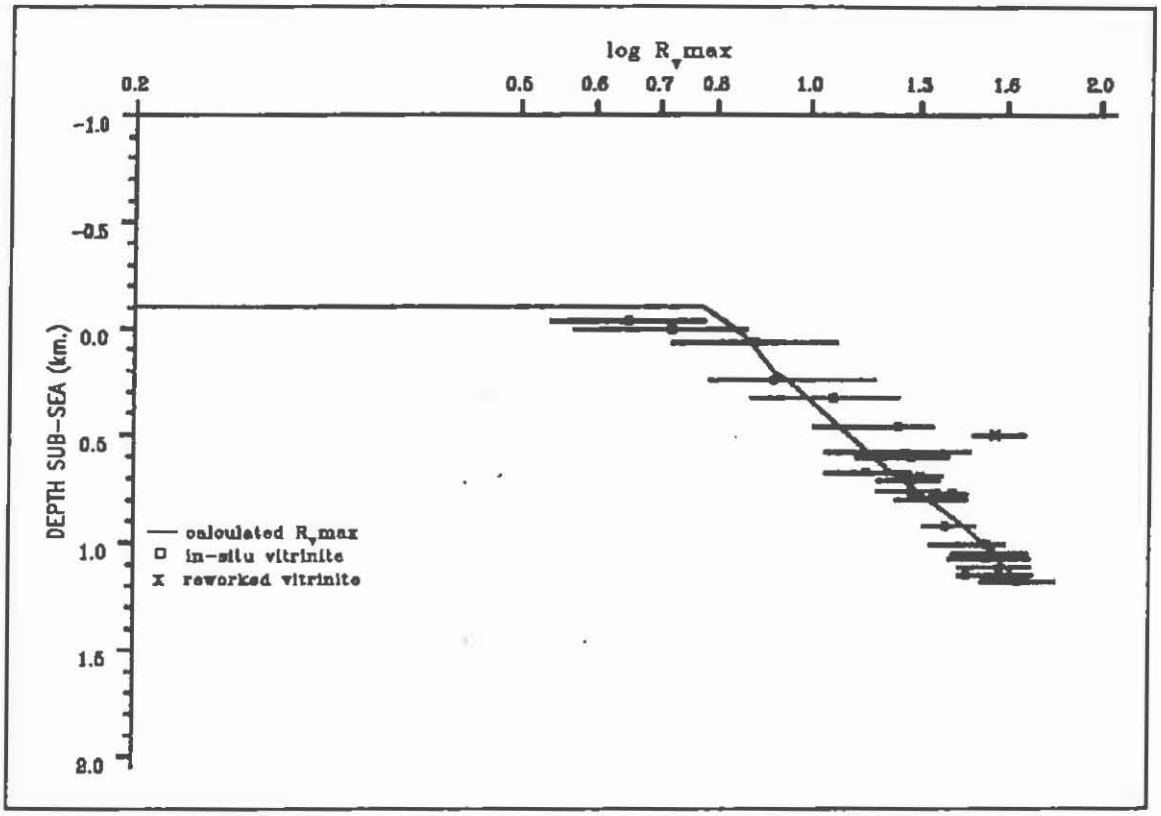

Figure 1 Observed *vs* calculated vitrinite reflectance profile for BL-8.

HYDROGEOLOGICAL PROPERTIES OF THE BOTANY SANDS AQUIFER, SYDNEY

X.W. YU, J. JANKOWSKI & I.R. ACWORTH
Groundwater Management & Hydrogeology Centre, UNSW

Abstract

An accurate evaluation of the hydrogeological properties and their spatial distribution in an aquifer is an important component of the study of groundwater flow and solute transport. The Botany Sands have been classified into different units for this study, depending on their hydrogeological and sedimentalogical properties. Geostatistics has been used to analyze the spatial distribution and variability of the units. The results provide the quantitative data that can be directly used in the groundwater modeling of the aquifer.

1. Introduction

The Botany sands form a high yielding aquifer system which provides an economical water supply system for industrial processes and irrigation in the Botany district. Studies have been carried out on various aspects of the aquifer since 1937. Smart (1974) conducted a pumping test at the North eastern end of the ICI Botany site. The test shows that the horizontal hydraulic conductivity is 26 to 36 m/day, and the storage coefficient ranges from 0.024 to 0.26. He noted the heterogeneity of the aquifer and claimed that quartz sands, clay and peat are three end elements, representing the compositions of the aquifer. The heterogeneity of the aquifer is determined by the ratio entropy of each element. Another comprehensive pumping test was conducted by Webb and Watson (1979) at David Phillip field, at Daceyville. This test provided not only data on the hydraulic conductivity, but also useful information about the peat materials interbedded in the sands and their impact on the groundwater flow regime. The results shown that the aquifer is a semi-confined with a hydraulic conductivity of 28 m/day in sands, and 0.012 m/day in the peat layers. The storage coefficient ranged between 0.001 and 0.003.

Our study is to evaluate the hydrogeological properties of the Botany sands, and their spatial distribution in the basin. We firstly classify the Botany sands into different units based on their sedimentalogical and hydrogeological properties, by means of laboratory experiments, field test and numerical analysis. Finally we use geo-statistics to study the spatial variability of the Botany Sands aquifer.

2. Hydrogeological Units of the Botany Sands Aquifer

Grain size analysis, Photo microscope and X-ray defractometry analyses were conducted on 50 sediment samples taken throughout the Botany Basin. The results of the analyses confirm that the Botany Sands Aquifer consists of different units. While clean medium quartz sand is the predominant composition. silty/peaty sand and sandy peat/clay form miner components, which usually form thin layers or lenses, embedded in the sands. The

hydrogeological properties of these units were evaluated using empirical equations and laboratory experiments.

2.1 Empirical Calculation

Empirical equation expresses the relationships between grain size parameters and hydrogeological properties. Here the permeability is calculated by Hazen's equation expressed as

$$k = A\,(d_{10})^2$$

where d10 is the effective diameter at which 10 % of the sample is of finer size; And A is 1.0 for k in cm/sec and d10 in mm. The results of this method are listed in Table 1.

Dispersivity is an another intrinsic property of the porous medium. It is determined by grain size, shape and roundness, compositions and combination of grain, and geometry and channel width of porous. Many studies have shown that grain size analysis can be used to estimate dispersivity. Klotz (1980) suggested that the dispersivity mainly depends on effective grain size and the uniformity coefficient. Milne-Home (1989) derived an equation

$$\alpha = 0.026\,(UC)^{0.63}\,d_{50}^{0.76}$$

where UC = d60 / d10, is uniformity coefficient; d50 is effective grain size. The results are shown in Table 1.

Table 1. Grain size parameters and hydrogeological properties of the Botany Sands

Parameters	Quartz sands	Silty/Peaty sands	Sandy peat/clay
mean (ϕ)	1.50 - 1.90	1.50 - 1.90	1.59
median (ϕ)	1.55 - 1.93	1.55 - 1.93	1.50 - 1.60
Stand. Deviation	0.35 - 0.45	0.35 - 0.45	0.40 - 0.50
Skewness	0.02 - 0.10	0.02 - 0.10	0.02 - 0.05
Roundness	0.60 - 0.80	0.60 - 0.80	0.60 - 0.74
Silt content (%)	< 1	1.0 - 4.0	> 5.0
Clay/Peat content	negligible	> 1 %, negligible for silty sands	> 5.0
Uniformity Coe.	1.70 - 2.20	1.40 - 1.70	< 1.40
d_{10}	0.16 - 0.20	0.15 - 0.18	< 0.15
Porosity	0.32 - 0.38	0.34 - 0.38	0.39 - 0.42
Permeability (m/day)	12.0 - 25.0	4.0 - 12.0	0 - 0.01
Dispersivity (m)	$6 - 9 \times 10^{-5}$	$3.0 - 5.0 \times 10^{-5}$	$0 - 4.21 \times 10^{-5}$

2.2 Permeameter Tests

The apparatus used in the study is a multiport Permeameter in which hydraulic head and volumetric flow rate are measured directly. Hydraulic conductivity is then calculated from the measurements according to Dacey's equation and the configurations of the Permeameter used, by equation

$$K = \frac{10\,Q}{44.2 * t * dl}$$

where K is the hydraulic conductivity (cm/sec), Q is the volumetric flow rate through the column (cm^3/sec), dl is the length of the section of column between two probes (cm), t is time period(sec). The results are listed in Table 1. The correlation of permeability from Hazen's equation and Permeameter test is shown in Figure 1. As we can clearly see that the permeability separates into three groups. One is ranged from 0.017 to 0.023; Anther group ranges from 0.012 to 0.166; And a third group ranges between 0 and 0.0008.

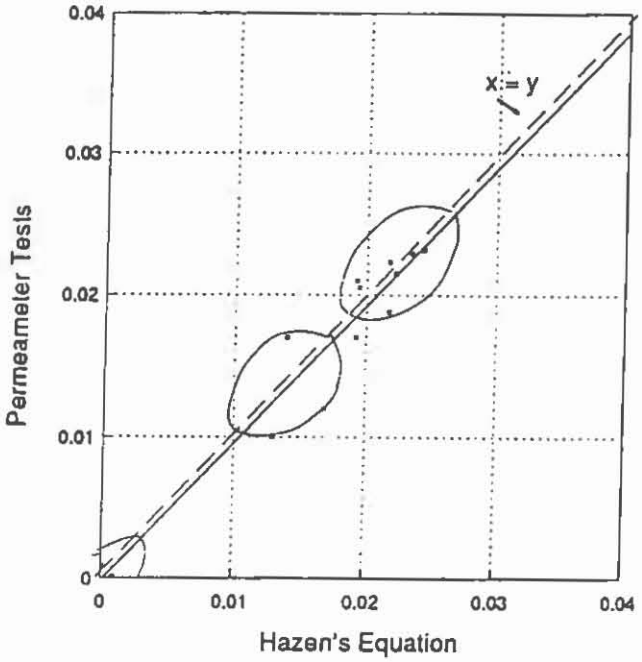

Figure 1 Permeability (cm/sec)

2.3 Classification of The Botany Sands Aquifer

Summary the sedimentalogical analyses and laboratory experiments, we classified the Botany Sands into three units.

Unit 1. Quartz sands

The quartz sand is predominant in the whole basin with color varying from light brown, golden brown, white to grey. It consists of almost 100 per cent quartz with minor heavy minerals and less than 1 percent silt.The X-ray defractometry analysis shows that the samples of this unit contain only negligible amount of clay. Under microscope, the grains appear as clean quartz with irregular fractures containing yellow iron oxides and sometime dark stains. The parameters are listed in Table 1. This type of sands represents an acolian dune deposition. Figure 2 shows grain size distribution curve.

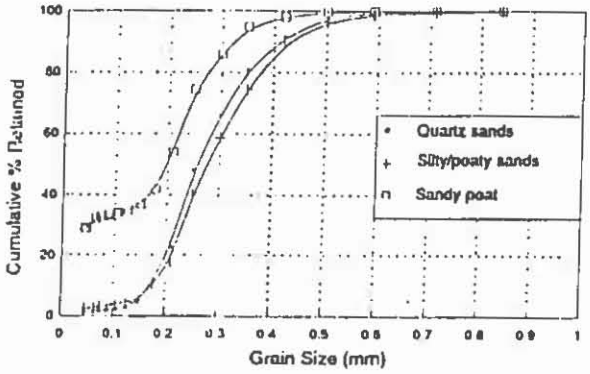

Figure 2 Cumulative Frequency Curves

Unit 2 Silty / Peaty sands

The sands of this unit contain significant amount of silt and peat. It is distinguished under microscope by silt/peat particles are adhered to quartz particles. The silty sands are also characterized by low clay contents, and strong iron oxide and cement, with yellowish color, which indicates a erosional deposition in a open environment. On the other hand, peaty sands are muddy with organic peat. The sands appear grey, dark blue or sometime white, smelling hydrogen sulphide odder from fresh core samples, that indicates a shallow and enclosed swampy environment. Field tests shown that this unit does not

affect groundwater flow regime, but it has significant effects on solute transport, in term of hydrodynamic dispersion.

Unit 3 Sandy peat/clay

This type can be subdivided into two groups. The first one is sandy peat, which is in black color, oily, with high organic and woody, fibrous contents. Sand and peat are both predominant compositions. The second type is peat or clay while peat or clay is predominant compositions.

Relationships between different parameters can provide meaningful information about the classifications of sands units. Figure 3 shows the relation between mean size and sorting, skewness and roundness of sands samples. As we can see the sorting and roundness slightly decreases as the average size reduces. In contrast, roundness slightly increases as sorting decrease.

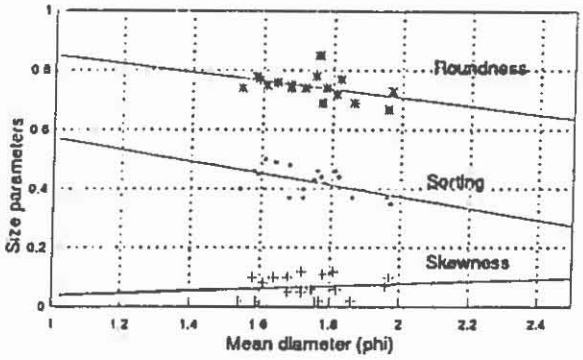

Figure 3 Correlation of Size Parameters

3. Spatial Distribution of Hydrogeological Units

The approach of the spatial variability of the Botany sands aquifer consists of three steps. First, Previous study and data acquisition. In this step initial data was collected and pre-processed. Secondly geostatistics analysis. Semi-variogram was calculated and geostatistical model determined. Heterogeneity and anisotropy of the properties were evaluated using directional variogram. Selected representative vertical cross sections was analyzed using indicator kriging to illustrate the boundaries of high and low permeability.

3.1 Geostatistical analysis

The basic premise in geostatistics is that the spatial variability can be described with a variogram, defined as a function of the correlation or of the covariance between pairs of data as the distance or lag between the data points increases. (Journel, el. at.,1978). For various practical and theoretical reasons, the most commonly used function is the semivariogram that can be expressed by equation

$$\gamma(h) = \frac{1}{2N(h)} \sum_{i=1}^{N(h)} [\, Z(Xi+h) - Z(Xi) \,]^2$$

where N(h) is the number of data pairs separated by lag h, Z(Xi) is observation value at point Xi. The semivariogram has another form once we assume the data has a mean of Zero

$$\gamma(h) = K(0) - K(h) \qquad \text{where } K(0) = \Sigma\, Z(Xi)^2 / n; \quad K(h) = \Sigma\, Z(Xi+h) * Z(Xi) / n$$

As the vector lag h increases, K(h) will decrease because there is a progressively greater independence between values Z(Xi) and Z(Xi+h). For large lag h such that Z(Xi) and Z(Xi+h) are not correlated, the semivariogram $\gamma(h)$ will reach a value, this limiting value is called the sill C of the semivariogram, and the distance at which r(h) reaches the sill is called the range which corresponds to the distance of influence of the given samples. The range is usually used to estimate the correlation of sample data, which can provide useful information in interpretation of data distributions.

Kriging is defined as a weight-moving-average interpolation method where a set of weights assigned to samples minimizes the estimation variance, which is computed as a function of the variogram model and locations of the samples relative to each other, and to the point or block being estimated. Kriging has the variety of ordinary kriging and simple kriging remarked by its theoretical basis of estimations. Ordinary kriging assumes that local means are not necessarily closely related to the population mean, and it therefore uses only the samples in the local neighborhood for the estimations. This kriging is the most commonly used method for environmental situations. While on the other hand, simple kriging assumes that local mean are relatively constant and equal to the population mean, so that the population mean is used in estimations of the samples.

2. Spatial distributions of hydrogeological units

Most of the original data used was gathered from lithological bore logs. All geological units in the bore log were incorporated into one of three units classified previously. The fractions of these unit were then calculated from each of those schematic representations by summing the thicknesses of each layer and dividing by the total depth of the drill hole. For example, fraction of sand is calculated as

$$\text{Fraction of sand (\%)} = \frac{\Sigma\, bi}{B} \times 100$$

where $\Sigma\, bi$ is the sum of thicknesses of sand layer along the drill hole; B is the total drill hole depth. The statistical parameters are also shown in Table 2

Table 2 Statistical parameters of sample data

q	x	y	Quartz sands	Silty/peaty sands	Sandy peat/clay
Mean	11.052	12.354	76.965	12.711	10.324
Variance	17.817	33.543	133.454	56.778	77.326
Std. Dev.	4.221	5.792	11.552	7.535	8.794
Coef. Var.	38.190	46.880	15.010	59.281	85.176
Skewness	0.176	0.554	- 0.321	0.268	1.296
Kurtosis	3.304	2.588	2.743	2.201	4.430
Minimum	1.000	2.300	44.440	0.000	0.000
25th %tile	8.050	7.938	68.783	6.113	4.775
Median	11.100	10.350	77.780	12.670	8.960
75th %tile	13.475	17.150	86.958	17.522	13.155
Maximum	22.950	28.650	100.000	31.480	35.710

Figure 4 shows the experimental variograms of quartz sands as an example. Three spherical models were matched to best fit the data. Estimations of the sill, the nugget and the range were obtained from the theoretical model (Table 3).

Table 3 Variogram model of the hydrogeological units

Parameters	Quartz sands	Silty/peat sands	Sandy peat/clay
Sill	60	30	30
Nugget	120	45	50
Range (m)	4000	2350	200
Model	Spherical	Spherical	Spherical

The estimates of the distributions of quartz sands, silty/peaty sands and sandy peat/clay were made by calculating kriging values of sample data using theoretical variogram models. These results are described by the block kriging maps and Contour maps of estimates. Figure 5 is a example of estimated distribution of quartz sands.

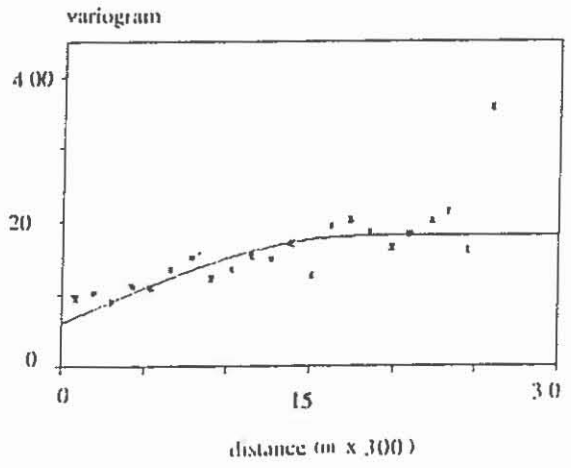

Figure 4 Variogram for quartz sands

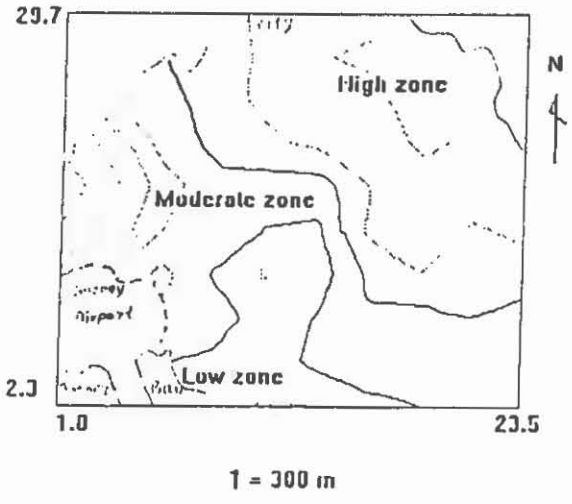

Figure 5 Estimated distribution of quartz sands

Hydrogeological Properties and their spatial distribution of the Botany Sands aquifer

As we can see in the maps, sand fraction predominantly occupies most of the basin. It gets largest value at north-east corner; And the lowest values distribute from middle of the basin to the Botany bay in form of a nearly north to south stripe, which getting wide towards the bay. One the other hand, sandy peat/clay fraction gets its largest values at almost the same stripe. Also it occupies a small area near east boundary, while it is absent from the middle to the upper part of the basin. The silty/peaty sands generally appear between the quartz sands and sandy peat/clay.

The variogram also indicates some important characters of the distributions of hydrogeological units. The range of spherical model, according to some studies, implicates the degree of correlation and continuity of the hydrogeological units. Therefore we can see in Table 3, that the sand fraction is of a large correlation and continuity in contrast to a very small correlation of sandy peat/clay.

Another indication of variogram is the anisotropic character of the units. It should be mentioned that general distribution maps were generated based on directional variogram and universal kriging. They represent the generalized estimates in all directions.

However, as we already know, the lag in variogram calculation is a vector with directional as well as distance properties, the variogram is valid or precise only for changes in a specified direction. To investigate the problem, four directional variograms at angles of 0 (parallel to x-direction), 45, 90, and 135 degree, with a tolerance of 22.5 degrees. The results were then compared. If they are the same, the distribution of units is considered to be isotropic, or it is anisotropic.

The variograms shown highly variable with directions. That indicates the distributions of hydrogeological units are anisotropic. Figure 6 illustrates the variations of variogram range against directions. As we can see, the largest ranges are filled in the degree of 45-90, 90-112 and 112-135 from x-direction, in respecting to sand, silty sand and sandy peat. That indicates that the predominant directions of distributions.

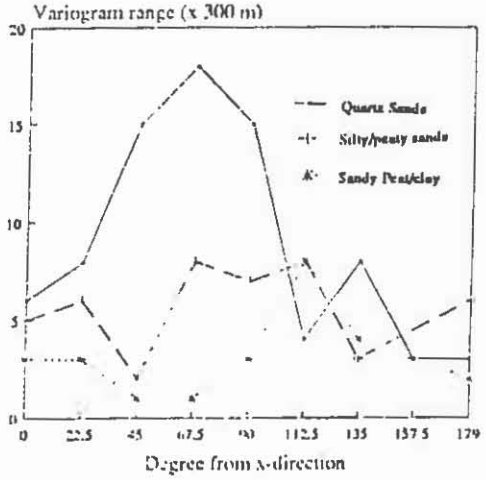

Figure 6 Variogram range vs direction

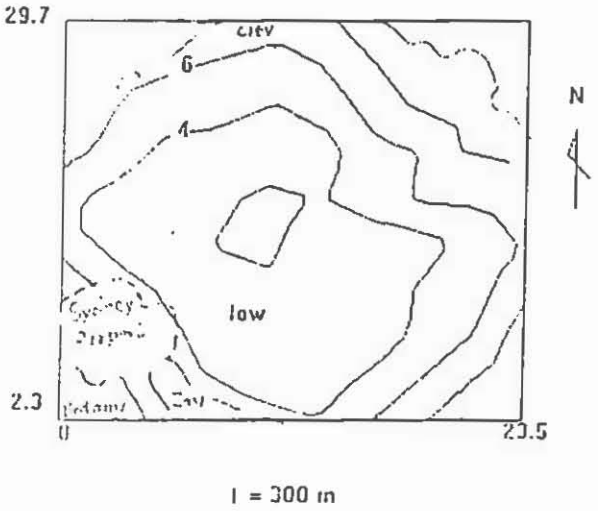

Figure 7 Kriging Standard Deviation

3.3 Error Evaluation of the Results

The error evaluation of the results by kriging can be done by calculating the kriging standard deviations, which implicates the standard error of estimate computed for a kriging estimate. It is notable that the kriging standard error highly dependents on the variogram model. Figure 7 shows contour maps of kriging standard deviation. They illustrate the reasonable results that the highest kriging errors are predicted in areas where the sample data is of lowest density.

4. Conclusion

The Botany sands aquifer consists of three hydrogeological units, they are quartz sands, silty/peaty sands and sandy peat/clay. The quartz sands are the predominant component and form the main aquifer of the Botany Basin. Their spatial distribution are heterogeneous and anisotropic. The silty/peaty sands have low to moderate permeability, The sandy peat/clay can be considered as impermeable material among the quartz sands. The last two units distribute in forms of lenses and thin layers in most of the area. However the continuity of these layers increases toward the Botany Bay, and therefore these layers divide the main aquifer into two parts. One is on the top, and is a unconfined aquifer with thickness of 7 to 15 meters; The other is a deeper confined or semi-confined aquifer with thickness of 10 to 20 meters.

References

Englund, E. and Sparks, A., 1988. Geostatistical Environmental Assesment Software User's Guide. U.S. E.P.A

Jounal. A.G. and Huijbregts, C.H., 1978. Mining Geostatistics. Academic press., London.

Smart, J.V. , 1974. The geology, hydrology, and groundwater chemistry of part of the Botany Basin, New South Wales. M.Sc. Thesis, University of Sydney (Unpub.).

Webb, S.N. and Watson, K.K., 1979. Hydraulic behaviour of an unconfined aquifer. Aust. Wat. Res. Council, Tech. Report.

THE GEOLOGY & RESOURCES OF THE NORTHERN PART OF THE SOUTHERN COALFIELD

M.B.L. HILL & M. ARMSTRONG
Department of Mineral Resources

The Southern Coalfield is the only source of hard coking coal in New South Wales. In 1991-92,a total of 16.4 million tonnes of coal were mined with 6.3 million tonnes being consumed by the domestic steel industry and 6.5 million tonnes of coking being exported to a number of countries including Japan, Korea, Taiwan and Great Britain. Hard coking coal has the highest value of all Australian coals and in 1991-92 the price per tonne averaged over $A64.

In 1985, The Department of Mineral Resources recognised that several of the existing colliery holdings had limited reserves or had difficulties with declining coal quality. New mine areas needed to be identified but the only unallocated high quality resources were in the northern part of the Coalfield, in the Picton, Camden, Campbelltown region. The delineation of new reserves was made more urgent by the rapid urbanisation of the region. Resource sterilisation is the likely outcome of urban expansion unless it is preceded by careful planning based on an adequate knowledge of the resource.

Existing data north of Picton-Appin was limited to a small number of coal and petroleum exploration boreholes. The majority of the coal holes were drilled during the 1960s and 1970s in the Cobbitty, Campbelltown and Holsworthy areas. Much of the coal quality data is inadequate by today's standards. The petroleum wells were drilled by several companies/joint-ventures in a series of programmes conducted from the 1950s to the 1980s. The older wells are of little use because of the unavailability or poor quality of down hole geophysics and analytical data, often combined with an inadequate intersection of the prospective units.

HILL AND ARMSTRONG

Since 1985, the Southern Section of the Coal and Petroleum Geology Branch, under the leadership of Mike Armstrong, has carried out four resource audit drilling programmes in the Southern Coalfield (figure 1). They are:

- The Picton Drilling Programme consisting of two wells drilled to the north and the south of Picton in 1986 . (Armstrong and Hill, 1988).
- The Camden Stage One Drilling programme consisting of . three wells drilled to the north, west and south of Camden, and one well drilled to the south of Oakdale during 1988 (Alder et al, 1992).
- The Camden Stage Two Drilling programme consisting of three wells drilled to the northeast, east and southeast of Camden during 1989-90 (Alder et al,1992).
- The South Creek Valley Drilling Programme consisting of two wells; one drilled to the northeast of Oran Park and one drilled near Bringelly during 1990 (Cozens et al, 1992).

The objectives of these programmes were:

- To assess the potential resources within the Bulli seam (and where possible to reduce bore hole spacing to a maximum of 4 km).
- To assess where possible the potential resources within the underlying seams down to the Woonona seam.
- To determine additional exploration required to prepare areas for release to industry.
- To provide sufficient data for meaningful land use planning.

In 1987, an additional objective was added:

- To assess the potential coal seam methane resources of the coal measure sequence, where possible, down to the Woonona seam.

Data collection from these programmes was maximised, with each bore hole being geologically, geophysically and geotechnically logged. Detailed coal quality and gas quantity and quality testing was conducted on all major seams intersected. Selected samples were submitted for sorption isotherm determination. A number of the holes were terminated immediately below the Cape Horn seam because of depth and financial constraints.

These drilling programmes, in conjunction with the pre-existing data, have enabled a broad understanding to be developed of the geology and the resources of the northern Southern Coalfield. There are however some significant gaps which require further work; in the Mt Hunter, the Bringelly (Lowes Creek), the

Leppington-Varroville and the Holsworthy-Menai areas. The Branch will complete the West Campbelltown Drilling Programme consisting of two holes near Leppington and Varroville during 1993. To the north, in what until recently was the Central Coalfield, there is little data. The closest wells being DM Cape Banks DDH 1 (Botany Bay), the Bunnerong Bore, Cremorne DDH 1 and 2, the Balmain Colliery Birthday Shaft bore, AOG Baulkham Hills, and AOG Kurrajong Heights. Data from these wells has been reinterpreted and is utilised in this study.

GEOLOGY

Bamberry (1991) provides a detailed discussion of the stratigraphy and sedimentation of the Southern Coalfield. The stratigraphy is set out in Figure 2. Bamberry has shown that the Sydney Subgroup thickens gradually to the north-northeast towards the depo-centre. There is no indication of any structural control of sedimentation for the Subgroup as a whole. Individual units however show a marked variation in thickness, lithology and facies across the Coalfield, that is, from the north-northwest to the south-southeast. In this paper discussion will be confined to the interval from the base of the Cape Horn Coal Member to the base of the Narrabeen Group.

The Cape Horn Coal Member occurs towards the top of the Eckersley Formation of the Sydney Subgroup. The unit is present throughout much of the central and northern parts of the coalfield. It consists of a thin coal seam which in the northwest is overlain by the Burragorang Claystone Member. To the northwest of Campbelltown, both of the units have been eroded by the Lawrence Sandstone Member. To the east and northeast, the Burragorang Claystone Member, which is a prominent marker horizon, is both over and underlain by coal and is in fact part of the seam. Further to the east, near Menai, the seam occurs directly above the Claystone Member. It is suggested that the Cape Horn Coal Member was originally much thicker but that it was deeply eroded by the Lawrence Sandstone. It is also suggested that the Coal Member may be time transgressive, younging to the east.

The Lawrence Sandstone Member occurs across the northern part of the Coalfield except in the far west. The Member comprises a relatively thin channel sandstone deposit except at Cape Banks and Cremorne where it consists of a lower laminite unit and an upper sandstone unit.

The Balgownie Coal Member is a well defined seam which is present across the central parts of the coalfield except near

the western margin. It averages over a metre in thickness. To the immediate west of Camden and to the north and northeast, the seam thickens, reaching over 3 metres in a narrow zone trending north-northeast from Camden. Further to the northeast, it appears to maintain a thickness of over 1.7 metres through the north of the Holsworthy area but it thins towards Cape Banks. The seam generally contains a few thin claystone bands.

The Loddon Sandstone Member overlies the Balgownie Coal Member (Bamberry, 1992) and is normally sand dominated. Near Cobbitty, in the northwest of the Coalfield, the Member consists of a lower unit comprising claystone and siltstone laminites, and an upper unit comprising sandstone channel deposits. A thin coal seam occurs at the top of the lower unit (informally named the 2b seam). To the east, between Camden and Bringelly, It consists of channel sandstone deposits. To the north and northeast of Campbelltown, a thin coal seam occurs towards the top separating two channel cycles. This seam (informally named the 2a seam) may not be laterally continuous. Around Menai and Heathcote, the Member comprises sandstone channel deposits but at Cape Banks, there is a thick lower claystone, siltstone and sandstone laminite unit which is terminated by a thin coal seam. Overlying the seam is a thin channel deposit. A similar sequence occurs at Cremorne but with a second seam developed towards the base of the lower unit.

The Bulli Coal conformably overlies the Eckersley Formation. It typically comprises between 1.5 and 2.4 metres of bright and dull coal with few minor discontinuous claystone bands in the central part of the Coalfield. The Formation thickens dramatically to the north of Picton reaching 5.2 metres at Narellan and 11.1 metres at Bringelly. Detailed brightness profiling of the coal in the Picton-Narellan area suggests that the increasing thickness is caused by the addition of plies to the top of the seam. These upper plies contain more dull coal than in the basal section and the proportion of dull coal increases towards the top. North of Narellan, the seam develops a claystone band towards the centre which thickens to the north and north west reaching 6.5 metres at Bringelly. The upper coal split deteriorates rapidly to the north. It consists of less than 1.5 metres of carbonaceous claystone with minor coal at Bringelly.

To the west of Mt Hunter and Cobbitty, the formation thins and the number and thickness of claystone bands increases. To the east and northeast of Narellan, the formation thins rapidly to 1.9 metres in thickness near Campbelltown. The band also thins but is still present. Further to the east, in the northern part

of the Holsworthy Military Reserve, the formation thickens again but the increase is due to the presence of a wedge of sandstone which splits the coal. The Formation is over 12 metres thick near Lucas Heights with less than 1.2 metres of coal in the upper split and 1.3 metres in the lower split. To the north and north east, the seam coalesces and does not contain major bands. The formation is 1.2 metres thick near Cronulla, 2 metres at Cape Banks and 3 metres at Cremorne. The Formation lies at depths between 450 metres at Picton, 625 metres at Camden, 830 metres at Bringelly, 600 metres at Campbelltown, 730 metres at Lucas Heights and 690 metres at Cape Banks.

COAL QUALITY AND RESOURCES

The available data suggests that only the Bulli and Balgownie seams have economic potential in the northern part of the coalfield. All other seams which exceed the minimum working section thickness of 1.8 metres required for longwall mining have unsatisfactory coal quality characteristics.

The Bulli seam working section closely corresponds to the formation geological thickness in the Picton-Camden-Narellan area, reaching a maximum thickness of 5 metres at Narellan. Raw coal ash ranges from 8.4% to 11.2%, volatile matter ranges from 21% to 24% and CSN ranges from 3.5 to 4.5. Washed coal quality in this area is high with yields between 90% and 95% at floats 1.50 with ash contents of between 8.1% and 8.5%. Vitrinite content is lower than normal between Camden and Narellan because of the effect of the thick, dull upper seam section. There is a restricted area east of Camden (near Glenlee) where the seam thins and coal quality deteriorates. The yield in this locality is 55% at floats 1.40 with ash of 19%.

To the north of Narellan, coal quality deteriorates due to the development of the bands within the seam. Immediately to the north, where the major band is up to 0.3 metres thick, ash at CF 1.50 remains at between 8% and 9%, but yields fall progressively to as low as 80%. North and northwest of the band 0.3 metre isopach, a working section is developed in the upper seam split in one bore only which is south of Cobbitty. A working section is developed in the lower split over a wide area. Coal quality in general deteriorates to the north and northwest as the number and thickness of claystone bands increases. Raw coal ash increases from 15% north of Narellan to over 22% near Bringelly. Washed coal quality declines, with concentric zones of coking blend, export thermal and domestic thermal coal (figure 3). The resource in the Camden-Narellan-

Oran Park area of the coalfield is in the order of 1,200 million tonnes of which 950 million tonnes is prime hard coking coal.

To the east and northeast of Narellan, there is limited coal quality data. Quality appears to deteriorate with coking blend coal near Campbelltown and domestic thermal coal immediately southwest of the seam split in the Holsworthy area. Further to the northeast, the coal quality appears to be high at Cape Banks. Phosphorous values are moderately high in the Camden area but increase further northwards with a maximum of 0.1% at Bringelly.

A working section is developed within the Balgownie seam immediately to the west, to the north and to the northeast of Camden reaching a maximum thickness of 3 metres. Coal quality increases to the north-north east due to a decline in raw coal ash from 15% west of Camden to 13% at Oran Park. Utilisation potential increases in the same direction (see figure 4). The resources of coking blend coal in the Camden-Narellan-Oran Park area are in the order of 330 million tonnes. Further to the northeast, under Campbelltown and Holsworthy, the seam appears to be of coking blend and/or export thermal quality.

GAS RESOURCES

The gas contents of the Bulli and Balgownie seams reach a maximum in the area to the east and southeast of Camden (Menangle). The contents decline gradually to the north and northwest, and more quickly to the west and southwest. The Bulli seam contains 17 cu.m/t near Menangle, 12 cu.m/t near Bringelly and 10 cu.m/t to the north and west of Camden. The gas contents increase with increasing depth of cover but also decrease with decreasing coal rank. Rank decreases to the north with vitrinite reflectance values of 1.24 at Menangle and 1.15 at Bringelly. Gas compositions range between 90% and 95% methane except in the west where high CO2 values occur close to the Nepean Structural Zone. Methane sorption isotherms were prepared for Bulli and Balgownie seam samples taken from a Departmental well drilled near Oran Park. The results show that the seams are fully saturated.

No permeability data is available, however the content and compositional data indicate that the gas will be a major concern for future coal mining and is a significant potential resource for the State.

CONCLUSIONS

The units of the upper part of the Sydney Subgroup can now be correlated across the northern part of the Coalfield and as far north as Cape Banks and Cremorne.

The resources of hard coking coal are finite and careful land use planning is vital to limit future sterilisation.

ACKNOWLEDGEMENT

Six Geoscientists have made significant contributions to the Department's Southern Coalfield drilling programmes since 1985. Their names are set out in the Reference List below as the authors of the appropriate programme reports.

REFERENCE LIST

ALDER J D, BYRNES J G, HILL M B L, COZENS S J, AND ARMSTRONG M, 1992. Camden Land Use Drilling Program Report, Southern Coalfield. Coal and Petroleum Geology Branch NSW Department of Mineral Resources - File GS 1992/363.

ARMSTRONG M & HILL M B L, 1988. Picton Land Use Drilling Programme, Coal and Petroleum Geology Branch. File GS 1988/03.

BAMBERRY W J, 1991. Stratigraphy and sedimentology of the Late Permian Illawarra Coal Measures, Southern Sydney Basin, New South Wales. The University of Wollongong, Wollongong. PhD thesis (unpubl) 262 pp.

COZENS S J, HILL M B L, ARMSTRONG M, BYRNES J, G AND ALDER J D, 1992. South Creek Valley Land Use Drilling Programme, Southern Coalfield. Coal and Petroleum Geology Branch NSW Department of Mineral Resources. File GS 1992/158.

MINE SUBSIDENCE BOARD, 1992. Camden area flood prone land study.

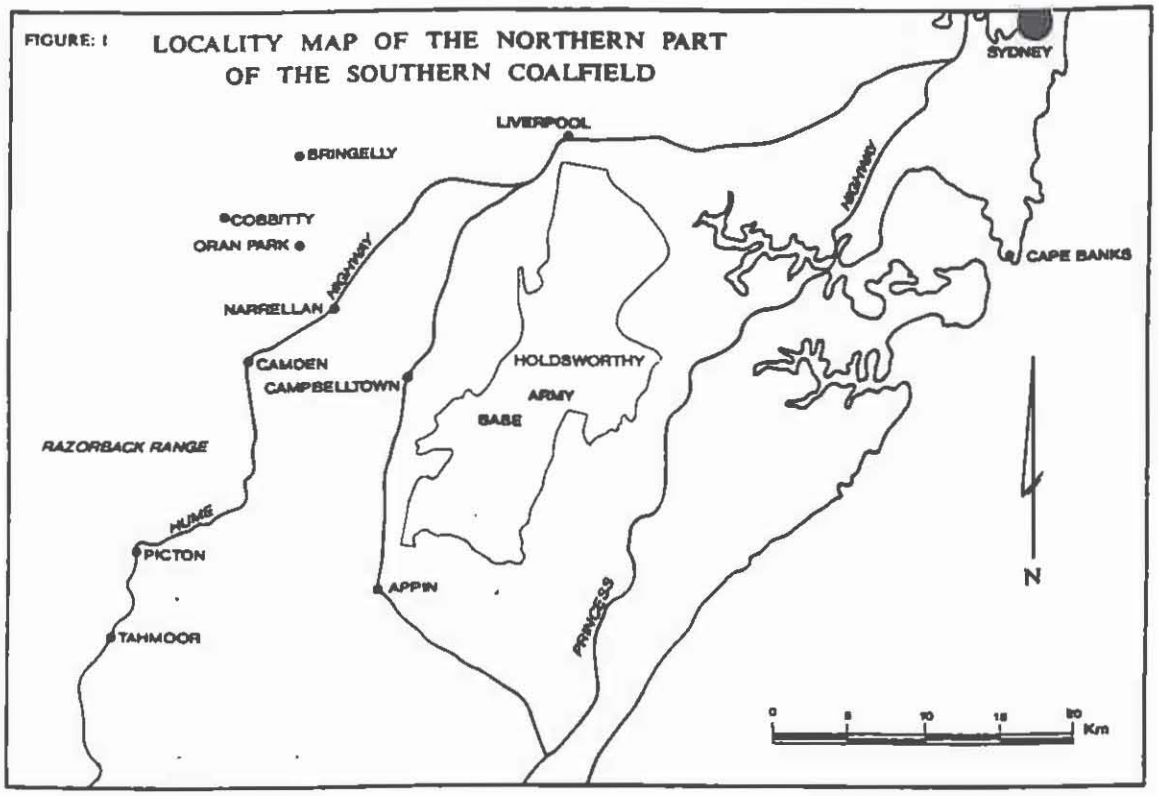

FIGURE: 2 REVISED STRATIGRAGRAPHY OF THE ILLAWARRA COAL MEASURES. SOUTHERN SYDNEY BASIN

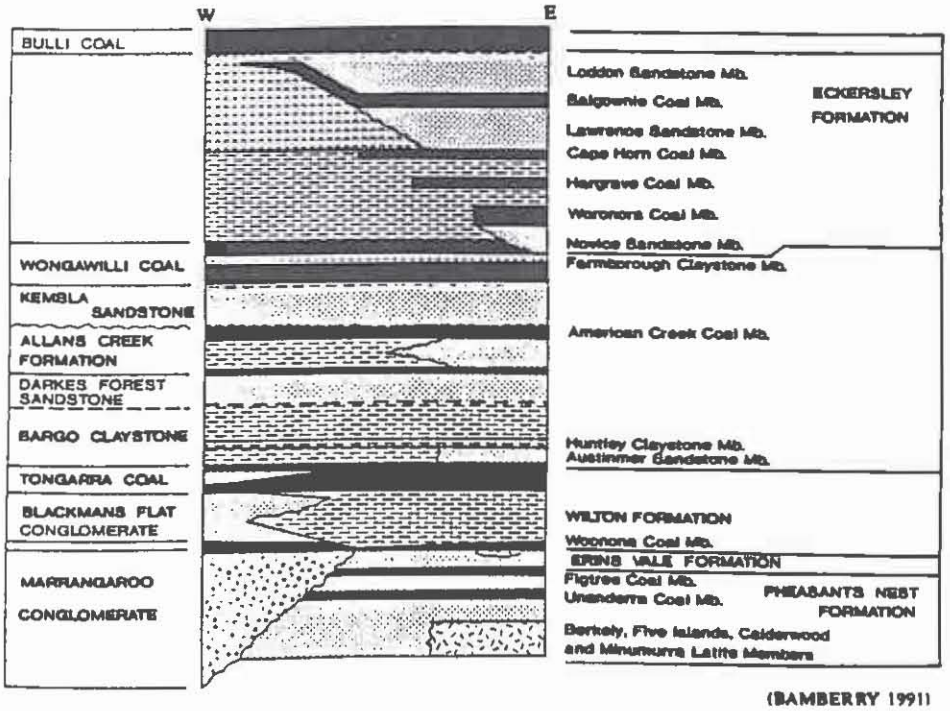

(BAMBERRY 1991)

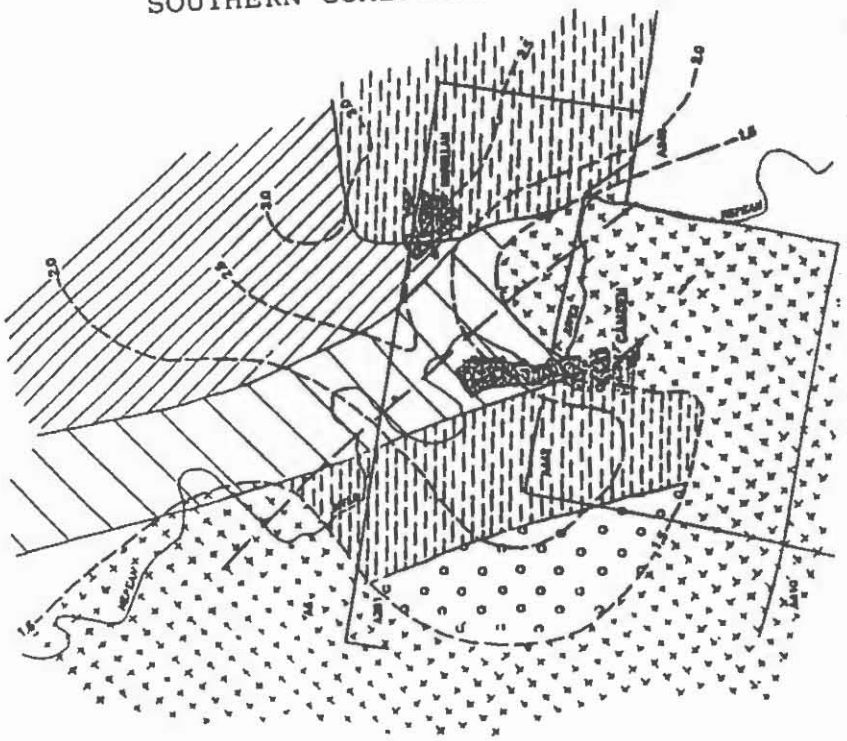

FIGURE: 4 COAL RESOURCES OF CAMDEN AREA - BALGOWNIE SEAM - SEAM THICKNESS AND UTILISATION POTENTIAL

MINE SUBSIDENCE BOARD 1992

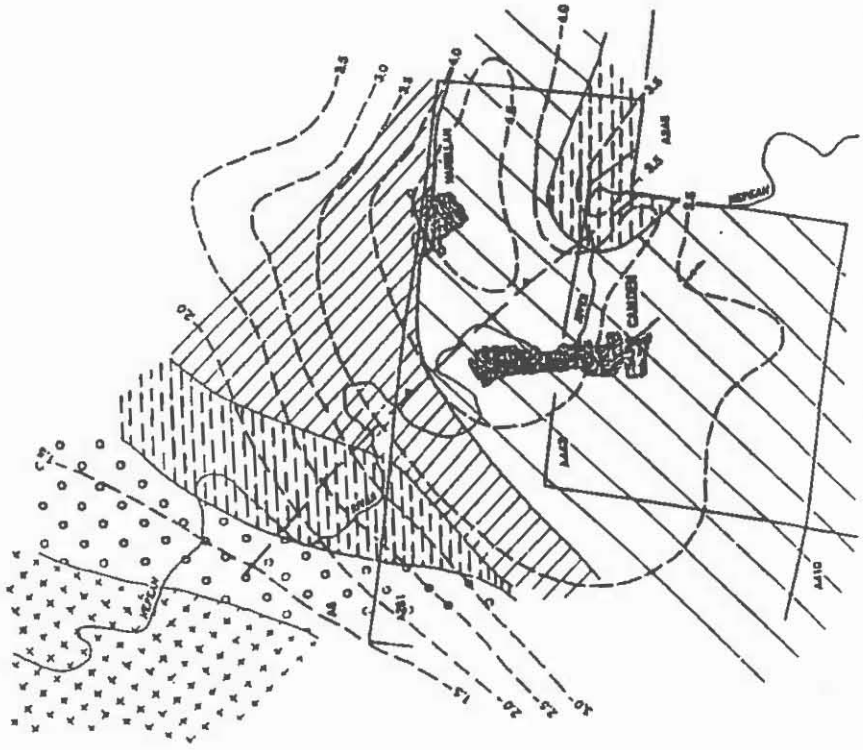

FIGURE: 3 COAL RESOURCES OF CAMDEN AREA - BULLI SEAM - SEAM THICKNESS AND UTILISATION POTENTIAL

MINE SUBSIDENCE BOARD 1992

PERMIAN DEPOSITIONAL SEQUENCES OF THE SYDNEY BOWEN BASIN

D.J.C. BRIGGS
University of New South Wales

Sequence stratigraphy has had a short, though now rapidly accelerating, history of application in the Permian of the Sydney - Bowen Basin. Of seminal importance were studies by AAR Ltd in the Denison Trough (Elliott, 1985; Ziolkowski and Taylor, 1985), which delineated a succession of seismic sequences based on extensive geophysical data and palynology. Fielding et al. (1990) and Ziolkowski et al. (1992) have presented additional thoughts on this succession, while AGSO is undertaking ongoing work in the adjacent Taroom Trough (Brakel et al., 1992). In the Sydney Basin, sequence stratigraphic concepts have been applied to the Late Permian succession in the southern coalfield (Arditto, 1991), to the relationship between the Permian coal measures and the overlying Narrabeen Group (Herbert, 1993) and to considerations of coal-forming environments in the northern Sydney Basin (Diessel, 1992). Prior to these studies, the broader but related concept of the "depositional episode" had been applied to the basin by Herbert (1980), and stratal relationships that can now be recognized as sequence boundaries had been described from a number of levels (e.g. McKelvey et al., 1971; Stuntz, 1972; Bowman, 1980; Herbert, 1980). A considerable acceleration of sequence stratigraphic investigations in the Sydney Basin Permian is projected for the very near future.

Theoretical models for the formation of depositional sequences have been summarized by Van Wagoner *et al.* (1988). In a predominantly marine depositional setting landward of the shelf break, such as that in which the Permian of the Sydney - Bowen Basin accumulated, the phase of lowest relative sea-level is represented either by an unconformity marked by subaerial exposure and erosion (in a type 1 sequence), or by a slightly progradational to aggradational interval of relatively shallow-marine or non-marine strata of the *lowstand systems tract* (in a type 2 sequence). This unconformity or relatively shallow-water interval is followed by a typically rather thin transgressive interval of the *transgressive systems tract*, followed by a generally much thicker and (usually) regressive interval of the *highstand systems tract*. In vertical section therefore, each depositional sequence in this setting is typically expressed as a broad-scale transgressive - regressive cycle, on which may be superimposed smaller scale fluctuations associated with parasequences. Transgressive - regressive cycles of this kind are in fact a pervasive feature of the Sydney - Bowen Basin Permian and, as foreshadowed earlier (Briggs, 1989), these cycles to a large extent can be correlated biostratigraphically throughout the Basin. The purpose of this paper is to delineate the succession of these major transgressive-regressive cycles, each of which is believed to correspond to one depositional sequence.

CORRELATION OF SEQUENCE BOUNDARIES AND TRANSGRESSIVE-REGRESSIVE CYCLES IN THE SYDNEY-BOWEN BASIN

Figure 1 summarizes the correlation of five relatively complete successions of transgressive-regressive cycles in the Sydney-Bowen Basin. The relative durations assigned to the various cycles in the chart follow those of the correlative chronostratigraphic units in the time scale of Ross and Ross (1987) (Briggs, this volume). Note that in a few places where biostratigraphic resolution is very poor (such as in the Late Permian coal measures of the Sydney Basin), the succession of transgressive -regressive cycles in itself has been used to suggest correlations; these speculative correlations are all qualified on the chart with question marks.

Sequence nomenclature used here is an informal system modified from that of Elliott (1985), in which sequence boundaries and their corresponding (underlying) sequences are given roman numeral - lower case letter designations (e.g. IIIa, IIIb etc.). Where Elliott's seismic sequences correlate with more than one regionally correlateable depositional sequence, the latter are designated as numbered subdivisions: for example, Elliott's seismic sequence IVa is divided here into, in ascending order, depositional sequences IVa1, IVa2 and IVa3.

Sequence II. Elliott (1985) applied the designation IIIa to the oldest sequence studied by him, and did not discuss older Permian sequences. Sequence II is used here for the interval in Sydney - Bowen Basin successions between the base of sequence IIIa (i.e. sequence boundary II) and the unconformity at the base of "Stage 2" units throughout much of Australia discussed by Powis (1984, p. 433). Roberts (1985) has argued that this latter unconformity marks the base of a regional transgression of probable eustatic origin. Biostratigraphically, sequence II spans palynological zones APP1 and lower APP2.1, and the *Lyonia* n. sp. to *Strophalosia subcircularis* brachiopod Zones.

Sequence boundary II is marked by onlap in Denison Trough (Elliott, 1985, fig. 3). In the northern Sydney Basin the correlative boundary, the base of the Rutherford Formation, is marked by truncation of underlying strata south of the Lochinvar Anticline (Mayne *et al.*, 1974, p. 150). In outcrop this boundary is marked by abrupt lithological change from greenish volcanolithic sandstone of the Allandale Formation to grey quartzo-felspathic sediments of the Rutherford Formation. In the offshore Sydney Basin a prominent reflector ("Horizon B": Mayne *et al.*, 1974, p. 101, pl. 9) marks the base of the Rutherford/Pebbley Beach Formations.

Sequence II spans three major transgressive cycles in the Sydney Basin. Sequence II1 at the base corresponds to the main "Stage 2" glacigene interval which, although apparently nonmarine within the Sydney-Bowen Basin, has been argued to have accumulated under the influence of a rising base level during a regional transgression (Roberts, 1985). Sequence II2 corresponds to a transgressive - regressive cycle associated with the "*Trigonotreta* n. sp. Zone". In both the Cranky Corner outlier and the Lochinvar Anticline this narrow transgressive interval is separated by a probable non-marine interval from the younger transgression associated with the *S. subcircularis* Zone (sequence II3). In the Gunnedah and eastern Bowen Basin, sequence II (and sequences IIIa-b) correlate with nonmarine volcanogenic units in which depositional sequences are not recognizable.

Sequences IIIa-IIIb. Sequence IIIa of Elliott (1985) corresponds to the lower division of the Reids Dome beds in the Denison Trough. Biostratigraphically, this unit spans the APP2.1 - APP2.2 palynological zonal boundary, and on this basis is correlated with the lower Rutherford Formation in the northern Sydney Basin, which contains the *Bandoproductus* n. sp. brachiopod Zone. Sequence IIIb of Elliott (1985) corresponds to the upper Reids Dome beds and occupies the remainder of APP2.2. On evidence from preceding and succeeding units, this upper division is correlated with the upper Rutherford Formation, which contains the *Tomiopsis strzeleckii* Zone.

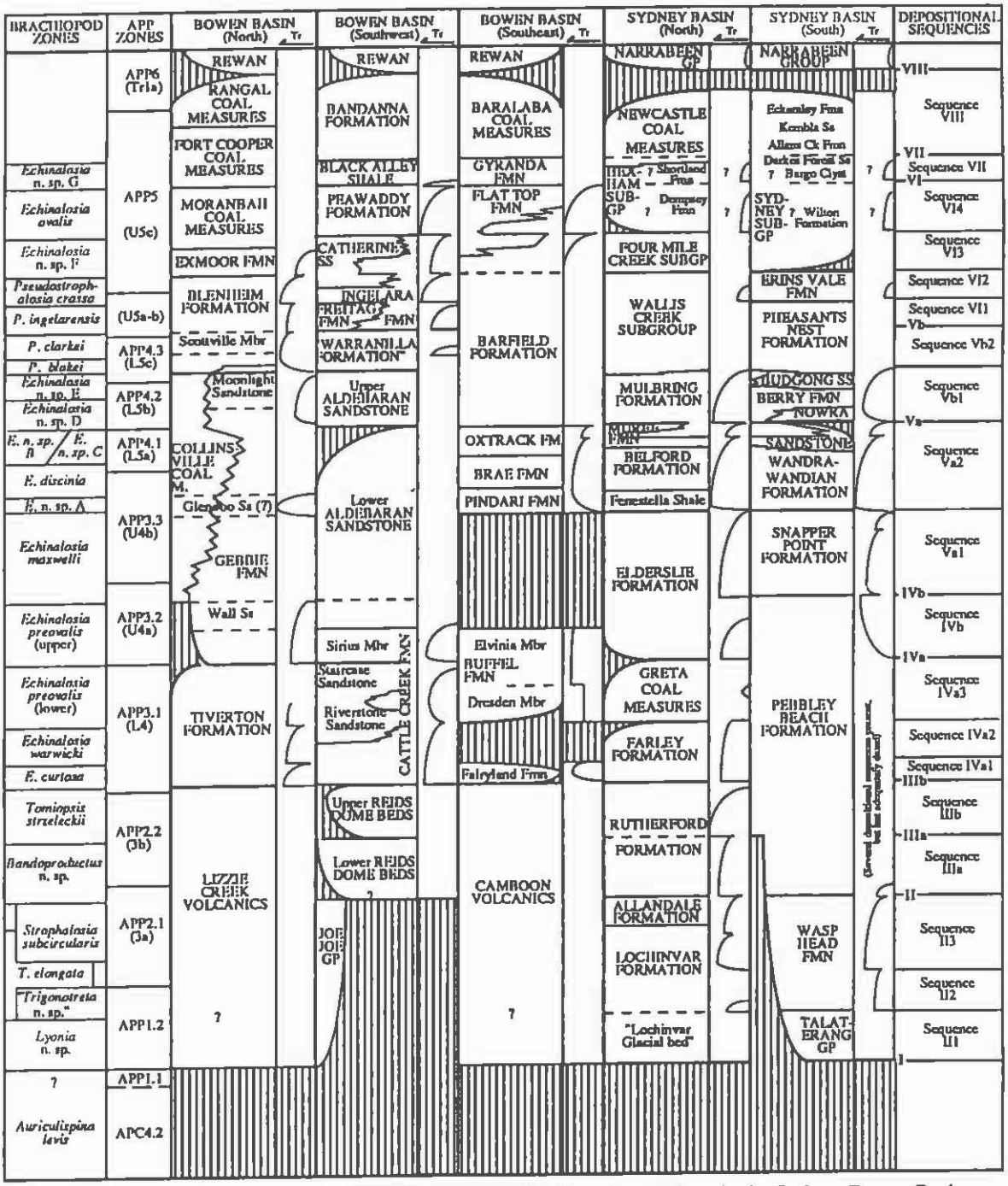

Figure 1. Correlation of depositional sequences in five standard Permian sections in the Sydney-Bowen Basin. Abbreviations: *P.* = *Pseudostrophalosia*, *E.* = *Echinalosia*, *T.* = *Tomiopsis*, Tr = transgression, GP = Group, FMN, FM = Formation, Mbr, M. = Member, Ss = Sandstone, Clyst = Claystone.

Sequence boundary IIIa is marked by onlap in the Denison Trough (Elliott, 1985). In the northern Sydney Basin this level is not marked by known onlap, but separates two transgressive-regressive cycles comprising respectively the lower and upper Rutherford Formation. The lower Rutherford Formation is a relatively thin, upward-coarsening, silty to sandy unit, containing quiet-water, fenestrate bryozoan-dominated faunas in its lower part, and moderately high energy large spiriferid/encrusting bryozoan faunas at its top. The upper Rutherford Formation comprises very low-energy mudstones and limestones in its lower part, followed by an upwards-coarsening succession of siltstones, sandstones and minor conglomerate. Thus, sequences IIIa and IIIb, recognized initially as seismic sequences in the Denison Trough, apparently each correspond to a single transgressive-regressive cycle in the northern Sydney Basin.

Sequence boundary IIIb is marked by truncation of the underlying Reids Dome beds in the Denison Trough (Elliott, 1985, fig. 3), and marks the base of a regional marine transgression seen at the base of the *Echinalosia curtosa* Zone and correlatives throughout the Bowen Basin. A renewal of marine conditions is also evident in the Sydney Basin at this level, where the laterally persistent Ravensfield Sandstone Member at the base of Farley Formation can be interpreted as a basal transgressive sand.

Sequence IVa in the Denison Trough spans the lower Cattle Creek Formation (*sensu* GSQ) up to a sequence boundary (IVa) near the top of the Staircase Sandstone Member, and also includes correlative freshwater sediments that have been included in the Reid's Dome beds (Elliott, 1985, Fig. 3). Biostratigraphically sequence IVa spans palynological zone APP3.1 (L4), and corresponds to the *Echinalosia curtosa*, *Echinalosia warwicki* and lower *Echinalosia preovalis* brachiopod Zones.

In the Denison Trough sequence boundary IVa is marked by onlap within the Cattle Creek Formation (Elliott, 1985, fig. 3). In the northern Bowen Basin this boundary correlates with the base of the Gebbie Formation as originally defined by Malone et al. (1966); at this boundary the Gebbie Formation overlaps the underlying Tiverton Formation to rest directly on the Lizzie Creek Volcanics. Evidence for truncation of Tiverton Formation strata below this boundary in the Exmoor area was recorded by Waterhouse and Jell (1983, p. 234) (who nevertheless suggested redefinition of the formation boundary at a higher level). In the southeastern Bowen Basin sequence boundary IVa correlates with the onset of rapid transgression at the base of the upper member (Briggs and Waterhouse, 1982) of the Buffel Formation. In the northern Sydney Basin, sequence boundary IVa correlates with the base of the Elderslie Formation, which overlaps and possibly truncates the underlying Greta Coal Measures to the east of the Lochinvar Anticline. A transgressive "depositional episode" boundary was recognized at this level by Herbert (1980, p. 26) who related it to the base of the Snapper Point Formation; the latter boundary however is now correlated on macrofaunal evidence with sequence boundary IVb.

Within sequence IVa, the *Echinalosia curtosa* , *E. warwicki* and lower *E. preovalis* Zones each appear to be associated with a separate transgressive - regressive cycle, and evidence of onlap and truncation near the base of the uppermost of these cycles has been recorded locally. The three cycles can be best illustrated from the succession in the Tiverton Formation near Homevale, using the subdivisions of Campbell (1961). Here relatively deep-water faunas, dominated by small brachiopods and preserved as unworn and usually conjoined shells, occur at three discrete levels: "Zone 1" of Campbell (*E. curtosa* Zone correlative), "Zone 3" to "Zone 7" of Campbell (*E. warwicki* Zone) and "Zone 10" to "Zone 13" of Campbell (lower *E. preovalis* Zone). These units are separated by two shallower-water units dominated by large brachiopods and molluscs, with taphonomic indications of higher energy conditions: "Zone 2" of Campbell , and "Zone 8" to "Zone 9" of Campbell respectively. In the southeastern Bowen Basin strata of the lower *E. preovalis* Zone (Dresden Limestone member of the Buffel Formation) onlap onto truncated strata of the *E. curtosa* Zone (now Fairyland Formation) on Cracow Station

(Briggs and Waterhouse, 1982). An at least locally unconformable contact also occurs at the base of the Greta Coal Measures in the northern Sydney Basin, which from faunas from overlying and underlying marine units is correlated with the lower *E. preovalis* Zone.

Sequence IVb. In the Denison Trough sequence IVb of Elliott (1985) spans from sequence boundary IVa, at the top of the Staircase Sandstone, to sequence boundary IVb, just above the base of the Aldebaran Sandstone. This interval spans most of palynological zone APP3.2, and corresponds to the upper *Echinalosia preovalis* Zone.

Sequence boundary IVb is marked by onlap in the Denison Trough (Elliott, 1985, fig. 3). The boundary in the northern Bowen Basin (within the lower Gebbie Formation) may be conformable, although biostratigraphic resolution is poor in this interval. In the southern Sydney Basin boundary IVb correlates with the base of the Snapper Point Formation, which Gostin and Herbert (1972) considered to be slightly unconformable on the underlying Pebbley Beach Formation, and which is marked by a prominent seismic reflecting horizon offshore ("horizon B" of Bembrick and Holmes, 1976). In the northern Sydney Basin this boundary correlates with a level within the lower Elderslie Formation, above the basal fossiliferous part. In each area sequence IVb corresponds to a single transgressive - regressive cycle.

Sequence Va. Sequence Va in the Denison Trough corresponds to the lower Aldebaran Sandstone, between sequence boundaries Va and IVb. Sequence Va spans the uppermost APP3.2 to APP4.1 palynological zones, which elsewhere in the basin correspond to the *Echinalosia maxwelli*, *Echinalosia* n. sp. A, *Echinalosia discinia* and *Echinalosia* n. sp. B/*Echinalosia* n. sp. C brachiopod Zones.

In the Denison Trough sequence boundary Va is a major unconformity within the Aldebaran Sandstone (Elliott, 1985). Successions in the northern and southeastern Bowen Basin may be conformable at this level. In the Sydney Basin sequence boundary Va correlates with a disconformity recognized by McKelvey *et al.* (1971) near the base of the Nowra Sandstone (i.e. near the base of the upper unit of the Nowra Sandstone *sensu* Mayne *et al.*, 1974), and with a level within the more continuous Muree Formation.

Outside the Denison Trough, sequence Va contains two major transgressive - regressive cycles, most clearly expressed in the Sydney Basin. The lower sequence (Va1), corresponding to the upper Elderslie Formation in the north and the Snapper Point Formation in the south, spans most of the *E. maxwelli* Zone, excluding its uppermost part. The shallowing-up succession in the Snapper Point Formation above its basal transgressive part has been documented in detail by Carey (1979). A similar shallowing-upward trend is evident in the correlative interval in the Elderslie Formation of the Lochinvar Anticline, where productid-bearing faunas in the middle part of the formation are replaced upwards by shallower-water communities consistently dominated by large spiriferids.

The upper transgressive-regressive cycle (Va2) comprises the uppermost Elderslie Formation-Fenestella Shale-Belford Formation-Muree Formation in the north, and the Wandrawandian Formation-lower Nowra Sandstone in the south, and spans the uppermost *E. maxwelli* to *E.* n. sp. B/*E.* n. sp. C Zones. In the SE Bowen Basin this sequence (Pindari-Brae-Oxtrack Formations) onlaps disconformably onto older strata.

Sequence Vb. Elliott (1985) showed his sequence Vb as spanning two sediment packages in the Denison Trough, the upper Aldebaran Sandstone and the thin overlying informally-named "Warranilla Formation", which was interpreted as a relict lag deposit below sequence boundary Vb. The upper Aldebaran Sandstone lacks diagnostic marine macrofossils, but in spanning palynological zones APP4.2 to lower APP4.3 can be correlated with the *Echinalosia* n. sp. D and *Echinalosia* n. sp. E Zones in the Sydney Basin. The "Warranilla Formation" spans the boundary between APP4.3 and APP5, and has yielded *Pseudostrophalosia clarkei* (Eth. Snr), typifying the *P. clarkei* Zone.

These two sediment packages correlate with two transgressive-regressive cycles (Vb1 and Vb2) in other parts of the Sydney-Bowen Basin. The upper Aldebaran Sandstone correlates with the youngest transgressive-regressive cycle of the Maitland/ Shoalhaven Groups in the Sydney Basin, comprising the Mulbring Formation to lowermost Tomago Coal Measures in the north and the upper Nowra Sandstone-Berry Formation-Budgong Sandstone-lowermost Illawarra Coal Measures in the south. In the northern Bowen Basin the *P. clarkei* Zone and the *P. blakei* Zone (associated with the immediately underlying transgressive sandstone) characterize the lowermost transgressive pulse of the Blenheim Formation. The two Zones occupy a similar position in the basal Back Creek Group in the Capella Block (W Bowen Basin).

Sequence VI. Sequence VI in the Denison Trough spans from the base of the Freitag Formation to the base of the Black Alley Shale. This succession occupies an interval within APP5, and spans the *Pseudostrophalosia ingelarensis*, *Pseudostrophalosia* n. sp., *Echinalosia* n. sp. F and *Echinalosia ovalis* Zones.

Sequence boundary VI is marked by onlap and offlap in the Denison Trough (Elliott, 1985). Brakel et al. (1992) also reported truncation of beds at this level (their B63) in several sections, supported by field evidence of an erosional contact. Sequence boundary VI is correlated biostratigraphically (by its position at the top of the *E. ovalis* Zone) with the top of the Flat Top Formation in the Taroom Trough, at which level Brakel *et al.* (1992) recognized a possible sequence boundary (their B64).

As shown in Figure 1, the *P. ingelarensis*, *P.* n. sp., *E.* n. sp. F and *E. ovalis* Zones are each apparently associated with a minor transgressive - regressive cycle, here numbered VI1, VI2, VI3 and VI4 respectively. In the Sydney Basin sequence VI correlates with most of the Tomago Coal Measures (excluding its lowermost and uppermost parts), but although a number of transgressive-regressive cycles may be present in this interval, only the *P.* n sp. Zone appears to be represented in the basin by marine macrofaunas, which have been encountered in a representative of the Kulnura Marine Tongue in the upper Wallis Creek Formation in DM Stockton DDH3. A sequence boundary recognized at the top of the Erins Vale Formation (Kulnura Marine Tongue correlative) in the southern Sydney Basin (Bowman, 1980; Arditto, 1991) therefore may correlate with sequence boundary VI2. In the northern Sydney Basin a sequence boundary at the base of the upper Tomago Coal Measures or Dempsey Formation is associated with truncation of underlying units on the flanks of the Lochinvar Anticline (Stuntz, 1972); this boundary seems to be a correlative of sequence boundary VI3, although direct biostratigraphic evidence is not available.

Sequence VII. Sequence VII in the Denison Trough corresponds to the Black Alley Shale *sensu* Elliott (1985). Sequence VII spans part of APP5, and is the youngest Permian depositional sequence in the Bowen Basin to show clear indications of marine influence, including a widespread acritarch swarm (the "P3c horizon") and locally marine macrofossils in the basal few metres of the unit. Marine macrofossils from the unit in the Bowen Basin are largely indeterminable, but based on its position directly above the *E. ovalis* Zone, sequence VII is a probable correlative of the *Echinalosia n.* sp. G Zone, typified by a fauna from the Gilgurry Mudstone (New England Orogen).

Elliott (1985) recorded onlap and truncation at sequence boundary VII in the Denison Trough. Brakel et el. (1992) reported a dubious sequence or parasequence boundary, marked by a distinct reflector (B17), at the top of the correlative Gyranda Formation.

Sequence VIII. Although not specifically labelled by Elliott (1985), sequence VIII is taken to span the Bandanna Formation, up to the major unconformity at the base of the Rewan Formation. Palynologically, sequence VIII spans upper APP5 and lower APP6. No marine fossils are known from this interval in the Sydney - Bowen Basin.

Sequence boundary VIII corresponds to the regional unconformity at the base of the Rewan Formation in the Bowen Basin, at which truncation of underlying strata has been reported in many areas. Brakel *et al.* (1992) regarded this boundary (their B33) as "one of the most obvious sequence boundaries" in the Taroom Trough succession. In the Sydney Basin the corresponding sequence boundary between the Newcastle and Illawarra Coal Measures and the overlying Narrabeen Group is marked by extensive truncation of strata on the flanks of the Lochinvar Anticline) and by a persistent, more subtle disconformity elsewhere (Retallack, 1980; Herbert, 1993).

REFERENCES

ARDITTO, P.A., 1991: A sequence stratigraphic analysis of the Late Permian succession in the Southern Coalfield, Sydney Basin, New South Wales. Aust. J. Earth Sci. 38, 125-137.

BEMBRICK, C.S., & HOLMES, G.G., 1976: An interpretation of the subsurface geology of the Nowra-Jervis bay area. Rec. geol. Surv. N.S.W. 18(1), 5-68.

BOWMAN, H.N., 1980: Southern Coalfield, Upper Shoalhaven Group and Illawarra Coal Measures. Bull. Geol. Surv. N.S.W. 26: 116-132.

BRAKEL, A.T., TOTTERDELL, J.M., & WELLS, A.T., 1992: Sequence boundaries interpreted from seismic data in the central Taroom Trough, SE Queensland. Adv. Stud. Sydn. Bas., 26th Newcastle Symp. Proc., 64-71.

BRIGGS, D.J.C., 1989: Can macropalaeontologists, palynologists and sequence stratigraphers ever agree on eastern Australian Permian correlations. Adv. Stud. Sydn. Bas., 23rd Newcastle Symp. Proc: 11-17.

BRIGGS, D.J.C., & WATERHOUSE, J.B., 1982: Summary of formations and faunas of the Permian Back Creek Group in the southeastern Bowen Basin. Pap. Dept Geol., Univ. Qd. 10(2), 69-82.

CAMPBELL, K.S.W., 1961: New species of the Permian spiriferoids *Ingelarella* and *Notospirifer* from Queensland and their stratigraphic implications. Palaeontographica A, 117, 159-192.

CAREY, J., 1979: Sedimentary environments and trace fossils of the Permian Snapper Point Formation, southern Sydney Basin. J. geol. Soc. Aust., 25: 433-458.

DIESSEL, C.F.K., 1992: Coal composition and sequence stratigraphy. Geol. Soc. Aust. Abstr. 32, 118.

ELLIOTT, L., 1985: The stratigraphy of the Denison Trough. Bowen Basin Coal Symposium, Geol. Soc. Aust. Abstr 17, 33-38.

FIELDING, C.R., FALKNER, A.J., KASSAN, J. & DRAPER, J.J., 1990: Permian and Triassic depositional systems in the Bowen Basin. Proceedings, Bowen Basin Symposium, Mackay, 1990, Geol. Soc. Aust., Qd Div.: 21-25.

GOSTIN, V. A. & HERBERT, C., 1972: Stratigraphy of the Upper Carboniferous and Lower Permian sequence, southern Sydney Basin. J. Geol. Soc. Aust., 20(1), 49-70.

HERBERT, C., 1980: Depositional development of the Sydney Basin. Bull. geol. Surv. N.S.W. 26, 11-52.

HERBERT, C., 1993: Tectonics of the New England Orogen reflected in the sequence stratigraphy of the Narrabeen Group/Coal Measures of the Sydney Basin. *In* P.G. Flood and J.C. Aitchson, New England Orogen eastern Australia: 127-135. Dept Geol. Geophys., Univ. New England, Armidale.

McKELVEY, B.C., McCLUNG, G.R., & RUNNEGAR, B., 1971: Nowra-Muree sands - Definition, internal morphology and age. Adv. Stud. Syd. Bas., 6th Newcastle Symposium, Progr. and Abstr. 22.

MALONE, E.J., JENSEN, A.R., GREGORY, C.M. and FORBES, V.R., 1966: Geology of the southern half of the Bowen 1:250,000 Sheet area, Queensland. Rep. Bur. Miner. Resour. Geol. Geophys. 100.

MAYNE, S.J., NICHOLAS, E., BIGG-WITHER, A.L., RASIDI, J.S., & RAINE, M.J., 1974: Geology of the Sydney Basin - A review. Bull. Bur. Miner. Resour. Geol. Geophys.149, 229 pp.

RETALLACK, G.J., 1980: Late Carboniferous to Middle Triassic megafossil floras from the Sydney Basin. Bull. geol. Surv. N.S.W. 26, 384-430.

ROBERTS, J., 1985: Carboniferous sea-level changes derived from depositional patterns in Australia. Dixieme Congres International de Stratigraphie et de Geologie du Carbonifere, Madrid, Compte Rendu 4, 43-64.

ROSS, C.A., & ROSS, J.R.P., 1987: Late Palaeozoic sea levels and depositional sequences. Cushman Foundation Foram. Res., Spec. Publ. 24, 151-168.

STUNTZ, J., 1972: The subsurface distribution of the "Upper Coal Measures", Sydney Basin, New South Wales. Pap. Conf. Australas. Insti. Min. Metall., Newcastle, 1-9.

VAN WAGONER, J.C., POSAMENTIER, H.W., MITCHUM, R.M., VAIL, P.R., SARG, J.F., LOUTIT, T.S., & HARDENBOL, J., 1988: An overview of the fundamentals of sequence stratigraphy and key definitions. Soc. Economic Palaeontologists Mineralogists, Spec. Publ. 42, 39-45.

WATERHOUSE, J.B., & JELL, J.S., 1983: The sequence of Permian rocks and faunas near Exmoor homestead, south of Collinsville, northern Bowen Basin. *In* FOSTER, C.B. (ed.), Permian geology of Queensland, Geological Society of Australia, Qld Division, Brisbane, 231-267.

ZIOLKOWSKI, V. & TAYLOR, R., 1985: The structure of the north Denison Trough. Geol. Soc. Austr. Abstr. 17, 129-135.

ZIOLKOWSKI, V. FIELDING, C.R., WILKINSON, M., & DRAPER, J.J., 1992: Sequence stratigraphic analysis of the Permian succession in the western Bowen Basin, Queensland; implications for hydrocarbon exploration. Geol. Soc. Austr. Abstr., 109-110.